

GOETHE



UNIVERSITÄT
FRANKFURT AM MAIN

**Substrate binding does not only mean catalysis:
internal regulation in the cytochrome *bc*₁ complex
from *Paracoccus denitrificans***

Dissertation

zur Erlangung des Doktorgrades der Naturwissenschaften

vorgelegt beim Fachbereich 14

Biochemie, Chemie und Pharmazie

von Michela Castellani

aus L'Aquila

Italien

Frankfurt am Main 2011

(D30)

Vom Fachbereich Biochemie, Chemie und Pharmazie der
Goethe-Universität als Dissertation angenommen

Dekan: Prof. Dr. Dieter Steinhilber

Erstgutachter: Prof. Dr. Bernd Ludwig

Zweitgutachter: Prof. Dr. Klaas Martinus Pos

Datum der Disputation _____

To my Italian-German family

Table of contents

1	Introduction.....	1
1.1	Function and structure of the respiratory chain.....	1
1.1.1	<i>Paracoccus denitrificans</i> as a model organism	4
1.2	The cytochrome <i>bc</i>₁ complex	5
1.2.1	Subunits of the cytochrome <i>bc</i>₁ complex	6
1.2.1.1	Cytochrome <i>b</i>	7
1.2.1.2	The Rieske iron sulphur protein (ISP)	9
1.2.1.3	Cytochrome <i>c</i> ₁	12
1.2.1.4	Accessory subunits	13
1.2.2	The cytochrome <i>bc</i>₁ complex from <i>P. denitrificans</i>.....	14
1.2.2.1	Genetic organization	14
1.2.2.2	Protein subunits	14
1.2.3	Interaction between the cytochrome <i>bc</i>₁ complex and the substrate	17
1.2.4	Cytochrome <i>bc</i>₁ complex mechanism.....	19
1.2.4.1	The modified Q-cycle	19
1.2.4.2	Quinol oxidation at the Q _o site	20
1.2.4.3	<i>Half-of-the-sites mechanism</i>	25
1.3	Cytochrome <i>c</i>₅₅₂	31
1.4	Aim of this work.....	32
2	Materials and methods	34
2.1	Materials	34
2.1.1	Chemicals.....	34
2.1.2	Proteins	35

Table of contents

2.1.2.1	Enzymes for molecular biology	35
2.1.2.2	Antibodies	36
2.1.2.3	Varia.....	36
2.1.3	Kits	36
2.1.4	Markers	36
2.1.5	Chromatography materials	36
2.1.6	Instruments.....	37
2.1.7	Softwares and databanks	38
2.1.7.1	Softwares	38
2.1.7.2	Databanks	38
2.1.8	Plasmids	39
2.1.8.1	Available plasmids.....	39
2.1.8.2	Plasmids produced in this work	40
2.1.9	Microorganisms.....	41
2.1.9.1	<i>Escherichia coli</i> K12	41
2.1.9.2	<i>Paracoccus denitrificans</i>	41
2.1.10	Oligonucleotides	42
2.1.11	Solutions.....	42
2.1.12	Antibiotics.....	47
2.1.13	Medium.....	47
2.2	Molecular biology methods	48
2.2.1	Growth and storage of microorganisms.....	48
2.2.1.1	<i>Escherichia coli</i>	48
2.2.1.2	<i>Paracoccus denitrificans</i>	48
2.2.2	Isolation of plasmidic DNA in small scale (Miniprep)	48
2.2.3	Plasmid DNA restriction.....	49

Table of contents

2.2.4	Electrophoretic separation of DNA.....	49
2.2.5	DNA extraction from agarose gels	50
2.2.6	Ligation of DNA fragments.....	50
2.2.7	Production <i>E.coli</i> competent cells.....	51
2.2.8	Transformation of <i>E.coli</i> competent cells	51
2.2.9	Conjugation: <i>Triparental Mating</i>.....	51
2.2.10	Phosphorilation of oligonucleotides	52
2.2.11	<i>Polymerase Chain Reaction</i>.....	52
2.2.12	Site directed mutagenesis.....	53
2.2.13	DNA Sequencing.....	53
2.3	Protein biochemistry	53
2.3.1	Analytic membrane preparation	53
2.3.2	Membrane preparation (preparative scale)	54
2.3.3	Membrane solubilisation	55
2.3.3.1	Classic purification of the cytochrome <i>bc</i> ₁ complex.....	55
2.3.3.2	Purification by affinity chromatography (Ni ²⁺ -NTA)	55
2.3.3.3	Purification by affinity chromatography (StrepTactin)	55
2.3.4	Chromatography.....	56
2.3.4.1	Classic purification of the cytochrome <i>bc</i> ₁ complex.....	56
2.3.4.2	Purification by affinity chromatography (Ni ²⁺ -NTA)	56
2.3.4.3	Purification by affinity chromatography (StrepTactin)	56
2.3.4.4	Purification of the cytochrome <i>C</i> _{552F}	57
2.3.5	Lowry	57
2.3.6	Polyacrylamide gel electrophoresis (PAGE).....	57
2.3.6.1	Tricine system (Schägger)	57
2.3.7	Gel staining	58

Table of contents

2.3.7.1	Coomassie staining	58
2.3.8	Westernblot (semidry).....	58
2.3.8.1	Western blot protocol.....	59
2.4	Biophysics methods	59
2.4.1	Enzymatic activity tests	59
2.4.1.1	Decylubiquinone reduction	60
2.4.1.2	Measurements.....	60
2.4.1.3	Redox spectra	61
2.4.1.4	Pre steady-state cytochrome c_1 reduction: Stopped-flow	61
2.4.1.5	Time resolved stopped-flow.....	63
2.4.1.6	Pre steady state reduction of cytochrome c_1 and cytochrome b in presence of antimycin	63
2.4.1.7	Steady-state cytochrome c reduction with and without antimycin.....	63
2.4.1.8	Flash photolysis experiments	64
2.4.1.9	Flash photolysis internal kinetics	64
3	Results	65
3.1	Dimeric nature of the complex	65
3.1.1	Purification and characterization of the deletion mutant	65
3.2	Heterodimeric cytochrome bc_1 complex.....	70
3.2.1	Genetic background, mating and purification.....	73
3.2.2	Pre steady-state ubiquinol oxidation by the cytochrome bc_1 complex in absence of antimycin.....	78
3.2.3	Steady-state kinetics.....	80
3.2.4	Pre steady-state ubiquinol oxidation by the cytochrome bc_1 complex in presence of antimycin	82
3.2.5	Antimycin titrations.....	84

Table of contents

3.3	Interaction between cytochrome bc_1 of <i>P. denitrificans</i> and its cytochrome c substrate	88
3.3.1	Pre-steady-state laser flash kinetic studies	89
3.3.2	Preparation of the ruthenium coupled electron acceptors	90
3.3.3	Redox mediators and reaction conditions	91
3.3.4	Salt titrations with the Ru_2-H39C-<i>Cc</i>.....	95
3.3.5	Salt titrations with the Ru_2-N23C-<i>C</i>_{552F}.....	99
3.4	Rapid flash kinetics for the internal electron transfer	102
3.4.1	Experimental setup and protocol description	102
3.4.2	Internal kinetics using TMPD and ascorbate to reduce the cytochrome bc_1 complex.....	104
3.4.3	Internal kinetics using TMPD, ascorbate, decylubiquinol, succinate and SQR to reduce the cytochrome bc_1 complex.....	114
3.5	Interaction between the ISP and the cytochrome c_1 by stopped flow kinetics	117
3.5.1	Experimental setup.....	117
3.5.2	Kinetics observed mixing against ascorbate, with and without inhibitors	120
3.5.3	Kinetic measurements using the <i>fbcF</i> gene with the S157C mutation	129
4	Discussion	141
4.1	Half-of-the-sites mechanism and dimeric nature of the cytochrome bc_1 complex.....	142
4.2	Internal electron transfer and ISP movements	148
4.3	Kinetics of reduction with ascorbate and interaction between the ISP and the cytochrome c_1.....	152
4.4	Deletion mutant of the cytochrome bc_1 complex from <i>P. denitrificans</i> and interaction with the substrate.....	157

Table of contents

5	Summary	162
6	Zusammenfassung	164
7	References	169
8	Publications	185
9	Abbreviations	186
	Eidesstattliche Erklärung	189
	Curriculum Vitae	190
	Acknowledgments	191

1 Introduction

The redox equivalent obtained from the oxidation of NADH and FAHD_2 are used for energy transduction and ATP synthesis in mitochondria. The most accredited theory on the evolution of mitochondria is the endosymbiotic theory of Margulis (1), according to which mitochondria derive from a α proteo-bacterium which established a symbiosis with a host cell. Some principles behind this theory were criticised, for example the exchange of ATP/ADP between host and and symbiont (2), on the basis of mitochondrial DNA analysis, indicating this eventual exchange as unlikely. The advantage for this symbiosis lies, probably, in the exchange of metabolic intermediates useful for the host, which could offer a protected environment to the simbiont, assuring advantages for both organisms.

1.1 Function and structure of the respiratory chain

By oxidative phosphorylation, living organism can transform and use energy. Organic molecules, introduced with the diet or obtained from the storage of nutrients such as sugar or fat, are oxidized by glycolysis, tricarboxylic acid cycle or β -oxidation to obtain FADH_2 (flavin adenine dinucleotide) and NADH (nicotinamide adenine dinucleotide). These high energy nucleotides are oxidized by protein complexes resident in the inner mitochondrial membrane. By transferring electrons to molecular oxygen and reducing it to water, protons are pumped across the membrane, generating a proton gradient. The protein complexes involved in the electron transfer to oxygen are known as the aerobic respiratory chain.

The chemio-osmotic theory of Peter Mitchell (3) describes how the proton gradient is generated across the inner mitochondrial membrane (and across the cytoplasmatic membrane in bacteria) and represents the basis for the production of ATP.

The back flow of protons along the chemical gradient across the membrane is used by the last complex of the oxidative phosphorylation to convert ADP (adenosine diphosphate) to ATP. Little is still known about the exact proton pumping mechanism of each complex, whereas the electron transfer process seems to be better understood. Five complexes in total are involved in the oxidative phosphorylation, highly conserved between bacteria and eukaryotes, not only for their functions but also for their basic structure and composition.

Introduction

The mitochondrial oxidative phosphorylation is situated in the inner membrane, and hosts five membrane-integral protein complexes. In the electron transfer process, also ubiquinol and a soluble cytochrome *c* operate as shuttles between complexes. As a result, protons are translocated into the intermembrane space generating the electro-chemical gradient which will be used by the last complex to regenerate ATP from ADP and inorganic phosphate.

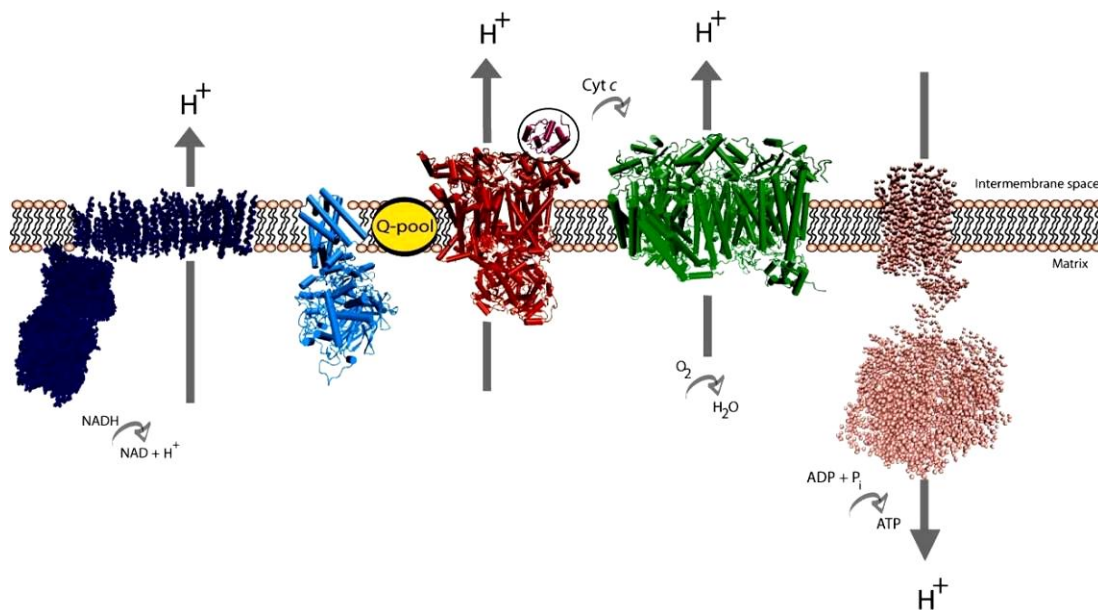


Fig. 1: Model for the mitochondrial respiratory chain. From the left, in dark blue the recently solved structure of complex I (taken from *Thermus thermophilus*; PDB: 3M9S, at present the only available structure for complex I). In light blue the structure of the mitochondrial complex II (PDB: 1ZOY). In red, the yeast complex III with bound cytochrome *c* in purple (PDB: 1KYO), and in green the mitochondrial cytochrome *c* oxidase (PDB: 1OCR). In pink, the structure of the mitochondrial ATP-synthase (PDB: 1QO1). The vertical gray arrows indicate the complexes able to transfer protons across the membrane. The stoichiometry is not represented here. The smaller arrows indicate reactions between the complexes.

The first complex is the NADH:ubiquinone oxidoreductase, or complex I, made up of approximately 45 polypeptide chains with a molecular weight of more than one MDa (4). It catalyzes the oxidation of NADH and the reduction of ubiquinol, with a stoichiometry of four protons per two electrons translocated to the intermembrane space. It has a very particular “L” shape, from which it is possible to identify at least two domains: a hydrophobic, transmembrane part and a hydrophilic arm which is protruding into the mitochondrial matrix. The latter includes the NADH binding site and all the cofactors (5-8), namely a non-covalently but tightly bound FMN (flavine

Introduction

mononucleotide) and eight iron sulphur clusters (two of them binuclear and the remaining six tetranuclear) (9). Recently (5, 10) crystal structures of the entire complex I have been obtained, from bacteria and mitochondria, showing a very interesting feature, implicated in the mechanism. The quinone binding site is not embedded in the membrane as it was previously thought due to its hydrophobic nature, but it is in the peripheral arm, where the two domains come in contact to form the whole complex. In the membrane arm, typical features of ion antiporters are found which are considered to be involved in the proton pumping mechanism. From the quinone reduction site a conformational change is transferred through the transmembrane domain by a very long amphipatic helix, coming in contact with discontinuous helices in the antiporter-like subunits, allowing proton pumping. Proton transfer coupled to the quinone electrochemistry is highly unprobable, since the binding site accommodates the substrate in the peripheral arm and not, as until recently believed, in the transmembrane part (6-8, 11).

Complex II (succinate:ubiquinone oxidoreductase) (12, 13) works as an alternative electron entry point, since it can oxidize succinate to fumarate and use FADH_2 as a cofactor obtained from the tricarboxylic acid cycle. The complex can be divided into two groups of subunits: two hydrophilic ones facing the mitochondrial matrix, containing a FAD and different iron sulphur centers, and a hydrophobic one spanning the inner membrane, being the binding site for ubiquinone and inhibitors. This is the only complex in the mitochondrial respiratory chain that transfers electrons without pumping protons. It allows, nevertheless, to re-oxidize FADH_2 to FAD, which enters again the Krebs cycle.

The reduced ubiquinol in the membrane is the substrate for the ubiquinol:cytochrome *c* oxidoreductase (complex III). This complex is composed of 11 subunits, and is a homodimer as confirmed from the analysis of different structures from several organisms (see 1.2). The redox cofactors included in the complex are a 2Fe-2S cluster, a cytochrome *c*₁ and a cytochrome *b* containing two heme groups. Its function is defined by the so called Q cycle mechanism, first described by Peter Mitchell (14), by which two ubiquinol molecules are oxidized and one ubiquinol is regenerated. The product of the reaction is reduced cytochrome *c*, which works as an electron shuttle to cytochrome *c* oxidase.

This last component, cytochrome *c* oxidase, is a homodimer in mitochondria and a monomer in bacteria (15-18). In total, four electrons have to be transferred to

Introduction

oxygen to reduce it to water, with a mechanism which is still at present intensively discussed and studied, since the different catalytic intermediates are spectroscopically distinguishable (19). Electrons are passed sequentially from cytochrome *c* to the Cu_A center, from here to the heme *a* and, at last, to the binuclear center heme *a*₃/Cu_B where oxygen reduction takes place. The proton pumping activity starts when electrons are passed from heme *a* to the binuclear center with a stoichiometry of one proton pumped per transferred electron.

The ATP-synthase (20-24) uses the backflow of protons along the gradient to regenerate ATP from ADP and phosphate.

1.1.1 *Paracoccus denitrificans* as a model organism

Paracoccus denitrificans is a gram negative bacterium belonging to the group of the α -proteobacteria. It was first isolated by Beijerinck (25) as *Micrococcus denitrificans*, being able to anaerobically convert nitrate into molecular nitrogen. Initially, *P. denitrificans* was the only member of its genus, but analysis of the 16S rRNA could show that other bacteria such as *Thiobacillus versutus* shared a high homology with *P. denitrificans* thus being included in the same taxonomic group (26-29). All bacteria belonging to the genus *Paracoccus* have a high GC content in their genomic DNA, estimated between 60 and 70 %. In this work, the strain PD1222 was used, whose genome sequence was published in 2006 (30); it includes two chromosomes (chromosome 1, 2.9 Mbp, Gene bank CP000489, and chromosome 2, 1.7 Mbp, Gene bank CP000490) and a megaplasmid (0.65 Mbp). The total GC content is 67 % and 2799 protein-coding genes have been identified.

The endosymbiotic theory from Margulis (1) discussed the origin of the mitochondrion and suggested it to be the development of an ancestral prokaryote having a respiratory chain, which established a symbiosis with its host, a protoeukaryote. The host was a plastid free, amoeboid cell, which used fermentation for ATP production. By taking up the prokaryote, the host acquired the possibility of performing aerobing respiration. According to this theory, the outer mitochondrial membrane derived from the host, whereas the inner one shows a high degree of homology with present-day bacteria. In this process, the prokaryote retained its respiratory chain and altered the properties of its membrane, in order to adapt to the

Introduction

new environment. The prokaryote in question is often identified with *Paracoccus denitrificans* (or other related bacteria), since the properties of its respiratory chain are quite close to mitochondria. For instance, the lipidic membrane composition, the use of ubiquinone 10, two *b*-type and two *c*-type cytochromes, the presence of an aa_3 oxidase and sensitivity to rotenone and antimycin A find correspondence in mitochondria (27).

Paracoccus denitrificans has a versatile respiratory chain: there are also two alternative terminal oxidases, the ba_3 oxidase (oxidizing quinol) and the cbb_3 oxidase (with high affinity for the substrate, and expressed under low oxygen conditions). Other metabolic pathways are also available (31), such as methanol and methylamine dehydrogenases, sulphur oxidation; moreover, also succinate can be used as an organic substrate and in anaerobic conditions nitrate can be used as an electron acceptor instead of oxygen.

In comparison with the mitochondrial complexes, *Paracoccus denitrificans* respiratory complexes are smaller: complex I is made of 14 subunits instead of 45 (32), complex III only three instead of 10 to 11 (33), and complex IV only four compared to 13 (34). Moreover, the latter is a monomer and not a dimer (as observed in mitochondria). The catalytic subunits, nevertheless, present a very high homology to the eukaryotic ones, while the accessory subunits are missing completely.

All those features make important working with *P. denitrificans* as a model organism, due also to the easy microbiological handling and to the accessibility to its genetic material.

1.2 The cytochrome bc_1 complex

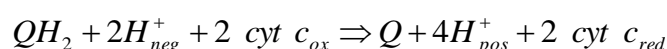
The bc_1 complex (ubihydroquinone-cytochrome *c* oxidoreductase) is a key component of several aerobic and anaerobic respiratory chains. It is not only involved in the electron transfer of mitochondria, but plays also a role in denitrification and nitrogen fixation. It belongs to the *bc* complex family, widely distributed in proteobacteria, archaea, cyanobacteria and eukarya (35). In photosynthetic organisms, a so called cytochrome b_6f complex is found, or plastoquinol-plastocyanin oxidoreductase. Several differences in comparison to the bc_1 complexes have been noted. In the cytochrome b_6f complex, cytochrome *b* is

Introduction

not a single subunit but two, there is a different number of residues between the histidines coordinating the *b* hemes than observed in the cytochrome *bc*₁ complex, a cytochrome *f* replaces cytochrome *c*₁ and the genes for cytochrome *b* and the Rieske protein are present on separate genetic loci (36-39). The *b₆f* complex is involved in the electron transfer between the photosynthetic centers II and I. The following discussion will focus on features of the *bc*₁ complex.

The *bc*₁ complex is a multi subunit enzymatic complex present in mitochondria in the inner membrane and in the cytoplasmic membrane of bacteria (22, 39-47) It catalyzes the oxidation of ubihydroquinone and the reduction of cytochrome *c*, which carries electrons to cytochrome *c* oxidase. The catalytic mechanism is described by an electron bifurcation reaction, in which one electron feeds into the high potential chain, i.e. Rieske cluster and cytochrome *c*₁, to be subsequently passed to cytochrome *c*, and the second electron is driven through the low potential chain (the two hemes *b*) to a quinone molecule from the Q-pool in the membrane. After two catalytic cycles, two ubihydroquinone molecules are oxidized, one ubiquinone is reduced and two cytochromes *c* molecules are reduced.

During the overall electron transfer process, protons originating from the oxidation of quinol are released on the positive side of the membrane (intermembrane space in mitochondria, or the periplasmic space in bacteria). Meanwhile, the re-reduction of a ubiquinone through the low potential chain leads to the uptake of protons from the matrix (in mitochondria, respectively the bacterial cytoplasm) increasing the electrochemical gradient. The overall reaction of the *bc*₁ complex is listed in Equation. 1.



Equation 1: Net reaction of two turnovers of the cytochrome *bc*₁ complex. QH₂: ubihydroquinone; Q: ubiquinone; Cyt *c*_{ox/red}: oxidized/reduced cytochrome *c*; neg, pos: negative/positive membrane side.

1.2.1 Subunits of the cytochrome *bc*₁ complex

The structural genes of the eukaryotic complex are all localised in the nuclear genome, with the exception of the cytochrome *b* gene present on the mitochondrial genome. Only three subunits (namely cytochrome *b*, cytochrome *c*₁ and Rieske protein) contribute to catalysis directly, and the accessory subunits (up to eight in the bovine, four in the avian and seven in yeast complexes) have unclear functions

until now. (Section 1.2.1.4 will later discuss some features of the additional subunits.) These facts make studies of the mitochondrial complex more complicated than in bacteria, where the only three to four subunit are present and the structural genes are typically organized in a gene cluster within the genome.

1.2.1.1 Cytochrome *b*

Cytochrome *b* is a central subunits taking part in the catalytic cycle. It is composed of eight transmembrane helices spanning the membrane so that the N- and the C-termini both face the matrix side in mitochondria (the cytoplasm in bacteria). The eight helices, denominated from A to H, are organised in two bundles: the helices A to E coordinating the two cofactors, and helices F to H (48). Seven loops in total are present in the cytochrome *b* protein: four large loops and three small ones. The large loops are *ab*, *cd*, *de* and *ef*. Of them, the *de* loop is the only one facing the matrix side and lacking a clear secondary structure, whereas the the *ab* and *ef* loops form a single helix each. The *cd* loop consists of two helices organized in a hairpin like arrangement, *cd1* and *cd2*. The two helix bundles make contact on the matrix side and diverge then into the intramembrane space to form the Q_o pocket where ubiquinol is oxidized. The ISP docks on cytochrome *b* on the so called ISP docking cavity, on the positive side of the membrane. The Q_o site is delimited by helices B, C and E and buried by the *ef* loop, capped by the *cd1* and *cd2* helices on top (49). When the ISP is bound transiently on cytochrome *b* for catalysis, the His¹⁶¹ (bovine numbering), ligand of the iron sulphur cluster, also contributes to the Q_o site (48-56).

Helices B and D coordinate the two cofactors in cytochrome *b*: the heme *b_L* (low potential) and the heme *b_H* (high potential). The names for the two hemes are derived from their redox potential properties: about 30 mV and 120 mV, respectively, as shown by potentiometric titrations (57). The hemes are coordinated by two His residues each, and along with four Gly residues in close contact with the heme ring, are extremely conserved among several organisms (39, 49, 58). It is interesting to note that the two *b_L* hemes in the dimeric complex are in close distance: in the bovine structure (49, 52) and in the avian structure (55) the distance between the two iron atoms is 21 Å and 20.7 Å respectively. The edge to edge distance is about 14 Å, as calculated for the yeast complex (59). This would allow electron transfer between the two monomers, as reported already (60-62) and analyzed and confirmed later in this work (63).

Introduction

A second quinone binding pocket is present in cytochrome *b*, the Q_i site, formed by helices A D and E with contributions from the small loop preceding the first helix (64), where the ubiquinone binds to be reduced, after two catalytic cycles, to ubihydroquinone.

Cytochrome *b* is a major binding site for inhibitors, which have historically been divided into two classes: class I for the Q_o site inhibitors and class II for the Q_i site. The first class was again divided into three subgroups: Ia for compounds containing a β -methoxyacrylate group such as MOA-stilbene and myxothiazol, Ib for the inhibitors having a chromone ring such as stigmatellin, and Ic for hydroxyquinone analogues such as 5-n-undecyl-6-hydroxy-4,7-dioxobenzothiazole (UHDBT). This subdivision was based on effects these different inhibitors exerted on the complex: the first group was characterized from a red-shift in the b_L spectrum, the second from an increase in the redox potential of the ISP and the spectral red-shift, and the third only for a slight change in the redox potential of the ISP.

According to Esser *et al.* (48) a new classification should be considered: class P for the Q_o site inhibitors, class N for the Q_i site and class PN for those molecules (i. e. NQNO) able to bind on both pockets. The class P should be then again divided into Pf for the inhibitors able to block the movement of the ISP globular domain, and Pm for the ones displacing it away from cytochrome *b*, according to the informations gained from the crystal structures. The new classification is summarized in Table 1.

Class	Sub-group	Examples	Structural features	ISP position
P	F	Famoxadone stigmatellin UHDBT	Benzoquinone analogues having a planar active group	ISP forced into a fixed conformation
	M	Myxothiazol MOAS azoxystrobin	Containing a common MOA moiety	ISP in mobile conformation
N		Antimycin A	Planar active group	No effect
PN		NQNO funiculosin	Planar active group	ISP in fixed conformation

Table 1: Classification of the bc_1 inhibitors. UHDBT: 5-n-undecyl-6-hydroxy-4,7-dioxobenzothiazole; MOAS: methoxyacrylate stilbene; MOA: methoxyacrylate; NQNO: 2-*n*-nonyl-4-hydroxyquinoline N-oxide (adapted by Esser *et al.* (65)).

In this work, stigmatellin, JG-144, mixothiazol and MOA-stilbene have been used to investigate the response of the iron sulphur protein (ISP) head domain. Stigmatellin binds at the Q_o site, and hydrogen-bonds the Glu²⁷² (bovine numbering) of the conserved PEWY sequence (also involved in the interaction with the substrate quinol, (66, 67)) and the His¹⁶¹ (bovine numbering) of the ISP (68, 69). The hydrogen bond is most likely what fixes the head domain in the *b* conformation, since other Pf inhibitors (such as JG-144) are not able to completely inhibit the ISP movements (see 1.2.1.2) (70). Mixothiazol and MOA-stilbene are both Pm inhibitors, sharing the same binding pocket at the Q_o site. Both hydrogen-bond the Glu²⁷² as all the methoxyacrylate containing inhibitors (48, 71-73). Both molecules diminish the occupancy of the ISP head domain to the surface of cytochrome *b* (48, 74).

1.2.1.2 The Rieske iron sulphur protein (ISP)

The iron sulphur protein is inserted in the membrane by the TAT translocation machinery (75). The signal sequence is N-terminal, and even if cleaved off from the mature subunit it stays in the bovine complex as an accessory subunit, strictly associated with the two core subunit on the matrix side (49, 52, 53).

A high resolution structure (1.5 Å) was obtained by Iwata *et al.* (76), where only the globular domain of the bovine ISP (residues 68-196) obtained by proteolysis by Link

Introduction

et al. (77) was described. The overall fold is made up by three layers of antiparallel β -sheets, and an α -helix followed by a long loop between the sheets β 3 and β 4. The globular domain is connected to a transmembrane helix, anchoring the subunit to the membrane. The β -sheets 1-2 and 2-3 form two sandwiches, the latter housing the cluster in the so called cluster binding fold, highly conserved. The Rieske cluster 2Fe-2S is coordinated by two Cys and two His residues: the Fe1 is ligated by the Cys¹³⁹ and Cys¹⁵⁸, and Fe2 by His¹⁴¹ and His¹⁶¹. Two more conserved Cys residues form a disulphide bridge (78) which is important for the stabilisation of the cluster: loss of one of those residues leads to the loss of the cluster. Another loop is also important in this respect: the Pro loop (residues 174-177), Gly-Pro-Ala-Pro, needed for the correct cluster insertion and positioning.

The overall stability of the cluster is further ensured by a network of hydrogen bonds with residues belonging to the base fold. The typical consensus sequence for the binding of the cluster is Cys-X-His-X₁₅₋₄₇-Cys-X-X-His. Even if the overall structures are quite different, almost all residues involved in the cluster binding and stabilisation are extremely conserved. The metal binding domain is similar to the one of rubredoxins (76), small electron transport proteins with Fe atoms coordinated by four Cys residues. The coordination of the Fe1 and the surrounding of the cluster itself share a high degree of similarity with the aforementioned proteins. The Rieske cluster in the hydroquinone oxidizing bc_1 complexes has a higher redox potential (~ 300 mV) compared to the one of other menaquinone oxidizing complexes and of plant ferredoxins. This difference is due to several factors, such as the overall charge of the cluster, its solvent exposure (since just the liganding histidines are shielding it from the solvent environment), the nature of the ligands (since histidines are more electronegative than the sulphur atoms coordinating the cluster in plants ferredoxins) and the strong hydrogen bond pattern (56, 76, 79-81). The higher redox potential of the cluster has implications for quinol oxidation and the catalytic cycle, avoiding two electrons to short circuit in the same turnover and flow into the high potential chain (see paragraph 1.2.4.1).

The redox potential of the Rieske cluster is also pH dependent: in the studies on the water soluble ISP fragment (76) increasing the pH from 5 up to 10 gave a drastic change in the E_m values. With electrochemical experiments, two residues were found responsible for this dependency, being identified with the two liganding histidines (56, 68, 82-84). No other residue in the proximity of the cluster is likely to

Introduction

undergo redox dependent deprotonation. No conformational changes were observed in the overall ISP structure. The His¹⁶¹ (bovine numbering) is thought to deprotonate the semiquinone to yield the correspondent anion. This implication will be further analysed in the section 1.2.4.1.

Several mutations were tested on the cluster and the surrounding residues in order to study the properties of the cluster itself and gain information on the electron transfer mechanism of the bc_1 complex. From these studies it was concluded that the hydrogen bond network is extremely important not only for the stability of the subunit and indirectly of the complete complex but also for the redox potential (85). Moreover, it could be stated that the position Ser¹⁸³ (bovine numbering) is important not only for being a part of the hydrogen bonding network, but also for the correct insertion of the cluster in the apoprotein which can affect inhibitor binding on the Q_o and Q_i sites (86).

An important feature of the ISP is its movement: from the crystal structures obtained by different groups (50, 51, 55, 65, 87, 88) it was observed that the head domain of the iron sulphur protein assumed different positions. Iwata *et al.* (49) indicated that the subunit could have three different states: the “ c_1 state”, the “intermediate state”, and the “ b state”. The three states reflect different positions of the head domain and the neck region. Contacts with cytochrome c_1 and the ef loop of cytochrome b were recorded, mostly van der Waals interactions apart from the hydrogen bond between the propionate of heme c_1 and the His¹⁶¹, the latter thought to allow fast electron transfer. In the intermediate state, the distance Rieske-cytochrome c_1 and Rieske-cytochrome b is similar, as calculated from the crystal structures, and no specific interaction between the subunits was observed. No more contacts are visible between cytochrome c_1 and ISP head domain at all, while there are now hydrogen bonds with cytochrome b (ISP Lys⁹⁰ with cytochrome b Asp¹⁷¹) and extensive contacts with the ef loop. In the b position, obtained in presence of stigmatellin, the ISP head domain is fixed close to the cytochrome b , not allowing electron transfer in the high potential chain, not only for the long distance to cytochrome c_1 , but also for the hydrogen bond connecting the His¹⁶¹ to the inhibitor molecule, simulating the situation in presence of semiquinone. Zhang *et al.* (88) named the relative positions of the ISP as “proximal” and “distal”, respectively corresponding to the “ b ” and the “ c_1 ” positions described by Iwata (49).

Introduction

The movements of the head domain of the ISP are due to the flexibility of the so called hinge region, residues 63-72 in the bovine complex. The overall structure of the head domain does not change when it moves, therefore the neck appears flexible and lets the domain swing. Several studies were performed using random and directed mutagenesis on the region in order to assess the criteria regulating the movements. The first studies indicated that the flexibility is more important than the length (89, 90), showing that reducing the flexibility diminished the activity of the complex of about 70% compared to wild type. Later, Darrouzet *et al.* (91) indicated that no single residue is strictly necessary in the hinge region: all the residues in the sequence could be changed individually without particular loss of activity. Diminishing the length of the region brings a loss of activity, but it does not completely inhibit the complex, which indicates that the neck region is extremely flexible and still able to let the head domain move. Other studies in yeast (92) showed that residues deletion doesn't produce drastic consequences, but insertion of single amino acids is not tolerated, since brings to improper fold of the subunit and therefore total loss of enzymatic activity.

1.2.1.3 Cytochrome c_1

The cytochrome c_1 receives electrons from the ISP in the bc_1 complex and transfers them to the acceptor cytochrome c . It is structurally composed of a transmembrane helix with the C-terminal extension in the mitochondrial matrix (or cytoplasmic side in bacteria) and a N-terminal globular domain. Cytochrome c_1 is made up of 7 helices (6 in the globular domain) and a double stranded β -sheet. Three helices (namely α_1 , α_2 and α_3) are conserved in all class I cytochromes c in general, and also very well conserved in this subunit. A tripeptide Pro-Asn-Leu (present in mitochondrial cytochromes c) starting from residue 111 in the aforementioned structure is another typical sequence, where the Pro provides a hydrogen bond for the heme liganding His (49). The structure of the globular domain, compared to the one of cytochrome c , presents some insertions and deletions, underlying the different functions of the two proteins and also reflecting the different interaction partners (ISP for cytochrome c_1 and complex IV for cytochrome c). The globular domain houses a c -type heme, covalently bound by thio-ether bonds to Cys³⁷ and Cys⁴⁰ (bovine numbering) present in the typical consensus sequence CXXCH. The heme iron is coordinated by residues His⁴¹ and Met¹⁶⁰, and one of its propionates makes a salt bridge with His¹⁶¹

of the ISP when the latter is in the “ c_1 position”. The N-terminal sequence of cytochrome c_1 is in close contact with subunit 8, also called the hinge protein, rich in acidic aminoacids (47, 93, 94) (about the function and features of subunit 8, see section 1.2.1.4).

1.2.1.4 Accessory subunits

In the bovine crystal structure some additional subunits are presents, whose function is not yet clear. Some insights have been gained for the subunits Core I and Core II, subunit 8 (the hinge protein) and subunit 9 (signal sequence cleaved off the mature ISP).

Core I und Core II

The two core subunits face the matrix of the mitochondrion and they are members of the MMP family (membrane metallo-proteins), indicating that the bc_1 complex may be bifunctional and also involved in mitochondrial protein processing. The MMP family members are heterodimers made up of an α and a β monomer, and located in the mitochondrial matrix. The first monomer is involved in recognizing and binding the signal sequence, and the second one contains the metal binding site. The core proteins II and I are respectively homologues to the α and the β monomers, and dependent on Zn^{2+} for the catalysis. After purification, the bc_1 complex shoes no cleavage activity anymore (49, 52, 95)

Hinge-Protein

It plays a role in the correct transient complex formation between cytochrome c_1 and cytochrome c (see paragraph 1.2.3). It is also known as acidic protein, since it contains 24 acidic residues out of 78 in total. It is composed of two helices connected by a disulphide bridge, and together with cytochrome c_1 forms a negatively charged docking position for the highly basic cytochrome c (96-98)

Subunit 9

Subunit 9 represents the N-terminal signal sequence of the ISP after the cleavage by the two core subunits. It is 78 amino acids long and contains two β -sheets, of which the one on the C-terminal side is in close contact with the N-terminal domain of the core II. This seems to be essential for the recognition by the core subunits of the cleavage site on the ISP. After cleavage, this peptide remains with the bc_1

complex as an additional subunit, but no specific function could be identified until now.

1.2.2 The cytochrome bc_1 complex from *P. denitrificans*

The cytochrome bc_1 complex from *Paracoccus denitrificans* is composed only by the three redox active subunits (33, 99-101). The three subunits form a minimal complex, if compared with the 11 subunit mitochondrial complex.

1.2.2.1 Genetic organization

The genes coding for the proteins in the bc_1 complex are present in the *fbc* operon localised on the chromosome 1, containing the *fbc F*, *fbc B* and *fbc C* genes, respectively coding for the ISP, cytochrome *b* and cytochrome c_1 . The structural genes are most likely transcribed in a polycistronic mRNA, since they are separated only by short sequences of 10 to 12 nucleotides, where Shine-Dalgarno sequences are present for ribosome binding (102).

1.2.2.2 Protein subunits

Cytochrome *b* contains 440 amino acids and has a calculated molecular weight of ~51 kDa. On SDS PAGE, the subunit shows an apparent molecular weight of about 45 kDa. Also the bacterial cytochrome *b* subunit has eight transmembrane helices and the two *b*-type hemes. The sequence homology with other organism (such as those of the *Rhodobacter* group, and the mitochondrial one as well (27, 103) is very high, once again pointing towards the use of *P. denitrificans* as a model organism.

The ISP shows the properties similar to Rieske proteins from other bc_1 complexes. In *P. denitrificans*, it has 190 amino acids and a molecular weight of about 20 kDa.

The cytochrome c_1 , the last gene on the operon sequence, has a feature that is found neither in other bacteria nor in the eukaryotic complexes. The protein can be divided into three domains, as shown in Fig. 2.

Introduction

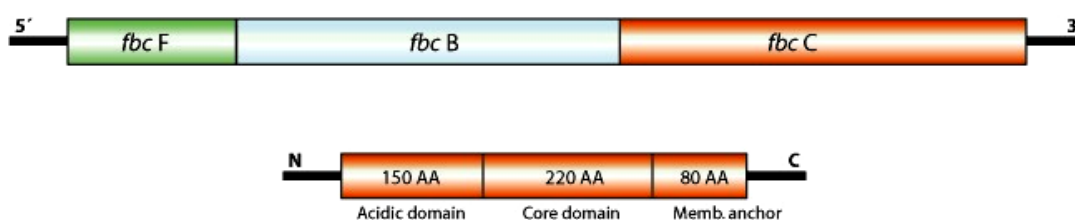


Fig. 2: Top, the *fbc* operon from *P. denitrificans*, schematic view. Bottom, representation of the three domains in the cytochrome *c*₁ gene product.

The N-terminal domain is unique: it has a very peculiar composition, between residues 46 and 197. Following a 24 residue N-terminal signal sequence which is cut to obtain the mature protein, a fairly monotonous stretch of 150 amino acids can be identified, composed of 40 % Ala, 14 % Pro and 38 % negatively charged residues (mostly Glu), arranged in a specific fashion so that tandem repeats of the sequence APA EEA AAE EAP AE and the repetition of the trimer PAA are found. No positive charge is found in the so called “acidic domain” (Fig 3).

```
MTLRNASLTAVAALTVALAGGAVAQDASTAPGTTAPAGSSYHTNEAAPAAADTAPAAEAADEPAAEEAEA  
GAEVTEEPAAETETPAEEPAADEPAADEPAADEPDAEAEPAEEEAQATTEEAPAEPAEEPAEEPAEEPAADAPAE  
EAAEEAPAEPEAAAEPAEEPEATEEEAPAEAAAEAPAEVVEDEAAADHGDAAAQEAGDSHAAAH  
EDISFSFEGPFKFDQHQQLRGLQVYEVCSACHGLRYVPLRRLADEGGPQLPEDQVRAYAANFDITDPETEEDRPRV  
PTDHFPTVSGEGMGPDLSLMAKARAGFHGPGYGTGLSQLFNGIGGPEYIHAVLTGYDGEEKEEAGAVLYHNAAFAGN  
WIQMAAPLSDDQVYEDGTPATVDQMATDVA AFLMWTAEPKMMMDRKQVGFVSVIFLIVLAALLYLTNKKLWQPIKH
```

Fig. 3: Cytochrome *c*₁ amino acid sequence from *P. denitrificans*. In blue the tandem repeats and in red the PAA trimer. In bold, the signal sequence.

The mature subunit has a molecular weight of about 45 kDa, but on SDS PAGE shows an apparent molecular weight of 60-68 kDa, according to the percentage used for the acrylamide gel. This behaviour could be due to an anomalous binding of SDS on the acidic domain during the denaturation step before the gel run, as described by Rath *et al.* (104, 105).

The acidic domain has no homology to any of the other *bc*₁ complexes known, but resembles the small acidic subunit found in the eukaryotic complex, the so called “hinge protein” in the bovine complex (98, 106) and its equivalent in yeast, the QCR6p (97, 107, 108). In the section 1.2.3 the interaction between cytochrome *bc*₁ and cytochrome *c* will be addressed.

Introduction

Some years ago, a deletion mutant missing the acidic domain in the *bc₁* C gene was obtained by E. Gerhus in our lab (109). By XhoI/ NotI restriction and subsequent ligation the domain was deleted, but this brought several problems in the purification procedure. The wild type complex is normally purified by anion-exchange chromatography since the acidic domain rich in negatively charged aminoacids binds quite strongly on the column. The deletion caused the loss of this highly charged domain, and therefore the classical purification procedure could no longer be followed. During my diploma thesis (110) I introduced at the C-terminus of cytochrome *b* a 10X His tag to allow purification by affinity chromatography, Ni²⁺-NTA, and succeeded in obtaining a pure complex further used for characterization. At the same time, in collaboration with the group of Prof. Carola Hunte, Thomas Kleinschroth obtained crystals of the deletion mutant and could define the structure (manuscript submitted, Fig. 4).

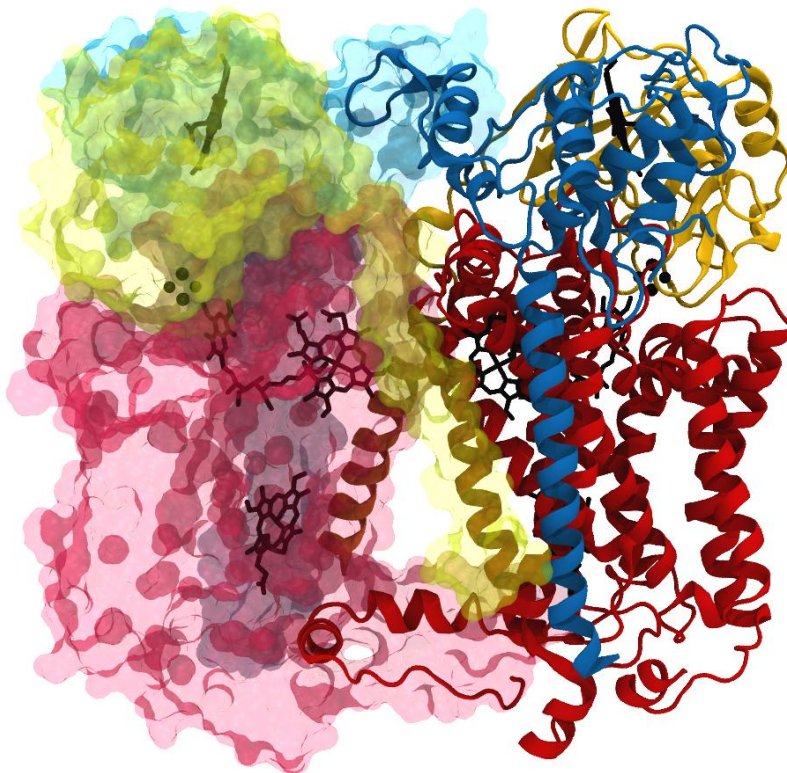


Fig. 4: Structure of the deletion mutant of the *bc₁* complex from *Paracoccus denitrificans*: the left monomer highlights the cofactors and the stigmatellin molecule used in the crystallization, the right monomer shows the three subunits in their α -traces. In yellow the ISP, in red the cytochrome *b* and in blue the cytochrome *c₁* (Kleinschroth *et al.*, manuscript submitted).

1.2.3 Interaction between the cytochrome *bc*₁ complex and the substrate

Extensive studies have been performed on the yeast complex, and the protein crystallized with both cytochrome *c* isoforms bound on the cytochrome *c*₁ (93, 94, 111). The Qcr6p subunit has 79 % acidic residues on its N-terminal part, which is also interacting with cytochrome *c*₁. In the high resolution structure with the isoform 1 about 40 residues cannot be defined, indicating that this domain has a large degree of mobility. A similar result was obtained by Iwata *et al.* (49) in the bovine enzyme: the first 14 amino acids, mainly Glu, could not be assigned on the structure. The subunit is involved in the interaction with cytochrome *c*. Several groups (96, 98, 107, 112) indicated that the loss of the acidic subunit leads to a reduction of the cytochrome *c* reductase activity. Other studies (108) indicated also the involvement of the acidic subunit in the half-of-the-sites mechanism. Interestingly, the yeast structure (111) gave no indication for interactions occurring between Qcr6p and cytochrome *c* at 1.9 Å resolution. In the bovine complex, it was speculated that the missing N-terminal domain of subunit 8 could form a negatively charged docking site for the basic cytochrome *c* (49).

Hunte *et al.* (94, 111, 113, 114) defined the binding domain and properties of isoform 1 cytochrome *c* for the yeast complex. The past literature demonstrated that the interaction between the two proteins was governed by the ionic strength. Interestingly, only two short range weak interactions, peripheral to the interaction site, are visible (Glu²³⁵ and Lys⁹², and Ala¹⁶⁴ backbone oxygen and Lys⁸⁵, respectively on the complex and cytochrome *c*), and two more were envisaged being mediated through water molecules. The residues involved in those interactions are highly conserved, suggesting in any case an important role for the ionic interaction between the two partners.

The contact area between cytochrome *c* and the *bc*₁ complex in yeast is quite hydrophobic: the interaction is mediated by non-polar residues around the heme crevices on both proteins (Ala¹⁰³ and Ala⁸⁷, Met²³³ and Arg¹⁹, Phe²³⁰ and Thr¹⁸, Ala¹⁶⁸ and Val³⁴, and Phe²³⁰ and Arg¹⁹ respectively on the *bc*₁ complex and cytochrome *c*), the latter being a cation π interaction (114). The two hemes are quite close to each other and no residue is likely to be involved in the electron transfer reaction, strongly suggesting a direct heme-to-heme electron exchange. The definition of the interaction area between the proteins lead to the hypothesis of a two-step model,

Introduction

also applied to the interaction plastocyanin-cytochrome b_6f (115) in which the two protein partners are directed to each other by long range electrostatic interactions so that the encounter happens in a directed fashion, maximizing the probability of a successful collision between them, and hydrophobic short range interactions stabilize the complex allowing electron transfer (111, 114, 116-118). The short range ionic interactions are quite weak, and no water molecule mediates the binding of cytochrome c on the enzyme, indicating the presence of a transient complex formation required for efficient electron transfer. The surface of cytochrome c is highly hydrated, possibly indicating that water molecules can have a role in destabilizing the interaction between the two proteins and help the release of cytochrome c (114). The acidic subunit is believed to regulate the interaction with cytochrome c_1 so that the two proteins come close to each other in an orientation suitable for electron transfer, therefore enhancing the probability of a successful collision.

Using a ruthenium photoexcitation technique the electron transfer between cytochrome c_1 and cytochrome c in the bovine complex was measured, and once again the two step model could be confirmed (119). The results indicated that at low ionic strength the proteins formed a complex which showed intracomplex electron transfer with very high rates. Increasing of the ionic strength makes the process diffusion-limited with the long range interactions directing the partners towards each other so that the interaction between them allows a successful electron transfer event, and a further stabilisation of the transient complex by short range hydrophobic interaction. The electron transfer rate measured was $6.0 \cdot 10^4 \text{ s}^{-1}$, three orders of magnitude slower than the rate calculated from the structural data, which was explained by the presence of the ruthenium derivative on the cytochrome c . Studies on the *Rhodobacter sphaeroides* complex revealed no intracomplex electron transfer, but a very important role of the acidic residues found on the cytochrome c_1 subunit.

Previous investigations in our group (118), analyzing soluble fragments of the interaction partners, confirmed the two step model and revealed that the acidic domain in *Paracoccus denitrificans* cytochrome c_1 is not directly involved in the electron transfer process, as no difference in the electron transfer reaction between the wild type and the domain deletion mutant was observed. It must be noted that the soluble fragments have a higher degree of diffusion and mobility in the

measurements than the membrane-bound counterpart, which more closely represent the situation found in the membrane-embedded complex. However, this should not change the way the two proteins interact, giving hints on the kind of forces coming into play. The interaction between cytochrome c_1 and its partners will be further analyzed in the section 1.2.3

1.2.4 Cytochrome bc_1 complex mechanism

The mechanism by which the bc_1 complex is able to couple electron transfer and proton pumping is widely accepted nowadays, and has become known as the “modified Q cycle”. In the beginning, Peter Mitchell proposed the first version of the Q cycle, which could not take into account all the structural informations we have now (14).

With the information gained from the high resolution crystal structures in the second half of the 1990's, several models could be postulated, all of them sharing the same idea: electron transfer is bifurcated at the Q_o site, to lead to the high-potential chain to cytochrome c_1 , and over the low-potential chain to a quinone molecule which is then fully reduced in two turnovers (120). How the bifurcation happens, what the mechanism of quinol oxidation is, how any shortcircuit reaction could be avoided and the ways by which protons are transported are a matter of debate, and several groups proposed different ideas.

1.2.4.1 The modified Q-cycle

The ubiquinol oxidation in the Q_o site funnels electrons into two separated pathways: one electron is transferred to the ISP docked in the proximal position, and after the head domain moves in direction of the cytochrome c_1 this electron reduces the c_1 heme. Cytochrome c docked to the complex receives the electron and dissociates. The second electron from the ubihydroquinone is delivered into the low potential chain, to the b_L heme, and from here to the b_H to the Q_i site, where a ubiquinone molecule is reduced in two steps to ubihydroquinone and released into the Q-pool. The oxidation of two ubihydroquinone molecules at the Q_o site releases four protons into the positive side of the membrane, whereas the reduction of one ubihydroquinone subtracts two protons from the matrix side, by this producing an electrochemical gradient (Fig. 5).

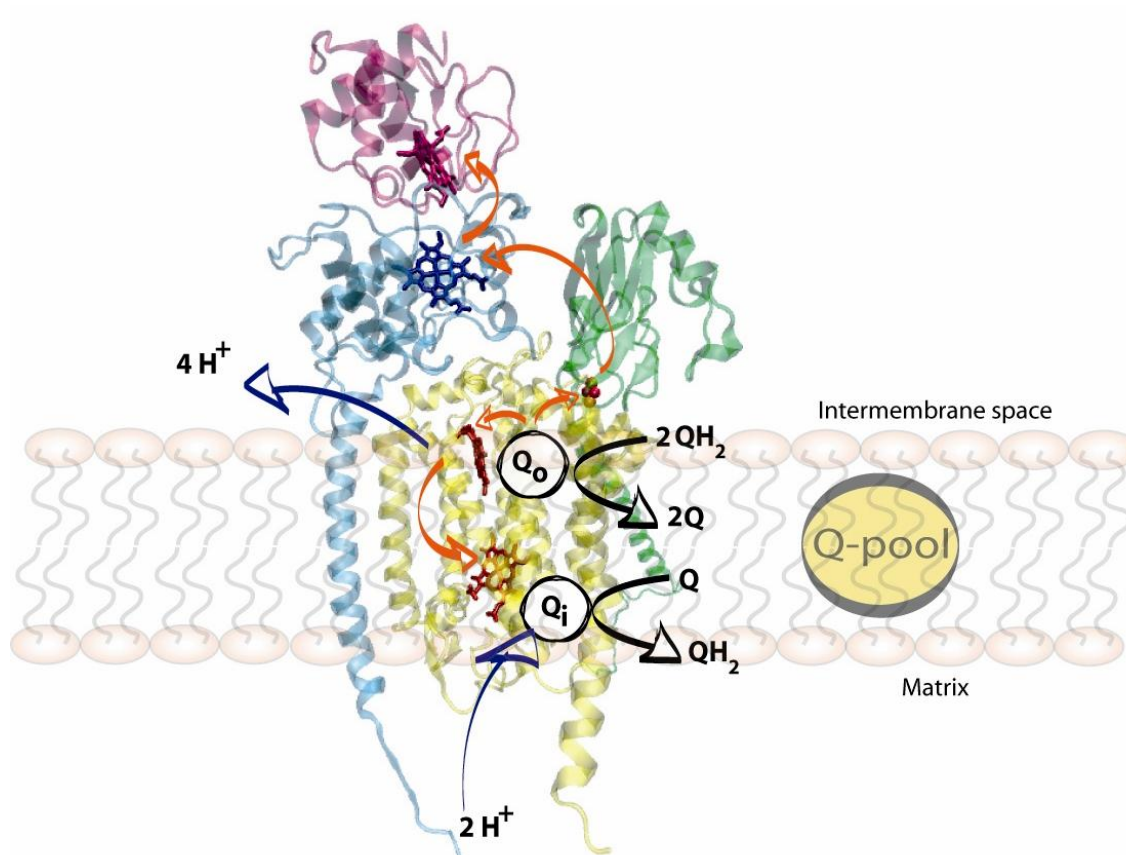


Fig. 5: Schematic representation of the Q cycle: quinol and quinone (from the Q-pool, black arrows) are oxidized and reduced respectively at the Q_o and the Q_i site. After quinol oxidation, one electron is transferred to the FeS cluster in the ISP (green), and from here to the cytochrome c_1 (blue) and to the electron acceptor, cytochrome c . The second electron from quinol oxidation goes into the low potential chain, to the two b hemes in cytochrome b (yellow) to finally reduce, in two turnovers, quinone to quinol. During the cycle, four protons are transferred to the intermembrane space, and two protons are taken up from the matrix for quinone reduction. The orange arrows indicate the electron transfer steps, while the blue ones the proton transfer across the membrane.

1.2.4.2 Quinol oxidation at the Q_o site

The electron bifurcation is essential for the coupling of proton pumping. The second electron coming from quinol does not enter the high potential chain even in the complex inhibited by antimycin (120) and it can therefore be stated that the bifurcation is obligatory for the complex.

Until now, it was not possible to obtain a structure with a quinol molecule bound at the Q_o site, since all the complexes were crystallized with inhibitors. In the native complex without inhibitors, it is not possible to identify clearly the ISP head domain since its mobility makes the electron density not unequivocal enough. An important

Introduction

information gained from the structures is the hydrogen bonding occurring between the ISP and stigmatellin which is thought to stabilise the binding of the substrate (121-123). In this case, stigmatellin would be considered as a quinone intermediate bound at the Q_o site, since the ISP is reduced when stigmatellin is bound and stays docked in the proximal position.

Some groups (83, 122, 124-126) could identify the typical EPR signal of a semiquinone in the complex, identifying it with a semiquinone bound at the Q_o site as an intermediate of the quinol oxidation. This led to the hypothesis of the so called “double occupancy” models, which proposes that the Q_o site can accommodate more than just one quinol molecule. According to Ding *et al.* (124), there are two binding sites for quinol, Q_{os} and Q_{ow} , to indicate a strong and a weak affinity for the substrate. In this way, the two quinol molecules necessary for a complete reduction of quinone at the Q_i site are already present at the Q_o site, and no exchange with the Q-pool is needed. According to Brandt (122) in the Q_{os} site, a prosthetic quinone binds, and the quinol binding at the Q_{ow} site works as the “real” substrate. The latter would be deprotonated, and a symproportion share the two electrons of the substrate with the Q_{os} bound quinone, so that two semiquinone radicals could be produced each of them serving as electron donor for the b_L (Q_{ow}) and the ISP (Q_{os}). A different vision of the double occupancy model (73) proposes that only one quinol is present in the Q_o site but able to move between the proximal and distal pockets and deliver electrons to the ISP and to the cytochrome b_L , ensuring the bifurcation of electrons.

Another mechanism proposed for the bc_1 complex is the so called “proton-gated affinity change” mechanism (56), according to which after deprotonation of the quinol the anion binds one of the liganding histidines of the ISC, and transfers the electron to the Rieske center. After being reduced, the ISP would have a high affinity for the semiquinone remaining in the proximal position and transferring the second electron obligatorily to the b_L heme. This way, the bifurcation of the electrons is maintained, and also provides an explanation why the redox potential of the ISP is higher than the one of cytochrome c_1 is given. This would guarantee that after reduction of the ISC the electron stays on the Rieske cluster instead of being transferred to the cytochrome c_1 , so that the second electron coming from the quinol is forced to enter the low potential chain.

Introduction

Recently, from observations derived from the structures and from site-directed mutagenesis, a new mechanism has been proposed, which is also supported by kinetic studies. Two residues are thought to be important in the substrate recognition: the Ile¹⁶⁶ and the Pro²⁷⁰ (bovine numbering) on cytochrome *b*, the first in the *cd1* helix and the second in the highly conserved PEWY sequence. The first one is involved in binding to each inhibitor until now seen in structures (48), and the second is hydrogen bonding the quinol in the Q_o site. In this model, the ISP head domain is constantly scanning the docking position on the cytochrome *b*, but is not fixed in any position (as observed from the structures where inhibitors are bound). Upon binding of the substrate in the Q_o site, the two residues would sense it and the *cd1* helix move, opening up the docking site for the ISP on cytochrome *b*. The Rieske protein is now able to dock on the proximal position. Almost simultaneously, the second electron enters the low-potential chain, since the reduced ISP is still in the *b* position and the electron cannot be transferred to cytochrome *c*₁. As the electron from the *b*_L is passed to the *b*_H heme, only then the ISP is free to move and deliver its electron to the cytochrome *c*₁ (70, 127).

The bifurcation is guaranteed by the fixed position the ISP has in the reduced state, and the completion of the electron transfer to the *b*_H heme closes the conformation of the *cd1* helix to set the ISP free to move towards the cytochrome *c*₁. The model is supported by the experiments of Zhu *et al.* (128) where it is shown by stopped-flow that the rate of electron transfer from quinol to the ISP and from quinol to the *b*_L is the same, and therefore the electron transfer to the high- and low-potential chain is thought to occur simultaneously, without the formation of a semiquinone anion at the Q_o site. Other groups (127, 129, 130) support with their experiments the concept that the movement of the ISP happens after electron transfer events in cytochrome *b* have taken place

The semiquinone in the Q_o site was discussed for long time. It is necessary for the double occupancy models, either with two or just one quinone in the binding pocket, and some groups (131, 132) claimed to have registered an EPR signal attributed to the Q_o site. A semiquinone has also been postulated by Link *et al.* (56), but this would be not detectable since it is electronically coupled with the ISP and therefore EPR-silent. In other studies, a highly unstable semiquinone would be transiently present in the Q_o site, but be almost immediately oxidized to quinone and therefore having a concentration too low to detect (73). A semiquinone anion is certainly

Introduction

dangerous for the complex, since it can rapidly react with oxygen and create reactive oxygen species (ROS). Therefore, a more attractive hypothesis would be a simultaneous oxidation of the substrate, to avoid side reactions. More recently, it has been shown (133, 134) that the radical signal is insensitive to the Q_o site inhibitors myxothiazol and stigmatellin, but it is sensitive to Q_i site inhibitors, such as antimycin A. This indicates that this signal was wrongly attributed before to the Q_o site. More investigations lead to the conclusion that the semiquinone is to be found at the Q_o site, and is derived from the direct reduction of the b_H heme in presence of quinol. The Q_i site has a high affinity for the quinon only when the b_H heme is reduced, otherwise quinol would preferentially bind (60). The binding of quinol to the Q_i site would then lead to the reduction of it and the stabilisation of a semiquinone at the Q_i site, possibly in both monomers according to the reduction state of the Q pool and the electron transfer across monomers over the b_H hemes. This hypothesis has very strong implications in the formulation of the half-of-the-sites reactivity, which will be explained in the section 1.2.4.3.

The presence of quinone radicals could be, as already observed, detrimental to the cell, for the possible formation of ROS, with consequent lipidic peroxidation and cell aging. It is therefore important, if any semiquinone is at all present in the complex, that it is stabilized or sealed within the reaction site. It is important in that sense that the bc_1 complex is not inhibited for example by Q_i site inhibitors, since blocking the low potential chain could possibly bring about a semiquinone in the Q_o site able to react with oxygen. Studies with mutants lacking the b_H or the b_L heme (135) indicated that the complexes where the low potential chain was modified to a certain extent could produce ROS with the same efficiency as the wild type antimycin A inhibited complex.

Forquer *et al.* (134) investigated the production of ROS by the bc_1 complex and studied the activation energy for the catalytic turnover and for the side reaction with oxygen. It resulted that the two processes have the same activation energy, not depending on the electron transfer to cytochrome c_1 or cytochrome b_L , neither on the movement of the ISP. The key process is the ISP reduction, since the activation energy increases by diminishing the redox potential of the Rieske cluster. These results indicate that both the catalytic cycle and the superoxide production share the same activation energy and that most likely a semiquinone is responsible for the electron transfer to oxygen. Such a finding is in contrast to models supporting a

Introduction

simultaneous quinol oxidation. In 2007, Cape *et al.* (131) applied the freeze-quench EPR spectroscopy to the antimycin inhibited bc_1 complex finding the presence of a semiquinone anion at the Q_o site which is sensitive to class P inhibitors and is likely to be responsible for ROS production. They propose that the redox properties of the couple SQ/Q controls the rate of ROS production, and that the structure of the Q_o site may be involved since it can probably act as a barrier limiting oxygen permeability in the Q_o site.

In 2004 Osyczka *et al.* (136) proposed the double gated model, by which the bifurcation of electrons is ensured and side reactions avoided. The quinol oxidation would only take place if both ISP and heme b_L are oxidized, being regulated by the pattern of hydrogen bonding around the Rieske cluster and the b_L heme in the oxidized and the reduced state. This model does not exclude the presence of more than one quinol in the Q_o site participating to the turnover.

Also Rich *et al.* (137) in 2004 proposed a mechanism which emphasises the hydrogen bonding pattern of the His and the Glu residues involved in the binding of the quinol at the Q_o site. Only if the hydrogen bonding pattern is correct, then the quinol oxidation can take place in an “all-or-nothing” fashion, in which the two electrons are transferred simultaneously to ISP and cytochrome b .

Mulkiđjanan (138) proposed recently the “activated Q-cycle”, in which one Q_i site contains a stabilised semiquinone and the b_H heme in the other monomer is reduced. Starting from this “activated state”, a quinol enters the Q_o site and makes hydrogen bond with the His¹⁶¹ on the ISP and the Glu²⁷² (bovine numbering) on cytochrome b . After the first coupled electron and proton transfer to the ISC, a semiquinone anion is present at the Q_o site, and the ISP stays docked in the proximal position. Thereafter, the second electron is transferred to the oxidised b_L heme which then reduces the semiquinone to quinol in just one catalytic turnover, without the need of any exchange with the Q-pool. In such a model, no interaction between the bc_1 monomers is expected, in terms of Q_o - Q_i site interaction as postulated by the half-of-the-sites mechanism.

The bc_1 complex establishes a proton gradient across the membrane. The proton translocation activity originates from the release of four protons from quinol oxidation on the positive side of the membrane, and the uptake of two protons on the negative side for quinone reduction. The quinol substrate is hydrogen bonded by the His¹⁶¹,

Introduction

one of the cluster ligands, and the Glu²⁷² of the conserved PEWY sequence (59, 66). The His¹⁶¹ shares the hydrogen bond with quinol and as the substrate has been oxidized, the ISP moves in direction of cytochrome c_1 releasing the proton. The second proton from quinol is transferred to the Glu²⁷² after the second electron has been passed further to the b_L heme. Then, the Glu side chain rotates 170° to make a hydrogen bond with a water molecule, itself in hydrogen bond distance with the propionate group of heme b_L . The proton release to the aqueous solvent is mediated by a chain of hydrogen bonds of water molecules stabilised by cytochrome b residues Arg⁷⁹, Asn²⁵⁶, Glu⁶⁶ and Arg⁷⁰ (yeast numbering).

At the Q_i site, two protons are taken up from the matrix side for the reduction of quinone to quinol. In yeast, two different pathways have been shown to be important for the proton uptake: the E/R pathway and the CL/K pathway. The yeast substrate is UQ6, which is stabilised at the Q_i site by the residue Asp²²⁹ and by a water molecule hydrogen bonded to the His²⁰². On the Asp²²⁹ side is present the CL/K pathway, where the water molecules in the quinone binding pocket are in hydrogen bond with the Lys²²⁸, connecting them with the cardiolipin molecule present on the surface of the protein (59, 94, 139, 140). Upon reduction of the UQ6, a proton would be taken from the Lys²²⁸, which, through the hydrogen bond network, has access to the aqueous phase and can replenish the proton. In this way, the cardiolipin is not only an important lipid for the structural integrity of the Q_i site but also plays a role in the protonation pathway for UQ6.

The second pathway is closer to the residue His²⁰². In this case, an important Arg residue (Arg²¹⁸ in yeast) is connected by hydrogen bond with a water molecule and involved in a network of interaction with several water molecules and neighbouring residues. At the exit of this array, a hydrophilic cavity formed by Qcr 7 and Qcr 8 in yeast opens to the solvent, allowing replenishment of the protons when the Arg²¹⁸ donates a proton to the UQ6 (59).

1.2.4.3 *Half-of-the-sites mechanism*

An important observation obtained from the structures until now available is the dimeric structure of the bc_1 complex. The ISP structurally belonging to one monomer delivers electrons to the cytochrome c_1 of the second monomer (50). Interestingly, the distance between the b_L hemes is short, comparable to the b_L - b_H distance in a single monomer, so short to allow inter-monomer electron transfer and electron

Introduction

equilibration between monomers. This feature is conserved in all structures solved so far, and it has been discussed at length whether or not the two monomers are both involved in the catalytic cycle of the enzyme. The work of Trumpower and Covian opened the way for the identification of the so called half-of-the-sites reactivity by using stopped-flow measurements and computer simulations. Their work provided evidence for the electron equilibration and for inter-monomer communication able to regulate the activity of the complex and offer a base to prevent detrimental electron leakage eventually capable of forming ROS.

To avoid deleterious electron transfer to oxygen, control on the mechanism of quinol oxidation is necessary. With the bc_1 complex being a dimer, it is theoretically possible to oxidize two quinol molecules at the same time. This could eventually overload the enzyme with electrons, as is indicated by ischemia studies where the physiological membrane potential in the mitochondrion and the reduction of the Q-pool are altered (60, 141). Kinetic studies with several bc_1 inhibitors indicated non-linear inhibition curves for the binding of stigmatellin to the Q_o site. Only one stigmatellin molecule (Pf inhibitor) was necessary per dimer in order to completely inhibit the enzyme (142) and the binding of the inhibitor to the complex was found to be anti-cooperative. On the other hand, myxothiazol (a class I Pm inhibitor) showed a linear inhibition curve, binding tightly to the complex in a homogeneous way in respect to the two monomers. The same results were confirmed not only on the eukaryotic but also on the bacterial complex (143), hint of a conserved behaviour dependent on intrinsic protein properties. Covian *et al.* (62, 143-145) explained the results by proposing a mechanism by which the two monomers could communicate and the Q_o site of the inhibited monomer would, by a conformational change, block the activity of the second one. From the stigmatellin titration curves it was clear that the inhibitor could bind to the first monomer in a fast phase, followed by a slow phase independent on the inhibitor concentration, during which the one inhibited monomer could undergo the conformational change needed to impede the quinol oxidation on the other monomer. Moreover, in presence of an inhibited Q_o site, only one Q_i site was able to bind antimycin or the substrate quinone, therefore regulating the occupancy of the quinone reduction site. The explanation given involved the position of head domain of the ISP: in the situation where the two ISP are docked on cytochrome *b*, virtually ready to oxidize quinol, only one Q_i site is able to bind semiquinone. When semiquinone is bound to both Q_i sites just one ISP head

Introduction

domain is able to react with the substrate. Stigmatellin was considered a good mimic of the quinol molecule bound at the Q_o site, since it resembles both the binding and the properties of the substrate right before oxidation, in a situation where the ISP is blocked on the b conformation. How exactly the conformational change should cross the monomers to get to the second active quinol oxidation site is not yet clear, but the authors suggested that the ef loop and the helices D and E could be involved in sensing the position of the ISP and, by the N-terminal helix at the cytochrome b , transfer the blocking to the other monomer (62). Myxothiazol does not directly interact with the ISP and its binding is insensitive to the ISP position, and therefore does not show the same behaviour as stigmatellin, giving linear titration curves, expected for the independent inhibitor binding in the two monomers.

The half-of-the-sites reactivity can be explained also studying the binding properties of quinol and quinone at the Q_i site. In presence of Q_o site inhibitors, the b_H hemes can be reduced from the quinol at the Q_i site. Under these conditions is possible to observe an EPR signal, sensitive to antimycin and other class II inhibitors, which can be identified with a semiquinone at the Q_i site. For the first time it was shown that the EPR signal was not localized at the Q_o site, possible intermediate of the Q-cycle, as initially thought (124, 146) but a semiquinone at the Q_i site originating from the backreaction of the b_H hemes from quinol (133, 144, 147). Fig. 6 shows the proposed mechanism which regulates the Q_i site occupancy. Covian *et al.* measured the affinity of quinol and quinone for the Q_i site and concluded that quinol is binding at the Q_i site preferentially when the b_H heme is oxidized, and quinone when it is reduced. This redox specificity is essential to ensure that quinol would leave the Q_i site each time the heme b_H is reduced and ready to reduce a quinone molecule (60). From the triphasic cytochrome b reduction kinetics, Covian *et al.* (145, 147) identified from the the basis for semiquinone stabilisation at the Q_i site: the b_H heme can interact with quinol and be reduced when its concentration is higher than that of quinone; even a few quinone molecules are enough to accept the electrons from the turnover of the bc_1 complex, such avoiding that electrons could accumulate in the high- and low-potential chains; once the turnover has produced again enough quinol molecules, they can as well interact with both the Q_o and Q_i site and be used in a normal turnover or as reductant for the b_H heme. This way, the dimeric structure can use the electron equilibration between monomers in order to have available as many oxidized cofactors as possible and avoid the formation of ROS.

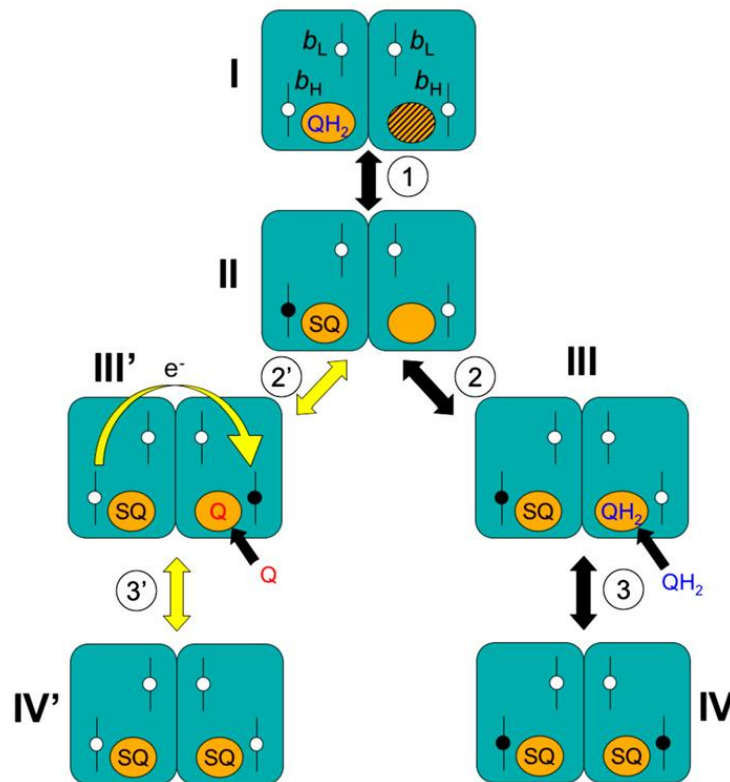


Fig. 6: Semiquinone stabilisation at the Q_i site. The blue rectangles represent the cytochrome b subunits, and only the Q_i site is shown, for simplicity. The reduction of a b -type heme is shown with a black circle, the oxidized form with a white circle. Semiquinone: SQ; Q: quinone; QH_2 : quinol (62). After binding of one quinol molecule to the Q_i site, a semiquinone is formed and the b_H heme reduced. At this point, several possibilities are open: the electron can be equilibrated to the other monomer and the reduced Q_i site binds a quinone which is then reduced to semiquinone. The b_H hemes in both monomers are oxidized (intermediate III' and IV'). Alternatively, another quinol could bind to the free Q_i site and give a semiquinone. Both monomers have finally a reduced b_H heme and a stabilized semiquinone at the Q_i site (intermediates III and IV).

Necessary for the semiquinone stabilisation at center N is the inter-monomer electron transfer across the b_L hemes. In the yeast complex (62) the edge-to-edge distance between the two b_L hemes is 13.8 Å, similar to the 12.4 between the b_L and b_H heme in each monomer. Intradimeric electron equilibration gains particular importance in situations where the b_H hemes are pre-reduced by reverse electron transfer at the Q_i site, or the low potential chain is inhibited. In the latter case, after two turnovers, cytochrome b is fully reduced but the ISP can still oxidize quinol and reduce cytochrome c_1 . In the Q_o site a semiquinone anion would remain, eventually responsible of side reactions with oxygen, as indicated in the study of Cape *et*

Introduction

al.(131). It is still unclear whether or not a semiquinone is a real intermediate of the turnover, but considering the damages derivating from an eventual electron leakage, the electron equilibration between monomers may be of critical importance.

When antimycin is added in substoichiometric amounts in respect to the bc_1 complex, a fraction of dimers will bind only one antimycin molecule. In such a scenario, one b_H heme is reducible directly by quinol at the Q_i site, the second b_H heme in the inhibited monomer is only available in case of inter-monomer electron equilibration. The binding of antimycin (which neither modifies the redox potential of the b_H hemes, nor can it dissociate easily from the binding site, being a tightly bound inhibitor) can be followed by the red shift in the redox spectrum of cytochrome b , and by this experiment one of the proofs of the b_L - b_L electron transport was obtained (62). Covian *et al.* (144, 148) measured pre-steady-state kinetics of cytochrome c_1 and b reduction in the presence of antimycin, showing that one cytochrome c and at the same time two cytochromes b_H per dimer were reduced by decylubiquinol. If the two monomers were both at the same time able to oxidize quinol, two cytochromes c_1 and two b_H would have been expected to be reduced after a single turnover. Simulations presented in the work could explain the reduction kinetics only if a mechanism was operating by which the two monomers work one at a given time and allow for inter-monomer electron transfer. At the same time, the crystal structure of the bc_1 complex from yeast complexed with the electron acceptor, cytochrome c , was published (94) interestingly showing only one cytochrome c bound to the dimer and ubiquinone in only one monomer, supporting the half-of-the-site mechanism.

Taken together all present data favour a model as presented in Fig. 7, which summarizes the inhibitor studies, the relationship between the Q_i site occupancy, the Q_i site semiquinone stabilisation and the inter-monomer electron transport.

Introduction

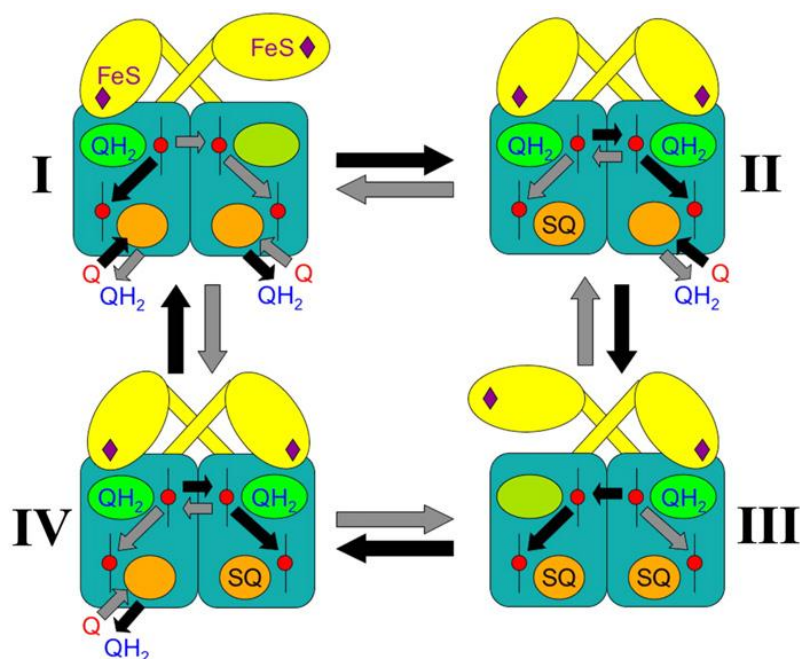


Fig. 7: Scheme of the half-of-the-sites mechanism. The blue rectangles represent cytochrome *b*, with the Q_o site as a green oval and the Q_i site as an orange oval. In yellow, the ISP. This model shows that the occupancy of the Q_i site regulates the activity of the Q_o site (62).

The semiquinone is simulated by antimycin in the experiments presented until now. In the case of a vacant Q_i site, only one ISP domain is able to dock on cytochrome *b* and oxidize quinol. One electron is transferred to the high-potential chain, and the second to the low-potential chain. At the b_L level, the electron has an approximately equal probability to be transferred to the b_H of the same monomer or to the other by inter-monomer electron transfer. The semiquinone stabilisation at the Q_i site (Fig. 6, intermediate IV) represents a state of the enzyme with the two b_L hemes, the two b_H hemes and two semiquinone ready to accept an electron from the catalysis at the Q_o site, preventing efficiently any form of electron leakage and oxygen side reaction. In the intermediates II and IV, the catalytically favourable position for the ISP destabilizes the interaction with a semiquinone at the Q_i site in the other monomer, and the half-of-the-sites mechanism makes sure that electrons are quickly delivered to quinone, avoiding them to accumulate in the complex. Since electrons have the same probability to be distributed between the two monomers, randomly in a given time span the two monomers will swing between the double active form (intermediates II and IV) and the single active form (intermediates I and III), statistically undergoing each the same number of turnovers.

Intermediates II and IV are simulated by antimycin titration curves (62, 148), where a stimulation of the initial rates, instead of an inhibition, can be observed in presence of a substoichiometric amount of antimycin. The inhibitor mimics the presence of a semiquinone bound at the Q_i site: in the intermediates where just one monomer binds antimycin, both Rieske head domains are ready to oxidize quinol, so that the stimulation observed is explained as the sum of the activity of the free monomers and twice as much the activity of the inhibitor binding monomers (148). If no inhibitor is bound at the Q_i site, or no semiquinone is stabilized there, only one monomer accounts for the activity. For a more detailed discussion on the implication of the antimycin titration curves, see the section 3.1.1.6.

1.3 Cytochrome c_{552}

Cytochrome c_{552} is the physiological electron acceptor for the bc_1 complex in *P. denitrificans*. It shuttles electrons to the aa_3 oxidase and is only one among several cytochrome c molecules involved in electron transfer in the different metabolic pathways of this organism. The cytochrome c_{552} can be divided into three domains (118, 149, 150): an N-terminal transmembrane helix, anchoring it to the cytoplasmatic membrane, a highly negatively charged linker region, and a C-terminal class I cytochrome domain. It carries a covalently bound c -type heme, liganded by a His and a Met.

Previously the crystal structure of a soluble fragment containing only the cytochrome c binding domain has been solved (149) and recently a new structure could be achieved, containing the linker and the C-terminal domain (150). A loop region (residues 1-12) could be identified, followed by the residues 13-31 which lacked any electron density. A small helix formed by the residues 34-41 precedes the heme binding domain. From the new data, it was concluded that the head domain of cytochrome c_{552} is flexible to interact with the bc_1 complex on the one side and with the cytochrome aa_3 oxidase on the other. The region not visible in the electron density map indeed indicates a high degree of mobility, which could be very important since cytochrome c_{552} is membrane bound and not able to diffuse as does the mitochondrial cytochrome c .

The mobile domain is thus of relevance in the light of a supercomplex, as already published (151): in this case, the movements of the C-terminal domain would allow a rapid and efficient electron transfer to the oxidase without any lateral diffusion.

1.4 Aim of this work

The acidic domain deletion mutant of the bc_1 complex of *P. denitrificans* is investigated, in terms of structural and kinetic properties. During my previous work, I achieved cloning and expression of the protein, and purified it by affinity chromatography. Due to some problems encountered during purification (110), I plan to modify and optimise elution condition and to characterise the complex by spectral and kinetic analysis.

By using flash photolysis kinetics, I investigate the role of the acidic domain in cytochrome c_1 in the interaction with cytochrome c_{552} , the physiological electron acceptor. In fact, the domain resembles the small acidic subunit in the eukaryotic complex, known to facilitate the interaction with the substrate (114). A similar analysis was already performed by Janzon *et al.* (118) by using soluble fragments of the reaction partner. The measurements with whole complexes reflect more closely the situation in membranes and offer the possibility to verify the kind of interaction between bc_1 complex and cytochrome c_{552} . Until now, the interaction mechanism has been widely described in yeast, and previous experiments in *P. denitrificans* have shown similarities with that system.

With the use of stopped-flow spectroscopy, the internal electron transfer pathway will be studied to define the rate of cytochrome c_1 reduction from ascorbate and the role that the ISP plays in the complex. In particular, it should be analyzed how electrons can be transferred from the Rieske cluster to cytochrome c_1 , the latter having a lower redox potential.

The second part of my work consists in structure-function analysis and internal regulation in the bc_1 complex from *P. denitrificans*. By using a different experimental setup, flash photolysis kinetics represent a powerful tool to measure internal electron transfer and investigate inhibitor effects on specific reactions in the catalytic cycle. Class P inhibitors bind in different positions at the Q_o site and lead to inhibition of electron transfer by using different mechanisms. In this work, I analyse the position of the head domain of the ISP in presence of different molecules at the Q_o site, either quinol or inhibitors, to study the mechanism which regulates the ISP movement allowing fast electron transfer and catalysis.

Finally, I plan the construction a heterodimeric bc_1 complex in order to prove the aforementioned internal regulation system (half-of-the-sites mechanism). This

Introduction

experiment will be carried out with the deletion mutant of the complex, since it has been shown to have a dimeric structure, in contrast with the wild type protein (152). One of the two monomers in the complex carries an inactivating mutation in the Q_o site (153, 154), which does not allow quinol oxidation. The other monomer is fully active. A sequential purification due to the differential tagging at the genetic level of the two halves will be used to purify the complex. The resulting heterodimer, homologously expressed in *Paracoccus denitrificans*, shall be analysed by time resolved stopped slow experiments to demonstrate the regulatory function of the dimeric structure.

2 Materials and methods

2.1 Materials

2.1.1 Chemicals

All the chemicals, also the ones not explicitly included in this list, were purchased in *p.a.* quality from different companies (AppliChem, Merck, Roche, Roth or Sigma-Aldrich). Water was desalted with an instrument from the company Seral for biochemical application, and with a PRO 90 CN apparatus from the same company for molecular biology experiments. In the second case, water has always been autoclaved.

Acrylamide, Bisacrylamide	Roth
Antimycin A	Sigma-Aldrich
Agar-agar	Roth
Agarose	peqlab
Ammoniumpersulfate (APS)	Roth
Ampicillin-sodium salt	Applichem
Avidin	Gebro
Bactotryptone	Becton-Dickinson
Succinic acid	Fluka
Bromo phenol blue	Sigma-Aldrich
5-bromo-4-chloro-3-indolylphosphate (BCIP)	Sigma-Aldrich
Coomassie brilliant blue R250	Roth
Decylubiquinone	Sigma-Aldrich
Desoxyribonucleosidtriphosphate (dNTPs)	Fermentas
Dimethylsulfoxid (DMSO)	Merck
Ethidium bromide	Gibco BRL
Folin-ciocalteau	Merck
Yeast extract	Gibco BRL
Histidine	Roth
Imidazole	Applichem
Isopropyl- β -D-thiogalactopyranoside (IPTG)	Fermentas
Kanamycinsulfate	Roth
β -Mercaptoethanol	Sigma-Aldrich

Materials and methods

Potassium ferricyanide	Fluka
Sodium ascorbate	Fluka
Sodium dithionite	Sigma-Aldrich
Sodium dodecylsulfate (SDS)	Roth
n-Dodecyl- β -D-maltoside (DDM)	Biomol/Roth
Bovine serum albumine (BSA)	Roth
Nicotinamidadenindinucleotide (NADH)	AppliChem
Nitro blue tetrazolium (NBT)	Sigma-Aldrich
2-(<i>N</i> -morpholino)ethanesulfonic acid (MES)	AppliChem
3-(<i>N</i> -morpholino)propanesulfonic acid (MOPS)	Roth
N,N,N',N'-Tetramethylethylenediamine (TEMED)	Roth
Pefabloc SC	Biomol
Ponceau S	Merck
Rifampicin	Fluka
Stigmatellin	Sigma-Aldrich
Streptomycinsulfate	Applichem
3,3',5,5'-Tetramethylbenzidine (TMBZ)	Sigma-Aldrich

2.1.2 Proteins

For the enzymes needed in molecular biology applications, were used buffer delivered from the company. Enzymes, antibodies and cytochrome *c* from horse heart were kept at -20 °C, all other proteins at -80 °C.

2.1.2.1 Enzymes for molecular biology

Calf intestinal alkaline phosphatase (CIAP)	NEB
Phusion-DNA Polymerase	Finnzymes
Ribonuclease A (RNAse)	Roche
T4-DNA-Ligase	Fermentas
T4-Polynucleotide kinase (PNK)	Fermentas
Restriction endonucleases	NEB, Fermentas

Materials and methods

2.1.2.2 Antibodies

All antibodies for the respiratory chain of <i>Paracoccus denitrificans</i>	Prof. Ludwig
Penta-His-Antibody	Novagen
Protein A-Alkaline Phosphatase	Sigma-Aldrich
Goat-anti-Mouse IgG / Alkaline Phosphatase-Conjugate	Sigma-Aldrich
Streptavidin / Protein A- Alkaline Phosphatase -Conjugate	Sigma-Aldrich

2.1.2.3 Varia

Cytochrome <i>c</i> from horse heart	Sigma-Aldrich
Lysozyme	Biomol
Cytochrome <i>c</i> ₅₅₂ from <i>P. denitrificans</i>	Prof. Ludwig
Cytochrome <i>c</i> ₅₅₂ N23C from <i>P. denitrificans</i>	Prof. Ludwig
Isoform 1 cytochrome <i>c</i> from <i>S. cerevisiae</i>	Prof. Millett, Arkansas

2.1.3 Kits

Gel extraction/PCR purification	Zymoclean
---------------------------------	-----------

2.1.4 Markers

λ Phage DNA cut with EcoRI/HindIII	Produced in the lab
Unstained Protein Molecular Weight Marker	Fermentas
PageRuler Protein Ladder	Fermentas

2.1.5 Chromatography materials

Chromatography materials were washed with 20 % ethanol at 4 °C for long time storage and with 1 mM sodium azide at 4 °C for short time storage.

Diethylaminoethyl-(DEAE)-Sepharose CL-6B	GE Healthcare
Ni ²⁺ -NTA-Agarose Superflow	Qiagen
StrepTactin-Sepharose	Novagen
Sephadex G-25	GE Healthcare

Materials and methods

2.1.6 Instruments

Analytical balance	Basic Sartorius
Air-bath shaker	New Brunswick Scientific
Autoclave	Bioklav Schütt
Centrifuges Sorvall RC 5B, RC 36	Dupont
Concentrators	Millipore, Sartorius
Dialysis tubes 4-6 kDa	Roth
Drying cupboard	Memmert
Electrophoresis-Camera Powershot G5	Canon
FPLC Pharmacia LKB	GE Healthcare
Freezer	Heraeus
Ice machine	Ziegra
Incubator	Heraeus
Laser flash	Phase R model DL 1400 flash lamp-pumped dye laser
Manton-Gaulin-Homogenisator	APV Schröder
Microwave	Hitachi
Nitrocellulose membrane BA 85	Whatman
pH-Meter	pH340i WTW
Pipettes	Eppendorf, Gilson
Power supplier Powerpac 300	Biorad
Protein electrophoresis Mini Protean II	BIORAD
Shaker	New Brunswick Scientific
Spectrophotometer U-3000	Hitachi
Sterile bench	Heraeus
Stopped Flow	Applied Photophysics apparatus, Leatherhead, UK
Time resolved Stopped Flow	OLIS Rapid Scanning Monochromator
Table centrifuge Biofuge 13	Heraeus
Thermocycler	Biorad
Thermomixer 5436	Eppendorf
Ultracentrifuge L-70	Beckman
Ultrasound generator Sonifier 250	Branson

Materials and methods

Ultra-Turrax-Homogenisator T25	IKA Labortechnik
UV-Transilluminator	UVP
Vortex Reax 2000	Heidolph
Water bath	Bachofer

2.1.7 Softwares and databanks

2.1.7.1 Softwares

Adobe Illustrator 9.0	Adobe
Adobe Photoshop 6.0	Adobe
Visual Molecular Dynamics (VMD) Version 1.8.6	http://www.ks.uiuc.edu/Research/vmd/ (155)
Clone Manager	Scientific & Educational Software
Origin 8.0	OriginLabCorporation

2.1.7.2 Databanks

NCBI Entrez Pubmed	http://www.ncbi.nlm.nih.gov/entrez/query.fcgi?db=PubMed
Expasy Swissprot	http://www.expasy.org/sprot/
Kazusa Codon-usage Databank	http://www.kazusa.or.jp/codon/
Protein Data Bank (PDB)	http://www.rcsb.org/pdb/home/home.do
Elektronische Zeitschriften Bibliothek	http://rzblx1.uni-regensburg.de/ezeit/fl.phtml?bibid=UBFM

2.1.8 Plasmids

2.1.8.1 Available plasmids

Plasmids	Description	Resistance	Origin
pBluescript	cloning vector, f1 ori, lacZ α	Amp	Stratagene (Heidelberg)
pRI2	broad host range vector, pBBR1MCS derivative, expression vector	Sm, Cm	(156)
pRI2 (436)	<i>fbc</i> operon HindIII/SacI in pRI2, expression vector for wt complex III	Sm, Cm	M. Korn (Institute)
pSL1180	Cloning vector, superlinker, pMB1 ori, M13 ori, lacZ α	Amp	Pharmazia
pUC18	Cloning vector, lacZ α	Amp	(157)
pEG400	incP, broad host range-vector, expression vector	Sm	(109)
pBBR1-MCS5	broad host range-vector, expression vector	Gm	(158)
pMC1	expression vector for the <i>fbc</i> operon with N-terminal <i>fbcC</i> deletion and C-terminal <i>fbcB</i> 10x His tag	Sm, Cm	(110)
pTK33	pRI2 (436) derivative (HindIII/SacI) + <i>fbcB</i> C-terminal 10x His tagged <i>fbc</i> operon	Sm, Cm	(152)
pTK44	pTK33 derivative (Eco147I+Pfl23II) with a Y147S mutation in <i>fbcB</i> with a Eco24I restriction site) + <i>fbcB</i> C-terminal 10x His tag	Sm, Cm	(152)
pTK56	pMC1 derivative, + <i>fbc B</i> C-terminal Strep tag,	Gm	Kleinschroth (institute)
pTSP1	pAlter with <i>fbc</i> operon from <i>P. denitrificans</i> with S157A mutation in <i>fbcF</i>	Amp, Tet	(85)
pTSP2	pAlter with <i>fbc</i> operon from <i>P. denitrificans</i> with Y159F mutation in <i>fbcF</i>	Amp, Tet	(85)
pEC86	Heme maturation plasmid, pACYC184, <i>ccm</i> ABCDEFGH	Cm	(159)
pBR2	<i>P. denitrificans</i> <i>cycM</i> (cyt. c_{552} functional domain) NcoI/HindIII in pET22b(+)	Amp	(160)

Materials and methods

2.1.8.2 Plasmids produced in this work

Plasmid	Description	Resistance
pMC8	pMC1 with Pfl23II/SacI fragment from pTSP2 contains the mutation Y159F in the <i>fbcF</i> gene	Sm, Cm
pMC9	pTK33 with Pfl23II/SacI fragment from pTSP1 contains the mutation S157A in the <i>fbcF</i> gene	Sm, Cm
pMC10	pTK33 with Pfl23II/SacI fragment from pTSP2 contains the mutation Y159F in the <i>fbcF</i> gene	Sm, Cm
pMC11	pMC1 with Pfl23II/SacI fragment from pTSP1 contains the mutation S157A in the <i>fbcF</i> gene	Sm, Cm
pMC12 a	<i>fbc</i> operon from pMC1 HindIII/SacI in pUC18	Amp
pMC12 b	pMC12 a with Pfl23II/SacI from pTK44 in pUC18 contains the Y147S mutation in <i>fbcB</i>	Amp
pMC12	HindIII/SacI fragment from pMC12 b in pEG400 contains the <i>fbc</i> operon with N-terminal cytochrome <i>c</i> ₁ domain deletion and Y147S mutation in <i>fbcB</i>	Sm
pMC13	HindIII/SacI fragment from pTK33 in pUC18 Contains the 10X His tagged <i>fbc</i> operon	Amp
pMC14	<i>fbc</i> operon from pMC12 a with a S157C mutation in <i>fbcF</i>	Amp
pMC15	<i>fbc</i> operon from pMC13 a with a S157C mutation in <i>fbcF</i>	Amp
pMC16	HindIII/SacI fragment from pMC14 in pRI2 contains the <i>fbc</i> operon with N-terminal <i>fbcC</i> domain deletion and S157C mutation in <i>fbcF</i>	Sm
pMC17	Pfl23II/SacI fragment from pMC14 in pTK33 contains the <i>fbc</i> operon with C-terminal <i>fbcB</i> 10X His tag and S157C mutation in <i>fbcF</i>	Sm
pMC18	Pfl23II/SacI fragment from pMC14 in pRI2(436) contains the <i>fbc</i> operon from <i>P. denitrificans</i> with S157C mutation in <i>fbcF</i>	Sm

2.1.9 Microorganisms

2.1.9.1 *Escherichia coli* K12

Strain	Genetic markers	Origin
DH5 α	SupE44, Δ lacU169 (Φ 80lacZ Δ M15), hsdR17, recA1, endA1, gyrA96, thi-1, relA1	(161-163)
pMC8	DH5 α , transformed with pMC8	this thesis
pMC9	DH5 α transformed with pMC9	this thesis
pMC10	DH5 α transformed with pMC10	this thesis
pMC11	DH5 α transformed with pMC11	this thesis
pMC12 a	DH5 α transformed with pMC12 a	this thesis
pMC12 b	DH5 α transformed with pMC12 b	this thesis
pMC12	DH5 α transformed with pMC12	this thesis
pMC13	DH5 α transformed with pMC13	this thesis
pMC14	DH5 α transformed with pMC14	this thesis
pMC15	DH5 α transformed with pMC15	this thesis
pMC16	DH5 α transformed with pMC16	this thesis
pMC17	DH5 α transformed with pMC17	this thesis
pMC18	DH5 α transformed with pMC18	this thesis

2.1.9.2 *Paracoccus denitrificans*

Strain	Genetic marker	Origin
Pd1222	Spc ^R , Rif ^R , „enhanced mating frequency“	(164)
MK6	Pd1222 derivative chromosomal deletion mutant for the <i>fbc</i> -Operon Δ (<i>fbc</i> ::Km ^R), Spc ^R , Rif ^R	(85)
MC1	MK6 derivative contains pMC1	(110)
pMC8	MK6 derivative contains pMC8	this thesis
pMC9	MK6 derivative contains pMC9	this thesis
pMC10	MK6 derivative contains pMC10	this thesis
pMC11	MK6 derivative contains pMC11	this thesis
pMC12	MK6 derivative contains pMC12	this thesis
pMC16	MK6 derivative contains pMC16	this thesis
pMC17	MK6 derivative contains pMC17	this thesis
pMC18	MK6 derivative contains pMC18	this thesis

Materials and methods

2.1.10 Oligonucleotides

Oligonucleotides for PCR applications were purchased from Biospring.

Oligonucleotide	Sequence
fS157C_III	5'- CCGTGCCACGGGTGCCATTACGACACC -3'
fS157C_III_reverse	5'- GCAGAACCAGCCGCCGAAATCGC -3'
ende_cytb_rev_seq	5'- GCAACAGCCGTGAGCGAT -3'
Seq_cytb_mitte	5'- CCCTTCGTCATCGCGGCG -3'
Seq_ISP_mutagenese	5'- ATTTGATCGCTAGAACCGCG -3'

2.1.11 Solutions

All the solutions were prepared with the described water. Solutions for protein purification were sterile filtered. All the solution for molecular biology application were sterile filtered or autoclaved.

DNA Agarose gel electrophoresis

DNA sample buffer	0.02 % bromo phenol blue, 30 mM EDTA, 5 % glycerol in TBE buffer
TBE buffer (10x)	1 M Tris, 1 M boric acid, 25 mM EDTA, pH 8
Ethidium bromide stock solution	10 mg/ml ethidium bromide in H ₂ O

Activity measurements

<i>bc</i> ₁ dilution buffer	50 mM MOPS/NaOH pH 7.5, 100 mM NaCl, 0.04 % DDM, 5 % glycerol, 0.05 % BSA
<i>bc</i> ₁ measurement buffer	50 mM MOPS/NaOH pH 7.5, 100 mM NaCl, 0.04 % DDM, 1 mM EDTA, 1 mM KCN

Materials and methods

Kinetic measurements

Stopped Flow	50 mM MOPS/NaOH pH 7.5, 0.04 % DDM, 1 mM EDTA, 1 mM KCN
Time resolved Stopped Flow	100 mM Tris-HCl, pH 8.0, 2 mM sodium azide, 0.2 mM EDTA, 0.05% dodecylmaltoside
Laser flash Ru _Z -H39C-Cc	20 mM Tris/HCl pH 8.0, 0.02% DDM, 2 mM sodium ascorbate, 2 μM N, N, N',N' tetramethylphenylendiamine (TMPD)
Laser flash Ru _Z -N23C-C _{552F}	10 mM Tris/HCl pH 8.0, 0.02% DDM, 2 mM sodium ascorbate, 2 μM N, N, N',N' tetramethylphenylendiamine (TMPD)

Purification bc₁ complex from *P. denitrificans* (ion exchange column)

Solubilisation buffer (2x)	100 mM MES/NaOH pH 6, 600 mM saccharose, 2,4 M NaCl
Equilibration buffer	50 mM MES/NaOH pH 6, 350 mM NaCl
Low salt buffer	50 mM MES/NaOH pH 6, 350 mM NaCl, 0.02 %DDM
High salt buffer	50 mM MES/NaOH pH 6, 600 mM NaCl, 0.02 % DDM
Wash buffer	50 mM MES/NaOH pH 6, 1 M NaCl

Purification bc₁ complex from *P. denitrificans* (affinity chromatography, Ni²⁺-NTA with imidazole)

Solubilisation buffer (2x)	100 mM NaPi pH 8, 600 mM saccharose, 2.4 M NaCl, 20 mM imidazole
Equilibration buffer	50 mM NaPi pH 8, 300 mM NaCl
Low imidazole buffer	50 mM NaPi pH 8, 300 mM NaCl, 0.02 % DDM, 10 mM imidazole
High imidazole buffer	50 mM NaPi pH 8, 300 mM NaCl, 0.02 % DDM, 250 mM imidazole
Wash buffer	50 mM NaPi pH 8, 500 mM imidazole, 1 M NaCl

Materials and methods

Purification bc_1 complex from *P. denitrificans* (affinity chromatography, Ni^{2+} -NTA with histidine)

Solubilisation buffer (2x)	100 mM NaPi pH 8, 600 mM saccharose, 2,4 M NaCl
Equilibration buffer	50 mM NaPi pH 8, 300 mM NaCl
Low histidine buffer	50 mM NaPi pH 8, 300 mM NaCl, 0,02 %DDM
High histidine buffer	50 mM NaPi pH 8, 300 mM NaCl, 0,02 % DDM 250 mM histidine
Wash buffer	50 mM NaPi pH 8, 500 mM histidine, 1 M NaCl

Purification bc_1 complex from *P. denitrificans* (Strep-Tactin column)

Solubilisation buffer (2x)	100 mM NaPi pH 8, 600 mM saccharose, 2.4 M NaCl, 5 mg avidin
Equilibration buffer	50 mM NaPi pH 8, 300 mM NaCl, 0.02 % DDM
Elution buffer	50 mM NaPi pH 8, 300 mM NaCl, 0.02 % DDM, 2.5 mM desthiobiotin

Purification c_{552F} from *E.coli* cells

Q-Sepharose washing buffer	50 mM Tris/HCl pH 8, 1 mM EDTA
Q-Sepharose gradient buffer	50 mM Tris/HCl pH 8, 350 mM NaCl, 1 mM EDTA
Q- Sepharose high salt buffer	50 mM Tris/HCl pH 8, 2 M NaCl, 1 mM EDTA
Gel filtration buffer	50 mM Tris/HCl pH 8, 150 mM NaCl, 1 mM EDTA

Coomassie staining

Staining solution	0.2 % Coomassie brilliant blue R 250, 10 % acetic acid, 20 % methanol
Destaining solution	10 % acetic acid, 20 % methanol

Materials and methods

Plasmidic DNA isolation (Miniprep)

Mini II	50 mM glucose, 0,2 M NaOH, 1 % SDS
Mini III	potassium acetate solution 3 M, 11.5 % acetic acid, pH 5 (4 °C)
Chloroform/Isoamyl alcohol	24:1 (v/v)

Competent cells

TFB-I-Puffer	30 mM potassium acetate pH 5.8, 10 mM CaCl ₂ , 50 mM MnCl ₂ , 100 mM RbCl, 15 % glycerol
TFB-II-Puffer	10 mM MOPS/KOH pH 6.8, 10 mM RbCl, 75 mM CaCl ₂ , 15 % glycerol
TE-Puffer	10 mM Tris/HCl pH 7.5, 1 mM EDTA

Membrane preparation

Lysis buffer	100 mM KP _i pH 8, 1 mM EDTA
Membrane buffer	20 mM KP _i pH 8, 1 mM EDTA
<i>bc</i> ₁ membrane buffer	50 mM MES/NaOH pH 6, 300 mM saccharose, 1 mM EDTA
<i>bc</i> ₁ membrane buffer NaP _i	50 mM NaP _i pH 8, 300 mM saccharose, 1 mM EDTA
Membrane spectrum buffer	50 mM KP _i pH 8, 0.5 % Triton X-100

Protein concentration (Lowry)

Lowry A	2 % Na ₂ CO ₃ , 0.1 M NaOH
Lowry B1	1 % CuSO ₄ ·5H ₂ O
Lowry B2	2 % potassium sodium tartrate
SDS solution	20 % SDS
Folin solution	50 % (v/v) Folin-ciocalteu in H ₂ O

Materials and methods

Periplasma prep

Periplasma buffer	100 mM Tris/HCl pH 8, 0,5 M saccharose, 1 mM EDTA
-------------------	--

SDS polyacrylamide gel electrophoresis (Tricine-System from Schagger)

Anode buffer (10x)	1 M Tris/HCl pH 8.9
Cathode buffer (5x)	0.5 M Tris/HCl, 0.5 M tricin, 0.5 % SDS, pH 8,3
Acrylamide solution	48 % acrylamide, 1.5 % Bis-acrylamide
Gel buffer	3 M Tris/HCl pH 8.5, 0.3 % SDS
Sample buffer	100 mM Tris pH 6.8, 4 % SDS, 200 mM DTT, 20 % glycerol, 0.02 % bromo phenol blue

Trace element solution for succinate medium

Trace element solution	15g CaCl ₂ * 2 H ₂ O, 24.5g FeCl ₃ * 6 H ₂ O, 10g MnCl ₂ * 4 H ₂ O, 3.4 g ZnCl ₂ , 2.4 g CoCl ₂ * 6 H ₂ O, 1.25 g CuSO ₄ * 5 H ₂ O, 0.6 g H ₃ BO ₃ * 6 H ₂ O, 2.4 g Na ₂ MoO ₄ * 2 H ₂ O, resuspend in 250 ml HCl _{conc.} and 250 ml H ₂ O, to 1 L with H ₂ O
------------------------	--

Western Blot solutions

Semidry buffer	11.64 g Tris, 5.86 g glycine, 3.75 ml SDS 20 %, 400 ml methanol, to 2 L with H ₂ O
Ponceau solution	0.2 % Ponceau, 3 % TCA
BSA solution	3 % BSA in TBS
TBS	50 mM Tris/HCl pH 7.5, 150 mM NaCl
TBS-TT	0.05 % (v/v) Tween-20, 0.2 % Triton X-100, 20 mM Tris/HCl pH 7.5, 500 mM NaCl
TNM	100 mM Tris/HCl pH 9.5, 100 mM NaCl, 50 mM MgCl ₂
BCIP	BCIP 25 mg/ml in dimethylformamide (DMF)
NBT	NBT 50 mg/ml in 70 % DMF
Stop solution	50 mM EDTA pH 8

2.1.12 Antibiotics

Antibiotic	Stock solution
Ampicillin (Amp)	50 mg/ml in 50 % (v/v) glycerol
Gentamycin (Gm)	10 mg/ml in 50 % (v/v) glycerol (<i>E. coli</i>) 20 mg/ml in 50 % (v/v) glycerol (<i>P. denitrificans</i>)
Kanamycin (Km)	25 mg/ml in 50 % (v/v) glycerol
Rifampicin (Rif)	15 mg/ml in methanol
Streptomycinsulfat (Sm)	25 mg/ml in 50 % (v/v) glycerol

Antibiotics have been (except rifampicin) sterile filtered and stored at -80 °C. After opening an aliquot, it was stored at -20 °C and used between 4 and 6 weeks. The dilution in the medium is 1:250 for rifampicin, and 1:1000 for all the other antibiotics.

2.1.13 Medium

Medium	Protocol
Luria-Bertani (LB)-Medium (Sambrook <i>et al.</i> , 1989)	Pepton 1 % (w/v), yeast extract 0.5 % (w/v), NaCl 0.5 % (w/v)
Succinate medium (Ludwig, 1986)	50 Mm K ₂ HPO ₄ , 10 mM NH ₄ Cl, 1mM citrate, 1 mM MgSO ₄ , 40 mM succinate, 0.2 ‰ (v/v) trace elements solution, pH with KOH to 6.2
Frozen cultures medium, (Sambrook <i>et al.</i> , 1989)	Pepton 1.6 % (w/v), yeast extract 1 % (w/v), NaCl 1 % (w/v), 20 % glycerol

To prepare Agar plates, 1,5 % (w/v) Agar-Agar has been added to the mediums. The plates are stored at 4 °C four to six weeks. Rifampicin plates were stored in a dry and dark place, since rifampicin is light sensitive.

2.2 Molecular biology methods

2.2.1 Growth and storage of microorganisms

2.2.1.1 *Escherichia coli*

E. coli liquid cultures were obtained by shaking the inoculated LB medium at 37 °C in air bath shaker (Multitron Shaker, type Aerotron, 37 °C, 240 rpm). The cells can be streaked on a plate and kept in the incubator over night. After that, the plate can be stored at 4 °C for six weeks. For frozen cultures, the colony from the backup plate was inoculated in 2 ml LB medium with the correspondent antibiotic and grown over night. The cells are then harvested, resuspended in frozen cultures medium, vortexed and frozen in liquid nitrogen before storing them at -80 °C

2.2.1.2 *Paracoccus denitrificans*

P. denitrificans cells can be grown in LB medium or in succinate medium. For small amounts, the cells are grown in the shaker (Multitron shaker, Typ Aerotron, 32 °C, 240 rpm) over night, similar to *E.coli*. To grow them on a plate, the strains are normally streaked on the corresponding antibiotic plates and kept over night in a incubator at 32 °C (Heraeus B 6120). It is then possible to store the plates at room temperature for one week.

For a preparative scale (10 to 50 L), a frozen culture is streaked out on a plate and left over night in the incubator at 32 °C. The so obtained cell layer was then resuspended in 2 ml and used to inoculate a 2 L pre-culture flask. After 24 hours of growth, 50 ml of it are inoculated in each 2.5 L succinate medium flask. The cells can be harvested after 18-22 hours of growth, at an OD₆₀₀ value of 3-5.

For *P. denitrificans* frozen cultures, see the protocol described for *E.coli*.

2.2.2 Isolation of plasmidic DNA in small scale (Miniprep)

1.5 ml of a 2 ml overnight culture were harvested using a table centrifuge (13.000 rpm, 2 minutes at room temperature). The supernatant is discarded and the cell pellet completely resuspended in 100 µl water. 200 µl from the Mini II solution are added and the Eppendorf cup inverted several times, to mix the two solutions and lyse the cells. This will make the solution viscous. It is important not to vortex or to shake the Eppendorf cup, since this can lead to problems in the separation of

Materials and methods

genomic DNA from the plasmidic one. After 5 minutes incubation on ice, 150 μ l of the Mini III solution are added, and the cup again mixed by inversion. After 5 minutes incubation on ice, white flakes of complexes containing SDS, genomic DNA, protein and membrane lipids are visible, which are pelleted by centrifugation (13000 rpm, 10 min, 4 °C). The supernatant will be transferred to a new Eppendorf cup avoiding the white pellet and mixed with an equal volume of chloroform/isoamyl alcohol (24:1) and vortexed for a minute. After centrifugation (13000 rpm, 5 min, RT) the aqueous phase is again mixed with an equal volume of chloroform/isoamyl alcohol and again vortexed and centrifuged as before.

The aqueous phase is transferred to a new Eppendorf cup and mixed with 2 volumes of cold ethanol 100%, and incubated for 30 minutes at -20 °C. After centrifugation (30 minutes at 4 °C, the supernatant is discarded and the pellet washed with 1 ml 70 % ethanol, without resuspending it, and again centrifuged 10 minutes, 13000 rpm, at 4 °C. The supernatant is discarded and the pellet kept 5 minutes at 37 °C in the opened Eppendorf cup to let ethanol evaporate completely. The pellet is then completely resuspended in 50 μ l water and incubated with 1 μ l from a 2 mg/ml RNase A stock, to remove RNA from the preparation.

2.2.3 Plasmid DNA restriction

DNA restrictions have a final volume of 20 μ l. This includes the 10X buffer supplied with the enzyme from the company, in a 1X final concentration, and 100-300 ng plasmidic DNA for an analytic restriction. If requested, 2 μ l 10X BSA are also added if not included in the supplied buffer. For a preparative restriction, it is necessary to calculate the enzyme amount according to the indications of the supplier and to the amount of DNA. For a standard restriction, 2.5 U of the enzyme are added. The mixture is vortexed and incubated for an hour at the optimal temperature. Most reactions can be stopped by heat-inactivation of the enzyme or by addition of 5 μ l of DNA sample buffer, and the mixture stored at -20 °C or directly analyzed on an agarose gel.

2.2.4 Electrophoretic separation of DNA

The separation of DNA is achieved in 0.7 to 2 % agarose gels, according to the expected fragment size. The smaller the fragments, the higher has to be the percentage of the gels. To prepare the gels, the calculated agarose amount has to

Materials and methods

be cooked in the microwave, until the powder is solved. When the solution is hand-warm, 5 μ l ethidium bromide (10 mg/ml) can be added pro 100 ml of liquid agarose solution and carefully mixed by gentle shaking. The solution is then poured into a casting chamber with the combs where the sample has to be loaded afterwards. The agarose is put in a running chamber filled with TBE buffer so that it stays wet during the electrophoretic run. The probe is pipetted in the pockets and the run started using a constant voltage (5 V / cm). At the end of the run, the gel is taken out from the chamber and put on a transilluminator (TMW 20, Firma UVP) to reveal the DNA fragments using the fluorescence of ethidium bromide at 254 nm when it is intercalated in DNA. To reveal fragments which should be recovered from the gel, a UV light at 365 nm is used, to avoid the formation of thymin dimers in the DNA, which could lead to mutations. At the end of the observation, a picture is taken to document the gel.

2.2.5 DNA extraction from agarose gels

The bands of interest can be cut out the gel using a scalpel and transferred to an Eppendorf cup. To extract them from the gel, the Zymoclean Gel Extraction kit from the company Zymo Reasearch has been used. At the end, the desired DNA is purified from the gel and resuspended in water (30 μ l or 10 μ l, according to further use).

2.2.6 Ligation of DNA fragments

Ligations are pipetted to a final volume of 10 μ l, adding 1 μ l of ligation buffer supplied by Fermentas together with the enzyme, 1 μ l of DNA ligase (1 U), equimolar amounts of vector and insert (at least 25 ng for a *sticky end* ligation, and 200 ng for a *blunt end* one) and the rest filled with water up to 10 μ l. The reactions takes place at least for an hour (overnight for *blunt end* ligations) at 22 °C, and subsequently the ligase is inactivated at 65 °C for 10 minutes. To improve the yield of the ligation in case of a blunt end ligation or ligation with two identical sticky ends, or to avoid the insertion of a chain of inserts into the vector, the vector can be dephosphorylated with the Calf Intestinal Alkaline Phosphatase (CIAP).

2.2.7 Production *E.coli* competent cells

2 ml of an *E.coli* overnight culture are prepared from a frozen culture. The next day 50 ml LB medium are inoculated to have a 0.5 % culture. The culture is shaken at 37 °C until an OD₅₅₀ of 0,45/0,5 is reached, and kept for 10 minutes on ice. Then the cells are pelleted (Megafuge 3400 rpm, at 2000 g and 0 °C, 10 min). The supernatant is thrown away carefully, and any remaining medium is pipetted away. The pellet is then resuspended in 1 ml cold TFB I buffer, and again 6.5 ml of the same buffer added and mixed by inverting it. The cell suspension is incubated one hour on ice and afterwards pelleted (BIORAD Megafuge 4800 rpm, bei 3000 g und 0 °C). The pellet is then carefully resuspended in 2 ml cold TFB II buffer. The cell suspension is aliquoted (100 µl) and frozen in liquid nitrogen. Afterwards, the cells can be stored at -80 °C.

2.2.8 Transformation of *E.coli* competent cells

An aliquot of competent cells is thawed on ice (20 minutes) and 20-50 ng DNA from the ligation or 1 ng from the plasmidic DNA which is needed to be retransformed added, and carefully mixed with the pipette tip. After 20 minutes incubation on ice, follows the heat shock at 42 °C for one minute, 900 µl of fresh LB medium are then added and the cell suspension left 1 h at 37 °C in an Eppendorf Thermomixer under shaking. At the end, the cells can be plated (100% or splitting them in two aliquots, 90 % and 10 %) on plates with the appropriate antibiotics.

2.2.9 Conjugation: *Triparental Mating*

The *P. denitrificans* strains used in this work possess no natural or chemical competence. Therefore conjugation is normally used. The plasmids and the strains used in the normal laboratory work possess no *tra* functions, necessary for the conjugation. These genes are present in a helper strain, *E. coli* MM294, having a mobile plasmid (pRP4-7) which will be transferred in the donor strain (DH5α), now made able to transfer the desired vector into the recipient strain (MK6: *bc₁* deletion mutant). The three strains are inoculated in a 2 ml overnight culture with the corresponding antibiotic. The next day, 300 µl of the recipient strain and 100 µl from the helper and the donor strains are mixed together and the cells pelleted with a table centrifuge (6000 rpm, 3 minutes, room temperature). The supernatant is discarded and the cells resuspended in 100 µl fresh LB medium and in a single drop

Materials and methods

transferred to a LB plate without any antibiotic. The plate is incubated overnight at 32 °C, and the next day the cells scratched away and resuspended in 500 µl LB medium. This suspension is diluted in a row from 1:4 to 1:32 and plated on Rif/Km/Sm or Rif/Km/Gm₂₀ or Rif/Km/Sm/Gm₂₀ plates, according to the desired selection. Km, Sm and Gm select *P. denitrificans* cells which have received a plasmid after conjugation. Rif kills the *E. coli* cells. The plates are incubated 24 hours at 32 °C and single colonies are picked and transferred to a backup plate for further analysis.

2.2.10 Phosphorilation of oligonucleotides

In an Eppendorf cup 2 µl PNK 10x reaction buffer supplied from the company are pipetted, plus 4 µl of a 5 mM ATP solution, 1 µl T4-Polynucleotid-Kinase, 100 pmol of the oligonucleotide and distilled water up to 20 µl final volume. After 30 minutes at 37 °C, the mixture is inactivated at 70 °C for 10 minutes.

2.2.11 Polymerase Chain Reaction

The *polymerase chain reaction*, PCR, is used to amplify DNA. The polymerases used are thermostabile, and this makes possible to achieve several cycles of amplification without adding after each denaturation step new enzyme. An amplification cycle starts with a denaturation step at 98 °C, during which the two DNA strands are separated. In the annealing step, oligonucleotides anneal specifically to the complementary sequence on the DNA strand. The melting temperature for the primers is calculated *in silico* with the software Clone Manager and the annealing temperature calculated by subtracting 10 °C. During the elongation step, the primer is elongated in direction 5' to 3' at 72 °C by the thermostabile polymerase. The cycles duration and number can vary, according to the different application of the PCR and the kind of polymerase used. In this work, the Phusion polymerase from Finnzymes has been used, which has a polymerisation rate of 3500 bp*min⁻¹. For a PCR reaction, 20-50 ng of oligonucleotide are used and 1-2 ng of template DNA. For a 50 µl reaction, 2.5 U of enzyme and 100 µM dNTPs are required. Annealing temperatures and protocols are adapted to each application and polymerase.

Cycles	Steps	Time [min]	Temperature [°C]	Function
1	1	1	95	Pre-denaturation
30	1	0:30	95	DNA strands separation
30	2	0:30	50→60	Annealing
30	3	0:15→60	72	Elongation

2.2.12 Site directed mutagenesis

The mutation of a specific amino acid in a protein is achieved by changing the DNA sequence which codes for that rest, using the directed mutagenesis. In this work, directed mutagenesis was achieved by inverse PCR. With this technique, the plasmid which has to be mutagenised is used as template in a PCR which uses two primers: the forward contains the mutation, and the reverse without the mutation binds exactly where the forward starts and runs in the opposite direction. Therefore, are produced copies of the plasmidic DNA which contains the mutation in the desired position and are open. The PCR product is run on a preparative gel, and purified using the DNA Gel Extraction kit and eluted using 20 µl of water. Then, 5 µl of the eluted DNA are phosphorylated and ligated at the same time and after 2 hours of ligation transformed into DH5α competent cells. The next day, colonies are picked from the plate, inoculated in LB medium with the corresponding antibiotic and the plasmidic DNA analyzed by restriction and sequencing.

2.2.13 DNA Sequencing

DNA has been sequenced from the company Scientific Research and Development GmbH (SRD GmbH) Köhlerweg 20 D-61440 Oberursel, with the chain termination method (165)

2.3 Protein biochemistry

2.3.1 Analytic membrane preparation

Initially, a 2 ml culture of the desired *P. denitrificans* strain is grown over night at 32 °C with the needed antibiotics. The pre-culture is then inoculated in a 2 L flask containing 400 ml of succinate medium with antibiotics and grown over night at 32 °C and 250 rpm. The next day, the cultures are cooled down on ice and the cells

Materials and methods

harvested in a Sorvall centrifuge at 6000 rpm and 4 °C. The supernatant is discarded and the cell pellet resuspended in 5-10 ml of 50 mM KP_i buffer pH 7, 10 mM EDTA. Cells are lysated using lysozyme (0.1 mg/ml) and incubated 30 minutes on ice. The solution is now viscous, due to the cell disruption and the release of genomic DNA. To achieve a complete cell disruption, the solution is shock frozen in liquid nitrogen creating so water crystals which help disrupting completely the cells. After thawing the sample at room temperature, it follows a 5-10 minutes treatment with a Branson Sonifier 250 (duty cycle 30 %, output 40 %) on ice, until the solution is not anymore viscous since the genomic DNA is completely destroyed. The sample is afterwards centrifuged (Sorvall Centrifuge SS34-Rotor in 10 ml tubes, 10 minutes at 10000 rpm and 4 °C) and the supernatant transferred in ultracentrifuge tubes to be again centrifuged (Beckman ultracentrifuge, Ti-70-Rotor, 1 hour, 35000 rpm at 4 °C). Membranes are present in the pellet fraction, which is then recovered from the ultracentrifuge tubes and resuspended using a Teflon pistil in 200 μ l 20 mM KP_i pH 8, 1 mM EDTA. Membranes are frozen in liquid nitrogen and stored at -80 °C

2.3.2 Membrane preparation (preparative scale)

2.5 L flasks of *P. denitrificans* cells are prepared as previously described. Cells are then harvested at an OD_{600} of 3-5 in a Sorvall RC36 for 20 min at 5000 rpm and 4 °C after cooling down the flasks. The cell pellet is resuspended in 100-200 ml of cold 100 mM KP_i , pH 8, 1 mM EDTA buffer and frozen at -80 °C. This helps also the cell disruption later. To lysate the cells, after thawing, the protease inhibitor Pefabloc SC is added to a 100 μ M final concentration and a Monton-Gaulin homogenisator (APV Schröder, Lübeck) used for 5 minutes at 400 bar pression. The warmth generated from the homogenisator is compensated by the presence of an ice bath. The instrument is washed with buffer in order to recover all the cell material and subsequently with 20 % ethanol to eliminate any cell rest. The sample is centrifuged in a Sorvall RC36 centrifuge at 5000 rpm for 15 min in order to sediment big cell fragments and granules. The supernatant is centrifuged again over night in a Sorvall centrifuge, GS3 Rotor at 8000 rpm, presenting the next day a hard, white core (granules) and a soft, red external part where the membranes are. This red pellet is transferred to a becker and resuspended in 50 mM MES/NaOH pH 6, 300 mM Saccharose (or 50 mM NaP_i pH 8, 300 mM Saccharose according to the desired applications) using an Ultra Turrax Homogenisator. It follows the last centrifugation

step (Beckmann ultracentrifuge Ti 45-Rotor, 1 hour, 35000 rpm at 4 °C) to better separate the membranes from the storage ganula. The so obtained membranes are then resuspended in a small volume of the same buffer previously used, aliquoted and frozen at -80 °C.

2.3.3 Membrane solubilisation

2.3.3.1 Classic purification of the cytochrome *bc₁* complex

Membrane aliquots are thawed and the protein concentration is set to 35 mg/ml using the membrane buffer. Membranes are solubilised upon addition of Pefabloc SC, 100 µM final concentration, and one volume of solubilisation buffer 2X, 1.2 times DDM compared to the protein amount (w/w) and water to final volume. The solution is then stirred one hour at 4 °C. The solubilisate is then centrifuged (Beckmann Ti 45 Rotor 35000 rpm, 1 hour at 4 °C) and the supernatant, which now has a NaCl concentration of 600 mM, diluted to 350 mM NaCl using the dilution buffer and filtered using a paper filter.

2.3.3.2 Purification by affinity chromatography (Ni²⁺-NTA)

Membrane aliquots are thawed and the protein concentration is set to 35 mg/ml using the membrane buffer NaP_i. Membranes are solubilised upon addition of Pefabloc SC, 100 µM final concentration, and one volume of solubilisation buffer imidazol or histidine 2X, 1.2 times DDM compared to the protein amount (w/w) and water to final volume. The solution is then stirred one hour at 4 °C. The solubilisate is then centrifuged (Beckmann Ti 45 Rotor, 35000 rpm, 1 hour at 4 °C) and the supernatant filtered using a paper filter.

2.3.3.3 Purification by affinity chromatography (StrepTactin)

Membrane aliquots are thawed and the protein concentration is set to 35 mg/ml using the membrane buffer NaP_i. Membranes are solubilised upon addition of Pefabloc SC, 100 µM final concentration, and one volume of solubilisation buffer with avidin 2X, 1.2 times DDM compared to the total protein amount (w/w) and water to final volume. The solution is then stirred one hour at 4 °C. The solubilisate is then centrifuged (Beckmann Ti 45 Rotor 35000 rpm, 1 hour at 4 °C) and the supernatant filtered using a paper filter.

2.3.4 Chromatography

All the chromatographic experiments are done at 4 °C

2.3.4.1 Classic purification of the cytochrome *bc*₁ complex

The column (DEAE-Sepharose CL-6B, ca. 250 ml, FPLC Pharmacia LKB) is equilibrated with 4 column volumes (CV) equilibration buffer and 2 CV low salt buffer. The solubilisate is applied to the column with a flow rate of 3.5 ml/min, and afterwards washed with 1 CV of low salt buffer. All proteins not tightly bound to the column are washed away. The *bc*₁ complex is eluted with a 6 CV NaCl gradient (350-600 mM NaCl). The elution profile is registered with a detector (Pharmacia Optical Unit UV-1, 280 nm) and a writer (Pharmacia Rec 102). The elution of the red fractions containing the *bc*₁ complex happens around 420-450 mM NaCl, and the fractions are analysed spectroscopically and by SDS-PAGE and Western Blot. The fractions containing no undesired protein are collected and concentrated to a factor of 150-200 (Satorius Vivaspin cutoff 100 kDa).

2.3.4.2 Purification by affinity chromatography (Ni²⁺-NTA)

The column (Ni²⁺-NTA-Superflow, ca. 20 ml, FPLC Pharmacia LKB) is equilibrated with 4 column volumes (CV) equilibration buffer and 2 CV low imidazole or low histidine buffer. The solubilisate is applied to the column with a flow rate of 1 ml/min, and afterwards washed with 1 CV of low imidazole or low histidine buffer. All proteins not tightly binding to the column are washed away. The *bc*₁ complex is eluted with a 5 CV gradient (10-250 mM imidazole or 10-200 mM histidine). The elution profile is registered with a detector (Pharmacia Optical Unit UV-1, 280 nm) and a writer (Pharmacia Rec 102). The elution of the red fractions containing the *bc*₁ complex happens about 150 mM imidazole and 80 mM histidine. The fractions are analysed spectroscopically and by SDS and Western Blot. The fractions containing no undesired protein are collected and concentrated to a factor of 150-200 (Satorius Vivaspin cutoff 100 kDa).

2.3.4.3 Purification by affinity chromatography (StrepTactin)

The column (Core-Streptavidin, 5 ml, FPLC Pharmacia LKB, 0,5 ml/min) is washed with 6 CV equilibration buffer. The solubilisate is loaded and the column washed with 1 CV equilibration buffer to wash away the protein not tightly bound. The

Materials and methods

complex is eluted with 2 CV elution buffer in a single step. The fractions are analysed spectroscopically and by SDS-PAGE and Western Blot. The fractions containing no undesired protein are collected and concentrated to a factor of 150-200 (Satorius Vivaspin cutoff 100 kDa).

2.3.4.4 Purification of the cytochrome c_{552F}

Two different columns are used to purify the cytochrome c_{552F} heterologously expressed in *E.coli*, an ion exchange (Q-Sepharose) and the gel filtration (Sephacryl S-100). The first column is equilibrated with the 4 CV Q-Sepharose washing buffer, and the periplasma loaded on it. After loading the column, it is washed with 1 CV of the same buffer. The protein is eluted with 5 CV NaCl gradient (0-350 mM). The fractions (ca. 5 ml) are analyzed with SDS PAGE, and where no impurity has been found, collected and concentrated. The concentrated sample is run on the second column, previously equilibrated with 4 CV of the gel filtration buffer. The run occurs with the same buffer. The protein is eluted in 0.5 ml fractions, analyzed by SDS PAGE and collected to be concentrated

2.3.5 Lowry

The solution for the Lowry measurement has always to be prepared fresh. It contains 20 ml Lowry A, 0.5 ml Lowry SDS solution, 0.2 ml Lowry B1 and 0.2 ml Lowry B2. The standards are prepared with BSA in the following amounts: 0.0, 2.0, 4.0, 6.0, 8.0, 1.0 and 1.5 mg/ml. Standards and samples have a total volume of 50 μ l. To these, 850 μ l from the Lowry solution are added, vortexed well and incubated in the dark for 10 minutes. Next, 100 μ l of the Folin solution are added and kept 30 minutes in the dark. Reading the OD_{750} of the standards and making a linear regression, is then possible to determine the protein concentration of the sample (166).

2.3.6 Polyacrylamide gel electrophoresis (PAGE)

2.3.6.1 Tricine system (Schägger)

For the SDS PAGE has been used the Schägger system, specific for proteins with a $M_r < 1-100$ kDa (167). The 10 % lower gel is prepared pipetting 2 ml acrylamide solution, 3.5 ml H_2O , 3.3 ml Gel buffer, 1 ml Glycerol, 20 μ l TEMED and 100 μ l of a 10 % APS solution, mixing and quickly pouring in the casting chamber (Mini Protean

Materials and methods

II, BIORAD). After polymerisation, the upper gel is prepared (0.5 ml acrylamide solution, 6 ml H₂O, 1.5 ml Gel buffer, 20 µl TEMED und 100 µl 10 % APS) and poured over it, using a comb for the pockets. The samples are mixed with Sample buffer (1:1) and kept 30 minutes at 37 °C to allow denaturation of the proteins. The gel apparatus is then put in a running chamber and the inside of it is filled with catode buffer while the rest with anode buffer. The probes are loaded onto the gel using a Hamilton syringe; the gel runs with a constant voltage (100 V for 100 minutes).

2.3.7 Gel staining

2.3.7.1 Coomassie staining

The gel is kept in the Coomassie staining solution for 20 minutes at room temperature. The extra Coomassie bound to the gel can be washed away until the desired background is obtained with the Coomassie destaining solution.

2.3.8 Westernblot (semidry)

Three pieces filter paper wet with some semidry buffer are put in the semidry blot apparatus (BIORAD), upon them a layer of nitrocellulose membrane (Whatman) also previously wet with the same buffer and the acrylamide gel on it. It is important to avoid air bubbles which can lead to an improper protein transfer during the Blot. Upon the gel, again wet filter paper is put, ad the “sandwich” is then closed in the Blot apparatus. The upper part of it is the negative pole, and the negatively charged proteins are forced, by applying voltage (15 V, 1 hour) to move in the direction of the positive pole, meaning to the nitrocellulose membrane. After one hour, the gel and the filter paper are discarded and the nitrocellulose membrane is washed with some distilled water in order to wash away ions which would interfere with the Ponceau staining. The membrane is then stained with the Ponceau solution for five minutes. The protein bands will appear on it, since Ponceau binds reversibly to proteins when no ions are present and can be easily and totally be washed away with distilled water. The marker bands are marked with a pen and the membrane destained.

Materials and methods

2.3.8.1 Western blot protocol

The membrane is “blocked” with BSA 3 % in TBS for one hour. BSA binds onto the membrane and occupies all the positions where no proteins are bound, avoiding that the antibody later could bind on an unspecific position and give background staining.

The primary antibody (monoclonal from mouse against the His tag, or polyclonal from rabbit for the protein of the respiratory chain from *Paracoccus denitrificans*) is diluted 1:1000 in BSA solution and incubated shaking with the membrane for two hours or over night. Subsequently, the membrane is washed three times with TBS-TT and again with TBS to wash away residuals of the antibody not specifically bound to the protein of interest. The membrane is then incubated with the secondary antibody (also diluted 1:1000 in BSA solution) for one hour. The secondary antibody can be, in the case of the anti His-tag Blot, a *goat anti mouse* IgG directed against the primary one, or a Protein A-Alkaline Phosphatase conjugate (AAP) in the case of polyclonal antibody from rabbit. In the case of the anti Strep-tag Blot, a mouse IgG is used to bind the Strep-tag, directly coupled to the Alkaline Phosphatase, and therefore, after 30 minutes incubation with the first antibody, the membrane can be washed with TBS-TT and directly stained.

After the secondary antibody incubation, the membrane is then washed three times with TBS-TT, once with TBS and with TMN buffer. TMN is a buffer with pH 9.5, which equilibrates the membrane at the right pH to let the Alkaline Phosphatase work in presence of the two substrates.

The staining solution is 20 μ l TMN buffer and 90 μ l NBT and BCIP. After purging it on the membrane, it is incubated in the dark to avoid unspecific background and the reaction is then stopped, when the bands are visible, using 10 ml 50 mM EDTA. By keeping the membrane wet, it is now possible to document it

2.4 Biophysics methods

2.4.1 Enzymatic activity tests

To measure the activity of the cytochrome *bc*₁ complex, the change in absorption at 550 nm is detected, which shows the change in the redox state of the cytochrome *c* from horse heart. For the measurements with cytochrome *c*_{552F}, the absorption

Materials and methods

change at 552 nm has been recorded. The electron donor is decylquinol, analog to the native substrate, ubihydroquinone.

2.4.1.1 Decylubiquinone reduction

To reduce the substrate, 50 mg decylquinone are solved in 3 ml ethanol and 1 ml water is added. The solution is deep yellow. 100 μ l of 1 M HCl are added to regulate the pH. Decylubiquinone is reduced by the careful and slow addition of KBH_4 , which can be optically seen since the solution becomes transparent. Bubbles are produced during the reduction process. Afterwards, in 20 μ l steps, 1 M HCl is added until no more bubbles are visible, since the excess of KBH_4 has been removed. The pH has to be checked with pH indicators and has to be kept below 4. Then, 2 ml of water are added and the sample is mixed 3 times with 5 ml cyclohexane. The organic phases are then collected and again washed 2 times with water. The sample is then aliquoted in 150 μ l aliquots in small Eppendorf cups and the organic phase is evaporated using a SpeedVac. The aliquots are stored at $-80\text{ }^\circ\text{C}$, and resuspended in 40-60 μ l ethanol mit 100 μ M HCl give a solution of about 50 mM. To check the amount of reduction, a spectrum from the sample is measured, afterwards it is oxidized with some μ l of a fresh 1 M NaOH solution, and again measured. The difference spectrum allows the calculation of the decylubiquinol concentration (168, 169) using the extinction coefficient : $\epsilon_{275, \text{oxred}} = 12,5 \text{ mM}^{-1}\text{cm}^{-1}$.

2.4.1.2 Measurements

The complex III activity can be measured by following the increasing of absorption at 550 nm (for the measurement with horse heart cytochrome *c*) or 552 nm (for the case of cytochrome $\text{C}_{552\text{F}}$). In a 1 ml disposable cuvette, 1 ml of the measuring buffer is pipetted together with 10 μ l of a 2.5 cytochrome *c* from horse heart stock solution and 2 μ l of the aforementioned decylubiquinol stock solution (ca 50 μ M). When the spectrophotometer shows a stable baseline, the previously diluted protein sample (1:100 for membranes, 1:1000 for purified proteins) is then added, quickly mixed and the absorption change is measured. The activity is normally measured in a window between 40 and 120 mOD. The initial rate is measured in a time of 10 seconds and the slope calculated by linear regression. In the case of steady-state kinetics, different concentrations of cytochromes *c* and $\text{C}_{552\text{F}}$ are used instead of a fixed one

2.4.1.3 Redox spectra

Redox spectra can be made directly with purified proteins. In the case of membranes, it is necessary to solubilise the protein from the lipids. This occurs using the Spectra buffer, which is then mixed in ratio 20:1 with 25 % Triton X-100. The sample is afterwards vortexed and centrifuged (30 min at 4 °C in Heraeus table centrifuge at 13000 rpm). Thereby the solubilized proteins are separated from the lipid portion and a spectra can be measured. (In the case of purified protein, some μ l of the concentrated sample are diluted in the elution buffer and measured.) The supernatant is transferred to a glas cuvette, and the sample is first completely oxidized with potassium ferricyanide(III), to record an oxidized spectrum (Hitachi U-3000 Photometer, wavelengths 500-650 nm) which serves as baseline. The sample is afterwards reduced with sodium ascorbate (to reduce especially c-type hemes) and/or with sodium dithionite (to reduce all the cofactors) and again a spectrum recorded. The result is a typical redox spectrum which shows the kind of cofactors present and allows an estimation of their concentration by measuring the hight of the single peaks (normally the α - and β - bands between 500 und 650 nm are used for this aim).

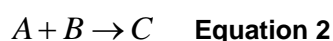
Protein	Heme	Wavelength [nm]	Extinction coefficient ϵ [mM ⁻¹ cm ⁻¹]	Reference
cyt <i>b</i>	<i>b</i>	560-574	28.5 / 29.3	(170, 171)
cyt <i>c</i>	<i>c</i>	550	19.4	(172)
cyt <i>c</i> ₁	<i>c</i> ₁	553-540	20.1 / 23.2	(170, 173)

2.4.1.4 Pre steady-state cytochrome *c*₁ reduction: Stopped-flow

To measure the rate of cytochrome *c*₁ reduction in the *bc*₁ complex from *P. denitrificans* the Stopped Flow has been used in collaboration with Prof. Francesco Malatesta in the lab of Prof. Maurizio Brunori at the university “La Sapienza” in Rome. A fixed amount of cytochrome *bc*₁ complex (ca. 5 μ M) has been mixed with increasing amounts of sodium ascorbate (1, 2, 4, 7 and 10 mM before mixing) and the signal at 420 nm recorded. The syringes with the samples were kept on ice until used, and the experiments made at 10 °C. The buffer used was 50 mM MOPS/NaOH pH 7.5, 100 mM NaCl, 0.04 % DDM, 1 mM EDTA and 1 mM KCN.

Materials and methods

The conditions used are **Pseudo First Order** conditions (PFO), meaning that the concentration of sodium ascorbate is so high compared to the bc_1 concentration that it can be considered constant during the reaction, since it does not vary much. This approximation is normally used to simplify the calculation of constant from bimolecular reactions, which would be otherwise calculated using the η -equation (174) in conditions where the PFO approximation cannot be assumed. The PFO approximation can be described as follows, for the reaction in equation 2.



In this case, the concentration of the product C in the time is:

$$\frac{d[C]}{dT} = k_{ET} [A][B] \quad \text{Equation 3}$$

If the concentration of one of the reagent (in this example B) is much higher than the concentration of A, it can be considered as constant.

$$k_{ET} [B] = k_{OBS} \quad \text{Equation 4}$$

The 2.1 can be then also written as follows:

$$\frac{d[C]}{dT} = k_{OBS} [A] \quad \text{Equation 5}$$

The k_{OBS} is a PFO constant, from which it is possible to calculate the second order kinetic constant by plotting the k_{OBS} against the concentration of B.

After recording the signals, they were fitted to a mon- or bi-exponential mathematic model described in Equations 6 and 7.

$$y = a * e^{-k*t} + offset \quad \text{Equation 6}$$

$$y = a1 * e^{-k1*t} + a2 * e^{-k2*t} + offset \quad \text{Equation 7}$$

2.4.1.5 Time resolved stopped-flow

The measurements were performed in collaboration with Prof. Bernard L. Trumpower and Dr. Raul Covian at the Dartmouth Medical School in New Hampshire, USA.

2.4.1.6 Pre steady state reduction of cytochrome c_1 and cytochrome b in presence of antimycin

Pre-steady state reduction of cytochrome c_1 and cytochrome b was followed at room temperature by stopped flow rapid scanning spectroscopy using the OLIS Rapid Scanning Monochromator. For the experiments 2 μM of enzyme were used, with and without 2.5 μM antimycin, in the measuring buffer (100 mM Tris-HCl, pH 8.0, 2 mM sodium azide, 0.2 mM EDTA, and 0.05% DDM). The cytochrome bc_1 complex was measured against an equal volume of buffer containing several concentrations of decylubiquinol. The traces were exported using software from OLIS and fitted to a monoexponential or a biexponential mathematical model using the software Origin 5.0.

2.4.1.7 Steady-state cytochrome c reduction with and without antimycin

The electron acceptor used in these experiments is the horse heart cytochrome c , whose reduction was followed at room temperature using OLIS Rapid Scanning Monochromator. 100 nM enzyme and horse heart cytochrome c have been mixed against an equal volume of buffer with different concentrations of decylubiquinol. The absorbance change between 550 and 539 nm has been extracted using a software from OLIS and exported to Origin 5.0, where the initial absorbance increase has been fitted to a linear regression and expressed as turnover numbers (mol cytochrome c reduced/mol bc_1 monomer/s), using an extinction coefficient of $21.5 \text{ mM}^{-1}\text{cm}^{-1}$ (63). The calculated initial rates are then fitted to the Michaelis-Menten equation. The enzyme (100 μM) was kept on ice. Several concentrations of inhibitor were added to this stock solution and left 2 minutes on ice to let the binding occur. After this incubation, the enzyme has been diluted to a final concentration of 100 nM, and 20 μM cytochrome c were added. The sample was then mixed against an equal volume of buffer containing 80 μM decylubiquinol. The absorbance change at 550 versus 539 nm has been extracted and rates calculated as described above.

Materials and methods

Six individual data sets per antimycin concentration are shown in the results and fitted to a model already described (148).

2.4.1.8 Flash photolysis experiments

For the laser flash experiments a *Phase R model DL 1400* Laser has been used, which generates an excitation pulse of 480 nm and 0.4 μ s period using a Coumarin LD 490 dye. The detection system used is the one described from Heacock *et. al.* (175). In a micro-glass cuvette were mixed 300 μ l of buffer (according to the different c-type cytochrome used), 5 μ M cytochrome c_{552F} (or isoform 1 of the yeast cytochrome *c*) coupled to ruthenium, 5 μ M cytochrome bc_1 complex from *P. denitrificans*, 2 mM sodium ascorbate, 2 μ M TMPD. Also a sacrificial oxidant was used according to the experiment, $[\text{Co}(\text{NH}_3)\text{Cl}]^{2+}$ and pentaamine osmium for, respectively, the cases of $\text{Ru}_z\text{-H39C-Cc}$ and $\text{Ru}_z\text{-N23C-}c_{552F}$. The salt concentration has been increased using a 2 M KCl stock solution and each time a new spectrum recorded in order to check the redox state of the bc_1 complex in the cuvette. The experiments were carried out at 10 °C, and each condition has been tested with different time scales and 2 different wavelengths (550 or 552 nm for the reduction of the substrate cytochromes and 558 nm for the oxidation of cytochrome c_1 (176), to make sure that the reaction was observed in each component. The transient obtained from the measurements were fitted using the program SIFitting 5.0 and mathematically fitted to a mono- or a bi-exponential equation and a k_{OBS} obtained which describes the electron transfer process between the two reaction partners. The k_{OBS} calculated from the transients have been plotted against the square root of the ionic strength to obtain the Brønsted plot which describes the interaction observed between the cytochrome bc_1 complex and the substrates.

2.4.1.9 Flash photolysis internal kinetics

With the same system, using a ruthenium dimer, it is possible to determine the rate for the reduction of cytochrome c_1 from the ISP. In this case, the same experimental setup as in 2.4.1.8 has been used, but instead of the cytochromes *c* coupled with ruthenium, a ruthenium dimer in solution takes an electron away from cytochrome c_1 and lets the ISP deliver an electron to the cytochrome c_1 . The measurements were performed with several inhibitors. The transients obtained from these measurements were fitted as previously described to a single or a double exponential equation.

3 Results

The results presented in this work will be divided into four sections, dealing with the dimeric nature of the complex, the interaction with its substrate, the internal regulation facilitated by the substrate and the electron transfer pathway

3.1 Dimeric nature of the complex

The aim of this section is to analyse the dimeric structure of the *bc₁* complex in *P. denitrificans* and prove the regulation mechanism already presented by Covian *et al.* (145) in the past. For the analysis, a deletion mutant of the acidic domain in cytochrome *c₁* has been used, since the wild type protein is a “dimer of dimers” (177) and this posed several problems, as already discussed by (152).

3.1.1 Purification and characterization of the deletion mutant

In a previous work (110), the *fbc* operon with a deletion in the *fbcC* gene and a C-terminal 10X His tag has been cloned and homologously expressed (MC1). The purification was obtained with Ni²⁺-NTA affinity chromatography and eluted with an imidazole gradient (0-200 mM). The complex normally eluted around 150 mM imidazole and the eluate was concentrated using 100 kDa cut off ultrafiltration membranes (Fig. 8).

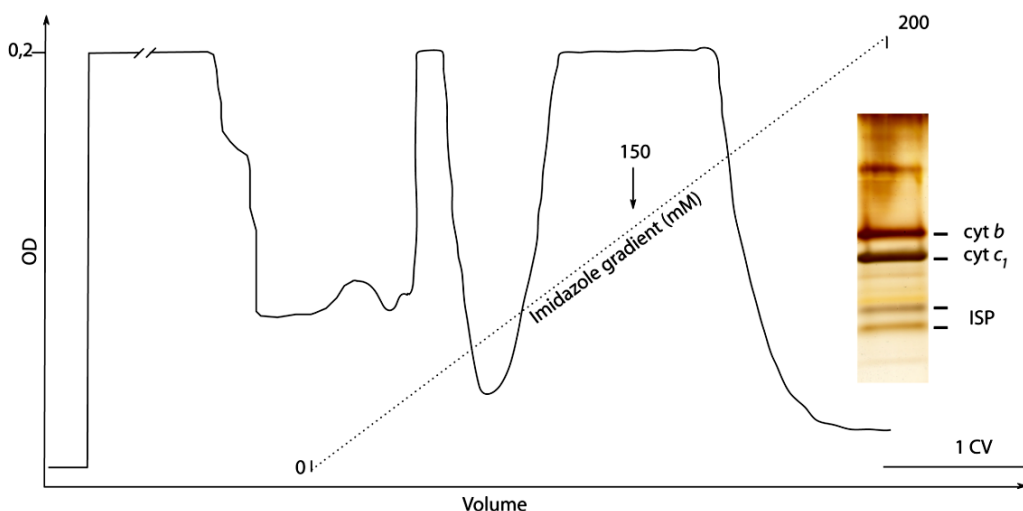


Fig. 8: Chromatogram of the purification of the deletion mutant of the cytochrome *bc₁* complex from *P. denitrificans* by a Ni²⁺-NTA column. The elution is obtained with an imidazole gradient. On the right, the concentrated protein on a SDS PAGE, silver stained (chromatogram from (152)).

Results

From redox spectra, it was clear that the reducibility of the mutated cytochrome c_1 was strongly impaired. In Fig. 9 static spectra are shown where the complex has been reduced with increasing amounts of ascorbate to selectively reduce cytochrome c_1 , and finally with dithionite to achieve a complete reduction of all redox cofactors. As control, the wild type complex (WT) and its His tagged version (TK33) were measured as well. Cytochrome c_1 in the wild type complex is completely reduced by ascorbate at 1 mM concentration, and later addition of reductant does not increase the signal in the spectra. On the other hand, a shoulder at 560 nm appears, speaking for reduction of cytochrome b . Dithionite reduces completely all the redox cofactors. In the His tagged and the mutant complex only a partial reduction of the c_1 heme can be observed, even with excess of reductant. At the same time, a more definite signal at 560 nm can be recorded, indicating cytochrome b reduction.

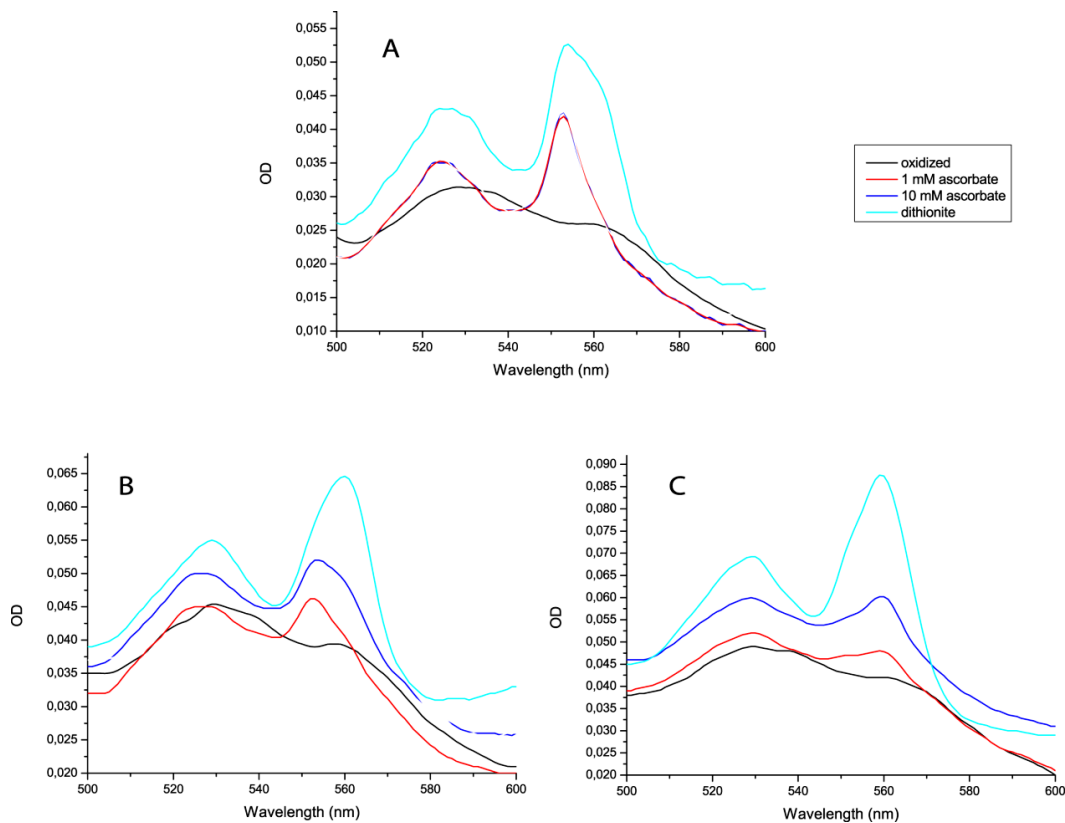


Fig. 9: Static spectra from the wild type (A), the His tagged (B) and the deletion mutant (C) bc_1 complexes from *P. denitrificans*. In panel A, the wild type complex is well reduced at 1 mM ascorbate. In panels B and C, even 10 mM ascorbate is not enough to achieve complete reduction of cytochrome c_1 . Dithionite, on the other hand, reduces completely all redox cofactors. In black, the oxidized spectrum; red: 1 mM ascorbate; green: 5 mM ascorbate; blue: 10 mM ascorbate; light blue: dithionite.

Results

The wild type complex is purified by ion exchange chromatography (DEAE), since the acidic domain, with its strong negative charge, binds the protein to the positively charged resin. The His tagged wild type and the mutant complex are both purified by a Ni^{2+} -NTA column and eluted with an imidazole gradient. It was already reported in the literature that imidazole is detrimental to cytochrome c_1 (for example in *Rhodobacter sphaeroides* cytochrome bc_1 (178, 179)), impairing the turnover number of the complex and the reducibility of the c_1 heme. This effect, in the case of the *P. denitrificans* cytochrome bc_1 complex was unknown. Thereafter, the His tagged proteins have been purified using a buffer containing histidine for elution instead of imidazole. The purification protocol remains, nevertheless, the same. Membranes are solubilised as described in section 2.3.3, ultracentrifuged and the column (equilibrated with 50 mM sodium phosphate, pH 8, 350 mM NaCl and 0.02 % dodecylmaltoside) loaded with the supernatant. A washing step with the equilibration buffer follows until the 280 nm trace reaches baseline, to wash away unbound proteins. Elution is obtained by a histidine gradient from 0 to 200 mM in the equilibration buffer. The chromatogram shows two peaks: the first has a green colour and contains the cytochrome c oxidase, the second one is deep red and contains the cytochrome bc_1 complex. The elution point is slightly shifted from 150 mM imidazole to 120 mM histidine but the peak containing the complex is very well separated from the rest of the membrane proteins (Fig. 10)

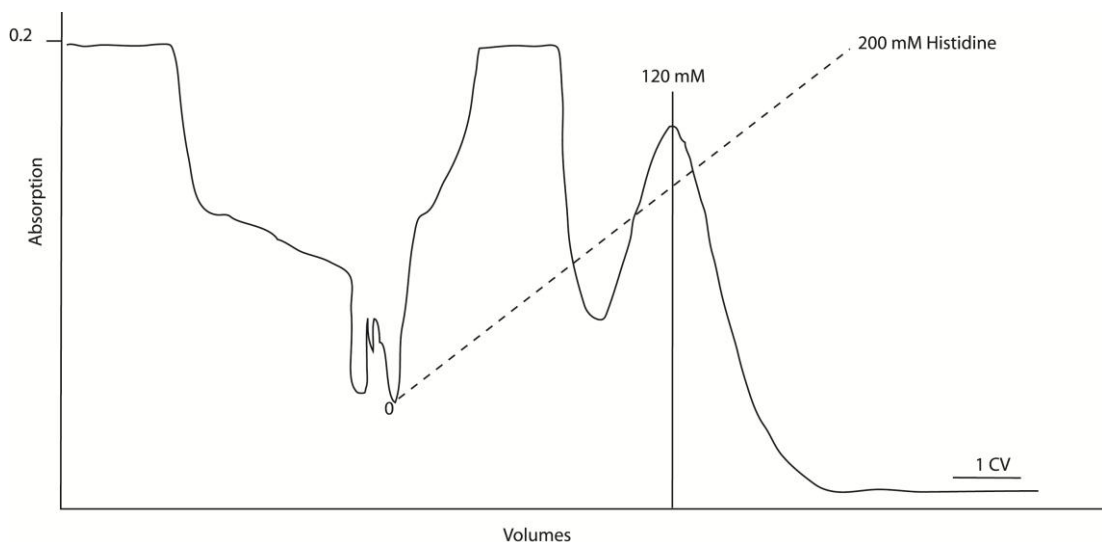


Fig. 10: Purification of MC1 by affinity chromatography (Ni^{2+} -NTA) and elution in presence of histidine. The chromatogram resembles the one obtained with the imidazole elution, with a slightly shifted elution point.

Results

Spectra have been measured also for the complexes purified using the histidine elution, showing that the redox properties are restored, as indicated in Fig. 11. Cytochrome c_1 is already fully reducible with 1 mM ascorbate. No reduction of cytochrome b is now visible.

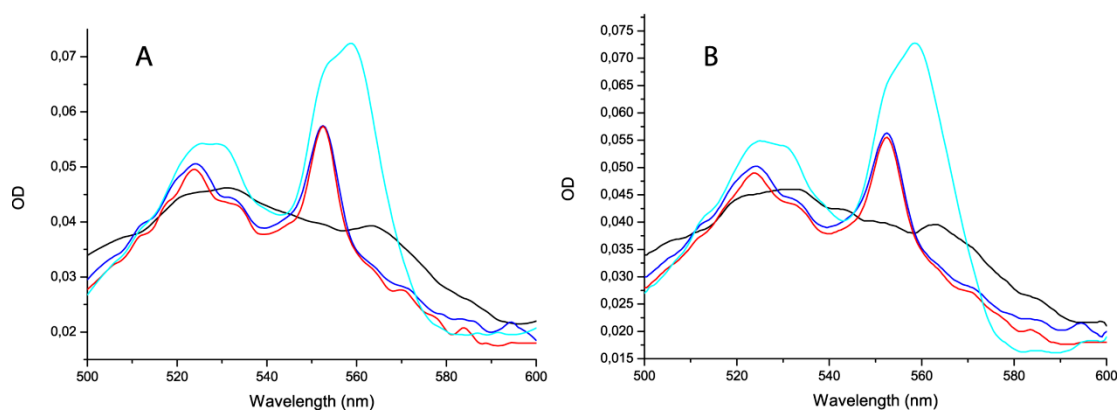


Fig. 11: Static spectra of the His tagged wild type (A) and the mutant (B) bc_1 complex. Small amounts of ascorbate fully reduce cytochrome c_1 , with dithionite also cytochrome b is reduced. In black, the oxidized spectrum; red: 1 mM ascorbate; green: 5 mM ascorbate; blue: 10 mM ascorbate; light blue: dithionite.

To characterize the newly obtained mutant complex and to check possible effects of the mutation on the interaction with the substrate, steady state kinetics were performed. Two different substrates were tested, horse heart cytochrome c and the physiological electron acceptor, cytochrome c_{552F} . Being the latter a membrane bound cytochrome, for all the experiments reported in this work a soluble fragment of it has been cloned and expressed (160) containing only the heme binding domain, from now on referred to as cytochrome c_{552F} . Steady-state kinetics were performed at room temperature measuring the initial velocity of the reaction at several substrate concentrations, repeating each measurement three times for reproducibility. In a disposable cuvette, the appropriate amount of horse heart cytochrome c or cytochrome c_{552F} has been mixed with 25 μ M decylubiquinol and buffer added up to 1 ml final volume. By addition of nanomolar amounts of enzyme, the absorbance increases at 550 nm (horse heart cytochrome c) or 552 nm (cytochrome c_{552F}), showing cytochrome c reduction. The obtained initial velocity has been plotted against several cytochromes c concentrations, and the catalytic constant (k_{CAT}) and the Michaelis constant (K_M) calculated by using the software

Results

Origin 8.0. Table 2 reports the results for the three complexes with both substrates. The catalytic constant is not influenced by the deletion, even though an entire domain (150 residues) is missing. The K_M does not show substantial changes between the wild type and the mutant protein, the latter exhibiting wild type kinetic properties. These results will be analysed in more detail in the section 1.2.3, where the interaction between the bc_1 complex and its substrate is discussed.

	Horse heart cytochrome <i>c</i>		Cytochrome <i>c</i> _{552F}	
	k_{CAT} [s^{-1}]	K_M [μM]	k_{CAT} [s^{-1}]	K_M [μM]
WT	273 ± 25	2,3 ± 0,5	251 ± 13	2,7 ± 0,3
TK33	328 ± 22	3,4 ± 0,3	322 ± 25	4,8 ± 0,9
MC1	357 ± 19	3,1 ± 0,3	315 ± 13	3,8 ± 0,2

Table 2: Steady-state kinetics with two different substrates. WT: wild type bc_1 complex; TK33: wild type His tagged complex; MC1: His tagged acidic domain deletion mutant.

In collaboration with the group of Prof. Petra Hellwig in Strassbourg redox potentials of the three complexes were measured, to be sure that the introduction of the His tag and the deletion of the acidic domain did not affect the redox potential of cytochrome *b* and c_1 . The results are shown in Table 3, clearly meaning that neither the affinity tag nor the deletion have influence on the redox potential of the hemes.

	cyt b_L	cyt b_H	cyt c_1
Wild type	-175 mV	80 mV	211 mV
Wild type His tagged	-141 mV	90 mV	227 mV
His tagged deletion mutant	-178 mV	95 mV	223 mV

Table 3: Redox potentials of the wild type, wild type His tag and the His tagged deletion mutant. The insertion of the His tag and the deletion of an entire domain do not affect the redox potentials of the two *b* hemes and the cytochrome c_1 .

In previous experiments, LILBID MS (177) was used to analyse the oligomerization state of the wild type and the deletion mutant protein. The wild type complex appears to be a “dimer of dimers”, where two dimeric structures stably associate.

Results

The reason for such an association is unknown. The same analysis on the deletion mutant gave unexpected results, since the association of dimers is not visible at all, and the spectra obtained clearly indicate the presence of dimeric structures in solutions. The results are confirmed by the crystallographic structure obtained by Thomas Kleinschroth in collaboration with the group of Prof. Carola Hunte (Kleinschroth *et al.*, manuscript submitted).

The deletion mutant of the *P. denitrificans* cytochrome bc_1 complex shows kinetic properties like the wild type protein, but the deletion of the acidic domain influences the oligomerisation state. Being a dimer and not an association of two dimers, the newly obtained complex was chosen as substrate for the studies to investigate the dimeric nature of the bc_1 complex and to validate the half-of-the-sites mechanism.

3.2 Heterodimeric cytochrome bc_1 complex

The half-of-the-sites mechanism describes an internal regulation mechanism (section 1.2.4.3) influencing the activity of the two monomers in the dimeric bc_1 complex. According to the results observed by Covian *et al.* (60, 62, 143, 144, 148), the Q_i site occupancy in one monomer can regulate the activity of the other one.

Intermonomeric electron transfer between the b_L hemes enables the complex to maximize the presence of electron acceptors in order to avoid the formation of ROS. One way to prove this mechanism is the inactivation of just one monomer by inserting a mutation in its Q_o site. The second monomer carries no mutation and is fully active. In this way, the stimulation observed in presence of antimycin should not be visible, with the second quinol oxidation site inactive. Still, the reduction of two cytochrome b_H per dimer can be achieved by b_L - b_L electron transfer between monomers. The protein needed for this approach is a heterodimeric bc_1 complex, as schematically indicated in Fig. 12. The heterodimeric cytochrome bc_1 complex is composed of a monomer which carries a mutation at the Q_o site inactivating quinol oxidation without affecting the K_M for the substrate. The second monomer shows full wild type properties. To be able to analyze the presence of the two monomers, they have been labelled with affinity tags, associating the inactivating mutation with the His tag and the wild type monomer with the Strep tag II. This allows performing a sequential purification, to isolate the heterodimeric complex.

Results

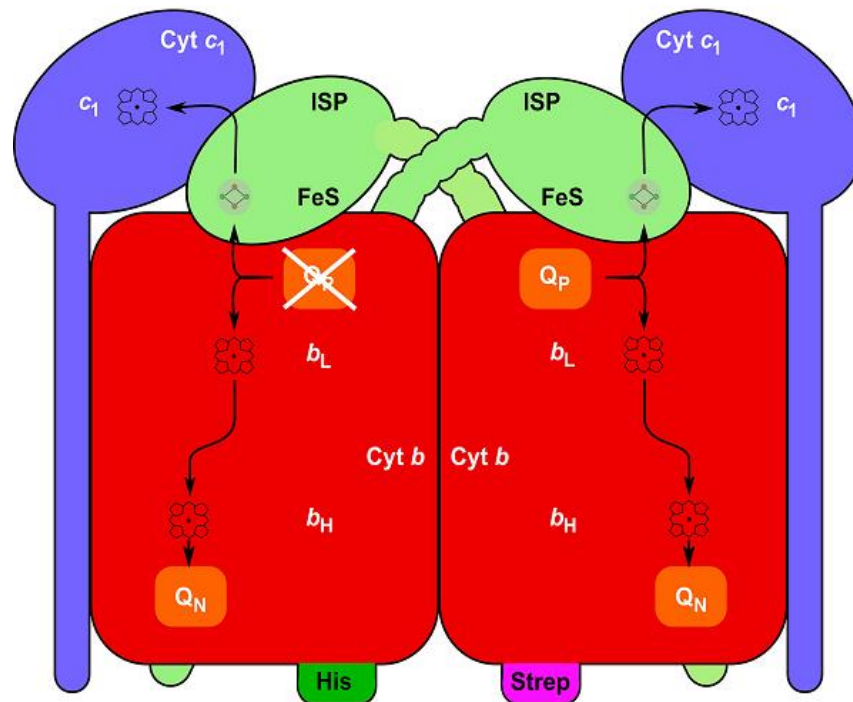


Fig. 12: Heterodimeric bc_1 complex from *P. denitrificans*. One monomer carries an inactivating mutation in the Q_o site, so that only one fully active quinol oxidation site is present in the dimer. The two monomers are separately cloned on two expression plasmids, each of them with a different tag. After homologous expression, the heterodimer is obtained by sequential purification.

The mutation used for the Q_o site has been described first by Saribas *et al.* in *Rhodobacter* (153): mutation of the Tyr¹⁴⁷ to a Ser impairs electron transfer to the heme b_L from the quinol oxidation, with a remaining activity of about 10 %, without modifying the affinity for the substrate (see 4.1, Fig 70). In this way, any effect on the activity of the second Q_o site is due only to the presence of the half-of-the-sites mechanism and not to changes in the K_M for quinol. To obtain the heterodimeric complex, it was necessary to clone two different versions of the *fbc* operon: one modified with the mutation in cytochrome *b* and the His tag at the C-terminus of cytochrome *b*, and the other carrying a Strep tag II, at the same position. Each operon was cloned in an expression vector and mated into *P. denitrificans* MK6 cells, where the *fbc* operon has been substituted with the Km resistance.

The plasmids used were a pEG400 (109), which was used with the mutated, His tagged version of the operon, and a pBBR1-MCS5 (158) with the wild-type, Strep

Results

tagged version of it. The two plasmids have different origins of replication. The vectors were chosen in order to avoid loss due to incompatibility. In fact, two vectors having the same origin of replication (*oriV*) are incompatible, meaning that just one of them is replicated and passed on to the daughter cells (180). The two copies of the operon cloned in the expression vectors are represented in Fig. 14. The resulting plasmids were pMC12 (S147Y mutation in cytochrome *b* and C-terminal 10X His tag) and pTK56 (wild type cytochrome *b* and C-terminal Strep tag II), respectively 11 kb and 8.1 kb. In the cell, the expressed subunits are able to freely associate and form three different kinds of dimers: one containing only monomers carrying the His tag (and therefore the mutation), one being just wild type and only Strep tagged, and the heterodimer. To separate heterodimers from the other two combinations, a sequential purification strategy has been developed, including a Ni^{2+} -NTA column followed by a StrepTactin, to first separate the only Strep tagged dimers and then the just His tagged ones. The purification strategy is exemplified in Fig. 13.

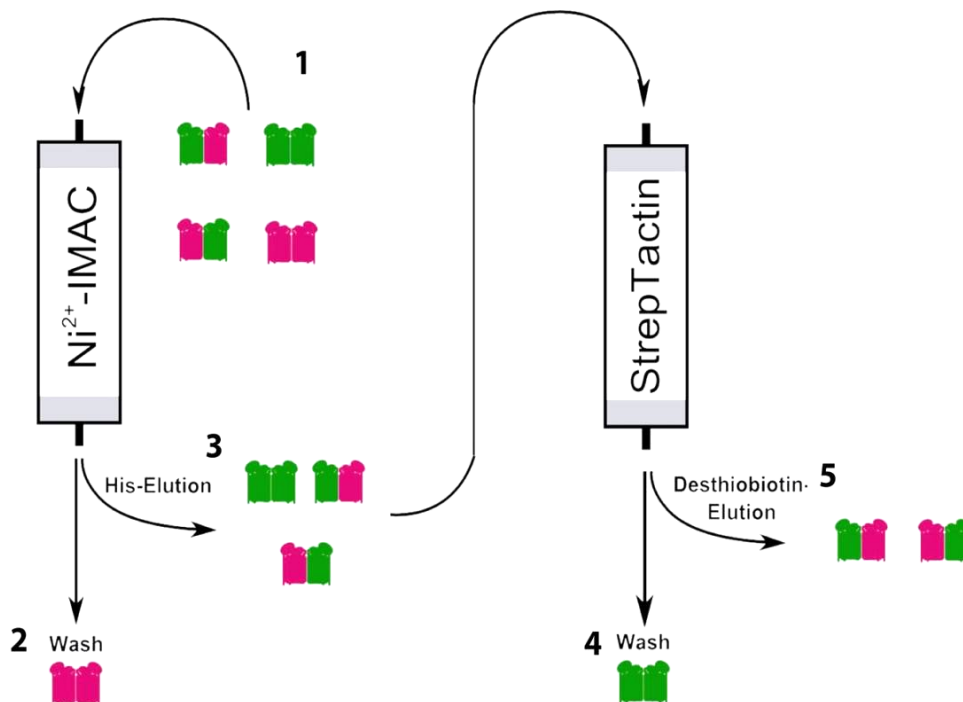


Fig. 13: Schematic representation of the purification strategy developed to obtain the bc_1 heterodimer. The pink monomers carry a Strep tag, whereas the green ones a His tag. After membrane solubilisation, three different combinations of the tags are possible (1). With the Ni^{2+} -NTA, the only Strep tagged monomers are washed away (2), and the eluate from the first column is loaded onto the StrepTactin (3). Here, monomers carrying only a His tag are separated (4) from the heterodimers (5).

3.2.1 Genetic background, mating and purification

As already mentioned, the protein used in this project is the deletion mutant of the *Paracoccus denitrificans* wild type complex. Two different versions of the *fbc* operon have been cloned, TK56 and MC12, as indicated in Fig. 14.

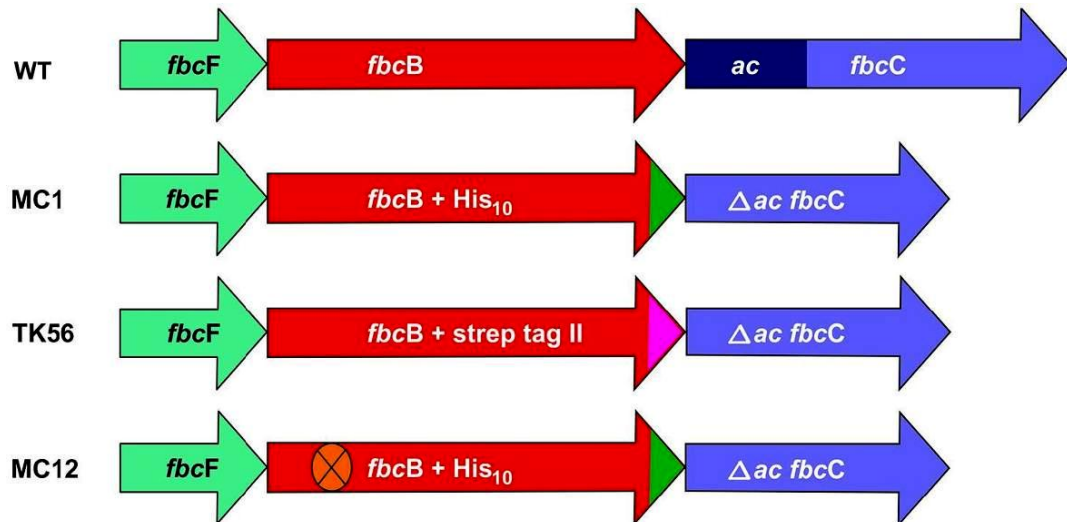


Fig. 14: *fbc* operon wild type and the Δac *fbc* operon (MC1). TK56 is the *fbc* operon with the Strep tag and MC12 is the His tagged one containing also the Y147S mutation in cytochrome *b*. Graphics from (152).

pTK56 (8132 bp) is a pBBR1-MCS5 derivative (158), containing the Δac *fbc* operon with a Strep tag at the C-terminus of cytochrome *b*, inserted by using a SOEing PCR (Splicing by Overlap Extension) [111, 124, 125]. pMC12 (11000 bp) is pEG400 derivative (109) with a His tagged Δac *fbc* operon and the mutation Y147S cloned by Pfl23II/SacI restriction from the plasmid pTK44 (152). pTK56 and pMC12 carry the resistance for Gm and Sm, respectively. Since the efficiency for chemical transformation or electroporation in *P. denitrificans* is not high, the strategy chosen to transfer the plasmids was conjugation. Vectors used in the laboratory do not possess *tra* functions, which would allow the bacterium to freely transfer genetic material to other bacterial cells. For conjugation to occur, it is necessary to use a helper strain, (*E. coli* RP4-4, Amp^R), which carries the plasmid-encoded *tra* genes necessary to transfer genetic material. The donor strains (containing each pTK56 and pMC12), the helper strain and the recipient *P. denitrificans* strain (MK6, Rif^R and Km^R) are mixed and pipetted in a single drop on a LB agar plate. This allows the helper strain to transfer its vector containing the *tra* functions to the two donor

Results

strains, which are now able to carry over the vectors to *P. denitrificans* cells. Selection occurs by pipetting a dilution series and streaking the cells on agar plates containing four antibiotics (Sm, Gm, Km and Rif) to select specifically *P. denitrificans* clones containing both expression vectors. After two days of incubation at 32° C, few clones were visible on the plates, with a much lower efficiency than the one normally observed for the conjugation of a single plasmid. The clones were inoculated and plasmid DNA prepared from them. The presence of the plasmid is the confirmation of the successful mating, since the strain used for the conjugation normally lacks plasmid DNA.



Fig. 15: Agarose gel from the plasmid DNA prepped from colonies 1 to 15 obtained after *P. denitrificans* conjugation with pTK56 and pMC12. The DNA was digested with Bpu1102I (single cutter in the Sm resistance gene) and BglII (single cutter in the Gm resistance gene). Ladder: λ phage DNA cut with EcoRI/HindIII.

The agarose gel in Fig. 15 shows the digestion of the plasmid DNA obtained from the colonies after conjugation. The enzymes used, Bpu1102I and BglII, are single cutters for the antibiotic resistances, Sm and Gm respectively. In lanes 2, 11, 13 and 15 the two bands at the top of the gel are respectively the linearized pMC12 and pTK56, followed by two more bands corresponding to supercoiled plasmids. *Paracoccus denitrificans* DNA has a high GC % content and a high degree of methylation, which leads sometimes to incomplete digestion.

From the colonies 3, 11, 13 and 15 cultures were used for the preparation of membranes on an analytical scale. Membranes with a total protein content of 150 μ g were applied on SDS PAGE. Western blot analysis using an antibody directed against the His tag and the Strep tag II indicated the presence of a band reacting

Results

with the two antibodies, at an apparent molecular weight of about 40 kDa, being most likely cytochrome *b*. Unexpectedly, also two unspecific bands appeared, in the Western blot for the Strep tag II, at low molecular weights, being with high probability biotinylated small proteins. The antibody directed against the Strep tag II binds with a high efficiency biotinylated proteins: to avoid this, traces of avidin are added to the blocking solution. In this way, avidin reacts promptly with biotin, leading to less unspecific bands. In order to obtain a much cleaner result, cells were grown on a preparative scale (50 L) and membranes prepared. For the purification, the same protocol was used as for the purification of the deletion mutant. The cytochrome *bc*₁ complex was solubilised using a 1.15 : 1 ratio detergent to total membrane protein in a 50 mM sodium phosphate buffer pH 8, containing 600 mM NaCl, and stirred for one hour on ice. After solubilisation, the sample was loaded onto the Ni²⁺-NTA column (Fig. 16). The flow rate was set to 1 ml/min, to allow efficient binding to the column. Not only the His tagged cytochrome *bc*₁ complex binds to the Ni²⁺-NTA, but also the cytochrome *c* oxidase from *P. denitrificans*, in an unspecific manner. The column was washed with 1 CV equilibration buffer, which washes away all the unbound protein, among these, also the Strep tagged dimers. The elution is performed with a 5 CV histidine gradient, from 0 to 200 mM, to elute first the unspecifically bound oxidase and finally the *bc*₁ complexes containing at least one His tag (heterodimeric complex and homodimer with the Y147S mutation in both monomers). In Fig 16, peak 1 shows a green colour, typical for the cytochrome *aa*₃ oxidase, and appears to be well separated from the peak number 2, red coloured, containing the cytochrome *bc*₁ complex. The eluate from the Ni²⁺-NTA column (peak 2) is loaded onto the StrepTactin column without concentrating the fraction. After loading, the StrepTactin column is washed with buffer until the chromatogram goes back to baseline, to avoid any contamination of the homodimer containing the mutation in both monomers. After the washing step, the protein bound on the StrepTactin (heterodimeric *bc*₁ complex) is eluted in a single step with a buffer containing 2.5 mM desthiobiotin (lower chromatogram in Fig. 16).

Results

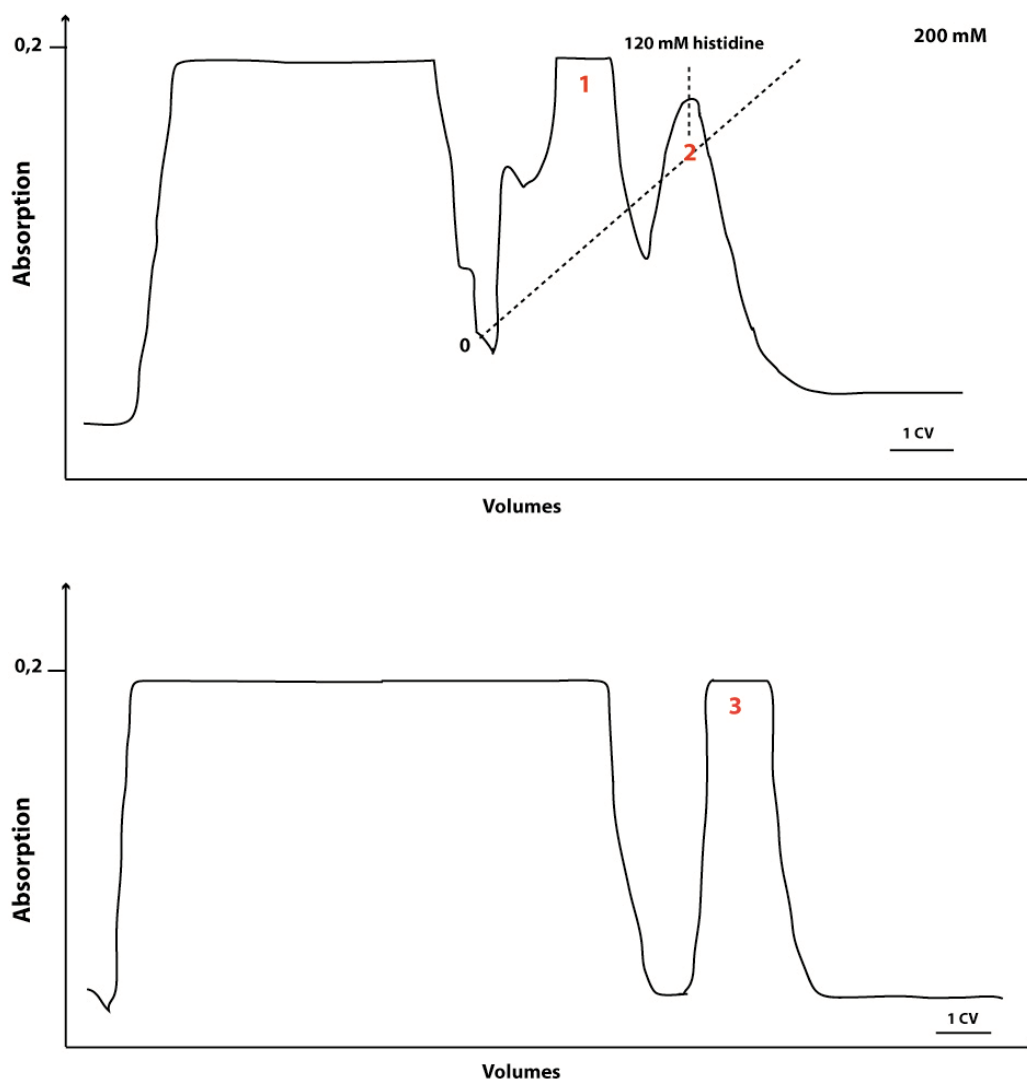


Fig. 16: Chromatograms of the sequential purification. Upper panel: Ni²⁺-NTA column. Two peaks are visible, the first one is the $\alpha\alpha_3$ oxidase which binds unspecifically on the column and elutes early as the gradient starts. When the gradient reaches 90 mM histidine, the bc_1 complex elutes. The eluate is directly loaded onto the StrepTactin column, where only the heterodimer binds. The column is washed until the absorption reaches baseline and eluted in a single step with a buffer containing 2.5 mM desthiobiotin.

The eluate has been concentrated and tested by redox spectra, SDS PAGE and Western blot (Fig. 17 and 18).

Results

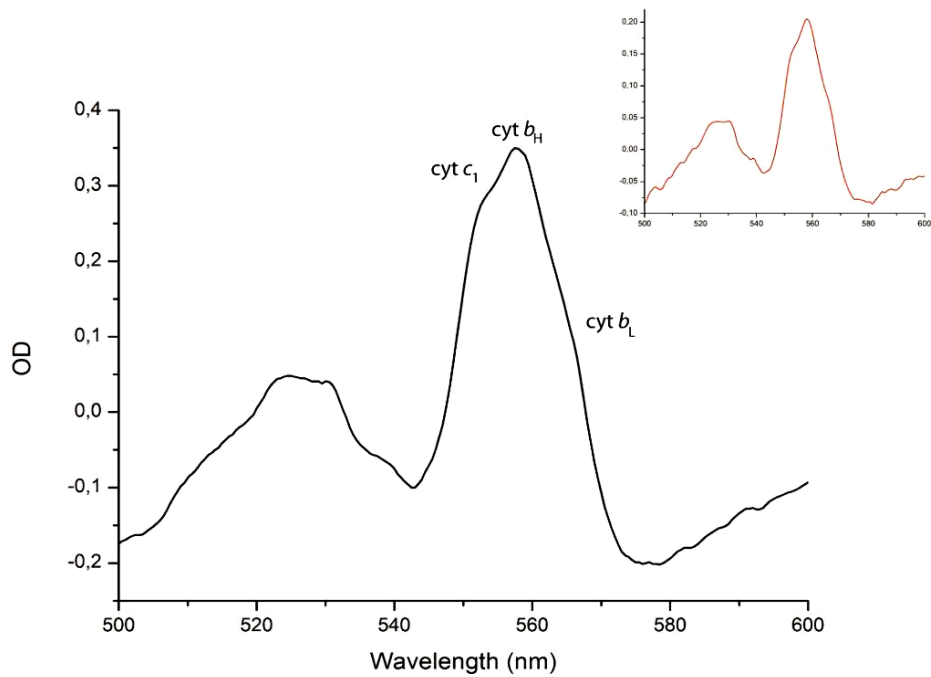


Fig. 17: Mixed dimer redox spectra. In the figure the absorbance peaks for cytochrome c_1 and cytochrome b are indicated. Inset, a redox spectrum of the $\Delta ac bc_1$ complex (MC1) from *P. denitrificans* as comparison.

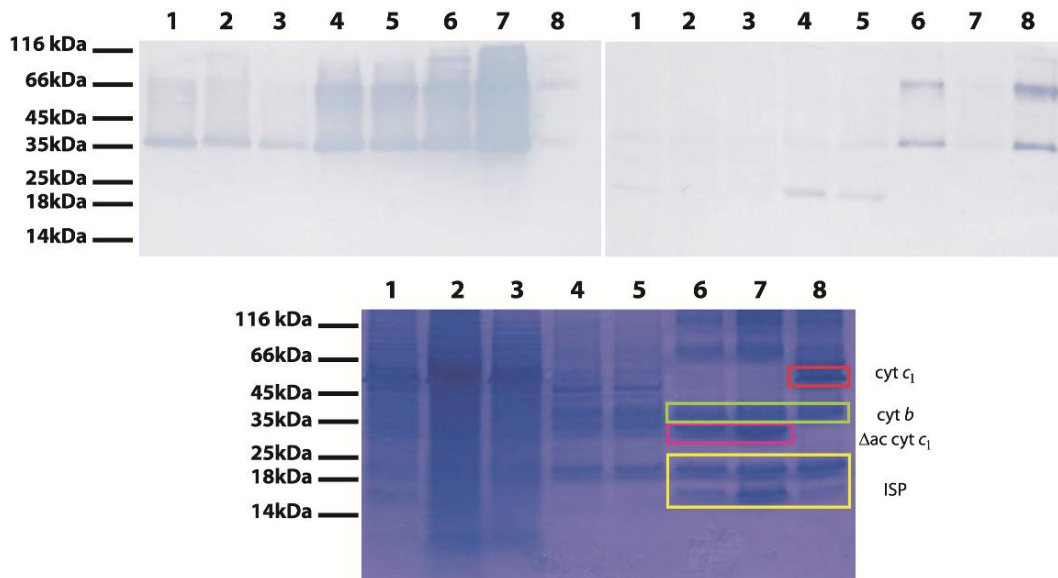


Fig. 18: anti His tag blot (top left) and anti Strep tag II blot (top right). Bottom: SDS PAGE with fractions from the purification. 1: solubilisate; 2: flowthrough Ni^{2+} -NTA; 3: wash Ni^{2+} -NTA; 4: flowthrough StrepTactin; 5: wash StrepTactin; 6: mixed dimer (TK56/MC12); 7: $\Delta ac bc_1$ complex (MC1); 8: WT Strep tagged bc_1 complex from *P. denitrificans*. In the red rectangle, the wild type cytochrome c_1 ; in the green one, cytochrome b ; in magenta the deletion form of the cytochrome c_1 and in yellow the ISP. The latter appears typically in two bands, most likely representing different unfolded states of the head domain.

Results

The redox spectra confirm that the mixed dimer presents no differences in comparison to the $\Delta ac bc_1$ complex, and that the mutation at the Q_o site shows no effects on the cytochrome b_L spectrum. As can be seen from the SDS PAGE in Fig. 15, the bands for the ISP, cytochrome c_1 and cytochrome b are visible (respectively 20 kDa, 30 kDa and 35 kDa), and the ISP presents two bands, as already described for the complex from *P. denitrificans* (152). Two additional bands are visible, most likely due to incomplete denaturation: around 65 kDa a band formed by cytochrome b and cytochrome c_1 associated, and around 130 kDa a complex dimer missing the ISP, as confirmed by Western blots with antibodies directed against the two tags both at the C terminus of cytochrome b . Notably the difference in the running behaviour between the wild type cytochrome c_1 and the one from the $\Delta ac bc_1$ complex: the presence of the acidic domain makes the subunit run at an apparent mass of about 65 kDa (calc. mass 47 kD), whereas without the domain it runs as expected. In summary, from the redox spectra, SDS PAGE and Western blots it is obvious that a complex has been purified, which shows wild type spectra and a signal for both the His tag and the Strep tag II. Therefore, it is possible to proceed with the kinetic studies to address the half-of-the-sites mechanism. As controls, two complexes were analysed: a dimer in which both monomers carry a C-terminal Strep tag II and cytochrome b is wild type, and a dimer with His tagged, mutated monomers. This permits to follow the behaviour of each monomer in the heterodimer.

3.2.2 Pre steady-state ubiquinol oxidation by the cytochrome bc_1 complex in absence of antimycin

After purification, the heterodimer (TK56/MC12) and the two controls (TK56/TK56 and MC12/MC12) have been tested by stopped flow analysis, in order to prove the composition of the heterodimer and to characterize it.

The first kinetic study was to follow cytochrome c_1 reduction. In the stopped flow apparatus, a volume of buffer containing 2 μ M of each complex was mixed with an equal volume of buffer containing 40 μ M ubiquinol. Eight different signals were averaged after subtracting the oxidized spectrum. The results are shown in Fig. 19.

Results

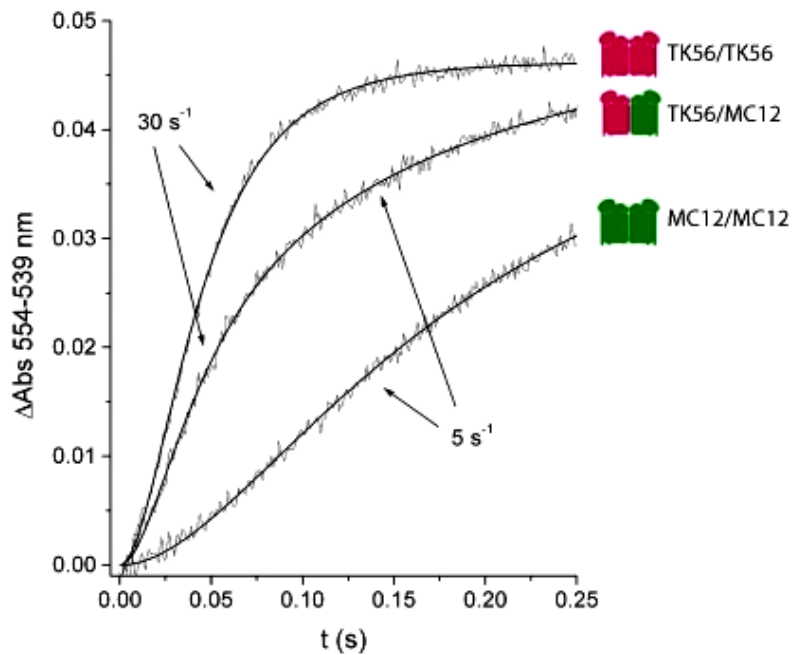


Fig. 19: Pre steady-state cytochrome c_1 reduction. Upper trace, wild type Δac homodimer. Middle trace: heterodimer. Lower trace: Y147S Δac homodimer. Cytochrome c_1 reduction was recorded at 554 nm and corrected by subtracting the oxidized spectrum.

The upper trace corresponds to the wild type $\Delta ac bc_1$ complex, and the lower to the mutated Δac complex. Both of them are single phase traces, with a rate of, respectively, 30 s^{-1} and 5 s^{-1} . The heterodimeric complex shows, on the contrary, a biphasic kinetic, with rates corresponding to the upper trace (fast phase) and to the lower trace (slow phase). The two phases have the same amplitude (about 50% each). This result indicates clearly the presence of a heterodimer, and confirms what already the Western blot analysis showed. In the heterodimer, one monomer carries the Y147S mutation at the cytochrome b , which reduces the activity of the complex to a residual 10 % without influencing the K_M for the substrate. The other monomer is a Δac wild type complex, and able to faster oxidize ubiquinol. The two phases are a reflection of the heterodimer composition: both monomers have the same affinity for ubiquinol, but the kinetic of the mutated monomer becomes visible only when the high potential chain of the wild type half starts accumulating electrons due to the faster turnover. At that point, the cytochrome c_1 from the wild type monomer cannot be reduced anymore, since no electron acceptor is present. The high potential chain is then blocked and the mutated monomer is now visible, due to its slower kinetic.

Results

At the beginning of the traces, a short lag phase is observable, better visible in the case of the mutant homodimer. This might be due to partitioning between the detergent micelles of the substrate after rapid mixing, which becomes more evident in the case of MC12 due to the slower turnover rate.

3.2.3 Steady-state kinetics

According to the half-of-the-sites mechanism, only one monomer is able to oxidize ubiquinol in a given turnover. In this way the production of ROS is minimized, since the production of a semiquinone at a single Q_o site allows having up to six electron acceptors in the dimer (see 1.2.4.3). This means that only one monomer at a time accounts for the activity of the complex. In the heterodimer, where one Q_o site has only a small residual activity, the turnover number is expected not to change, nor the affinity for ubiquinol. Therefore, Michaelis-Menten kinetics can verify two important aspects: first, that the heterodimer has the same affinity for ubiquinol, second whether there is any change in the v_{MAX} due to the insertion of the mutation.

In the stopped flow apparatus, one volume of buffer with 100 nM enzyme and 20 μ M cytochrome *c* from horse heart is mixed against an equal volume of buffer containing increasing concentrations of decylubiquinol. Six traces for each quinol concentration were recorded and the time course of absorbance change between 550 nm and 539 nm used to obtain the turnover numbers expressed as moles of cytochrome *c* reduced per moles of cytochrome bc_1 complex. The resulting turnover numbers have been plotted against the substrate concentration. As shown in Fig. 20 and indicated in Table 4, the upper trace (Δac bc_1 complex) and the middle trace (heterodimer) do not show any significant difference. The v_{MAX} is the same for the two complexes, meaning that the inactivation of one monomer does not influence the kinetics of the dimer. The Michaelis constant is also not changed: the apparent affinity for the substrate is not influenced from the mutation, as already described elsewhere (153). In the case of MC12/MC12, the v_{MAX} is about 10 fold lower than the wild type and the heterodimer; on the other side, the K_M is decreased, meaning a higher apparent affinity for the substrate. Actually, this could be due to the smaller contribution of k_{CAT} to the K_M of the mutant homodimer, which represents an apparent dissociation constant.

Results

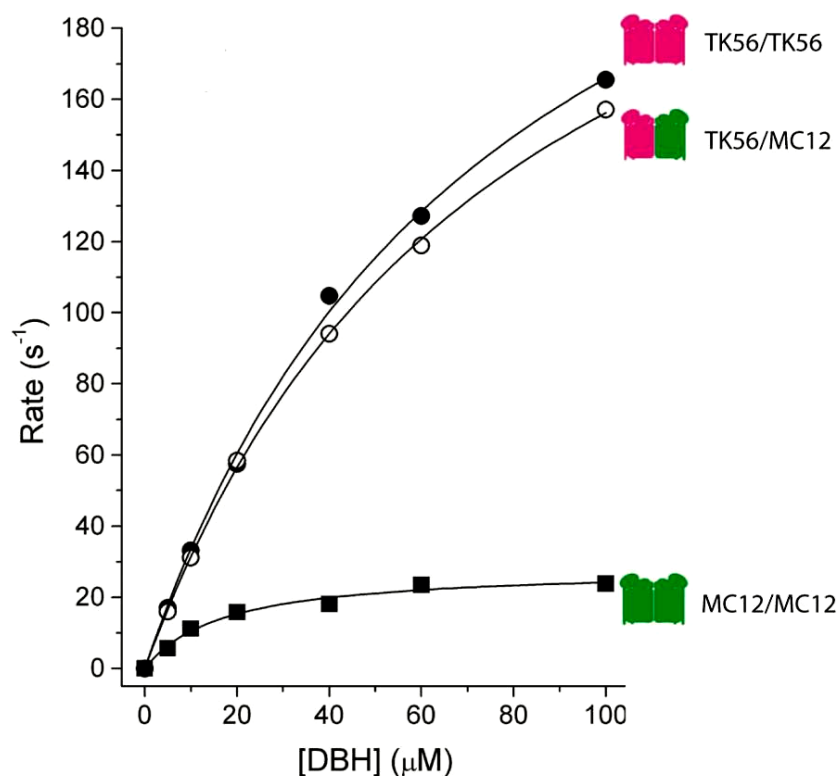


Fig. 20: Michaelis-Menten kinetics with the three complexes. Upper trace: $\Delta ac bc_1$ complex; middle trace: heterodimer; lower trace: $\Delta ac Y147S bc_1$ complex.

	$v_{MAX} [s^{-1}]$	$K_M [\mu M]$
TK56/TK56	294.6 ± 14	77.5 ± 6.6
TK56/MC12	279.3 ± 7.4	78.8 ± 3.7
MC12/MC12	28.2 ± 1.6	31.7 ± 2.9

Table 4: v_{MAX} and K_M values for the three complexes. As indicated, no significant difference can be seen between TK56/TK56 and the heterodimer TK56/MC12, meaning that only one monomer is working at a time in the dimeric complex.

The results from the steady-state kinetics represent a first confirmation of the half-of-the-sites mechanism, since they show that inactivating one of the monomers does not change the v_{MAX} of the enzyme. In the case of the two monomers working independently of each other, one would expect the heterodimer to be 50 % slower than the wild type homodimer, which is clearly not the case.

3.2.4 Pre steady-state ubiquinol oxidation by the cytochrome bc_1 complex in presence of antimycin

According to the half-of-the-sites mechanism, the cytochrome bc_1 complex equilibrates electrons between monomers in the dimer, in order to reduce the possibility of ROS production. When, for instance, antimycin is bound at the Q_i site, electrons are stuck in the high potential chain and may readily react with oxygen. Electron equilibration between monomers plays an important role by passing them to the other monomer in order to maximize the number of potential electron acceptors in the complex, to transfer them fast and avoid the side reaction with oxygen.

In presence of antimycin, a Q_i site inhibitor, electrons can enter the complex only through the Q_o site. Center N is blocked by the inhibitor, so quinol, semiquinone and quinone do not bind the complex. In the stopped flow apparatus, 2 μ M cytochrome bc_1 complex inhibited with 2,5 μ M antimycin have been mixed against 40 μ M decylubiquinol and the absorbance changes followed up to 800 ms at 554-539 nm for the cytochrome c_1 , and 563-578 nm for cytochrome b_H . The results can be seen in Fig. 21, 22 and 23. The Δac bc_1 complex (TK56/TK56) shows the reduction of one cytochrome c_1 and two cytochrome b_H per dimer. The reduction of cytochrome b_H is on the left panel, corresponding to the spectra taken at 20, 50, 100, 200 and 400 ms: only a peak at 560 nm (representing 70% of the total cytochrome b present in the observation chamber) can be seen (cytochrome b_H) and no shoulder at 566 (cytochrome b_L) is visible. The heterodimeric Δac bc_1 complex shows the same results: even if one of the two Q_o sites is inactivated, there is still reduction of two cytochrome b_H and one cytochrome c_1 . This supports the results obtained from the steady-state kinetics, according to which only one monomer is working at a time (if the monomers were working independently from each other it should be expected to see, in the first panel, reduction of two cytochromes c_1). It also shows that even in the case of inactivation of one center P, two cytochromes b_H are still getting reduced per dimer. The only way to achieve this is electrons to equilibrate between monomers. In the case of TK56/TK56 electrons can enter the complex through two centers P, but in the heterodimeric complex only one center P is able to oxidize quinol. The rates of reduction of cytochrome b_H in the two complexes are very similar, as indicated in table 5, whereas in the case of MC12/MC12, the Δac Y147S bc_1 complex, they are at least 7 times slower. At the given timescale, the reaction is

Results

far from being completed. If the two b_H hemes were reduced from electrons coming from two different centers P, slower cytochrome b reduction kinetics should be observed in the heterodimer, due to the much slower ubiquinol oxidation at the mutated center P. This result validates the occurrence of intermonomeric electron equilibration.

	Cyt b_H reduction [s ⁻¹]	Cyt c_1 reduction [s ⁻¹]
TK56/TK56	20	7.4
TK56/MC12	20.9	8.2
MC12/MC12	3.1	1.3

Table 5: Rates for the reduction of cytochromes b_H and c_1 in the three complexes in presence of antimycin. Errors are within 10% of the measurements.

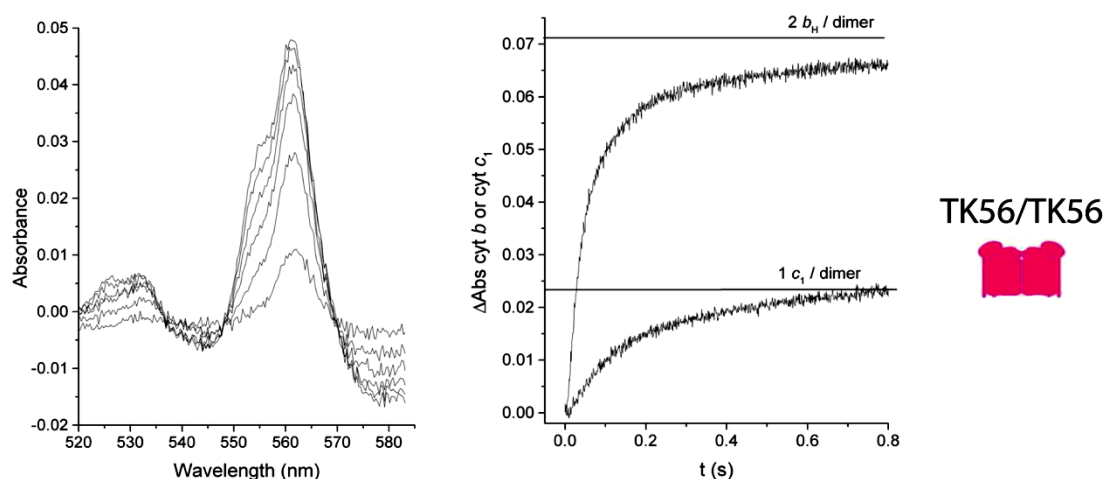


Fig. 21: Pre steady-state oxidation of ubiquinol at the Q_o site in presence of antimycin for the homodimeric $\Delta ac bc_1$ complex. Two cytochrome b_H and one cytochrome c_1 are reduced per dimer, when antimycin is bound at both Q_i sites in the dimer.

Results

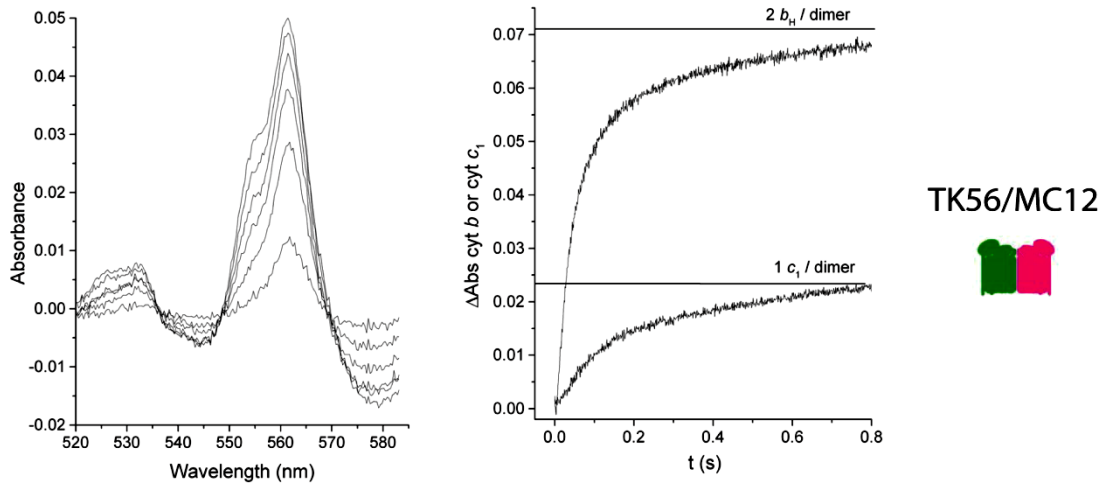


Fig. 22: Pre steady-state oxidation of ubiquinol at the Q_o site in presence of antimycin in the heterodimeric complex. The inactivation of one Q_o site still allows the reduction of both cytochromes b_H in the dimer and only one cytochrome c_1 is reduced.

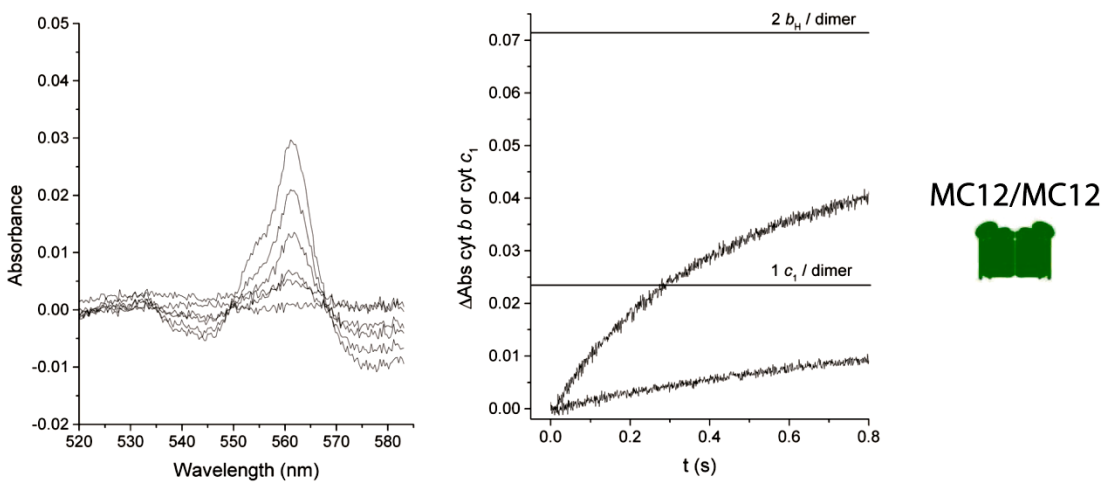


Fig. 23: Pre steady-state oxidation of ubiquinol at the Q_o site in presence of antimycin. In the homodimeric mutant complex, due to the mutation, the rate of cytochrome b_H and cytochrome c_1 reduction is much slower than the wild type complex.

3.2.5 Antimycin titrations

As shown with the yeast enzyme, substoichiometric amounts of antimycin increase the cytochrome c reduction. When the ratio antimycin : bc_1 monomer reaches 25 %, the activity of the complex increases, and decreases slowly as the inhibitor : monomer ratio increases further. This is a paradoxical effect, considering antimycin as an inhibitor, but can be explained by the half-of-the-sites mechanism, in which

Results

dimers having semiquinone bound at one center N are both able to react and oxidize quinol. On the other hand, when none or both centers N are occupied, only one monomer can oxidize the substrate. In other words, the occupancy of the Q_i site in the complex can stimulate the second, otherwise inactive monomer to react with quinol and participate in turnover. Antimycin simulates quite well a semiquinone bound at the Q_i site, so that titrating the enzyme with antimycin shows the aforementioned stimulation. In the case of the heterodimer, the second quinol oxidation site is almost totally inactivated due to the introduced mutation, so that the stimulation observed in the wild type complex should not be seen.

In order to test this, a 10 μM solution of enzyme kept on ice was incubated with the indicated amount of antimycin for two minutes, before diluting it to a final concentration of 100 nM with the buffer used for the measurements at room temperature. The final dilution used for the experiments contained also 20 mM horse heart cytochrome c. A volume of the diluted enzyme-inhibitor solution has been mixed with an equal volume of buffer containing 80 μM decylubiquinol, and the absorbance between 550-539 nm used to calculate the turnover number at a given inhibitor : monomer ratio. The results are shown in Fig. 24 for the $\Delta\text{ac } bc_1$ complex (TK56/TK56) and the heterodimer (TK56/MC12).

In the left panel, the titration with the $\Delta\text{ac } bc_1$ complex (TK56/TK56) is shown. The stimulation is visible (solid curve), due to the activation of the second monomer in response to the inhibitor binding to one of the Q_i sites in the dimer. As a consequence to the inhibitor binding on one monomer, the second, otherwise silent, center P is activated, and the enzyme is able to recycle electrons and reduce quinone to quinol through a single Q_i site, thanks to the intermonomer electron equilibration.

Results

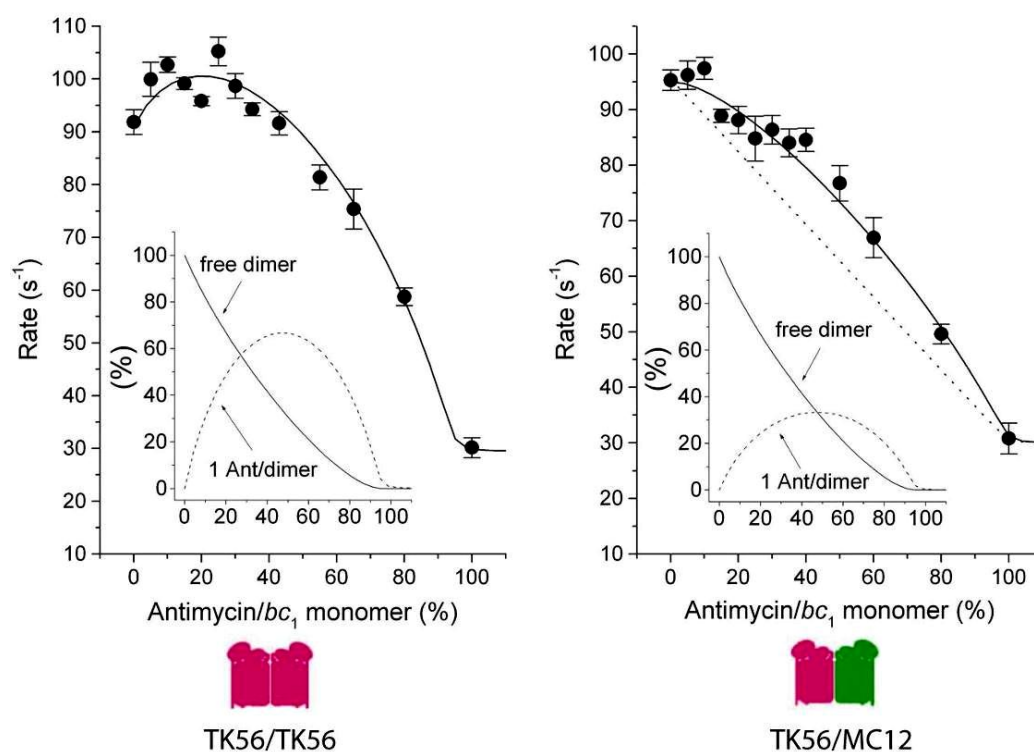


Fig. 24: antimycin titrations. Left: wild type $\Delta ac bc_1$ complex; right: heterodimeric complex. The inset curves indicate the percentages of the inhibitor-free dimer (solid line) and the dimer where one Q_i site is liganded varying with increasing antimycin concentrations.

In the case of the heterodimeric complex, the second otherwise inactivated Q_o site cannot oxidize quinol, at least not as efficiently as the wild type monomer at the timescale used for the measurements, so a stimulation is not observed. The solid curve in the right panel represents the expected behaviour in the case of the monomers with one inhibitor molecule bound having the same activity of the free ones. The dotted straight line in the right panel represents the simulation of the expected inhibition curve assuming that no intermonomer electron transfer takes place and no electron equilibration between the cytochromes b_L is possible.

In the inset, the curves represent how the concentrations of different intermediates vary by increasing the antimycin concentration. The free dimer concentration diminishes constantly. On the other side, the concentration of the intermediate where only one Q_i site binds the inhibitor increases in the beginning, to diminish in favour of the dimer with both Q_i sites occupied by the ligand.

An important feature of the half-of-the-sites mechanism is the electron equilibration between monomers. The solid curves simulate the activation of the second quinol

Results

oxidation site, given that electrons taken up from quinol oxidation at one Q_o site are able to be used for quinone reduction in the Q_i site of the other monomer. If this was not be the case, then the inhibitor bound monomer could oxidize quinol, but electrons coming into the low potential chain would be blocked at the cytochrome b_H in the same monomer without the possibility to reduce quinone (being the site occupied by antimycin). Assuming no electron equilibration, the antimycin bound monomer would have to be considered fully inactive, so that only free monomers could contribute to the activity. This would be the situation depicted in the absence of the half-of-the-sites reactivity.

It is interesting to note that even a 100 % ratio antimycin : bc_1 monomer does not give full inhibition of the cytochrome c reduction. The binding of antimycin leads to electrons accumulating in the low potential chain, blocking the electron flow to quinone or semiquinone. At the Q_o site, quinol can still be oxidized, but semiquinone, eventually present after the first electron has entered the high potential chain, stays at the Q_o site, unable to deliver its electron to the b_L heme, and reacts fast with oxygen increasing the concentration of superoxide in solution. The latter is a very good reductant for cytochrome c by itself, so that the absorbance change seen at high inhibitor concentration is dependent on the cytochrome c reduction in presence of ROS. This activity is sensitive to superoxide dismutase, which can abolish up to 50 % of the activity seen at high antimycin concentration (63). This depends on the fact that one electron coming from quinol oxidation reduces the ISP and cytochrome c_1 and finally the electron acceptor cytochrome c . The second electron bypasses cytochrome b and reacts directly with oxygen to produce ROS, part of which indirectly reduces cytochrome c (Fig. 25).

Results

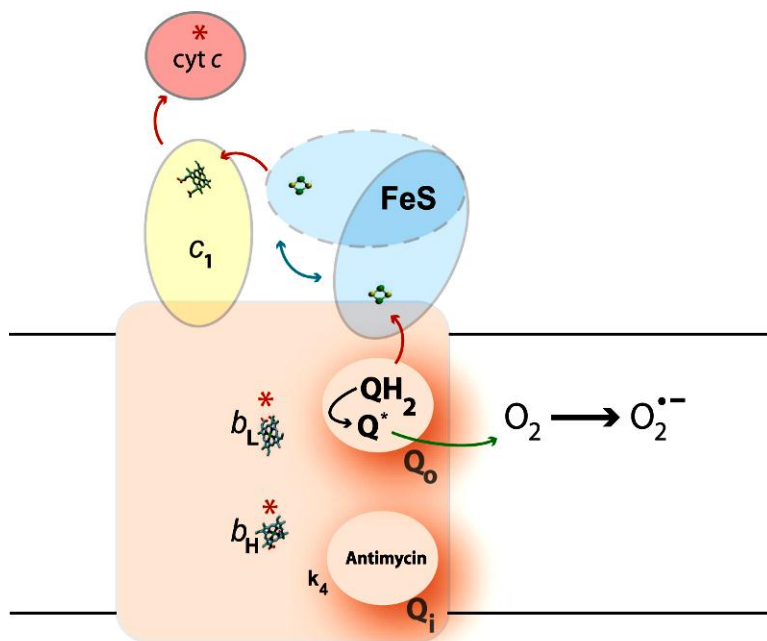


Fig. 25: With antimycin bound at the Q_i site, the low potential chain is blocked. When quinol is oxidized, electrons flow normally through the ISP and cytochrome c_1 to cytochrome c , but they are stuck in the low potential chain since no quinone is bound at the Q_i site. Therefore, after two turnover cytochrome b is fully reduced (red stars). If this is the case, subsequent quinol oxidations at the Q_o site will produce a semiquinone radical, which reacts readily with oxygen and produces superoxide ($O_2^{\bullet-}$).

3.3 Interaction between cytochrome bc_1 of *P. denitrificans* and its cytochrome c substrate

In this part of the work will be analysed the interaction between *P. denitrificans* bc_1 complex and its substrate, cytochrome c_{552} . As already described (1.2.2.2), *P. denitrificans* is the only organism with an acidic domain fused with the cytochrome c_1 protein. The acidic domain has a very peculiar composition, reminiscent of the hinge protein in the bovine complex and of the acidic part of the Qcr6p in the yeast enzyme, even if there is no direct homology. In the two mentioned systems, kinetic studies showed that these subunits are involved in the electron transfer to cytochrome c , the electron acceptor in mitochondria. The interaction is driven by opposite charges on the two interaction partner (cytochrome c_1 and cytochrome c) and the acidic subunits help pre-orienting the electron acceptor versus the donor. The interaction surface is rather hydrophobic, and this

Results

leads to a two-step model with long-range electrostatic interactions and short range hydrophobic ones tightening the transient interaction and making it specific (94, 96, 111, 114, 140). Crystal structures (111) showed that the Qcr6p in yeast has no direct interaction with cytochrome *c*, but the deletion affects the complex activity, probably since the pre-orientation effect is missing.

In most bacterial complexes, only the three catalytically active subunits are present. All the additional subunits present in the eukaryotic complexes are missing, but in *P. denitrificans* the acidic domain in cytochrome *c*₁ most likely resembles the eukaryotic situation. Previous investigations (118) using soluble fragments indicated that no specific role could be assigned to the acidic domain in the interaction with cytochrome *c*_{552F}. Soluble fragments are free to diffuse and to interact with the reaction partner, whereas the whole membrane protein complex, embedded in detergent micelles, are limited in this respect. This means a different experimental setup which is, on the other hand, similar to the situation in the membrane. For this reason, a new investigation was performed with the full membrane complex in order to analyze the kind and modality of interaction, and verify the previously obtained results.

3.3.1 Pre-steady-state laser flash kinetic studies

The interaction between the *bc*₁ complex and its native electron acceptors has first been analysed by stopped flow spectroscopy. The dead time of the instrument, i. e. the time occurring between the start of the mixing and the beginning of the measurement, is 1 ms. Since the reaction starts already in the dead time, the initial part of the kinetic traces was lost, so that only partial measurements could be obtained, not allowing a complete analysis. One way to overcome this problem was the use of laser flash kinetics. With this method, one of the reaction partners is covalently bound via a cysteine residue to a photoactive ruthenium complex. By flashing with an appropriate laser, the excited ruthenium is able to oxidize or reduce the redox center of the protein to which it is bound, according to the reaction conditions (structure and redox properties of the photoactive complex). This method is known as *metal to ligand charge transfer*; in this experiments Ru(2,2'-bipyrazine)₂(4-bromomethyl-4'-methyl-2,2'-bipyridine) (from now on referred as Ru₂) has been used as a photoactive complex. Ru₂-H39C-Cc is the yeast isocytochrome *c* with Cys¹⁰² mutated to Thr (C102T) and a surface Cys introduced in position 39

Results

(H39C), covalently attached to Ru_z. Ru_z-N23C-c_{552F} is the *P. denitrificans* cytochrome c_{552F} with the surface Asn²³ mutated to Cys (N23C) and covalently attached to Ru_z. Two cytochromes c have been used to better investigate the interaction with the cytochrome bc₁ complex: the yeast cytochrome c is known to have a very strong interaction with complex III (116), and this helps having a more complete picture of the effects the deletion brings.

In the following sections, the coupling between redox partner and ruthenium complex, as well as the reaction protocol and the results obtained will be discussed.

3.3.2 Preparation of the ruthenium coupled electron acceptors

The preparation of ruthenium labeled cytochrome c_{552F} was performed by Lois Geren at the University of Arkansas. The position of the cysteine residue for the ruthenium coupling was devised by Julia Janzon in her PhD thesis (116). 5 µl of N23C mutant cytochrome c_{552F} were treated with a 10-fold molar excess of dithiothreitol (DTT) to reduce the cysteines, then concentrated and buffer-exchanged three times using a Centricon Ultracel YM-10 concentrator. The sample was then diluted to 0.1 mM in a volume of 2.0 mL of 50 mM sodium borate buffer (pH 9.0). A 2-fold molar excess of DTT was added to the anaerobic solution of the protein and stirred for 15 minutes, followed by the addition of a 3-fold molar excess of Ru(2,2'-bipyrazine)2(4-bromomethyl-4'-methyl-2,2'-bipyridine) while stirring and under light protection. Ruthenium labeling was continued for 12–18 h in the dark under anaerobic conditions at room temperature. The reaction mixture was then dialyzed extensively against 5 mM sodium phosphate buffer (pH 7.0) to remove excess ruthenium reagent and to lower the ionic strength, then applied to a 5 mm × 50 mm DE53 (DEAE Cellulose) column equilibrated with 5 mM sodium phosphate (pH 7.0). Only unlabeled N23C cytochrome c_{552F} bound to the column while most of the multiple and singly labeled oxidized protein was eluted with 5 mM phosphate buffer in that order. The eluted sample was then again concentrated low salt buffer and minimal DTT (or ascorbate) was added to reduce the Ru_z-N23C-c_{552F} which was further purified by HPLC on a 1.5 cm × 30 cm high-resolution DEAE-52. Multilabeled protein eluted with a 5 mM sodium phosphate buffer washing step. Immediately after the start of a slow salt gradient, a single peak eluted off the DEAE-52 column which had a UV-visible spectrum equal to the sum of one equivalent of N23C cytochrome c_{552F} and 1 equivalent of ruthenium reagent, followed by a peak assigned to

Results

unlabeled N23C cytochrome c_{552F} . The purified Ru_z -N23C- c_{552F} was exchanged three times with 5 mM sodium phosphate buffer (pH 7.0), then concentrated, and frozen at $-80\text{ }^\circ\text{C}$. The overall yield of Ru_z -N23C- c_{552F} was 10-30%.

3.3.3 Redox mediators and reaction conditions

The laser flash system is regenerated after each flash, so that several measurements can be performed with the same sample. This allows reducing the variability in the experiments. In Fig. 26 is represented the scheme of the measurements. For the regeneration of the initial conditions, the redox centers have to be re-reduced after electron transfer. In the cuvette, the bc_1 complex and the ruthenium labeled electron acceptor are mixed, and reduced by using ascorbate and TMPD (N,N,N',N' tetramethyl-phenylendiamine) as a redox mediator. The redox state of the c -type hemes was checked by recording spectra, resulting in a complete reduction. Therefore, before each measurement, the c -type hemes are reduced. After flashing, one electron is transferred from the excited ruthenium photoactive complex to a sacrificial oxidant (step 1), stabilizing the electron vacancy by avoiding back-reactions. The electron acceptor transfers one electron to the ruthenium (step 2), which is then reduced and relaxes to the initial state. At this point, the electron acceptor can receive one electron from the cytochrome c_1 , and its reduction followed at 550 nm for the Ru_z -H39C-Cc or at 552 nm for Ru_z -N23C- c_{552F} . The oxidation of cytochrome c_1 was followed at 557 nm, the isosbestic for Ru_z -N23C- c_{552F} . The wavelengths have been chosen according to the work of Janzon, who analyzed the spectral properties of the electron acceptors used also in this work (116).

Results

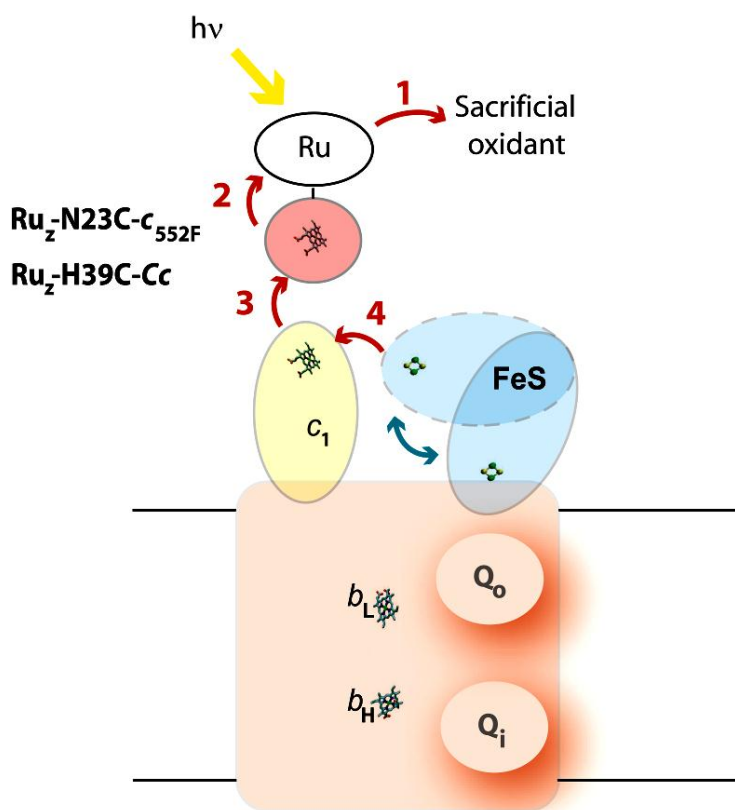


Fig. 26: Mechanism of the laser flash experiments to study the interaction between cytochrome c_1 and several electron acceptors. The red arrows represent the electron transfer steps after flashing and initiating the reaction. The blue arrow indicates the ISP movement to reach cytochrome c_1 (graphic from Castellani *et al.*, 2011, submitted).

After the laser pulse, ruthenium is in the excited state and the c -type heme in the electron acceptor is oxidized. Recording this signal, in absence of the bc_1 complex in the cuvette, gives a so called “step function” (Fig. 27), which reflects the oxidation of the acceptor protein in the photoactive complex. Since no electron donor is present in solution, no absorbance changes should be recorded. If this is the case, then the ruthenium labeled cytochrome is stable, and efficiently being oxidized after the laser pulse. If any absorbance change is recorded, or no step function at all can be seen, the system is not stable and the conditions have to be optimized or new photoactive complex prepared. As visible in Fig. 27, in the case of the ruthenium labeled cytochrome c_{552F} , a buffer containing pentaammineosmium nitrile ($[\text{Os}(\text{NH}_3)_5(\text{CH}_3\text{CN})](\text{CF}_3\text{SO}_3)^{3+}$) as sacrificial oxidant has been tried. After flashing, the signal goes down (cytochrome c_{552F} oxidation, yellow arrow) and stays stable (black arrow), with no absorbance changes in the time. This is a typical step function, meaning that the system was stable and cytochrome c_{552F} successfully oxidized.

Results

Normally, $[\text{Co}(\text{NH}_3)_5\text{Cl}]^{2+}$ is the preferred sacrificial oxidant, since it rapidly decomposes after reaction with ruthenium. This avoids back-reactions which could bring about unwanted reactions with hemes (see 3.3.1). In previous experiments, by Janzon *et al.* (116), was found out that the $[\text{Co}(\text{NH}_3)_5\text{Cl}]^{2+}$ precipitates the cytochrome c_{552F} , so they used Paraquat and aerobic conditions for the studies with the soluble fragments. For the experiments presented in this work, it was not possible to work under aerobic conditions, since small amounts of contaminating oxidase left from the protein preparation, not visible on the SDS PAGE or spectroscopically, could still be present and falsify the measurements. The use of Paraquat (Fig. 28) is not compatible with anaerobic conditions, since when it is reduced it is strongly coloured and interferes with the absorption between 540 and 570 nm. Therefore, the only sacrificial oxidant suitable for these experiments was the osmium complex, even if some backreactions could take place (see 3.3.5). For the experiments with $\text{Ru}_z\text{-H39C-Cc}$, $[\text{Co}(\text{NH}_3)_5\text{Cl}]^{2+}$ was the best experimental condition.

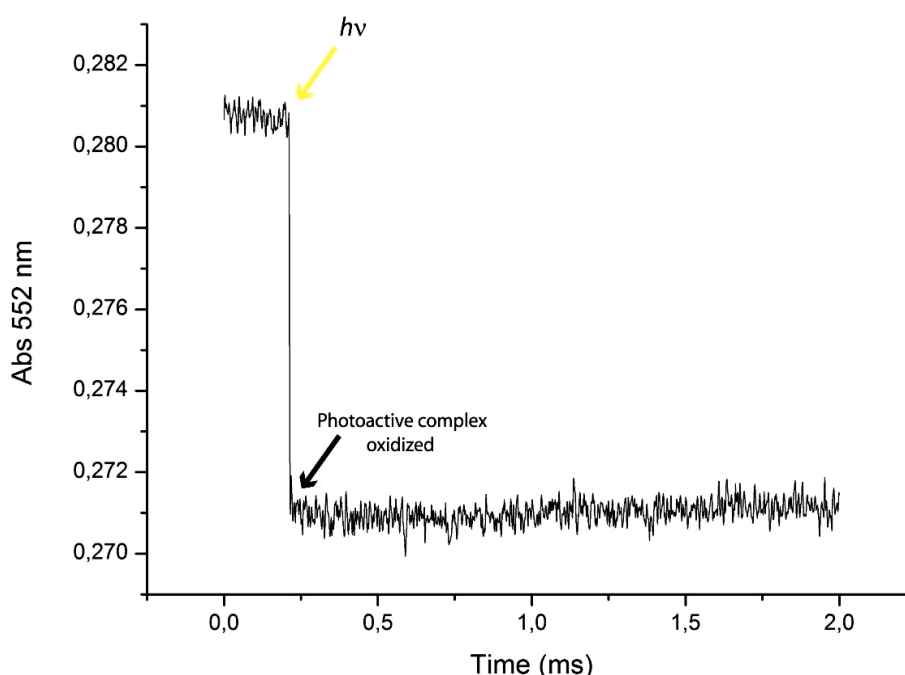


Fig. 27: Step function observed from the Ru-N23C-C_{552F} in presence of the osmium complex as sacrificial oxidant. After the flash (yellow arrow), the signal goes down in respect to the initial baseline (black arrow). This indicates the oxidation of the electron acceptor. Since no cytochrome bc_1 complex is present in this measurement, the signal remains constant. This means the photoactive complex can be oxidized, is stable and can be used for further experiments.

Results

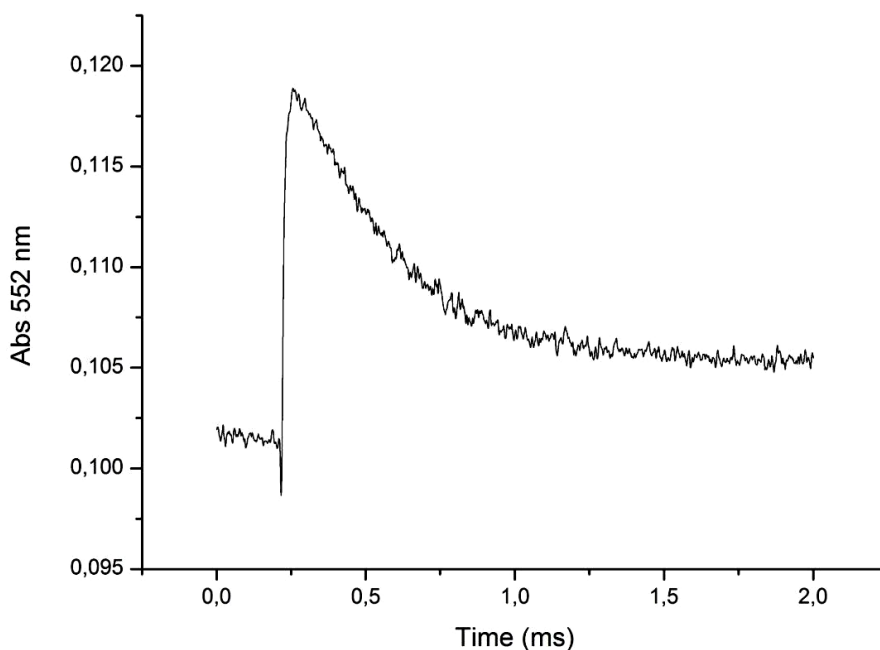


Fig. 28: Step function observed from the Ru-N23C-C_{552F} using Paraquat as sacrificial oxidant. After the flash, the signal goes up to decay slowly almost back to baseline. This is due to the absorption Paraquat has under anaerobic conditions as tested in this work. Therefore, it was not the sacrificial oxidant of choice for these experiments.

Flash photolysis experiments were carried out using a phase R model DL 1400 flash lamp-pumped dye laser and a detection system described by Heacock *et al.* (175). Solutions contained about 5 μM Ru_z-N23C-C_{552F} or Ru_z-H39C-Cc and approximately 6 μM cytochrome *bc*₁ in 300 μl of Tris/HCl buffer (20 mM in the case of Ru_z-39-Cc and 10 mM for Ru_z-23-C_{552F}) pH 8.0 with 0.02% dodecylmaltoside in semimicro glass cuvettes at 10 °C. 2 mM sodium ascorbate, and 2 μM TMPD were added to fully reduce the heme groups, as verified by recording the visible spectra before flash photolysis. In the photooxidation experiments with Ru_z-H39C-Cc, [Co(NH₃)₅Cl]²⁺ was added (5mM) as the sacrificial oxidant (Fig. 26), whereas in the case of Ru_z-N23C-C_{552F}, 1 mM pentaammineosmium nitrile was used. To establish and maintain anaerobic conditions, the cuvette was closed with an appropriate septum and flushed with N₂.

To test the dependence of the electron transfer reaction of the ionic strength [I], several amounts of a 2 M KCl stock solution were added to the sample before flashing in a sequential experiment series, spectra collected to check the cofactors reduction and eventually ascorbate added. The [I] was increased up to 430 mM, and for each increment was measured the rate of electron transfer to the accepting

Results

cytochrome *c*. Plotting the logarithm (log) of the rate constant against the square root of the [I] (Brønsted plot) allows to analyse the kind of interaction between the two proteins.

The wild type, the His tagged wild type and the His tagged deletion mutant were used in this study. The cytochrome *bc*₁ complex from *P. denitrificans* requires relatively high amounts of salt for the purification, and in the classical procedure (ionic exchange, DEAE) the protein elutes from the column at a concentration of 450 mM NaCl. As a consequence, a condition with zero mM ionic strength cannot be tested. On one side, this might appear as a limitation since the reaction cannot be studied in the absence of salt, but has the advantage that the complex is stable and does not show self oxidation. Janzon (116) showed that in absence of salt it was not possible to achieve a complete and stable reduction of the hemes. In these experiments, the hemes appeared to be fully reduced before the flash and maintained their state throughout the measurements. In the case of the intact complex, the cytochrome *c*₁ can be reduced directly by ascorbate (see the section 3.5.1) or via the ISP, which is easily reduced by ascorbate due to its redox potential (higher than that of the cytochrome *c*₁) at the pH used for the experiments. The kinetics of cytochrome *c*₁ reduction by the ISP will be discussed in section 3.5. This double reduction pathway ensures that the *c*₁ heme is fully reduced before flash, as subsequent additions of ascorbate did not change its spectrum.

3.3.4 Salt titrations with the Ru₂-H39C-Cc

Fig. 29 shows a trace recorded in the salt titration involving the Ru₂-H39C-Cc and the cytochrome *bc*₁ complex (in this case, the wild type complex). The black upper trace recorded at 550 nm represent the reduction by cytochrome *c*₁ of the electron acceptor after fast oxidation due to the laser flash. At the same time and with the same rate, cytochrome *c*₁ is oxidized (grey transient).

Results

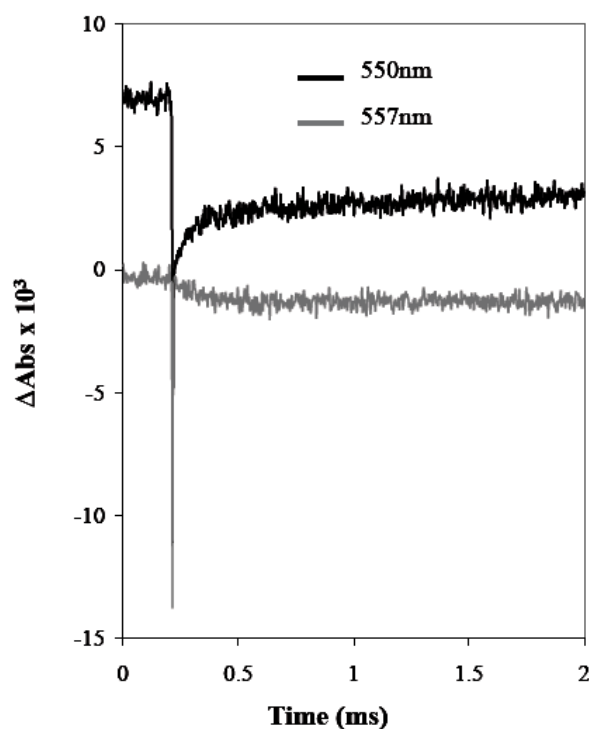


Fig. 29: Example of the kinetics between the wild type cytochrome bc_1 complex of *P. denitrificans* and the Ru₂-H39C-Cc. Upper trace: signal at 550 nm showing the reduction of the photoactivated complex. Lower trace: isosbestic at 557 nm for the Ru₂-H39C-Cc indicating the oxidation of cytochrome c_1 .

The signal at 550 nm shows two phases: a fast one, immediately after the flash, and a slower one on a long time scale, which is not present in the signal at 557 nm. This reaction mechanism is similarly observed in the three sets of measurements involving the wild type, the His tagged wild type and the His tagged deletion mutant complex. The rates for the fast phase are indicated in Table 6 and are very similar in the three experiments.

	WT [s ⁻¹]	WT His-tagged [s ⁻¹]	His-tagged deletion mutant [s ⁻¹]
550 nm	16,600	9,300	14,600
557 nm	16,700	8,400	11,200

Table 6: Rates recorded in the salt titrations obtained using the Ru₂-H39C-Cc as electron acceptor. The two transient reported here, at 550 nm and 557 nm, indicate the reduction of the ruthenium labeled cytochrome c from yeast and the oxidation of cytochrome c_1 respectively. Errors are within 10 % of the measured values.

Results

The fast phase represents the fast electron transfer between the cytochrome c_1 and the Ru_z-H39C-Cc, and finds correspondence in the signal recorded for the cytochrome c_1 oxidation. These rates are compatible with the previous results shown by Janzon *et al.*, which indicated a bimolecular reaction between the soluble fragments (118). The slow phase, on the other hand, shows very small amplitudes during the whole titration and is very slow, being completed in millisecond time scale and not microsecond as the electron transfer reaction between the bc_1 complex and the ruthenium labeled yeast cytochrome c . Moreover, it is not present in the 557 nm transient, suggesting a slow reduction of the photoactive complex by ascorbate. The amplitude of the 557 nm signal is slightly lower than the one recorded from the 550 nm transient. This is due to the fast reduction of cytochrome c_1 from the ISP, a process almost as fast as the electron transfer to the photoactive yeast cytochrome c (see 3.3.4-5).

The signal at 550 nm after flashing does not go back to baseline. This is due to the fact that 550 nm is not an isosbestic point for the ruthenium labeled yeast cytochrome c , so a small contribution in the absorbance from the cytochrome c_1 heme is also present. The signal could go back to the starting absorption value after complete re-reduction of all the cofactors operated by ascorbate and TMPD (see the slow kinetic in Fig. 29, upper trace).

By increasing the salt concentration, the rate observed for the electron transfer process is stable until a total ionic strength of 90 mM is reached. At higher salt concentrations, the rate starts becoming slower. This behaviour, shown in Fig. 30, reflects also what was already observed for the soluble fragments.

According to the Brønsted equation, the dependence of the observed rate constant from the [I] is defined by:

$$\log k_{\text{OBS}} = \log k_0 + 2B Z_A Z_B \log [I]^{1/2} \quad \text{Equation 8}$$

where the $\log k_{\text{OBS}}$ is dependent on the \log of the rate constant at $[I]=0$, and on the square root of the [I] multiplied by a term called $Z_A Z_B$ which is the product of the total charges involved in the interaction between two partners. B is a parameter derived from the Debye-Hückel theory keeping into account the dielectric constant of the

Results

medium and the temperature. For buffers made in water and at temperatures of 10 °C, the parameter B is equal to 0.5.

The Brønsted parameter $Z_A Z_B$ for the aforementioned electron transfer reaction is reported in Table 7.

WT	WT His-tagged	His-tagged deletion mutant
-5.57 ± 0.5	-5.68 ± 0.4	-4.59 ± 0.3

Table 7: Brønsted parameters for the three sets of experiments with the ruthenium labeled yeast cytochrome c.

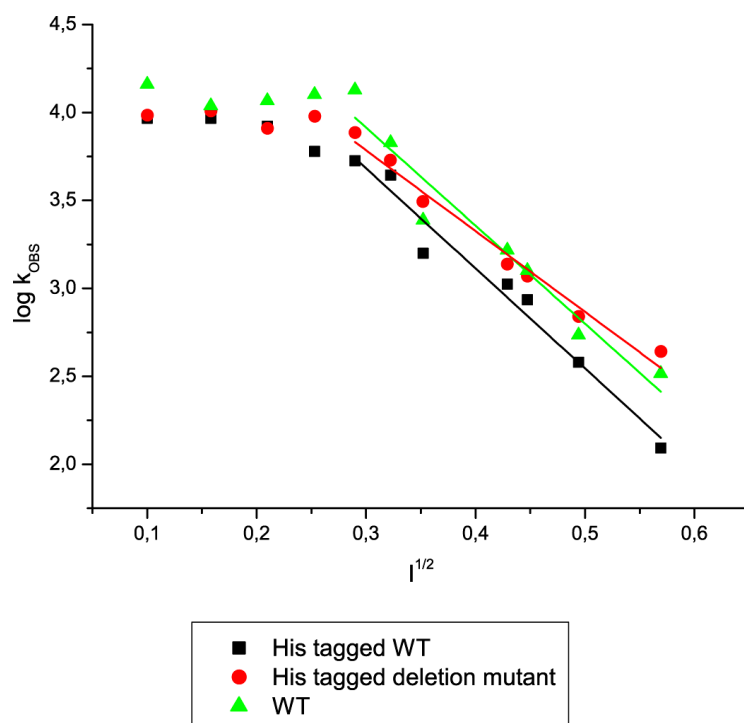


Fig. 30: Brønsted plot for the reaction between the cytochrome bc_1 complex and the photoactivated isoform 1 of the yeast cytochrome c. The slopes of the three experiments are very similar, indicating a similar reaction mechanism for the wild type and the deletion mutant.

The kinetics indicate that the electron acceptor and the bc_1 complex interact stably when the total ionic strength is low, forming a complex showing very high intramolecular transfer rates. This is a situation where cytochrome c_1 can transfer an electron to the ruthenium labeled cytochrome c very fast, since they do not have to

Results

diffuse and find each other. By increasing the ionic strength, above 90 mM, the association between the two reaction partners is less strong and they separate, so they diffuse and move to encounter each other for the electron transfer event (Fig. 31). The higher the ionic strength, the less probable is a successful encounter which leads to the transfer of an electron, so the observed rate decreases.

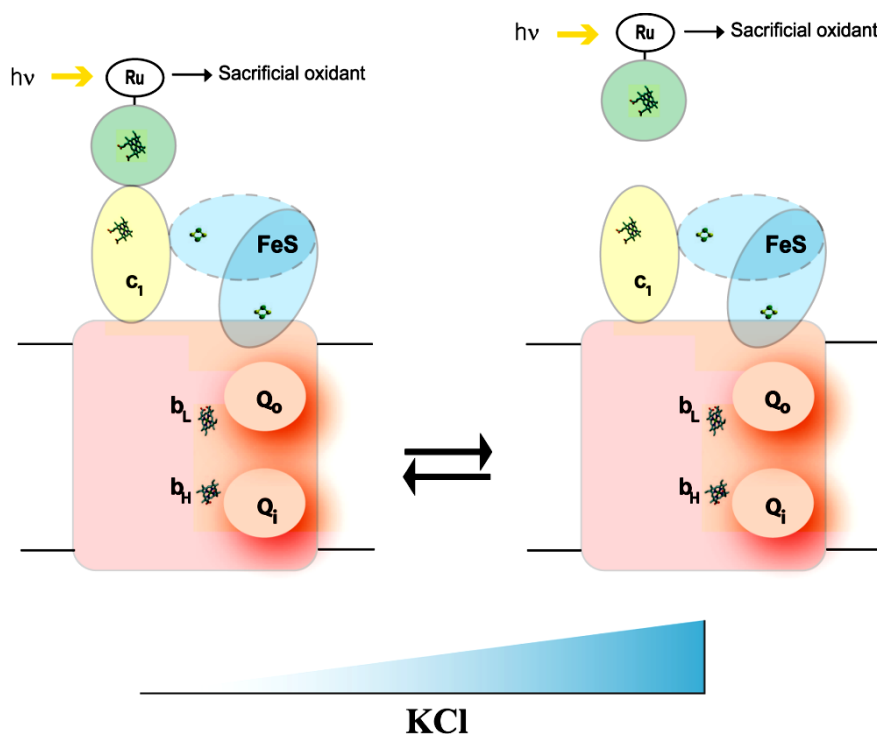


Fig. 31: Scheme showing the formation of stable complex with the photoactive complex in conditions of low ionic strength (left side). As the KCl concentration increases (blue triangle) the two reaction partners tend to separate and have to diffuse and encounter each other in the correct orientation to react. The long range interactions are shielded by the high ionic strength so that the successful collisions for electron transfer become more rare.

3.3.5 Salt titrations with the Ru_z-N23C-C_{552F}

The same experiment has been repeated with the ruthenium labeled substrate from *P. denitrificans*. Also here, the three complexes were tested with increasing salt concentrations, and the logarithm of the rate observed rate constant (k_{OBS}) plotted against the square root of the ionic strength. Fig. 32 shows an example of kinetics obtained in presence of the Ru_z-N23C-C_{552F}.

Results

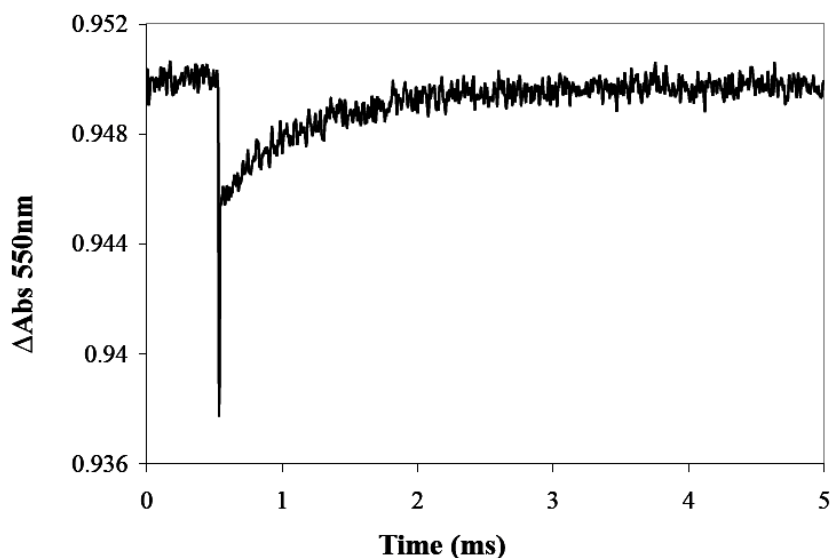


Fig. 32: Example of the kinetics between the cytochrome bc_1 complex of *P. denitrificans* and the $\text{Ru}_2\text{-N23C-c}_{552\text{F}}$, showing the reduction of the photoactivated substrate.

The rates observed for the electron transfer reaction between the *P. denitrificans* cytochrome bc_1 complex and the $\text{Ru}_2\text{-N23C-c}_{552\text{F}}$ are 1900 s^{-1} , 1500 s^{-1} and 1000 s^{-1} for the wild type, the His tagged wild type and the deletion mutant complex, respectively. The reaction is slower than what previously observed with the yeast cytochrome c , and the signal at 552 nm is monophasic, indicating that ascorbate is not able to re-reduce the photoactive complex as fast as in the previous experiments. In this case, the signal after the flash goes back to baseline. The reason is the choice of the sacrificial oxidant: the osmium complex was the only possibility for the experiments with the ruthenium labeled c_{552} , but it can back-react with cytochrome c_1 being positively charged, and reduce it, whereas it shows no interaction with the cytochrome c_{552} (otherwise to be observed in the step function). The latter repels the osmium complex due to the charges around the heme crevice. As cytochrome c_1 is oxidized by reaction with the ruthenium labeled cytochrome $c_{552\text{F}}$, it is rapidly reduced from the sacrificial oxidant, and therefore the signal goes back to baseline. This effect was not observed in the previous experiment, since the sacrificial oxidant chosen was the cobalt complex.

The Brønsted plot (Fig. 33) shows, for the bc_1 complex interaction with the physiological substrate, that there is almost no formation of a stable complex

Results

between the enzyme and its substrate. The plot starts rapidly going down after 60 mM, so the reaction with the ruthenium labeled cytochrome c_{552F} is more sensitive to the ionic strength. Moreover, the Brønsted parameters (shown in Table 8) indicate that no charge interaction is lost by the deletion of the acidic domain, not only in the aforementioned experiments nor with the native substrate. Therefore, these results confirm the observations obtained with the soluble fragments. The interaction model driven by long range electrostatic forces is also valid here, clearly showing no role of the charges of the acidic domain in interactions with the substrate. The acidic domain, similar (but not homologous) to the small acidic subunit of the eukaryotic complex, does not play any role in the interaction with the electron acceptor.

WT	WT His-tagged	His-tagged deletion mutant
-2.78 ± 0.08	-3.36 ± 0.26	-3.35 ± 0.17

Table 8: Brønsted parameters for the three sets of experiments with the ruthenium labeled cytochrome c_{552F} .

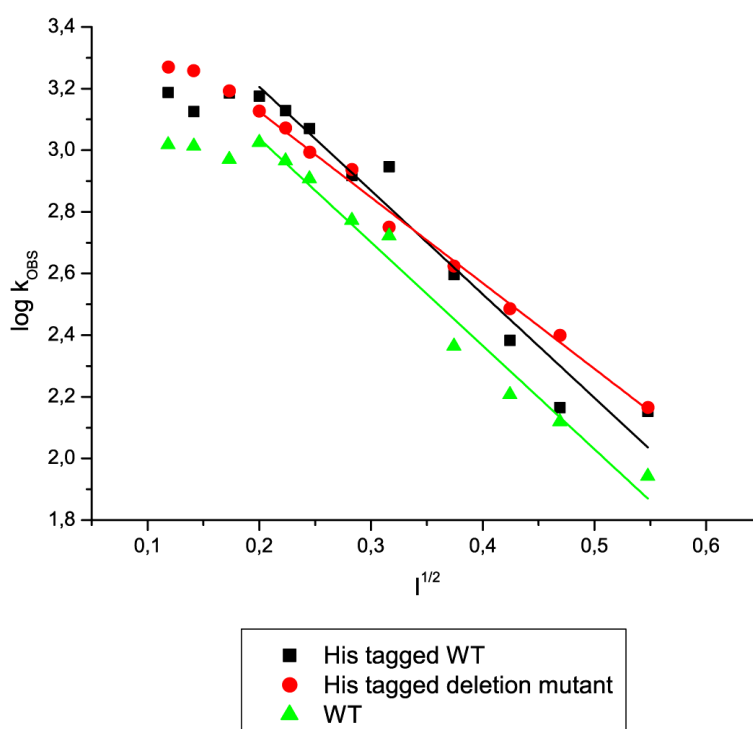


Fig. 33: Brønsted plot for the reaction of the cytochrome bc_1 complex and the Ru_z labeled substrate. The slopes of the three experiments are very similar, indicating a similar reaction mechanism for the wild type and the deletion mutant.

3.4 Rapid flash kinetics for the internal electron transfer

The laser flash technique can be also used for the investigation of internal electron transfer steps. In this case, a ruthenium dimer is used, which is not coupled to any electron acceptor. Its positive charge (+4) directs it to the cytochrome c_1 heme and allows its specific oxidation, creating an electron vacancy which is rapidly filled by the ISP. The reduction of cytochrome c_1 heme followed at 552 nm (α peak) permits an estimation of the internal electron transfer to the cytochrome c_1 . This electron transfer is governed by the movements of the ISP head domain, and several models have been developed so far (74, 127, 130) to explain the trigger of the ISP movements in direction to cytochrome c_1 . Measurements in the *R. sphaeroides* system have been carried out (181), describing a very fast electron transfer to the cytochrome c_1 with signals showing a single phase and rates of about 80000 s^{-1} (182). Until now, no data were available for the important model of the *P. denitrificans* enzyme. In this part of the work, the complexes used in the previous experiment (wild type, His tagged wild type and His tagged deletion mutant complex) were tested in order to study the electron transfer reaction from the ISP to the cytochrome c_1 , and to investigate possible effects of the deletion of the acidic domain for this interaction

3.4.1 Experimental setup and protocol description

The bc_1 complex (5 μM of each of the three aforementioned complexes) is mixed in 300 μl of a 20 mM TRIS/HCl buffer at pH 8.0, additionally containing 0.02% dodecylmaltoside and 5 mM of $[\text{Co}(\text{NH}_3)_5\text{Cl}]^{2+}$ as the sacrificial oxidant. Moreover, 2 mM succinate and 50 nM succinate dehydrogenase were added to ensure reduction of the low potential chain and regenerate the oxidized substrate (100 μM decylubiquinone) after flashing. To maintain the redox cofactors oxidized and avoid loss of reduction after several flashes (as observed already in (182)), 20 μM TMPD and 1 mM ascorbate were also added in the cuvette. The photoactive complex is the binuclear ruthenium complex, $[\text{Ru}(\text{bpy})_2]_2(\text{qpy})(\text{PF}_6)_4$; qpy, 2,2':4',4'':2'',2'''-quaterpyridine Ru_2D , in 20 μM concentration. The sample was made anaerobic by flushing with N_2 and using appropriate septa; the measurements were carried out at 10°C.

After a flash, one electron is abstracted from the excited ruthenium dimer and transferred to the sacrificial oxidant, which decomposes after reduction and thus

Results

avoids backreactions (see 3.3.4-5). In a timescale of 1 μ s, the cytochrome c_1 is rapidly oxidized, and can take up an electron from the ISP (k_1). After ISP oxidation, a turnover can take place at the Q_o site, since now the ISP is available to accept an electron from quinol (k_2). At this point, an increase in the absorption at 560 nm (isosbestic for cytochrome c_1) is observed, followed by a slower oxidation (k_4). The rate constant k_3 cannot be calculated, since the electron transfer from the b_L to the b_H is extremely fast due to the high redox potential of the latter and its short distance to the latter and, therefore, not rate limiting.

In Fig. 34 the experimental setup used for the experiments is depicted.

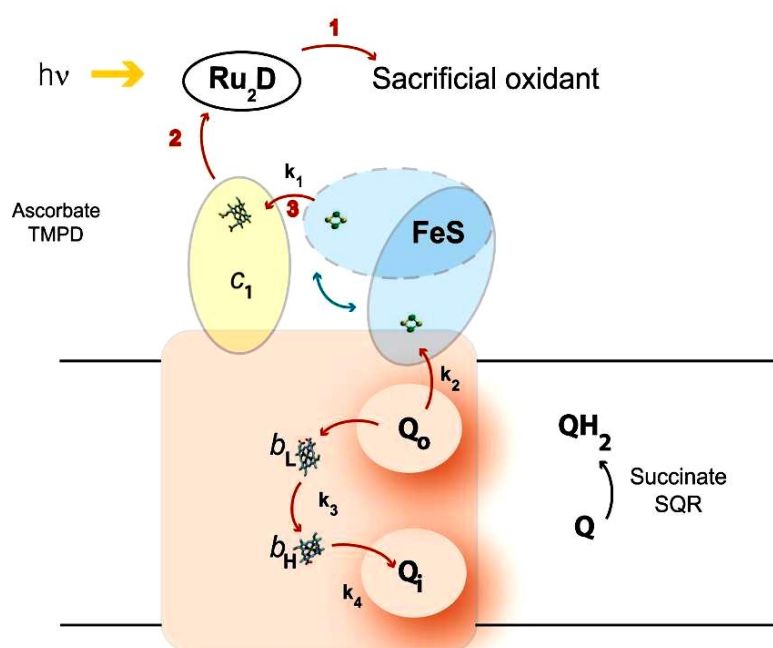


Fig. 34: Schematic representation of the experimental setup for the internal kinetic studies. In the cuvette, ascorbate and TMPD directly reduce the ISP and cytochrome c_1 , and the quinol reduces the low potential chain. After flashing, one electron is abstracted from the ruthenium dimer and subsequently transferred to the sacrificial oxidant. At this point, cytochrome c_1 is oxidized transferring its electron to the photoactive complex and the ISP can move to the c_1 heme and reduce it (k_1). As the ISP is oxidized, one turnover can take place and a quinol molecule is oxidized at the Q_o site. The ISP is then available to be reduced again (k_2) and reduction of a b -type heme is observed. The electron transfer between b_L and b_H is a fast process, driven by the high redox potential of the b_H heme, and k_3 cannot be resolved. k_4 represents the oxidation of b_H to reduce a quinone or a semiquinone at the Q_i site. SQR is the succinate dehydrogenase which regenerates with succinate the quinol pool after the turnover.

Results

Two different sets of experiments were tried: in the first one, the complexes were reduced by TMPD and ascorbate, so that only the high potential chain could be reduced. This implies no electron transfer processes at the level of the low potential chain, and permits to define whether or not the mobility of the ISP is affected from the presence of the substrate at the Q_o site. Several inhibitors were tested (stigmatellin, myxothiazol, MOA-stilbene, and JG-144) to study eventual effects in the cytochrome c_1 reduction in presence of Pm and Pf inhibitors. In the second set, the reduction of the complex was obtained by using ascorbate and TMPD and decylubiquinol, continuously regenerated by the presence of succinate and catalytic amounts of SQR. In this way, it is possible to observe also the kinetics at the low potential chain.

3.4.2 Internal kinetics using TMPD and ascorbate to reduce the cytochrome bc_1 complex

In the following tables the kinetics observed in presence of ascorbate and TMPD to reduce the high potential chain are reported. After flashing, the Ru_2D is able to oxidize cytochrome c_1 and the ISP transfers an electron to the c -type heme. In absence of quinol at the Q_o site, it is feasible to analyze the movements of the head domain of the ISP without any restriction due to possible interaction with the substrate. The Q_o site is, indeed, partially composed of the head domain of the ISP. Quinol forms a hydrogen bond with residues coordinating the Rieske cluster (His¹⁵⁵ in the *P. denitrificans* enzyme).

For each sample, three different inhibitors were tested and in all cases a measurement without inhibitor was included as reference. The transients were recorded at 552 nm to follow reduction of cytochrome c_1 and fitted to a mono- or bi-exponential equation. The wild type complex (Table 9) shows biphasic kinetics, with a fast phase of $9100 \pm 883 \text{ s}^{-1}$ and a slow phase of $910 \pm 112 \text{ s}^{-1}$. Upon addition of MOA-Stilbene to the sample, the fast phase is not considerably changed but the slow phase is two times faster than observed before ($1800 \pm 189 \text{ s}^{-1}$ in the wild type complex). The amplitude of the two phases (expressed as percentage of cytochrome c_1 reduced to the total amount of cytochrome c_1 oxidized) is sensibly increased, meaning that more cytochrome c_1 is reduced than in absence of inhibitors (Fig. 35)

Results

	k_1 (s^{-1})	Amplitude (%)	k_2 (s^{-1})	Amplitude (%)
no inhibitor	9100 ± 883	9	910 ± 112	15
MOA-stilbene	9900 ± 65	33	1800 ± 189	26
myxothiazol	8900 ± 1006	30	1700 ± 146	30
JG-144	1289 ± 94	17	257 ± 75	45

Table 9: Results from the experiments obtained using ascorbate and TMPD to reduce the wild type bc_1 complex from *P. denitrificans*. The amplitude shown is expressed as a percentage of the total heme c_1 flash-oxidized.

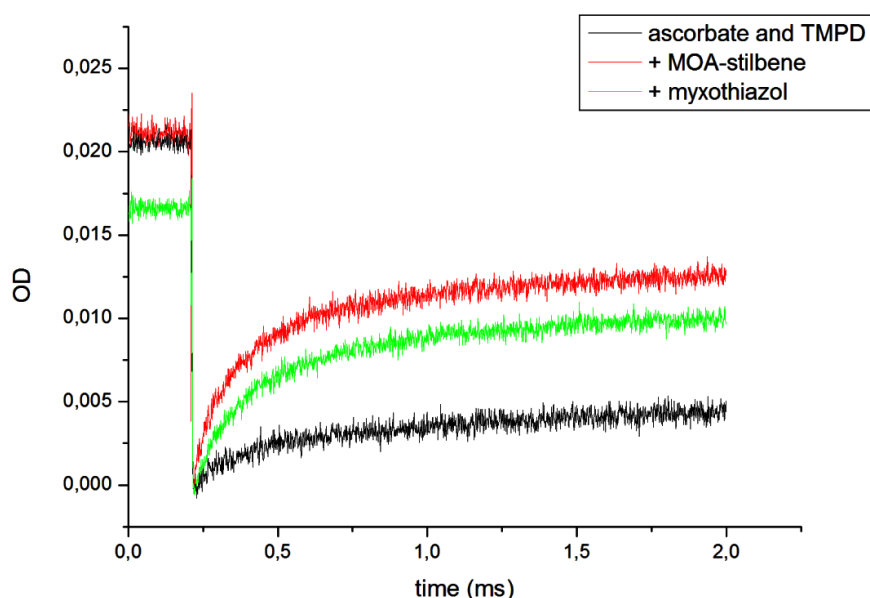


Fig. 35: Effect of Pm inhibitors on the electron transfer from the ISP to the cytochrome c_1 in the cytochrome bc_1 complex of *P. denitrificans*. In black, the transient obtained without inhibitors; in red and green the kinetics after addition of MOA-stilbene and myxothiazol respectively. The amplitude of the signal is increased, meaning a much higher reduction of cytochrome c_1 in presence of Pm inhibitors. The rate of reduction measured for the fast phase does not increase significantly, but the slow phase is two times faster than observed previously.

This result allows assigning the fast phase to the reduction of cytochrome c_1 when the ISP is in the so called c_1 position, and the electron transfer to the c_1 heme is not limited by the movements of the cluster. The slow phase represents the reduction of cytochrome c_1 by the ISP being in the b position, closer to the cytochrome b , therefore having to reach the c_1 heme and then to initiate electron transfer event. MOA-stilbene displaces the ISP from the b position, and makes the slow phase

Results

faster since the inhibitor forces the ISP to move towards the cytochrome c_1 . Hereby the distance the head domain has to transit before transferring an electron is lower than without inhibitor. The fast phase is not considerably faster than in absence of inhibitor, but the total amplitude increases (as visible in Fig. 35), as a consequence of the displacement of the ISP head domain. Myxothiazol shows an effect similar to the one of MOA-stilbene: the slow phase is 2-fold faster and the amplitude increases, meaning more cytochrome c_1 reduced.

The situation changes in presence of JG-144 (Fig. 36), a Pf type of inhibitor which was shown in crystal structures to keep the ISP head domain close to cytochrome b , even if no hydrogen bonding can be identified between the inhibitor molecule and the Rieske cluster as in the case of stigmatellin (48). JG-144 slows down both fast and slow phase observed, meaning that the ISP head domain is not able to interact anymore with the cytochrome c_1 as in absence of inhibitor, but not fixed in the b conformation since electron transfer to the c_1 heme is still observed (Table 9). Notably, the total amplitude is increased, indicating a higher amount of cytochrome c_1 reduced. This could indicate that a Q_o site occupied with a ligand allows a major portion of the ISP to be mobile compared to the situation where only endogenous quinone/quinol is bound in cytochrome b (see 3.4.2 and 3.4.3).

Stigmatellin, on the other side, completely blocks electron transfer, also when added in substoichiometric amounts (0.5 molecules per complex dimer). The hydrogen bond with the His¹⁵⁵ (*P. denitrificans* numbering) coordinating the cluster fixes the ISP head domain, as shown by the flat step function in Fig. 36. The electron transfer observed in presence of JG-144 can not be due to the re-reduction of cytochrome c_1 from ascorbate present in the reaction, since ascorbate only slowly reduces the c_1 heme in the *P. denitrificans* bc_1 complex, as confirmed by stopped-flow experiments, on a completely different timescale (seconds instead of microseconds). Therefore, such a slow electron transfer can not be observed in flash photolysis experiments, being far too slow for the considered timescale.

Results

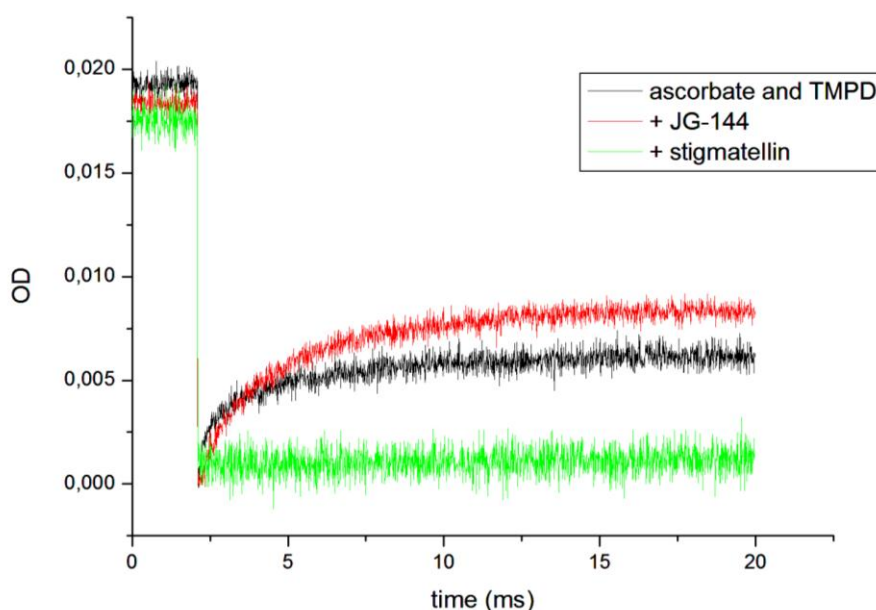


Fig. 36: Effect of the Pf inhibitors on the electron transfer to the cytochrome c_1 heme. In black, the transient obtained without inhibitors, and in red and green respectively the effects of JG-144 and stigmatellin. JG-144 slows both phases down, whereas stigmatellin blocks completely the electron transfer.

The results are similar also in the case of the His tagged wild type complex, although the observed rates are generally slower than those of the wild type. This could be due to variability of the samples, but also to the small amplitude of the phases in absence of inhibitor that making an accurate fitting difficult. Nevertheless, the behaviour observed upon binding of inhibitors is similar to the one observed with the wild type complex (Table 10 and Fig. 37).

	k_1 (s^{-1})	Amplitude (%)	k_2 (s^{-1})	Amplitude (%)
no inhibitor	5200 ± 488	9	600 ± 73	14
MOA-stilbene	9427 ± 509	33	1422 ± 127	24
myxothiazol	9736 ± 537	33	1714 ± 93	34
JG-144	733 ± 85	22	175 ± 19	26

Table 10: Results from the experiments obtained using ascorbate and TMPD to reduce the His tagged wild type bc_1 complex from *P. denitrificans*.

Results

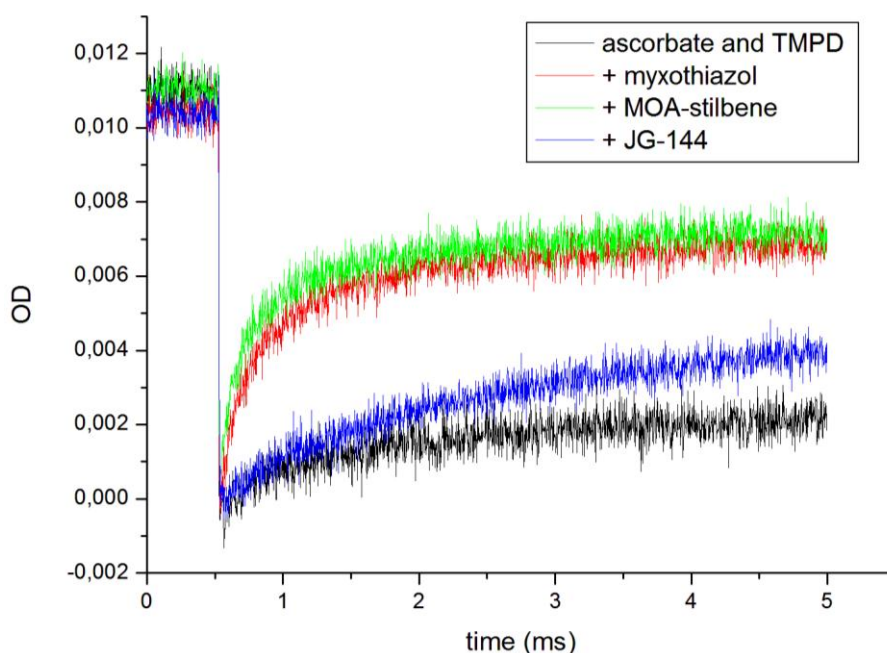


Fig. 37: Effects of the inhibitor on the electron transfer from the Rieske cluster to the c_1 heme for the His tagged wild type cytochrome bc_1 complex from *P. denitrificans*. In black, the complex reduced with ascorbate and TMPD and without any inhibitor. Following, in red the kinetics with myxothiazol, in green with MOA-stilbene, and in blue with the Pf inhibitor JG-144.

In the case of the deletion mutant complex, there is a significant increase of the fast phase in presence of inhibitors, with an increase also in the slow phase. The effect on the fast phase is unexpected and is present as well in the experiments where also the substrate quinol is used to reduce the complex (see 3.4.3). Moreover, a signal is visible also for the b hemes at 560 nm, which is not present in the wild type complexes (Fig. 38, 39).

Results

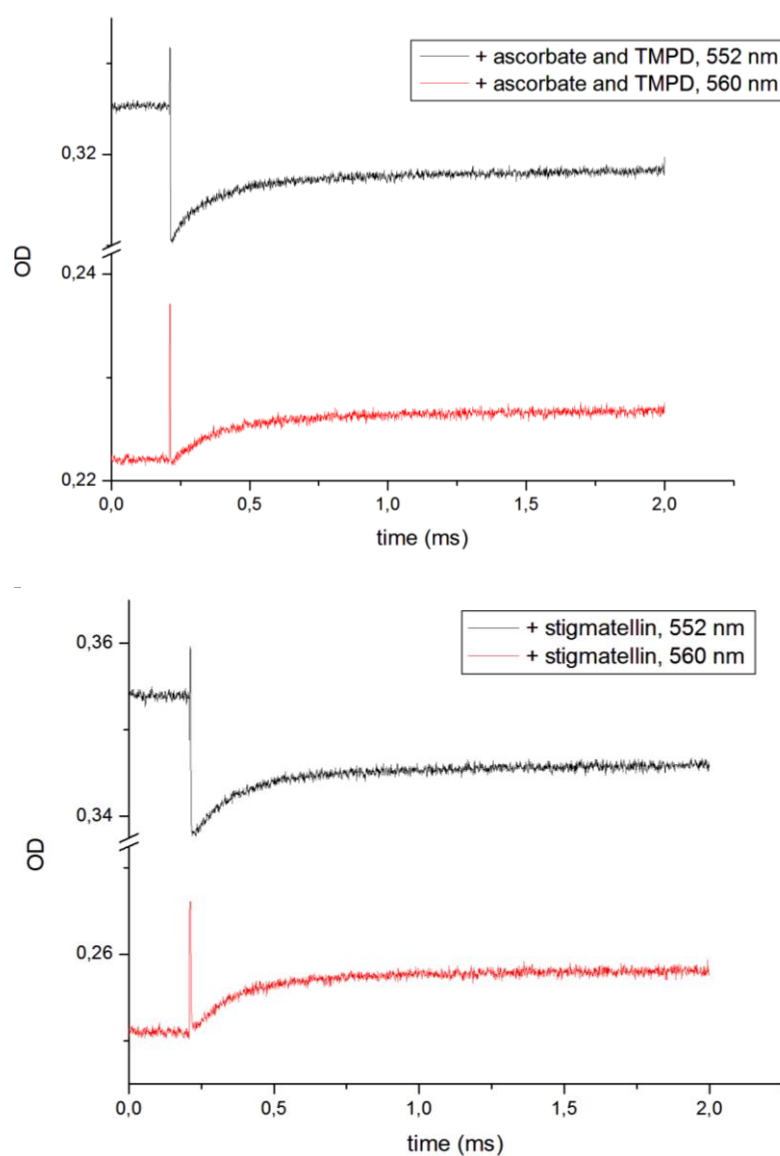


Fig. 38: Electron transfer from the ISP to the cytochrome c_1 in the deletion mutant of the cytochrome bc_1 complex from *P. denitrificans*. Upper panel, transient recorded only in presence of ascorbate and TMPD to reduce the complex. A signal is also evident at 560 nm, completely unexpected since electrons flow only through the ISP and cytochrome c_1 . Lower panel: adding stigmatellin to the sample shown in the upper panel, no change can be observed. Stigmatellin is, though, expected to quence the signal.

Results

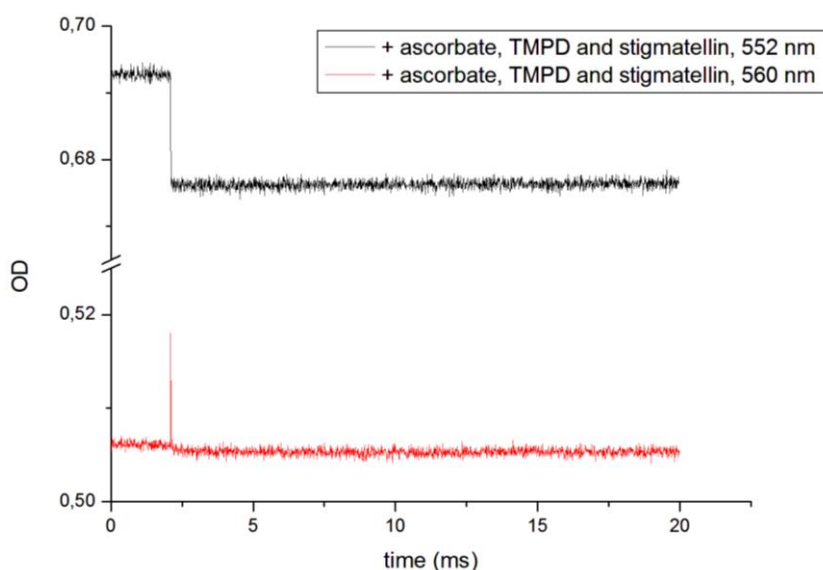


Fig. 39: Wild type cytochrome bc_1 complex from *P. denitrificans*, reduced with ascorbate and TMPD and blocked with stigmatellin. The black transient represent the electron transfer events at 552 nm and the red one at 560 nm. Both data indicate that in presence of stigmatellin, the electron flow to cytochrome c_1 is blocked and that no unexpected signal at 560 nm is recorded.

This is an indication for electron transfer taking place at the level of cytochrome b , which should not be observed since the complex is reduced only by ascorbate and TMPD, allowing only the reduction of ISP and cytochrome c_1 . In presence of stigmatellin, which locks the ISP away from the cytochrome c_1 , reduction of cytochrome b is still observed, as shown in Fig. 38 (lower panel). Fig. 39 shows the behaviour of the wild type complex upon binding of stigmatellin, with a flat step function indicating fixation of the ISP head domain onto cytochrome b . This unexpected feature in the deletion mutant complex could indicate that the inhibitor is not locking anymore the ISP and still allows electron transfer. This hypothesis looks quite improbable, since the introduced mutation is on cytochrome c_1 , not changing the inhibitor binding properties of the complex whereas the binding pocket is made up of cytochrome b and ISP. To check this, a test experiment has been performed, reducing the mutant complex using decylubiquinol and TMPD as redox mediator. After flashing, electrons are transferred to cytochrome c_1 and to cytochrome b , as shown in Fig. 40.

Results

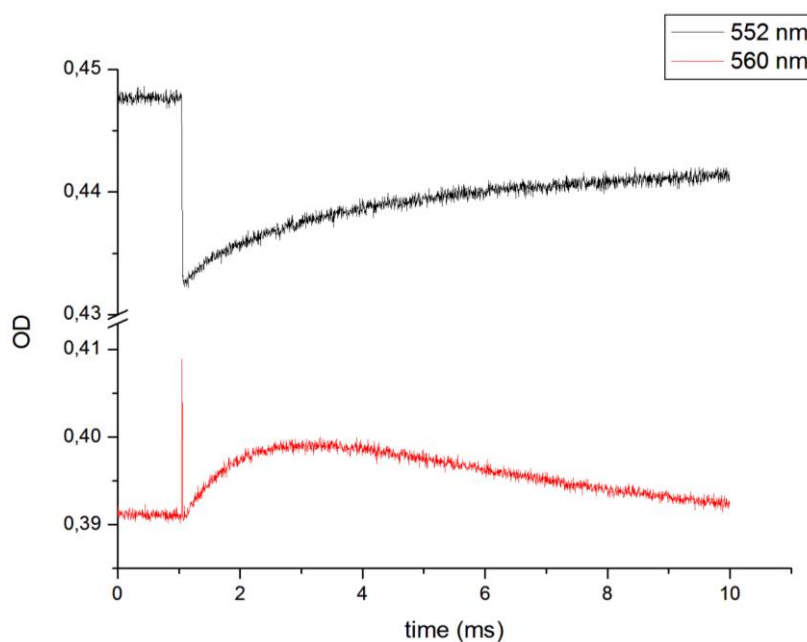


Fig. 40: Transients for the electron transfer to the cytochrome c_1 in the mutant cytochrome bc_1 complex from *P. denitrificans*, reduced with decylubiquinol and TMPD as redox mediator.

Addition of stigmatellin blocks the electron transfer, as expected, giving flat signals at both wavelengths. In Fig. 41, at 552 nm and at 560 nm the signals indicate that no electron is transferred, and therefore, that the inhibitor is binding and correctly inhibiting the electron flow through the complex, as expected.

Results

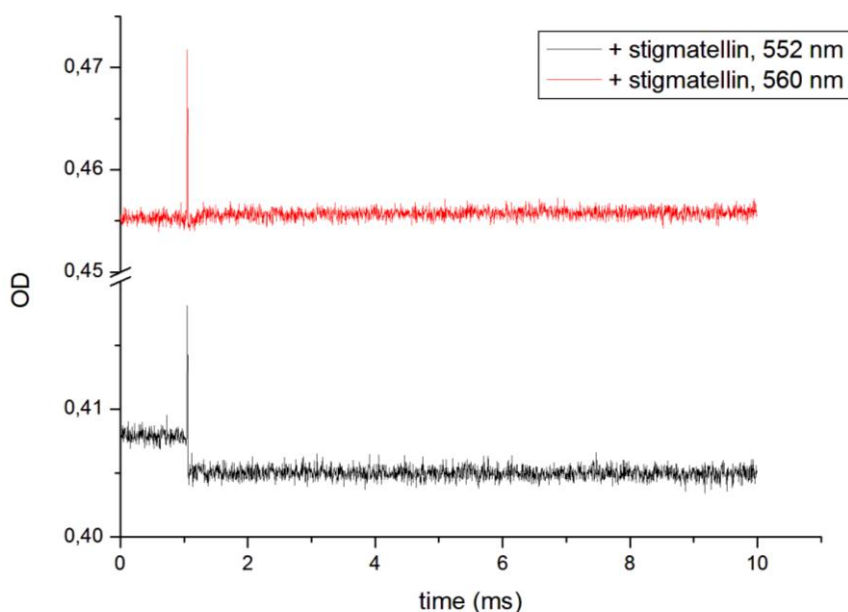


Fig. 41: Effect of stigmatellin on the ISP-cytochrome c_1 electron transfer kinetics on the mutated cytochrome bc_1 complex from *P. denitrificans*. In black, the transient at 552 nm and in red at 560 nm, both showing a flat line and indicating the inhibition of the complex by stigmatellin.

When ascorbate is added to the same sample, reduction of cytochrome c_1 and cytochrome b is again visible, even if the ISP is firmly docked on the Q_o site (Fig. 42). Therefore it is possible to conclude that ascorbate is responsible for the artefact observed in the case of the mutated complex. As shown from Fig. 40, the complex could be reduced also using quinol and avoiding artifacts, but the use of ascorbate allows analysing the behaviour of the ISP with no external added substrate. This is important since the occupancy of this site is thought to have a regulatory role in defining the gating of the ISP head domain movement (see 4.2). Moreover, the behaviour of the mutant in response to the inhibitor binding is the same as the wild type, even if the measured rate constants are faster as a result of the presence of ascorbate.

Results

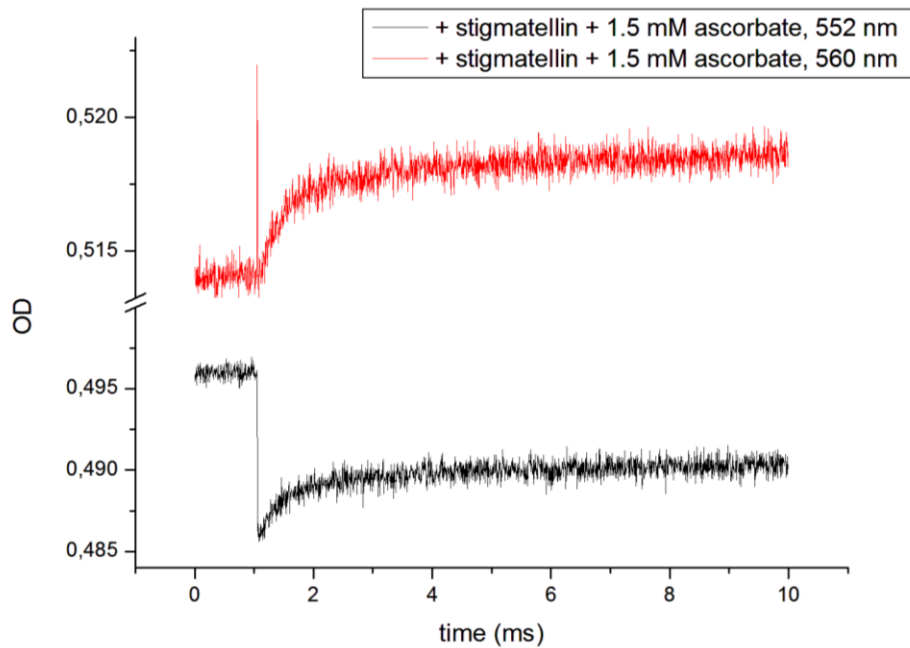


Fig. 42: Effects of ascorbate on the mutant cytochrome bc_1 complex from *P. denitrificans*. Adding ascorbate to the sample in Fig. 41 restores the reduction of cytochrome c_1 and cytochrome b even if the complex is blocked with stigmatellin. This shows that ascorbate is responsible for the artefact observed at 560 nm and for the faster electron transfer rates measured for the complex.

The reduction of cytochrome b recorded in these experiments was not observed in redox spectra using ascorbate to reduce the complex (see Fig. 11) and the steady-state kinetics showed values comparable with the wild type. Probably, the deletion of the acidic domain and the change in the oligomerisation state (see 4.4) render the complex more accessible for small molecules such as ascorbate, showing the aforementioned effects.

Even though the rates appear to be faster, the effects of inhibitors are similar: MOA-stilbene and myxothiazol increase the rate of electron transfer to the cytochrome c_1 , whereas JG-144, by constraining the ISP close to cytochrome b , affects both phases, still allowing slow electron transfer.

Results

	k_1 (s^{-1})	Amplitude (%)	k_2 (s^{-1})	Amplitude (%)
no inhibitor	9400 \pm 939	26	1300 \pm 560	14
MOA-stilbene	22138 \pm 514	41	3005 \pm 87	24
myxothiazol	21776 \pm 842	51	4197 \pm 159	43
JG-144	5889 \pm 137	64	818 \pm 25	15

Table 11: Results from the experiments obtained using ascorbate and TMPD to reduce the His tagged deletion mutant bc_1 complex from *P. denitrificans*.

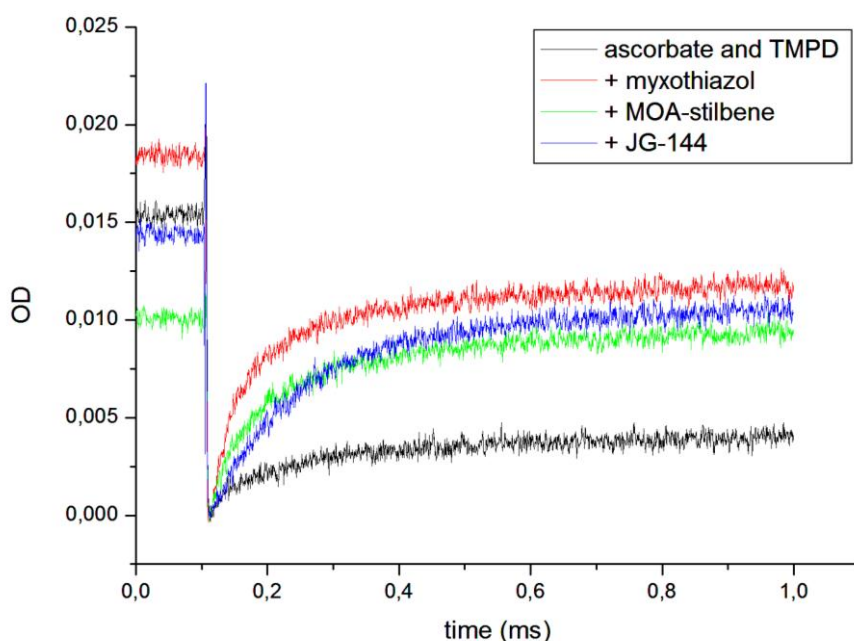


Fig. 43: Effects of the inhibitor on the electron transfer from the Rieske cluster to the c_1 heme for the His tagged deletion mutant cytochrome bc_1 complex from *P. denitrificans*. In black, the complex reduced with ascorbate and TMPD and without any inhibitor. Following, in red the kinetics with myxothiazol, in green with MOA-stilbene, and in blue with the Pf inhibitor JG-144.

3.4.3 Internal kinetics using TMPD, ascorbate, decylubiquinol, succinate and SQR to reduce the cytochrome bc_1 complex

In a further set of experiments, the electron transfer from the ISP to the cytochrome c_1 has been measured reducing the complex also in presence of quinol. This allows to observe effects on the kinetics in presence of substrate bound at the Q_o site. Moreover, quinol starts the turnover of the enzyme and, therefore, electron transfer

Results

at the level of the cytochrome *b* which can be followed at 560 nm. Ascorbate is still present in the reaction, to achieve complete reduction of the high potential chain and achieve good start conditions prior to flashing. In Table 12 the results for the three complexes are summarized, reduced with quinol and ascorbate, compared to what previously observed where the complexes were reduced by ascorbate and TMPD only. Again, cytochrome *c*₁ is reduced in two phases, with a scheme similar to what was observed in the experiments where only the high potential chain was reduced. The rates are comparable to the previous experiments, indicating that the binding of substrate does not influence the rates of electron transfer to the *c*₁ heme. On the other hand, the amplitude of the signals changes upon binding of inhibitor. This does not hold true for the fast phase of the cytochrome *c*₁ deletion mutant complex, but this effect might be due to the atypical reaction of the complex in presence of ascorbate described in the previous chapter.

Wild type complex						
	k₁	A₁	k₂	A₂	k₃	A₃
	[s ⁻¹]	[%]	[s ⁻¹]	[%]	[s ⁻¹]	[%]
Ascorbate and TMPD	9100	9	1000	15	0	0
Ascorbate, TMPD and quinol	9200	17	900	45	600	83
His tagged wild type complex						
Ascorbate and TMPD	5200	9	600	14	0	0
Ascorbate, TMPD and quinol	5900	17	400	46	300	88
His tagged deletion mutant complex						
Ascorbate and TMPD	9400	26	1300	14	5600	17
Ascorbate, TMPD and quinol	17700	26	1000	46	2200	67

Table 12: Results from the experiments obtained using TMPD, ascorbate, quinol, succinate and SQR to reduce the cytochrome *bc*₁ complex from *P. denitrificans*. Errors are within 10 % of the measured values.

Results

The presence of quinol in the assay, nevertheless, changes the distribution of amplitudes: the amount of cytochrome c_1 reduced increases, and especially the slow phase amplitude increases almost three fold compared to the experiments with no quinol added. This is consistent with the presence of substrate: the ISP docks onto cytochrome b to form the complete pocket for the binding and oxidation of quinol, and this increases the amplitude of the slow phase, since most electrons reducing cytochrome c_1 now come from the oxidation of quinol at the Q_o site. Turnover at the Q_o site is confirmed by the transients recorded at 560 nm, showing reduction of cytochrome b (Fig. 44) with a rate comparable to the one of the slow phase, consistent with electron bifurcation after quinol oxidation.

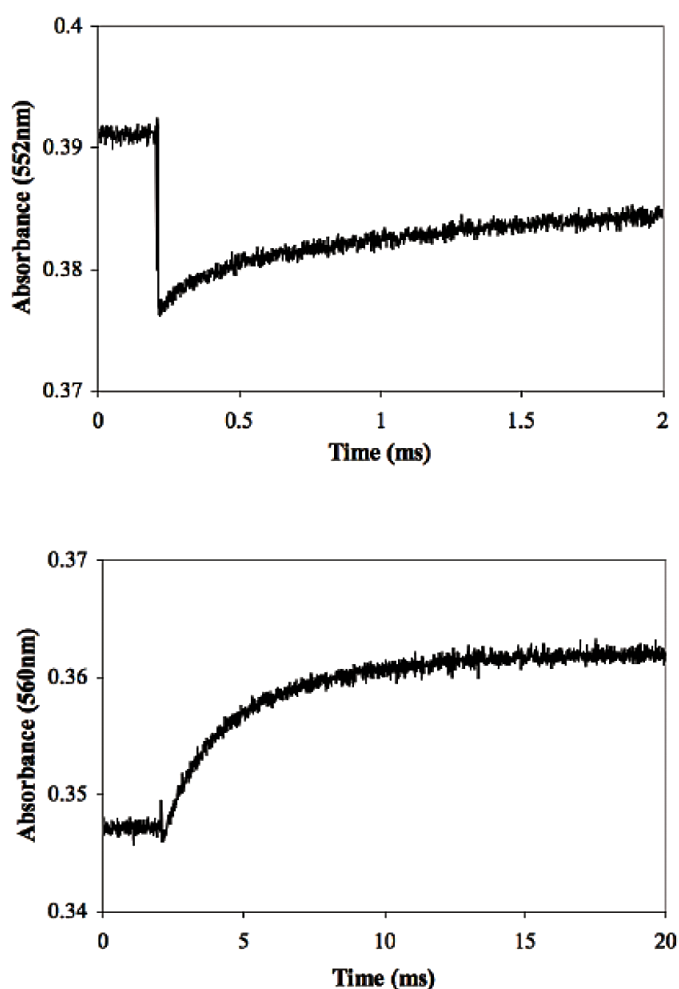


Fig. 44: Transients obtained from the wild type complex in presence of ascorbate and quinol to reduce both the high and the low potential chain. Upper panel, redox events at the cytochrome c_1 (552 nm); lower panel: cytochrome b reduction (560 nm).

Results

This result, taken together with the previous investigation where only the high potential chain is reduced, indicate that the ISP head domain, in absence of substrate, is not fixed in a single position but most likely continuously scanning between the Q_o site and the cytochrome c_1 , being randomly distributed. Binding of Pm inhibitors brings the ISP head domain closer to the the cytochrome c_1 and increases the amount of cytochrome c_1 reduced. Binding of Pf inhibitors, on the other side, forces the ISP in the b position with different efficiencies: stigmatellin blocks the electron transfer to cytochrome c_1 , whereas JG-144 lowers the rate of the process still allowing electron flow.. Binding of quinol at the Q_o site leads to an increase of the amplitude of the slow phase, indicating that the ISP head domain assumes preferentially the b position in order to bind and oxidize the substrate. Most important is that binding of ligands at the Q_o site (inhibitors or substrate) increases considerably the amount of cytochrome c_1 reduced compared to the total flash oxidized c_1 heme. The informations obtained with these experiments give evidence for a regulatory role for the ligand at the Q_o site, as proposed by Di Xia *et al.* (127). The mechanism seems to be controlled from the “sensory” *cd1* helix of cytochrome b , which allows the docking at the Q_o site when the substrate is bound. This will be discussed more in detail in section 4.2.

3.5 Interaction between the ISP and the cytochrome c_1 by stopped flow kinetics

3.5.1 Experimental setup

In the previous section, the kinetics of the cytochrome c_1 reduction by the ISP has been analysed on a very short time scale (μ s range), by using ascorbate and TMPD to pre-reduce the high potential chain. In the following experiments, the cytochrome c_1 reduction has been followed in the stopped flow apparatus by rapid mixing the oxidized protein against increasing amounts of ascorbate in pseudo-first-order (PFO) conditions. As visible in Fig. 45, a fixed amount of cytochrome bc_1 complex (3μ M) has been mixed against a large excess of ascorbate, in order to achieve PFO conditions and determine the bimolecular rate constant for the cytochrome c_1 reduction. The FeS cluster has a redox potential close to the one of cytochrome c_1 (85), so that also the ISP is reduced in presence of ascorbate. This implies that the reduction of cytochrome c_1 is not only achieved by direct electron transfer from ascorbate to the c_1 heme, but also by the electron transfer from the Rieske cluster.

Results

The picture is more complicated since it is necessary to consider also the movements the ISP head domain has to undergo in order to reduce the cytochrome c_1 as described in the previous chapter. A mechanism describing the electron transfer according to the experimental setup is described in section 3.4.2.

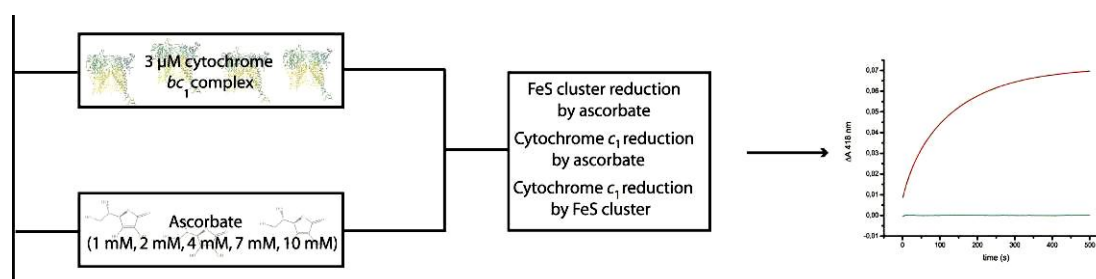


Fig. 45: Scheme of stopped flow experiments. A fixed amount of cytochrome bc_1 complex is mixed, under PFO conditions, with increasing concentrations of ascorbate. Cytochrome c_1 reduction can be followed at 418 nm, as a result of two processes: the direct reduction by ascorbate and the reduction by the Rieske cluster.

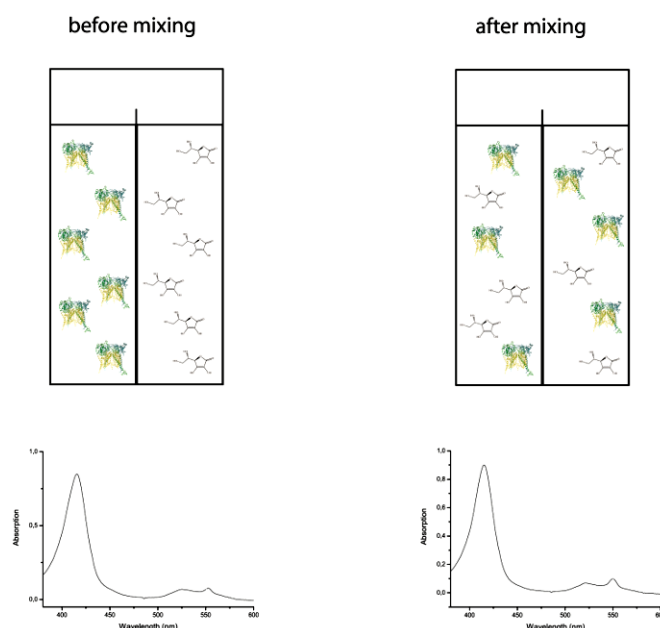


Fig. 46: Double sector cuvette (DSC) experimental setup. In a double sector cuvette two solutions are carefully pipetted: in one side 3 μM cytochrome bc_1 complex and in the other side 1 mM ascorbate. A spectrum is recorded (before mixing). After that, the cuvette is inverted to mix the two solutions and another spectrum recorded (after mixing). The difference spectrum ($a_m - b_m$) allows identifying the wavelength at which the change in absorption occurs; this wavelength is then used for the SF experiments.

Results

In the stopped flow apparatus, one syringe contained a protein solution (in some experiments incubated over night with Q_o site inhibitors) with $3\ \mu\text{M}$ oxidized cytochrome bc_1 complex, and the other one a solution containing 1 mM, 2 mM, 4 mM, 7 mM or 10 mM ascorbate in the same buffer. The two solutions were rapidly mixed and the absorption recorded at 418 nm. The wavelength has been chosen by double sector cuvette experiments, as depicted in Fig. 46. These cuvettes with two sectors have been used, in which one sector contains the oxidized cytochrome bc_1 complex and the second one a solution of 1 mM ascorbate. A spectrum is recorded before mixing the two solutions. After that, the cuvette is inverted and the two solutions can mix, reducing the protein. After waiting for five minutes to reach complete reduction, an after-mixing spectrum is recorded, and subtracted from the previous one. This gives a difference spectrum (Fig. 47): the peaks at 418 nm and 552 nm can be used to follow the spectral changes due to the complex reduction. The 418 nm peak is higher than the 552 nm one, indicating that the signal in the stopped flow will be more intense at 418 nm than at 552 nm.

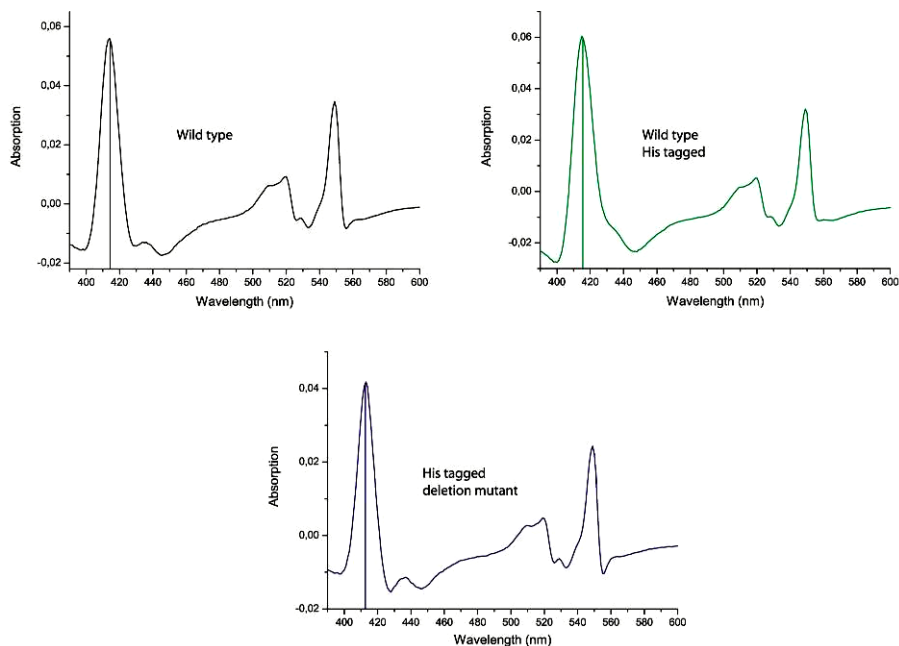


Fig. 47: DSC difference spectra. Here are represented the difference spectra from the three complexes, indicating that the same wavelength can be used for the experiments at the Stopped Flow. The peak at 418 nm is higher than the one at 552 nm, meaning that the signal at this wavelength is more sensible than at 552, therefore giving a better signal to noise ratio.

Results

The stopped flow measurements were performed with the three complexes analysed until now (wild type, wild type His tagged and acidic domain deletion mutant) at 418 nm, with syringes kept at 10 ° C by the use of a water bath. For each complex the effects of Pf inhibitors (such as stigmatellin) and Pm ones (such as MOA-stilbene and myxothiazol) were tested, after overnight incubation with a 10-fold excess of inhibitor.

3.5.2 Kinetics observed mixing against ascorbate, with and without inhibitors

Each of the three complexes studied showed a biphasic reduction in the stopped flow experiments: as seen in Fig. 48, the signal obtained can not be fitted to a monoexponential equation, since the residual plot shows a deviation of the model from the data. Fitting to a biexponential equation gives a much better result, indicating that the trace is composed of two phases, a fast and a slow one, whose constants are indicated in Table 13.

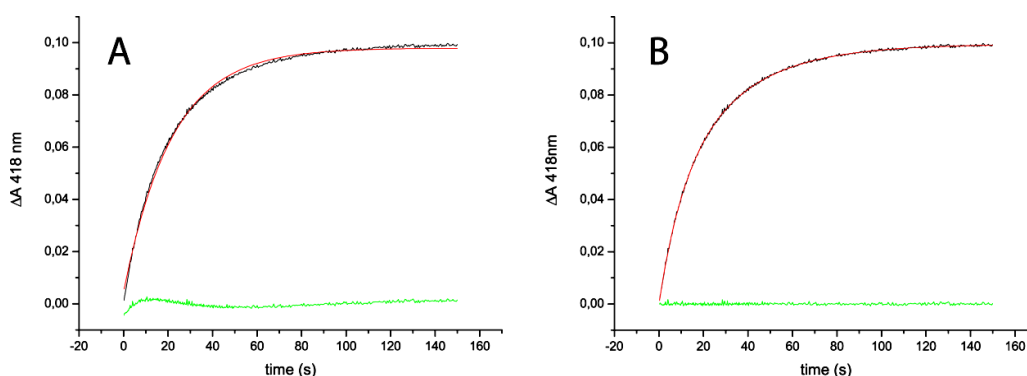


Fig. 48: Mono- and bi-exponential fit of one of the traces (black line) obtained with the wild type cytochrome bc_1 complex mixed with ascorbate. Left plot: the fit to a single exponential (red line) does not fit properly, since the residual plot (green line) is not flat indicating the model deviates from the experimental data. Right plot: fit to a double exponential equation, showing a much better correspondence between the model and the data.

The rate constants show different behaviours: the PFO constant for the fast phase increases linearly with the concentration of ascorbate, whereas for the slow phase shows a hyperbolic dependency (Fig. 49). The the slow phase tends to saturation, i. e. increasing the ascorbate concentration does not change the PFO rate constant anymore.

Results

	Wild type [M ⁻¹ s ⁻¹]	WT His tagged [M ⁻¹ s ⁻¹]	His tagged deletion mutant [M ⁻¹ s ⁻¹]
k_{FAST}	54.4	59.9	66.1

Table 13: Second order rate constant for the reduction of the cytochrome *bc*₁ complex in presence of ascorbate. The slow phase is hyperbolically dependent on ascorbate concentration, so no linear fitting can be done. Errors are within 10 % of the measured values.

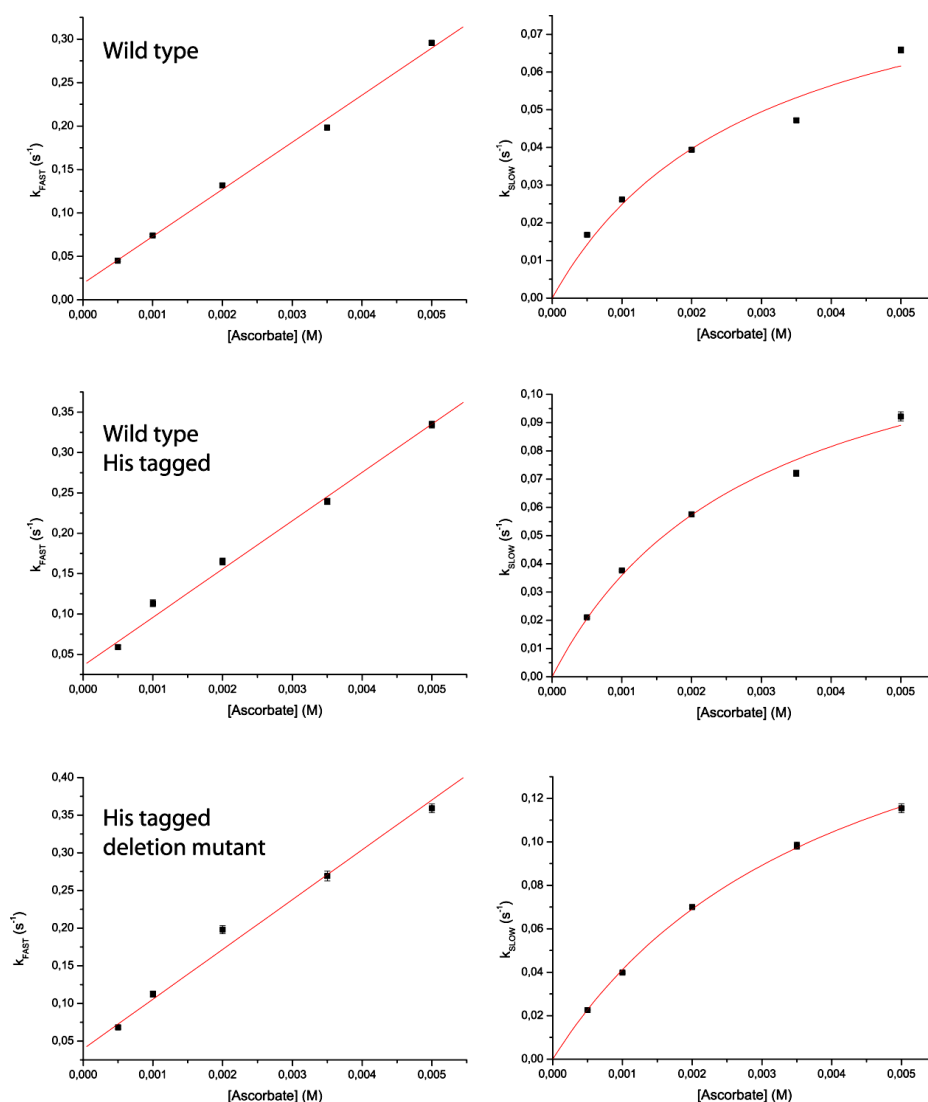


Fig. 49: Dependency of the PFO rate constants on the ascorbate concentration. Left column: k_{FAST} . The constant increases linearly with the ascorbate concentration. The slope from the plots is the second order kinetic constant (M⁻¹s⁻¹) of the fast phase. Right column: k_{SLOW} . The constant increases with the ascorbate concentration hyperbolically: at high ascorbate concentration, the process described by the slow constant tends to saturation, with no further increase of the k_{SLOW} .

Results

The amplitudes of the fast and the slow phase displaying that the first increases, whereas the second diminishes with increasing ascorbate concentrations, means that for low ascorbate concentrations the highest absorption change observed is due to the slow phase (about 70 % of the total amplitude). While increasing the ascorbate concentration, the curve reaches a point where the two processes contribute each of them with 50 % to the total absorption change. Further increasing ascorbate, the contribution of the slow phase becomes significantly lower reaching about 30 % of the total amplitude. This demonstrates that the kinetic process represented by the fast phase is predominant.

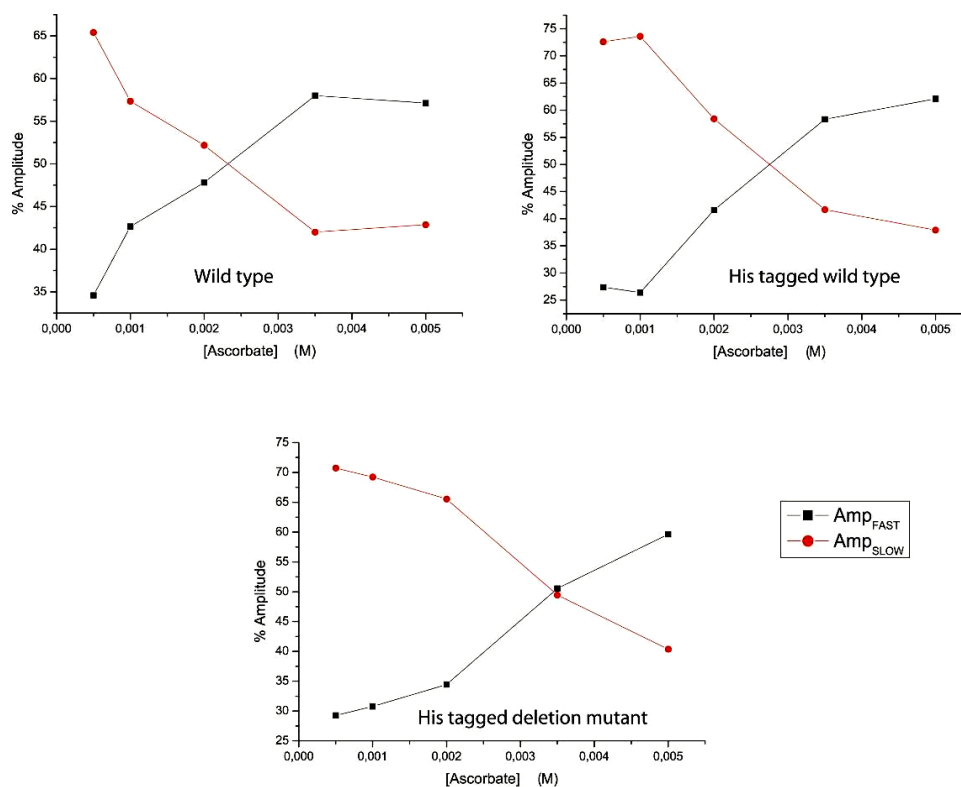


Fig. 50: Amplitudes (expressed as percentage of the total amplitude) of the two phases for the cytochrome *bc₁* complex reduction in presence of ascorbate. The amplitude of the fast phase increases with the ascorbate concentration (black line), whereas the one of the slow phase diminishes (red line).

Incubating the protein solution overnight with a 10 fold excess of stigmatellin, the kinetics are much slower than in the uninhibited complex: this effect is clear in Fig. 51, where a trace recorded with 4 mM ascorbate clearly shows the difference in the

Results

presence of stigmatellin. Cytochrome c_1 reduction is slower than in the absence of inhibitor.

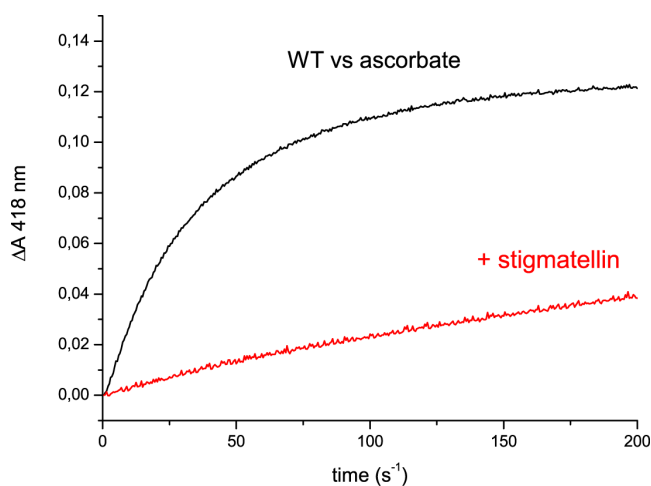


Fig. 51: Comparison between one of the traces obtained from the first experiment (inhibitor free, black line) and the trace in the same condition with excess of stigmatellin (red line).

Upon binding of stigmatellin to the Q_o site, the PFO constant for the fast phase becomes hyperbolically dependent on ascorbate concentration. The k_{SLOW} on the other hand is now showing a linear behaviour, with values indicated in Table 14. This indicates that the binding of stigmatellin, which docks the ISP head domain onto cytochrome b , fixing it, acts on the kinetics clearly reducing the rate of cytochrome c_1 reduction. It is interesting to note that the process is still biphasic. With the ISP fixed in the b position, ascorbate should transfer electrons directly to the cytochrome c_1 , resulting in monophasic signals. The biphasicity is, though, still observed (see 4.3).

	Wild type [$M^{-1}s^{-1}$]	His tagged wild type [$M^{-1}s^{-1}$]	His tagged deletion mutant [$M^{-1}s^{-1}$]
k_{SLOW}	0.2	0.1	0.2

Table 14: Linear fit of the PFO k_{SLOW} . Values of the second order rate constant for the reduction of the cytochrome bc_1 complex in presence of stigmatellin. Errors are within 10 % of the measured values.

Results

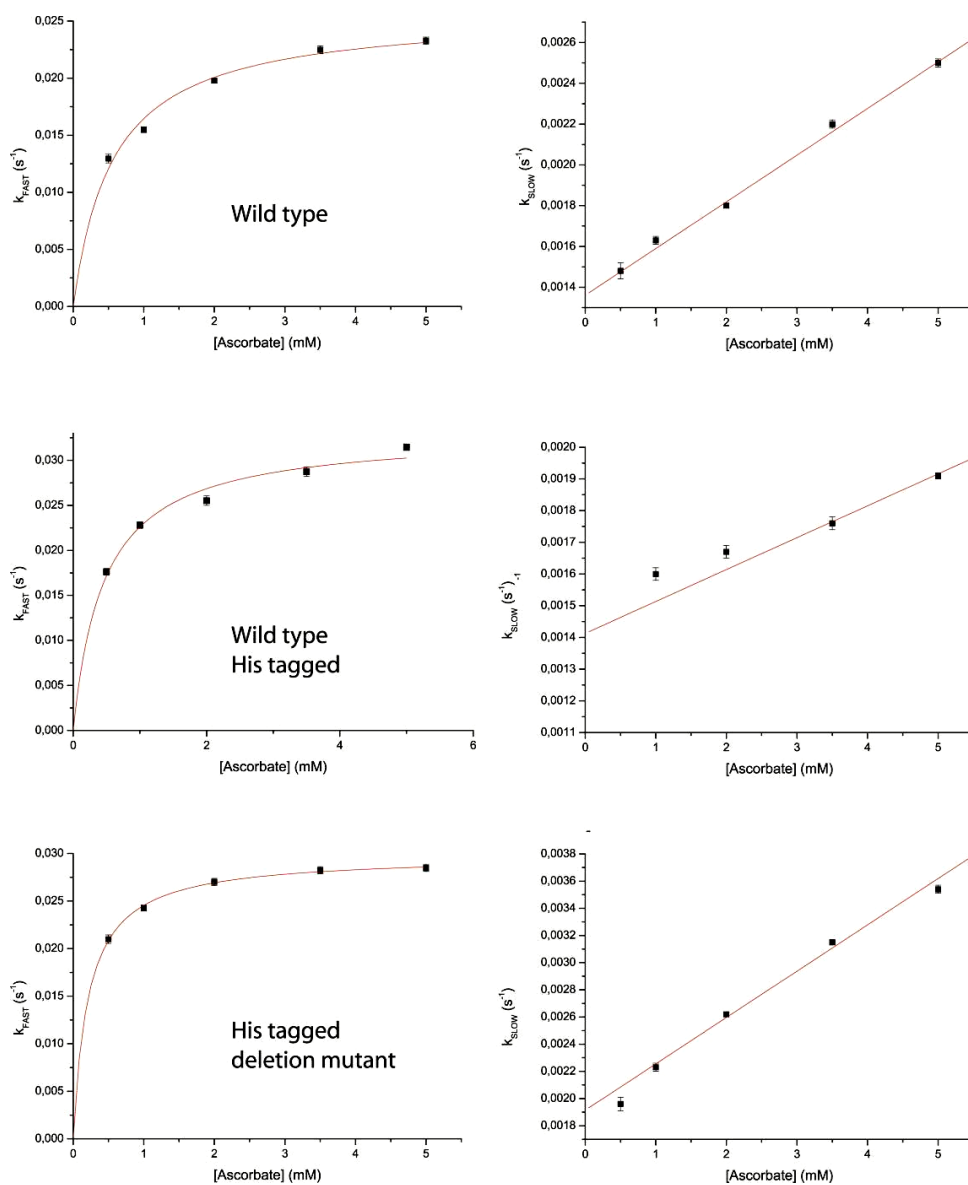


Fig. 52: PFO constants in presence of 40 μ M stigmatellin (in the left column, k_{FAST} ; right column; k_{SLOW}). The k_{SLOW} shows a linear behaviour now, and the k_{FAST} is hyperbolically dependent on the ascorbate concentration.

Results

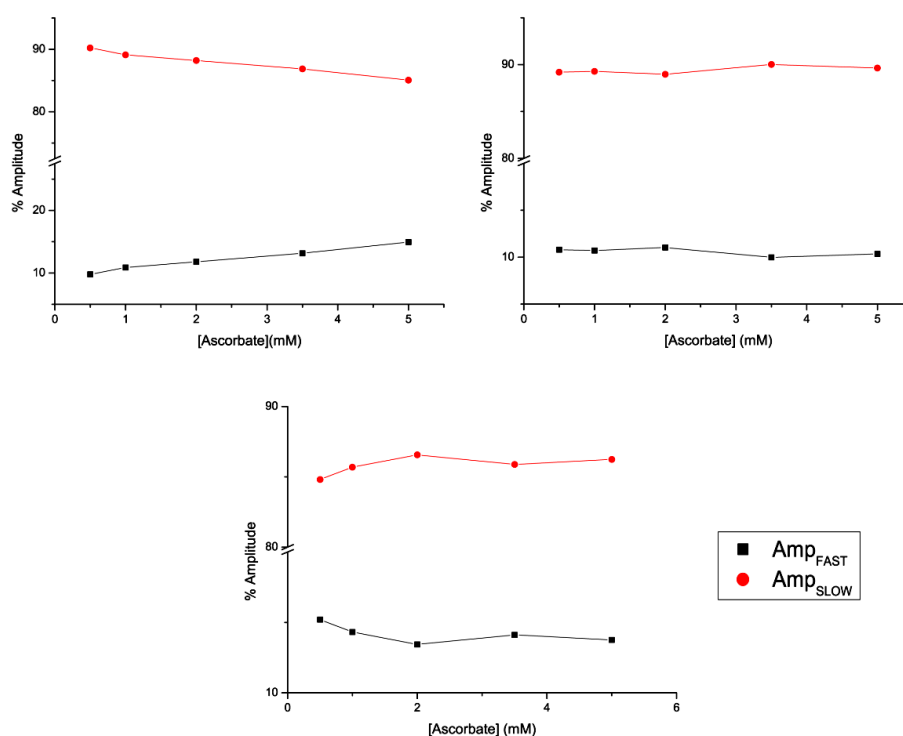


Fig. 53: Amplitudes of the kinetic process in presence of 40 μM stigmatellin. Upon addition of stigmatellin, the amplitude of the slow phase is predominant over the one of the fast phase. The amplitudes tend to remain constant throughout the experiment.

The amplitudes upon binding of stigmatellin are independent on the ascorbate concentration, meaning that the cytochrome c_1 amount reduced during the two phases is constant. The amplitude of the slow phase is now predominant, being 90 % of the total amplitude and stays constant during ascorbate titration.

In presence of MOA-stilbene, also a Pm inhibitors, the overall situation is changed: kinetics are faster, with a k_{FAST} increasing almost by a factor of two in comparison to the one uninhibited complex. Results are listed in Table 15, showing this remarkable effect. The dependence on ascorbate concentration is linear, exactly as observed for the uninhibited complex. The k_{SLOW} , on the other side, shows in a more definite way its hyperbolic dependency on ascorbate concentration, reaching saturation at lower ascorbate concentrations than in the first case (Fig. 54).

Results

	Wild type [M ⁻¹ s ⁻¹]	His tagged wild type [M ⁻¹ s ⁻¹]	His tagged deletion mutant [M ⁻¹ s ⁻¹]
k_{FAST}	79.7	82.4	94.0

Table 15: Linear fit of the PFO k_{FAST} results in values for the second order rate constant for the reduction of the cytochrome bc_1 complex in the presence of MOA-stilbene. Errors are within 10 % of the measured values.

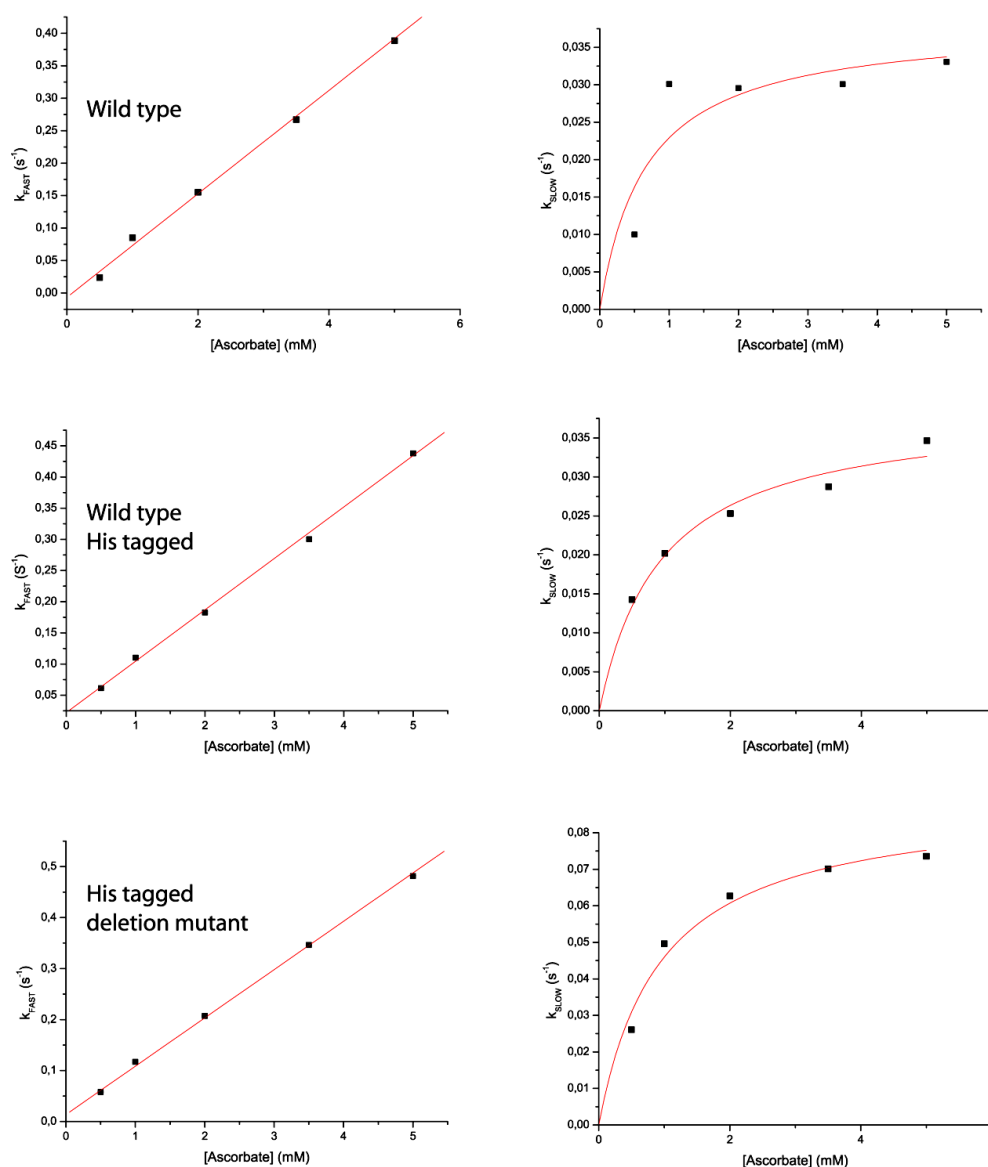


Fig. 54: PFO constants of 40 μM MOA-stilbene inhibited complex. The k_{FAST} increases linearly with ascorbate concentration, revealing a second order constant clearly faster than in the case depicted in Fig. 48 (uninhibited complex); k_{SLOW} shows the same hyperbolic dependence as observed before.

Results

The amplitudes for the MOA-stilbene inhibited complex are shown in Fig. 55. For the fast phase, the amplitude tends to diminish, whereas the one of the slow phase increases. A similar situation was already observed in the experiments without inhibitor, but the amplitude of the fast phase increases much faster than in the previous case. Indeed, the intersection of the two phases is reached at a lower ascorbate concentration than before (about 1 mM ascorbate after mixing).

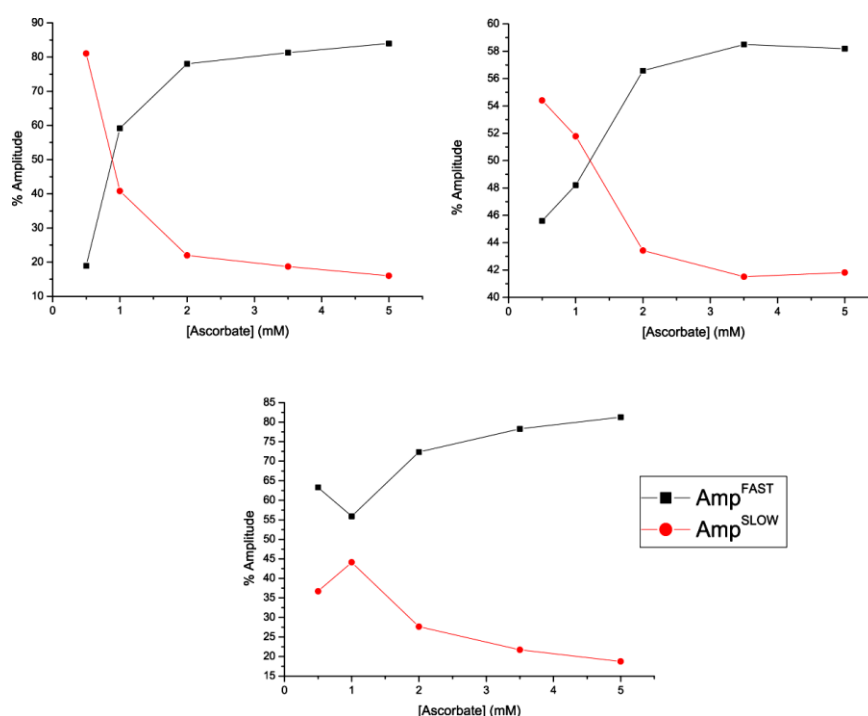


Fig. 55: Amplitudes of the fast and the slow phase in presence of 40 μ M MOA-stilbene. Upper left: wild type complex; upper right: His tagged wild type complex, and, lower panel, deletion mutant complex. At 1 mM ascorbate, both phases contribute each for 50 % of the total amplitude, opposite to what observed with the inhibitor free complex.

Another Pm inhibitor has been also tested, mixothiazol. Its effect is less evident than the one of MOA-stilbene (Fig. 56). In Table 16, the bimolecular rate constants for the experiments with mixothiazol are indicated. A slight increase in the rates, but less evident than in presence of MOA-stilbene, is observed. The amplitudes have a similar trend to the ones observed with the other Pm inhibitor and the wild type.

Results

	Wild type [M ⁻¹ s ⁻¹]	His tagged wild type [M ⁻¹ s ⁻¹]	His tagged deletion mutant [M ⁻¹ s ⁻¹]
k_{FAST}	64	71	60

Table 16: Second order rate constant for the fast phase describing the reduction of the cytochrome *bc*₁ complex after overnight incubation with excess (40 μM) of mixothiazol in presence of ascorbate. Errors are within 10 % of the measured values.

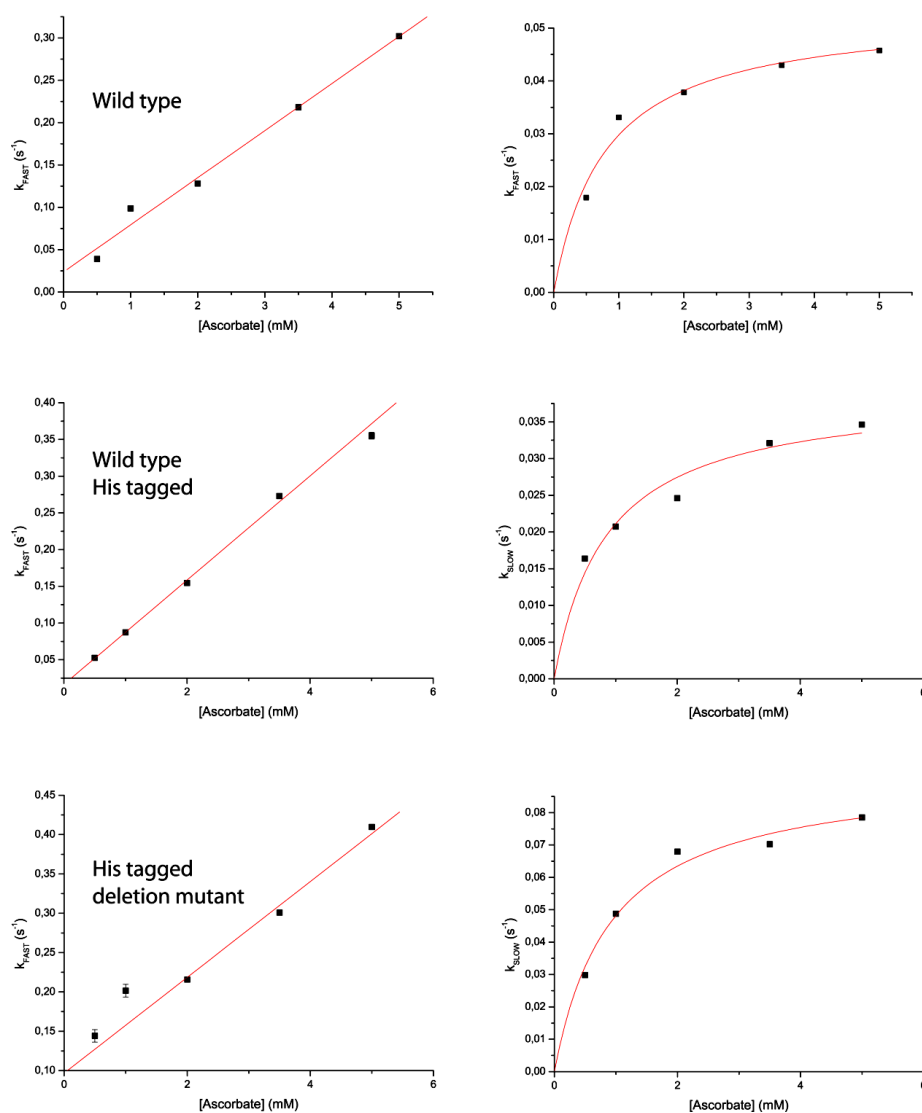


Fig. 56: Comparison of the PFO constants for the three complexes achieved by stopped flow experiments in presence of 40 μM myxothiazol. The k_{FAST} (left) has a linear behaviour, and the slope gives a slightly faster second order constant than in absence of inhibitors. The k_{SLOW} shows, even more clearly than in previous experiments, its hyperbolic dependence on the ascorbate concentration.

Results

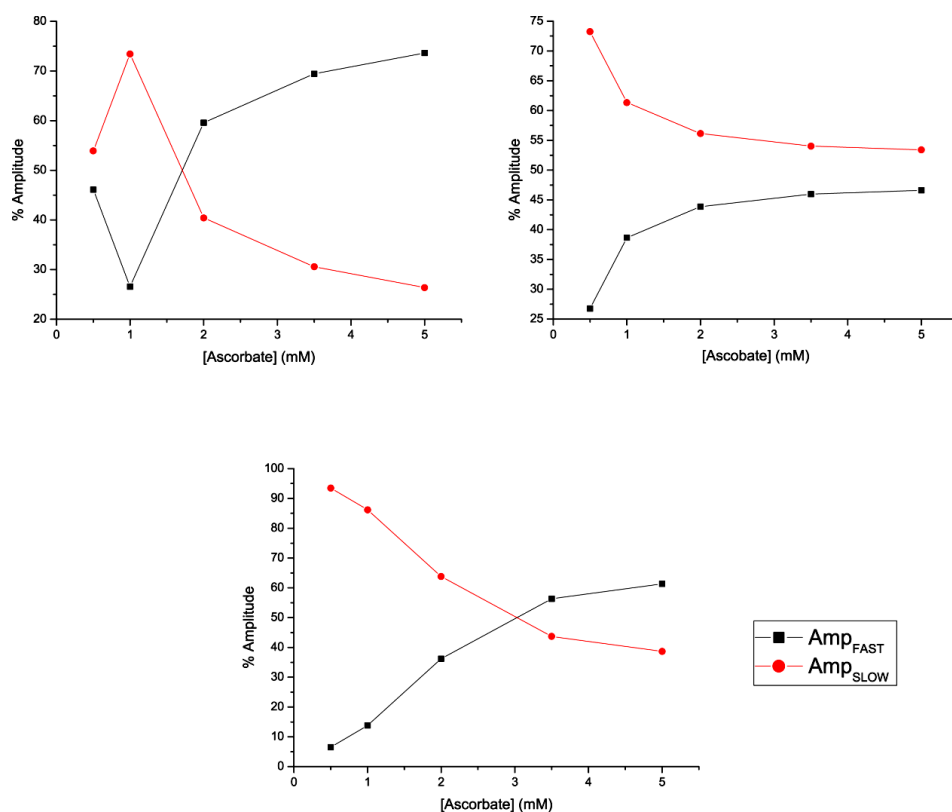


Fig. 57: Amplitudes of the fast and the slow phase in presence of 40 mM mixothiazol during the assay. From the upper right plot, wild type complex, His tagged wild type and deletion mutant complex respectively. The amplitude of the fast phase increases and the one of the slow phase diminishes throughout the experiment: a clear trend for the intersection is not visible as for the other cases.

3.5.3 Kinetic measurements using the *fbcF* gene with the S157C mutation

The contribution of the ISP cluster to the biphasic kinetic was studied more in detail with a mutant complex missing the Rieske cluster. The mutant was first described by Gutierrez-Cirlos *et al.* (86) where the mutation S183C (in the ISP gene from yeast) resulted in a complex where the apo-protein was still inserted but no signal for the Rieske cluster was detected in CD spectroscopy. The insertion of the Cys residue for the Ser leads, most likely, to the formation of an internal disulphide bridge with one of the Cys residues involved in the binding of the iron atom of the cluster, leading to loss of the cofactor (Fig. 58).

Results

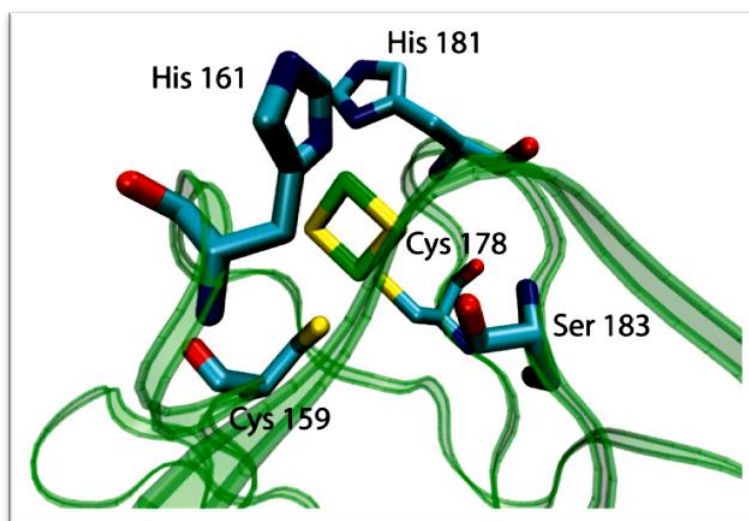


Fig. 58: Stick-representation of the Rieske cluster coordinating side chains in the yeast cytochrome bc_1 complex (PDB 1KY0). The protein backbone is shown in the ribbon representation in green. The Rieske cluster is in the middle, with the sulphur atoms in yellow and the iron ones in green. The residues Cys¹⁵⁹ and Cys¹⁷⁸ may be involved in the disulphide bridge with the thiol group of the Cys¹⁸³ in the mutant S183C (*P. denitrificans* numbering S157C).

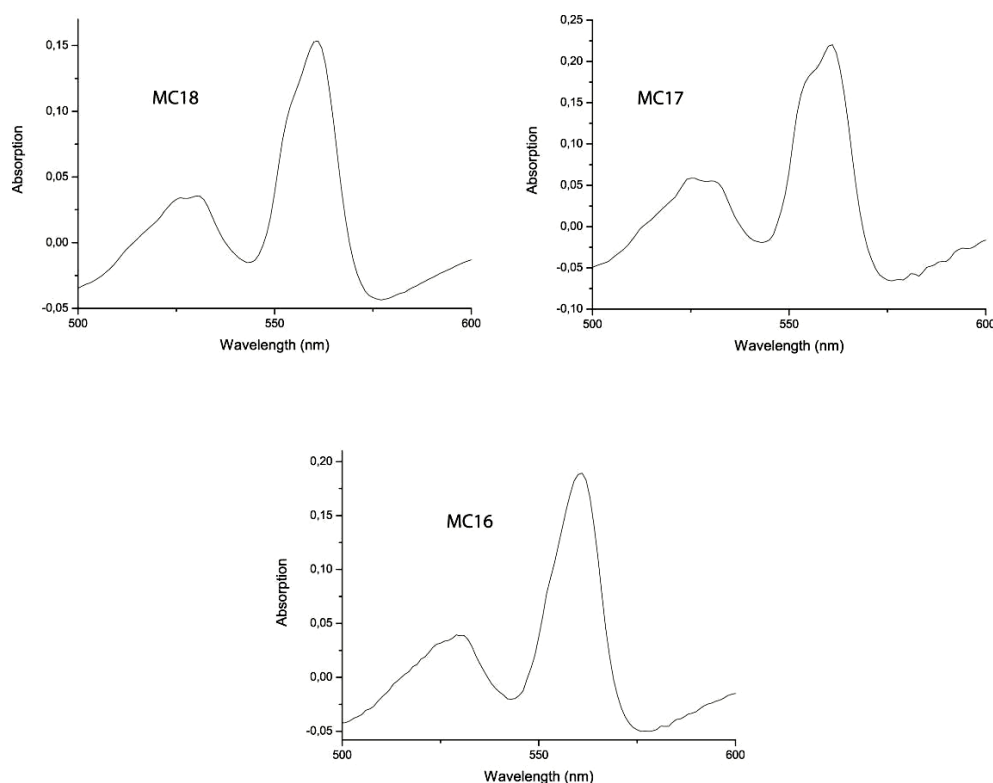


Fig. 59: redox spectra of the S157C mutants, demonstrating the presence of cytochrome c_1 and cytochrome b in the purified protein. The peaks observed correspond to the ones expected for a wild type protein (see Fig. 9, panel A).

Results

The mutation was inserted by inverse PCR into a cloning vector containing the acidic domain deletion mutant *fbc* operon (pMC14) and checked via sequencing. The operon was subcloned into the pRI2 expression vector to obtain the plasmid pMC16 and mated in *P. denitrificans* for expression. From pMC14, the fragment containing the mutation has been subcloned via Pfl23II/SacI directed cloning into pTK33 and pRI2(436) to obtain pMC17 and pMC18, respectively.

The membranes obtained from these strains were solubilised following the same protocol used for the corresponding wild type complex, and purified by ionic exchange or affinity chromatography. The redox spectra in Fig. 60 display the peaks for cytochrome *b* (560 nm) and cytochrome *c*₁ (553 nm) present in the purified complex. The presence of the iron sulphur apoprotein confirmed by a Western blot using an antibody against the ISP.

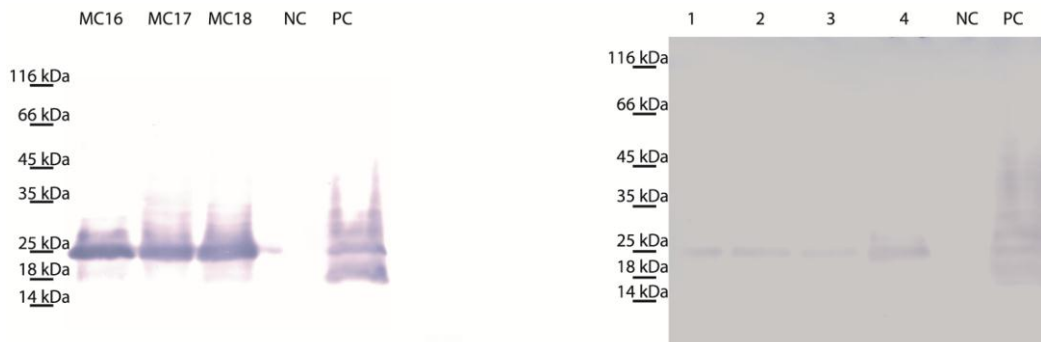


Fig. 60: Left panel: Western blot to reveal the ISP subunit of the strains MC16, MC17 and MC18. PC: positive control, TK56 *P. denitrificans* membranes with a Strep tagged version of the cytochrome *bc*₁ complex. NC: negative control, *T. thermophilus* wild type membranes, showing no cross reactivity with the used antibody. A signal is visible in the lanes MC16, MC17 and MC18. As expected the negative control does not show any band, and in the positive control the two typical bands for the ISP are visible. The presence of the 18 kDa molecular band could be the consequence of an incomplete denaturation of the sulphide bridges coordinating the cluster. Right panel: Western blot to follow the purification of MC16 as an example of the three strains on different fractions. Lane 1: solubilised membranes, lane 2: column flow through; lane 3: washing step; lane 4: eluted, and concentrated protein. Negative and positive control as described above. This Western blot shows that the iron sulphur apo-protein is present not only in the membrane but also in the purified protein, meaning that the absence of the cluster is not affecting the assembly and the stability of the complexes.

Results

The mutant complexes were also tested for turnover under steady-state conditions to check the functionality of the so obtained cytochrome bc_1 complex. With the cluster not present, as expected, no electron bifurcation can take place at the Q_o site and, therefore, no significant absorbance changes could be measured. Even if the kinetic tests indicated the mutants were inactive, the complexes were further analysed by CD spectroscopy to verify the presence of the characteristic signal the Rieske cluster shows in response to polarized light. The results are depicted in Fig. 61. From these, it becomes clear that there is no ellipticity change in the region where for the wild type the signal of the Rieske cluster is expected. All those evidence taken together confirm that the mutation caused the loss of the FeS cluster, but still allows expression and correct insertion of the Rieske apoprotein in the complex assembled in membranes.

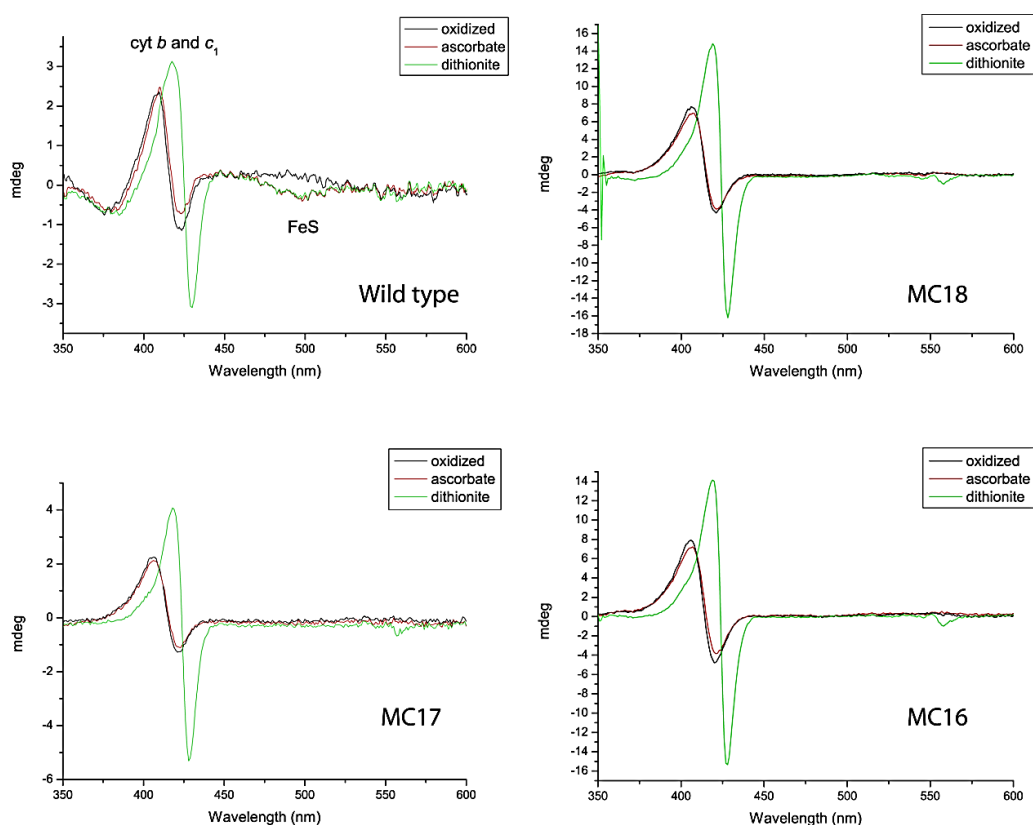


Fig. 61: CD spectra. Wild type: spectra obtained from the wild type cytochrome bc_1 complex. The complex has been measured in the oxidized state, ascorbate reduced and dithionite reduced. At wavelength 500 nm the signal for the ISP is visible. The complexes MC18, M17 and MC16 were also analysed by CD spectroscopy, and only the signals for the hemes are observed. This directly demonstrates that the cluster is not present as a consequence of the mutation S157C.

Results

The measurements were repeated with the complexes lacking the ISP, in the presence and absence of the inhibitors. The signals obtained from those measurements were monophasic, and the amplitude was independent of the ascorbate concentration. In Fig. 62 a typical signal obtained from the three complexes and the residual plot from the fitting to a single exponential is shown, clearly indicating that the previously observed biphasicity comes from the presence of the Rieske cluster. The presence of inhibitors did not show any effect on the kinetics anymore. This strikingly demonstrates that the biphasicity is beyond any doubt due to the Rieske cluster (Fig. 63, 64 and 65).

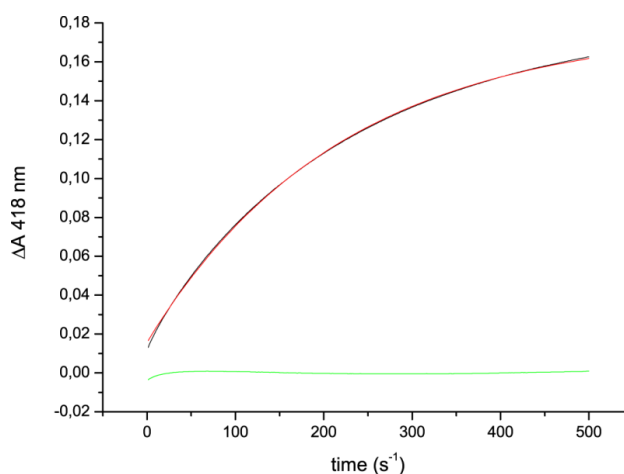


Fig. 62: Fitting of a trace obtained by the S157C mutated complexes (MC17) to a single exponential. The residual plot (green line) indicates a good correspondence of the data to the mathematical model used.

Results

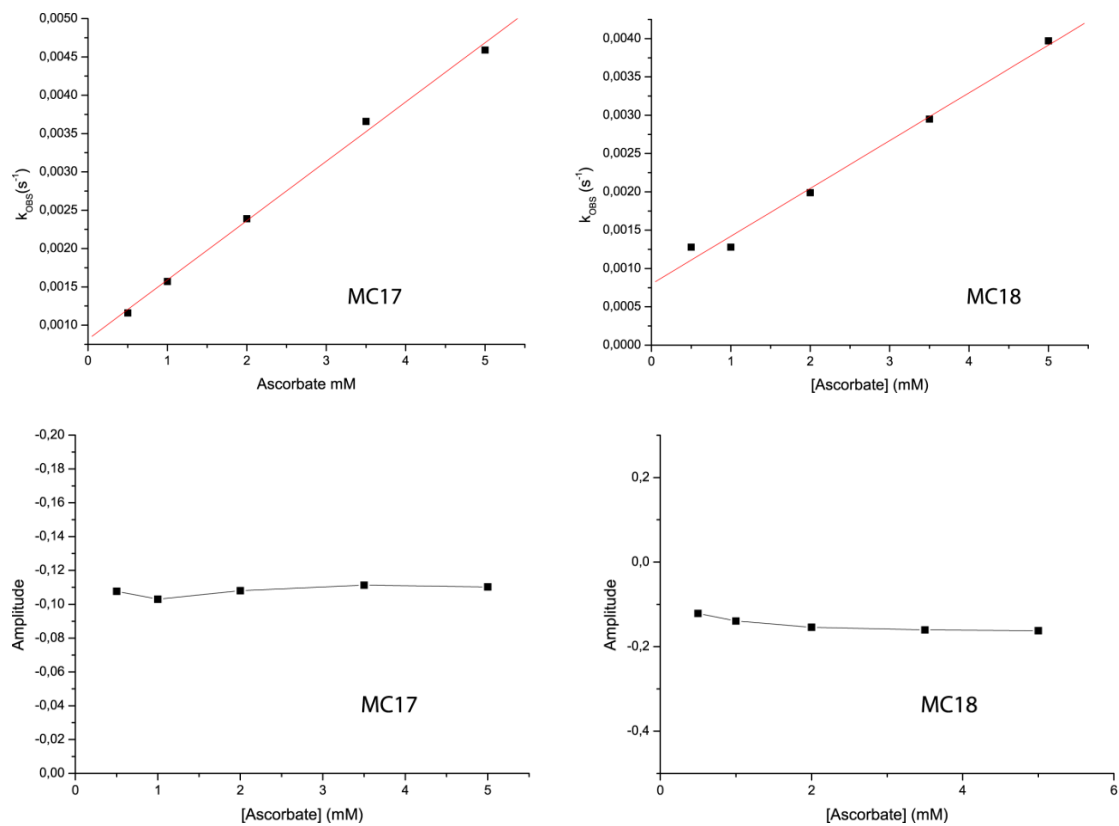


Fig. 63: PFO plots for the k_{OBS} obtained from the experiments with the complexes MC17 and MC18 (upper panels) and relative amplitudes (lower panels). The constants are linearly dependent on the ascorbate concentration. The amplitudes remain constant throughout the experiments, meaning a complete reduction of the cytochrome c_1 already at the lower ascorbate concentration (0.5 mM after mixing).

Results

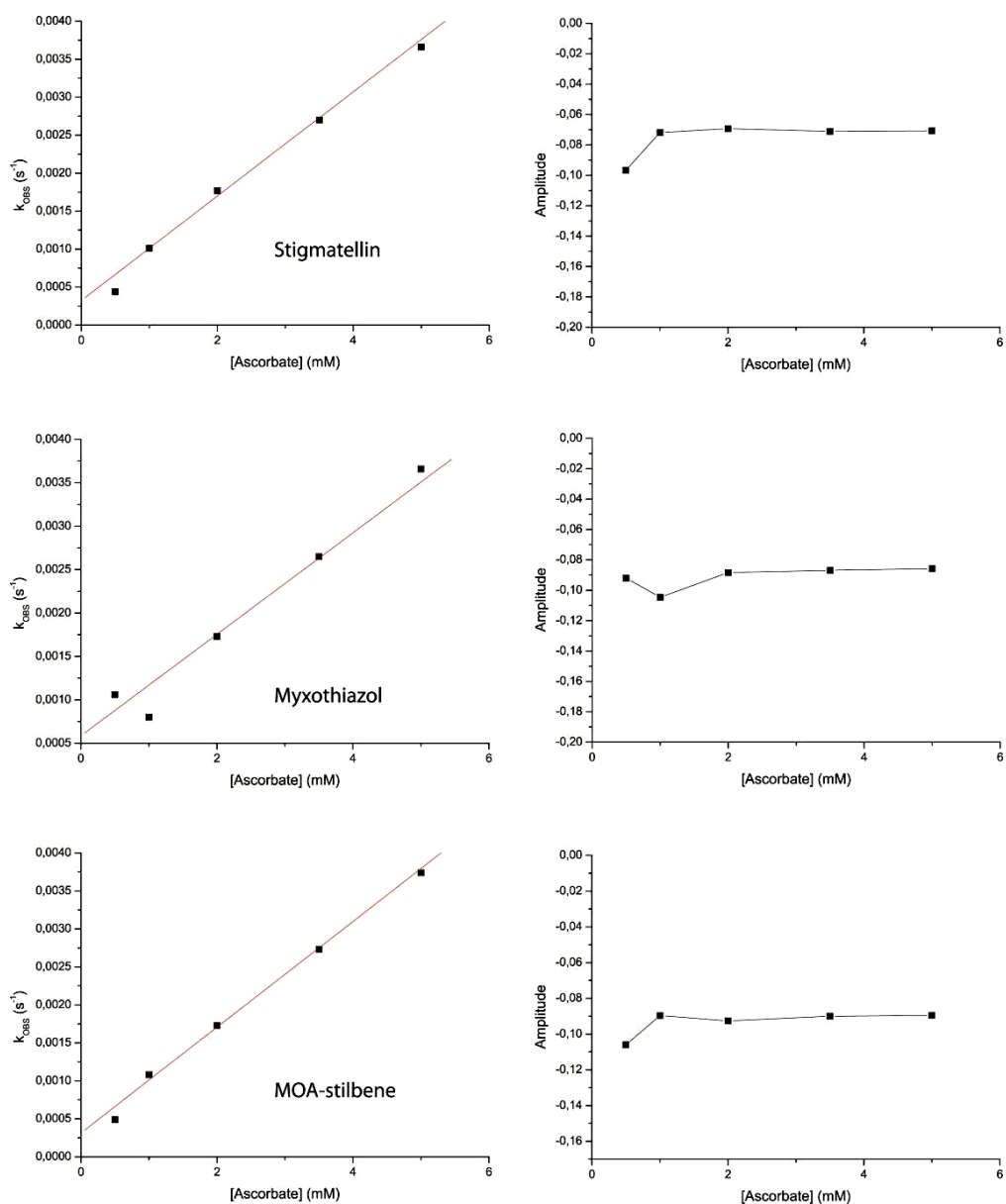


Fig. 64: PFO plots and amplitudes for the reduction of MC18 with ascorbate and inhibitors. Addition of inhibitors did not produce any change compared to the plot indicated in Fig. 62.

Results

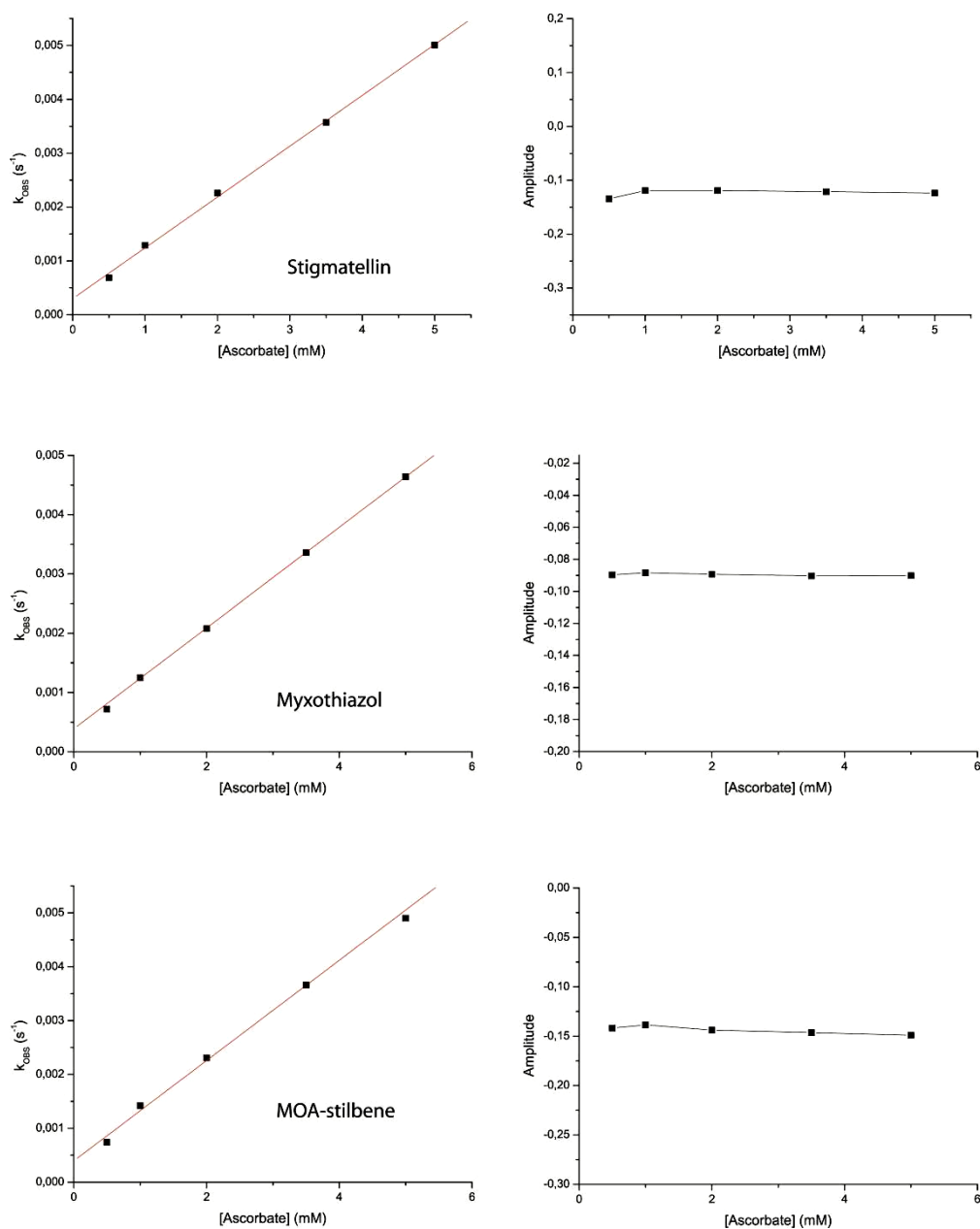


Fig. 65: PFO plots and amplitudes for the reduction of MC17 by ascorbate. As previously observed (Fig. 64), no change occurs upon binding of inhibitors.

In the case of MC16 (deletion mutant complex with the S157C mutation in the *fcfB* gene), a small biphasicity is still observed. The traces can still be fitted to a single exponential model for with low ascorbate, but the fitting tends to show deviation from the experimental data at higher concentrations (Fig. 66). In Fig. 67 is shown the PFO plot for the k_{FAST} and k_{SLOW} for the stopped flow experiment with MC16. The fast phase has very small amplitude (only 10 % of the total absorption change) and

Results

the constant is hyperbolically dependent on the ascorbate concentration, only in the case of MC16, and this could be due to the atypical behaviour already shown by the deletion mutant complex in the experiments of section 3.4.2, where the presence of ascorbate lead to reduction of both cytochrome c_1 and the cytochrome b . Nevertheless, the slow phase in Fig. 67 has a much bigger amplitude than the fast phase and the kinetic constant is in the range with the other two complexes, meaning that the fast phase observed is most likely to assign to the reduction of cytochrome c_1 in presence of ascorbate previously observed.

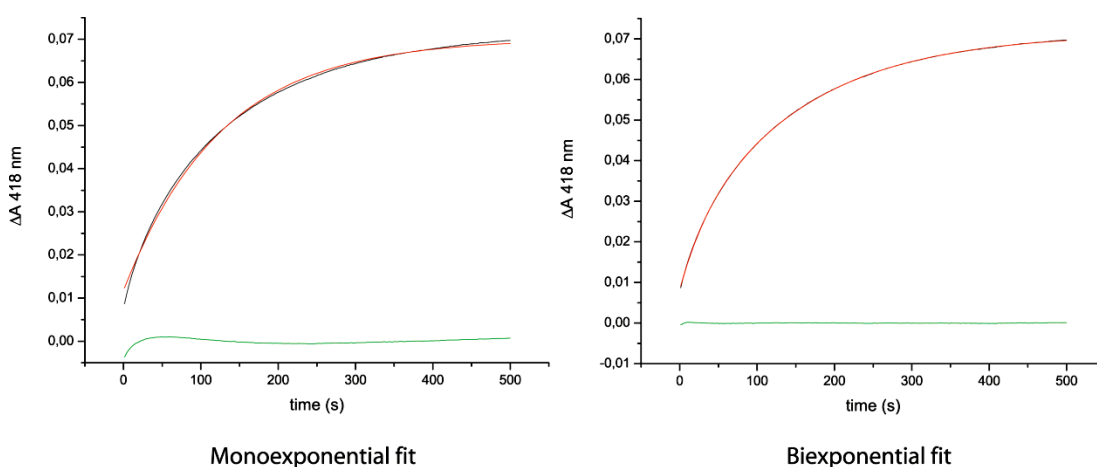


Fig. 66: Residual plot of the monoexponential and biexponential fit of one of the traces obtained from the SF experiments with MC16 (7 mM ascorbate). The biexponential fit indicates a very good correspondence with the experimental data, whereas the monoexponential fit leads to significant deviations. Therefore, the traces have been fitted to a biexponential equation and only the slow phase considered for the analysis.

Results

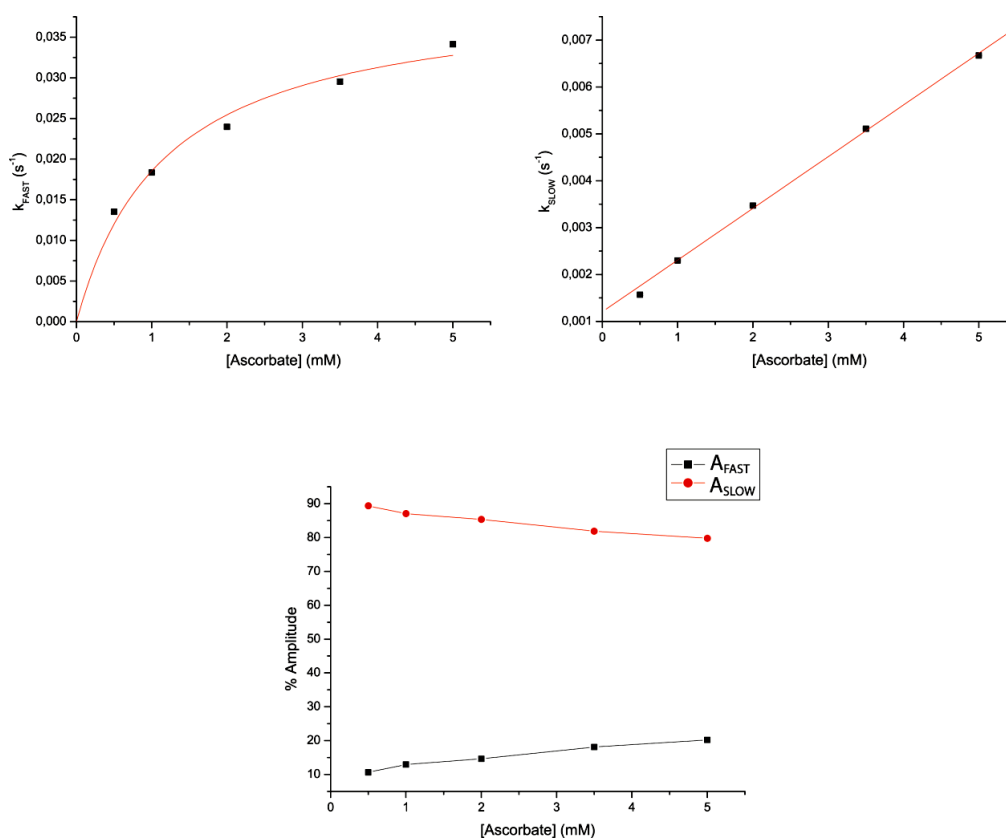


Fig. 67: PFO constants and amplitudes from the MC16 SF experiments with data fitted to a biexponential equation. Upper panel left: k_{FAST} , upper panel right: k_{SLOW} ; lower panel: amplitudes.

The assays in presence of inhibitors show no differences to the ones where the Q_o site is unoccupied, meaning that the biphasic kinetics observed in section 3.5.2 are due to the presence of the FeS cluster (Fig. 68). In table 17 all the kinetic constants are reported for the experiments with the complexes MC16, MC17 and MC18, showing no effect of the inhibitors on the reduction of cytochrome c_1 . This is in contrast to the observation of the complexes with the Rieske cluster.

Results

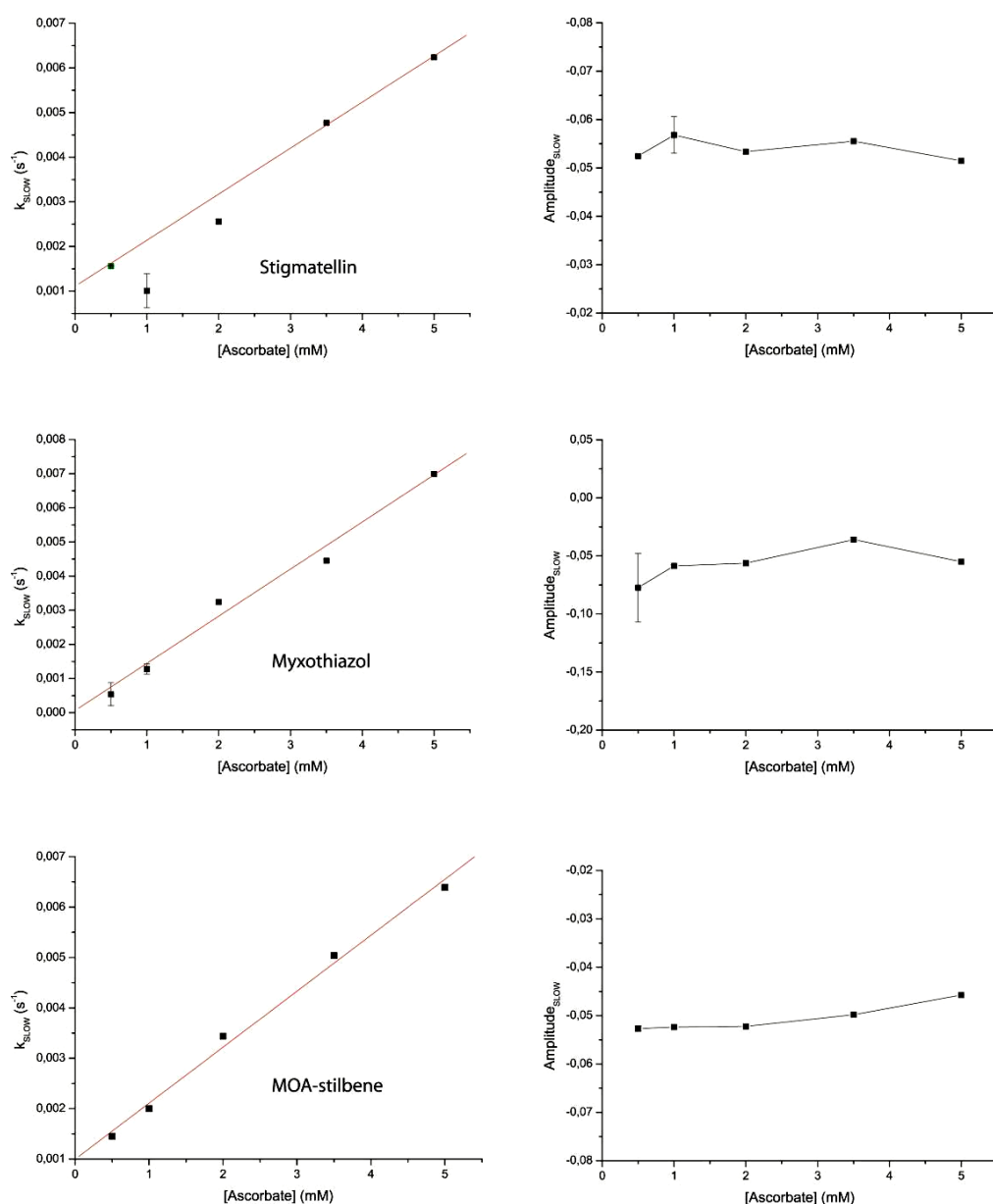


Fig. 68: PFO plots for the MC16 reduction kinetics in presence of different Q_o site inhibitors. Left column, the k_{SLOW} for MC16 in presence of stigmatellin (upper right), myxothiazol (middle right) and MOA-stilbene (lower right). Left column, the respective amplitudes. Only the k_{SLOW} and the amplitude of the slow phase are shown, since the fast phase is most likely due to an artifact seen only with the deletion mutant complex, as explained in the text.

Results

MC16	No inhibitor [M ⁻¹ s ⁻¹]	+ stigmatellin [M ⁻¹ s ⁻¹]	+ myxothiazol [M ⁻¹ s ⁻¹]	+MOA-stilbene [M ⁻¹ s ⁻¹]
	1.1	1.3	1.3	1.1
MC17	No inhibitor [M ⁻¹ s ⁻¹]	+ stigmatellin [M ⁻¹ s ⁻¹]	+ myxothiazol [M ⁻¹ s ⁻¹]	+MOA-stilbene [M ⁻¹ s ⁻¹]
	1.6	0.9	0.8	0.9
MC18	No inhibitor [M ⁻¹ s ⁻¹]	+ stigmatellin [M ⁻¹ s ⁻¹]	+ myxothiazol [M ⁻¹ s ⁻¹]	+MOA-stilbene [M ⁻¹ s ⁻¹]
	0.6	0.7	0.6	0.7

Table 17: Summary for the stopped flow experiments with the S157C mutants. No difference is present in the measurements in absence and presence of inhibitors, meaning that the Rieskecluster is effectively responsible for the biphasicity observed with the wild type complexes. Errors are within 10 % of the measured values.

The experiments presented here show that the cytochrome c_1 is reduced in two phases by ascorbate: a fast phase, with increasing amplitude at increasing ascorbate concentrations, and a slow phase, with diminishing amplitude. The PFO rate constant of the fast phase is linearly dependent on the ascorbate concentration, whereas the one of the slow phase shows a tendency to a hyperbolic dependency. This indicates that, at high ascorbate concentrations, the process defined by the rate constant is ascorbate independent. The presence of Pf inhibitors makes the k_{FAST} hyperbolically dependent on ascorbate concentration, while Pm inhibitors make the hyperbolic dependenc of k_{SLOW} from the substrate much more evident. The mutation S157C causes the lack of the Rieske cluster, abolishing the biphasicity and indicates no more effects of inhibitors on the cytochrome c_1 reduction.

4 Discussion

The aim of this work is the functional analysis of the cytochrome bc_1 complex, obtained by studying the dimeric nature of the complex, the interaction with its substrate and the inter-dimer electron transfer. For this study, the cytochrome bc_1 complex from *Paracoccus denitrificans* has been chosen as a model for several reasons: first of all, according to the endosymbiotic theory describing the origin of mitochondria (1), *P. denitrificans* shows a high degree of similarity with the ancestral α -proteobacterium which started the symbiosis at the origin of the eukaryotic cell. The respiratory chain of mitochondria corresponds to the one of *P. denitrificans*, composed of a complex I, II, a ubiquinone utilizing complex III, and an aa_3 cytochrome oxidase reducing O_2 to H_2O . Beside those, alternative oxidases are also present to allow fast adaptation to environmental changes (ba_3 quinol oxidase, cbb_3 oxidase, mostly expressed in conditions of low oxygen concentration). Moreover, the protein complexes of the aerobic respiratory chain in *P. denitrificans* are more basic versions of the mitochondrial ones, since no accessory subunit are present, allowing to work with smaller complexes still possessing the same properties as the eukaryotic counterparts. Bacteria offer the possibility of more convenient handling: as cultivation is less cumbersome and the genetic material is easily accessible for manipulation and modifications.

This work addresses open questions concerning the mechanism of the cytochrome bc_1 complex, such as the relationship between the putative dimeric nature of the complex and the catalytic cycle. Furthermore intermonomeric electron transfer, an internal regulation mechanism and how the two monomers communicate, were intensively discussed in the last ten years (108, 142, 143, 148, 183-185).

Additionally, the rotation of the ISP head domain has been investigated, by fast kinetic measurements, in order to gain insights on the mechanism which regulates the switching between cytochrome b and cytochrome c_1 and the electron bifurcation at the Q_o site. Several mechanisms have been proposed to explain how the ISP is kept in a specific position, and the regulation of its release from the Q_o site to reach cytochrome c_1 (67, 74, 127, 128, 130). The rotation of the ISP is a key step in the enzymatic turnover, since inhibitors binding at the Q_o site impair the electron transfer by blocking or displacing the ISP head domain (65). Several cytochrome bc_1 complex inhibitors are today used as herbicides (186), antimalaria agents (187-189)

Discussion

and fungicides (186, 190), so that the ISP movements and the interaction with inhibitors (from several crystal structures, (48, 65)) assume quite a big relevance.

P. denitrificans cytochrome bc_1 complex has a unique feature on the cytochrome c_1 gene, a 150 amino acid acidic domain (102, 104), which shows similarity to a small acidic subunit present in the eukaryotic complex involved in the interaction with the substrate (94, 111, 114). Since the domain is not present in any other organism, therefore representing a specific characteristic of *P. denitrificans* bc_1 complex, it has been deleted and the resulting complex tested with different kinetic approaches, in order to define the eventual role in regulating the interaction with cytochrome c_{552} , the physiological electron acceptor.

Finally, the internal electron transfer pathway has been analysed by stopped-flow kinetics. The complex has been reduced with increasing amounts of ascorbate and the bimolecular rate constants calculated for the reduction of the c_1 heme. Studies with mutants depleted of the Rieske cluster and inhibitor titrations (143) suggested that the Rieske cluster could affect the reduction of cytochrome c_1 , by acting as an intermediate affecting the rate of electron transfer to the c_1 heme.

4.1 Half-of-the-sites mechanism and dimeric nature of the cytochrome bc_1 complex

In all the crystal structures available at the moment, the cytochrome bc_1 complex is a homodimer (49, 52, 55, 65, 191). Each monomer contains cytochrome b , cytochrome c_1 and the Rieske ISP as catalytic subunits, plus up to 8 organism-specific additional subunits, according to the organism. Taking a closer look at the crystal structures and the position of the cofactors in the dimer, it is evident that the b_L hemes in the two cytochromes b in the dimer are in electron transfer distance (about 12 Å, edge to edge, Fig. 69 (65)), possibly allowing intermonomeric electron transfer.



Fig. 69: Cytochrome bc_1 complex from *S. cerevisiae* (PDB: 1KYO). In red, cytochrome b , in green the ISP and in light blue the cytochrome c_1 . In blue, the b_L hemes in the cytochrome b and in violet the b_H hemes. The b_L hemes are 12 Å apart, a distance allowing fast electron transfer across the dimer.

Electron transfer across the dimer has the aim to avoid the formation of detrimental ROS (192), which leads to cellular aging (193). In normal turnover conditions, quinol oxidation is so fast that both electrons are transferred almost simultaneously to the Rieske cluster and cytochrome b_L (194, 195). While an inhibitor is bound to the Q_i site, after the first electron reaches the Rieske cluster, the second electron coming from quinol cannot be transferred to a quinone/semiquinone molecule. A similar situation is obtained in presence of ischemia in tissues, where the low oxygen concentration impairs the electron flow in the respiratory chain and allowing them to react with molecular oxygen, producing superoxide (60). The protective distribution of electrons to the other monomer at the level of the b_L hemes allows electrons to find a quinone/semiquinone at the second Q_i site. The mechanism is effective only if the two monomers are not oxidizing quinol at the same time, so that for one electron entering the low potential chain there are two Q_i site theoretically available to accept it. Covian *et al.* (61) proposed a mechanism according to which

Discussion

only one Q_o site in the dimer is able to oxidize quinol at a given time, and electrons can equilibrate across the dimer. The occupancy of the Q_i site defines which monomer oxidizes quinol. The Q_i site can react with the Q-pool accommodating quinol and oxidizing it to a semiquinone or quinone, hereby reducing one (or two) b_H heme(s) in the process (141). This process stabilizes the species bound at the Q_i site, able to accept electrons coming from quinol oxidation, and at the same time impeding them to react with oxygen. The presence of a ligand at the Q_i site stimulates the other monomer to oxidize quinol at the Q_o site, communicating the presence of an available electron acceptor. The mechanism, called half-of-the-sites, is depicted in Fig. 7 (see Introduction 1.2.4.3). The way chosen here to verify the presence of such a regulation mechanism was the creation of a heterodimeric cytochrome bc_1 complex, where one Q_o site is inactivated by a mutation which impairs quinol oxidation but does not modify the affinity of the enzyme for the substrate. If the mechanism is valid, and only one monomer accounts for the activity of the complex at a given time, the introduced mutation would not diminish the turnover number in steady state conditions. Moreover, the stimulation of the second quinol oxidation site in the dimer should not occur in the heterodimeric complex, being the second Q_o site unable to oxidize the substrate. In the absence of any regulation mechanism, with each monomer responsible for 50% of the total activity, the mutation should allow only 50% of activity to be recorded.

The heterodimeric complex has been obtained by cloning the two different copies of the *fbc* operon in two separate expression vectors, with different origins of replication. As discussed more in detail in paragraph 4.4, the deletion mutant complex has been chosen for these experiments since LILBID analysis indicated that it has a dimeric structure (Kleinschroth *et al.*, manuscript submitted). The wild type complex is purified as a “dimer of dimers”(177): in this case, several combinations of affinity tags can be obtained, which do not allow purification of the heterodimer.

The two different expression vectors have been transferred by conjugation into *P. denitrificans* cells to allow homologous expression. The clones were screened by plasmidic DNA preparation and Western blotting to identify the presence of the two affinity tags. The separation of the heterodimer was achieved by a sequential purification, first on a Ni^{2+} -NTA column, followed by a Streptactin column. Once the cells are able to express the two versions of the Δfbc operon, three different

Discussion

combinations can be achieved: a dimer with only mutated, inactive monomers, one with fully active monomers and the desired heterodimer. On the first column is achieved the separation of just Strep tagged monomers from the ones containing two His tags and the heterodimer. With the second column, only heterodimers are eluted in a single step, using desthiobiotin. By Western blot, the presence of the two tags has been proven on the purified complex and redox spectra showed the expected peaks for the cytochrome bc_1 complex. Reduction of cytochrome c from horse heart in pre steady-state conditions confirmed that the complex measured is really a heterodimer: the kinetics of both monomers composing the heterodimer can be seen and identified (63).

To validate the half-of-the-sites mechanism, three experiments have been performed. In steady-state kinetics, it has been shown that the heterodimeric complex has a v_{MAX} comparable to the fully wild type dimer, meaning that only one monomer accounts for the activity measured. In the pre steady state kinetics in presence of antimycin was shown that when electrons can enter the complex through the only active Q_o site, the reduction of one cytochrome c_1 and two cytochrome b_H is obtained, due to intermonomer electron transfer. Finally, by titrating the complex with antimycin, a stimulation of the complex was demonstrated by activating the second monomer in the complex. The effects observed following the introduction of the mutation in one monomer are not due to changes in the affinity of the complex for the substrate, since steady state activity measurements showed that the K_M for quinol is not changed. Residue Tyr147 is thought to be involved in transferring the electron coming from quinol oxidation to the b_H heme, being halfway between the two. The substitution to Ser eliminates the aromatic ring blocking so the electron transfer.

A consequence of the half-of-the-sites mechanism is also the inhibition of the complex with one stigmatellin molecule per dimer: binding of stigmatellin at only one Q_o site blocks the ISP in the b position, kind of simulating the binding of substrate. As a consequence, quinol oxidation in the second monomer is blocked.

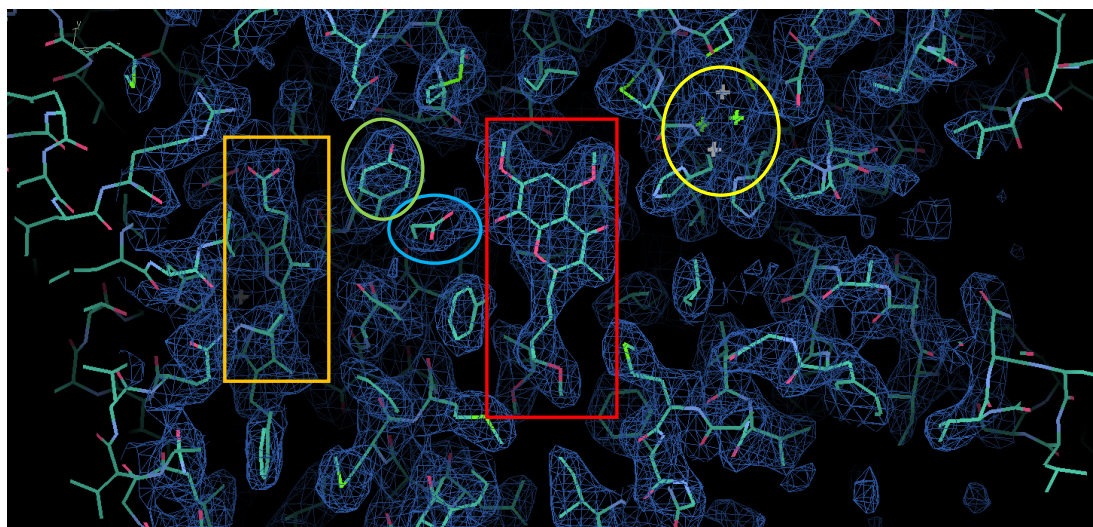


Fig. 70: electron density round the Q_o site from the deletion mutant cytochrome bc_1 complex from *P. denitrificans*. In yellow, the iron sulphur cluster. In red, stigmatellin. In light blue, the E^{272} of the PEWY sequence, hydrogen bonding stigmatellin (and quinol) and involved in substrate oxidation. In green, the Y^{147} , most likely being an electron bridge between the E^{272} and the b_L heme (side view, orange). Picture from Kleinschroth *et al.*, manuscript submitted)

The results show clearly that the half-of-the-sites mechanism is regulating the activity of the two monomers in the cytochrome bc_1 complex, and that the oligomerization state has not just a structural meaning (since the ISP structurally belonging to one monomer is catalytically active in the second one) but also a functional one.

It still is unclear how the activation of the second monomer takes place, even though hints come from the crystal structures available. Cytochrome b has both N- and C-termini facing the negative side of the membrane, the matrix in mitochondria and the cytoplasm in bacteria. The N-termini of the two cytochrome b are very close in the dimeric structure (Fig 43), and this could be the junction transferring the signal that the binding of antimycin/semiquinone at one Q_i site generates in one monomer. Conformational changes after the occupation of the Q_i site can be transferred by highly conserved residues in close contact with the His^{202} (yeast numbering), a key residue for catalysis at the Q_i site, and the N-terminus of the second cytochrome b (62).

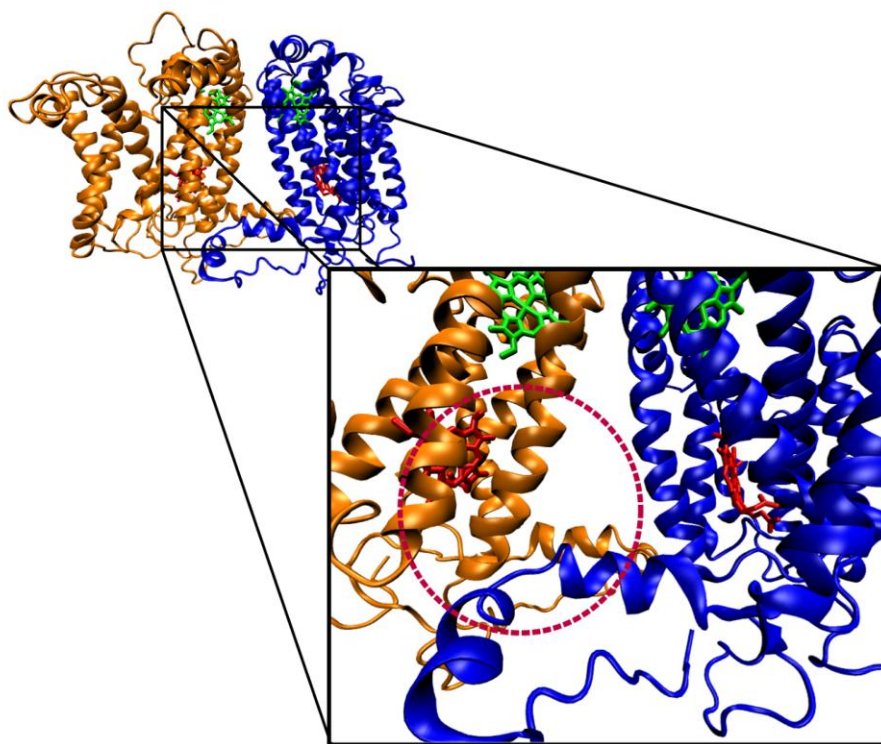


Fig. 43: Enlargement of the N-termini in the cytochrome *b* (PDN: 1zrt). In red, the b_H hemes and in green the b_L hemes. In the circle, the close contacts that the N-terminal sequence of the cytochrome *b* (blue monomer) makes with the helices surrounding the b_H heme in the cytochrome *b* (orange monomer).

A recent publication (196) discussed the presence of a regulation mechanism in the cytochrome bc_1 complex of *Rhodobacter capsulatus*. The approach used was to fuse together the genes for two cytochromes *b* in order to create a forced dimer, and have the possibility to introduce selectively in one or the other monomer inactivating mutations at the Q_o and Q_i site, to check not only the intermonomer electron transfer but also the regulation mechanism. The authors could not identify any kind of regulation in the activity of the cytochrome bc_1 complex, and affirmed that the two monomers are working in an independent manner. The weak point in this study is that by fusing together the C-terminus of a cytochrome *b* with the N-terminus of the cytochrome *b* in the second monomer, the proposed communication pathway is broken by fixating the termini. Therefore, it is to expect the absence of any regulation. Several groups now address this topic at the moment, all of them agreeing on the intermonomer electron transfer. The communication between

monomers and the controlled activation of the second quinol oxidation site is more highly debated.

4.2 Internal electron transfer and ISP movements

A central step in the Q cycle is the bifurcation of electrons at the Q_o site. From the oxidation of quinol, two electrons are released and split between the high and the low potential chain. The electron accepted from the Rieske cluster is transferred to cytochrome c_1 , after the ISP head domain moves towards the c_1 heme. To oxidize quinol, the ISP is fixed in the b position since a part of it is required to complete the Q_o site: one of the His coordinating the Rieske cluster has a hydrogen bond with quinol, forming a quinol-imidazolate complex (56, 68, 82, 85, 122, 125, 197-200). The same His is involved in coordination of stigmatellin via a hydrogen bond (71), blocking the movements of the head domain towards the cytochrome c_1 . Two different binding pockets have been identified in the Q_o site (73): a proximal and a distal part, where inhibitors like MOA-stilbene and stigmatellin, respectively, bind (48). This led to the idea that possibly two quinol molecules are accommodated at the Q_o site, one of them being completely oxidized and the second one working as a “cofactor”. This hypothesis is known as “double occupancy model” (83, 124, 201) and is just one of the many suggestions concerning the mechanism of quinol oxidation.

From crystal structures it was clear that whenever the ISP was not blocked in proximity of cytochrome b it was difficult to assign electron density to it, and only a part of the transmembrane helix was visible (52). This was the first hint towards the idea that movements were implicated in the catalytic cycle of the cytochrome bc_1 complex. On the other hand, it was difficult to state what the position of the head domain was in absence of inhibitors or in the case of no substrate bound and therefore no electron transfer taking place. Moreover, it is still unclear which signal allows the release of the head domain from cytochrome b after quinol oxidation. Di Xia *et al.* (127) proposed a mechanism based on observations made on crystal structures of inhibitor complexed bc_1 complexes, according to which the ISP head domain has, prior to substrate binding at the Q_o site, no fixed conformation. When quinol enters the Q_o site binds first in the distal pocket, and the $cd1$ helix of cytochrome b opens up allowing the ISP to fit perfectly onto cytochrome b and forming the complete Q_o site. Quinol now forms two hydrogen bonds, one with the

Discussion

His¹⁶¹ coordinating the Rieske cluster and one with the Glu²⁷² (bovine numbering) of the conserved PEWY sequence of the *ef* helix in cytochrome *b* (Fig. 71). Quinol is then oxidized and electrons are split between the ISP and the *b_L* heme. With the movement of the substrate to the proximal pocket, and/or with the electron transfer from *b_L* to *b_H*, the *cd1* helix goes back to the initial position and the ISP is released from cytochrome *b*, free to move in direction of cytochrome *c₁* and transfer its electron.

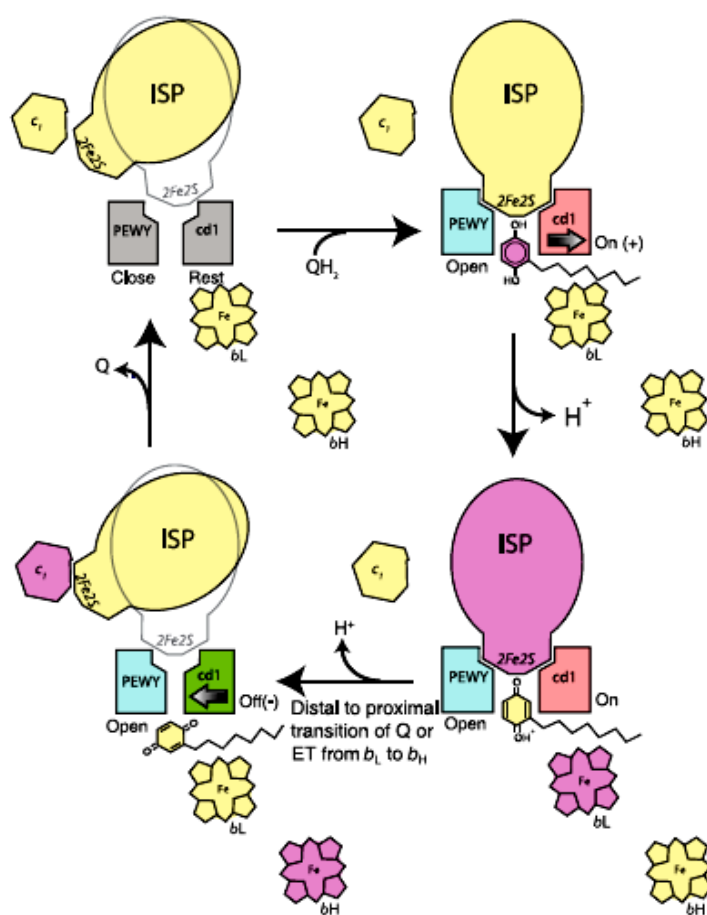


Fig. 71: Mechanism of electron bifurcation at the Q_o site. The mobile ISP head domain, normally oxidized (yellow) has no fixed position in the complex. As quinol enters the Q_o site distal part, the *cd1* helix moves (pink) and gives space so that the substrate is accommodated between the PEWY sequence (*ef* helix) and the *cd1* helix itself in cytochrome *b*. Now the ISP head domain can interact with the bound quinol and is blocked in the *b* position. The reduced ISP (violet) gets reduced but stays in the *b* position as long as semiquinone moves to the proximal part of the Q_o site or as soon as the electron from the *b_L* heme is transferred to the *b_H* heme. After one of the two events, the ISP is released and free to move towards cytochrome *c₁*, which is then reduced (graphic from (127)).

Discussion

In this work, flash photolysis experiments were used to investigate the movements of the ISP were studied, in presence and absence of ligands at the Q_o site. If the complex was reduced only with ascorbate and TMPD, meaning only endogenous quinone available in the dimer, two phases could be identified in reduction of cytochrome c_1 : a fast and a slow phase, with rates of $9,000\text{ s}^{-1}$ and $1,000\text{ s}^{-1}$, respectively. The amplitude of the two phases is relatively small: the fast phase is only 9 % of the total photooxidized cytochrome c_1 , and the fast phase only 17 %. The results until now indicate that a small fraction (9 %) of the reduced ISP without added Q_o site ligands is in proximity of the cytochrome c_1 , able of fast electron transfer, and another fraction (17 %) is in a position closer to cytochrome b , so that the electron transfer rate is lower. Another significant fraction of the ISP is not at all able to react and transfer electrons, since the amount of cytochrome c_1 reduced after flash is relatively small. In these experiments the Q_o site has no added ligands, and only endogenous quinol/quinone is present. The amount of endogenous quinone present in the preparations has been measured at the University of Strassbourg in the group of Prof. Petra Hellwig, and all three preparations used have two quinol/quinone molecules bound per complex monomer, most likely one at the Q_o and one at the Q_i site (data not shown).

Adding Pm inhibitors, such as MOA-stilbene or myxothiazol, significantly increases the amplitudes of the two phases. Hereby the total amount of reduced FeS cluster is able to transfer electrons to the cytochrome c_1 is now higher as a result of ligand added at the Q_o site. The rate of the fast phase remains changed, but the slow phase is two times faster than what previously measured. This clearly indicates that only one of the two conformations of the ISP is affected by the binding of Pm inhibitors at the Q_o site. This suggest that the slow phase represents the ISP close to the cytochrome b : binding of Pm inhibitors at the Q_o site causes a displacement of the ISP head domain from cytochrome b and allows faster electron transfer. The rate of the fast phase is not changed, since the amount of ISP closer to cytochrome c_1 is unaffected by the inhibitor binding.

Pf inhibitors (stigmatellin, JG-144) change the picture again: stigmatellin is the only inhibitor able to coordinate the His¹⁶¹ (bovine numbering) with a hydrogen bond which keeps the ISP head domain fixed in the b position. Hereby it does not allow any movement towards cytochrome c_1 , as shown by the results in section 3.4.2, where the signal is totally quenched in presence of stigmatellin. In presence of JG-

Discussion

144, the rate of both phases is drastically diminished, meaning that the inhibitor lowers the rate at which the ISP head domain can transfer electrons to the cytochrome c_1 . This is consistent with the information obtained from crystal structures (70) where JG-144 makes no hydrogen bonds with the ISP head domain, so that its movement is not blocked but significantly slower. This indicates as well that the hydrogen bond between stigmatellin and the His161 coordinating the cluster is necessary to keep the ISP head domain fixed in the b conformation. JG-144 cannot fix the ISP close to cytochrome b but affects the release of the ISP head domain from the b position, indicating that an intrinsic regulation mechanism has to be present.

Binding of quinol at the Q_o site does not change the electron transfer rates of the two phases but increases the amplitudes, meaning that its presence allows a larger ISP fraction to move towards the cytochrome c_1 . The fast phase is almost 20 % of the total flash-oxidized cytochrome c_1 , and the slow phase is about 45 %. The analysis of the data taken together confirm the mechanism proposed by Di Xia et al (70, 127), where the $cd1$ and the ef helices sense the binding of quinol at the Q_o site, and open up allowing the binding of the ISP onto cytochrome b . Binding of quinol at the Q_o site would allow the formation of a hydrogen bond with the His¹⁶¹ of the ISP and a proton coupled electron transfer would reduce the Rieske cluster. The subsequent electron transfer of the second electron to the heme b_L and then b_H causes quinol to leave the distal pocket and the sensory helices $cd1$ and ef to close. This releases the ISP head domain and after movement to the c position allows electron transfer to cytochrome c_1 . The effects of the two inhibitor classes (Pf and Pm) and the effects upon quinol binding are consistent with the proposed mechanism and could be verified by fast kinetics in this study. The results discussed here indicate that the binding of ligands at the Q_o site and the ISP head domain motions are tightly linked and most likely playing a role also in ensuring the electron bifurcation avoiding short circuits which lead to the generation of ROS with serious consequences for the organism. Some authors (128) proposed that the electron transfer from the b_L to the b_H represents the key factor in the electron bifurcation at the Q_o site, and the experiments presented in this work cannot exclude the presence of other factors (such as coulombic gating of the motion of the semiquinone (202, 203), the conformations of water or amino acid side chains in the Q_o pocket (66, 136,

137, 198, 202) or the redox state of cytochrome *b* (61-63, 86, 129, 130, 133, 138, 141, 142, 145, 204-207) being also involved in the regulation of this mechanism.

4.3 Kinetics of reduction with ascorbate and interaction between the ISP and the cytochrome *c*₁

The ISP to cytochrome *c*₁ interaction was analysed also on a different time scale than with the flash photolysis approach described before using stopped flow kinetics. The oxidized cytochrome *bc*₁ complex was mixed against increasing ascorbate concentrations used in high excess compared to the protein amount, in order to achieve pseudo-first-order conditions (PFO). In this way, a second order reaction can be studied as if it was of first order. By plotting the k_{OBS} against the substrate concentration the second order rate constant is obtained. The results from this analysis revealed the presence of two phases for the reduction of cytochrome *c*₁ by ascorbate: a fast phase, which is linearly dependent on the ascorbate concentration, with a second order rate constant of about $55 \text{ M}^{-1}\text{s}^{-1}$, and a slow phase. The slow phase is hyperbolically dependent on ascorbate concentration. This suggests that the slow phase defines a kinetic process, assuming a zero order trend by increasing ascorbate concentration. The presence of the two phases was surprising, since the expected result was a monoexponential kinetic, defined by only one kinetic constant and related to the direct electron transfer from ascorbate to the cytochrome *c*₁. The latter has a redox potential close to the one of the Rieske cluster (85), so ascorbate can actually not only reduce both redox centers. This suggests that the presence of the two phases is due to the combination of several processes, such as direct electron transfer to the cytochrome *c*₁ from ascorbate and from the reduced ISP to the *c*₁ heme. Therefore, also the movement of the ISP head domain towards cytochrome *c*₁ (see 3.4.2) plays an important role in the electron transfer kinetics with ascorbate. To test this hypothesis, the same experiment was performed in presence of stigmatellin. The oxidized protein was incubated with a 10 fold excess of stigmatellin over night and the following day kinetics with increasing amounts of ascorbate recorded at the stopped flow. The traces were still biphasic, and the rate constants were determined with a different dependence on ascorbate concentration: The second k_{FAST} was now hyperbolically dependent on ascorbate concentration, with values of $0.1 \text{ M}^{-1}\text{s}^{-1}$. The k_{SLOW} is now linear. Also the effects of other inhibitors, such as MOA-stilbene and myxothiazol were tested: both molecules indicate that the

Discussion

k_{FAST} is faster than without inhibitors and linearly dependent on substrate concentration, and the k_{SLOW} show in a more definite manner the hyperbolic trend. The slow phase is in the beginning predominant, with the fast phase increasing throughout the experiment to reach about 80 % of the observed kinetic. In presence of stigmatellin, though, the amplitudes remain constant.

This result was somehow surprising, since binding of stigmatellin at the Q_o site fixes the ISP in the b position. Preventing the cluster to take part in electron transfer to the cytochrome c_1 heme was expected to modify the behaviour of the kinetics, in particular a shift from a biphasic to a monophasic mechanism. In order to analyse the role of the ISP in the electron pathway in detail, a mutant has been cloned and expressed, where the Ser¹⁵⁷ (*P. denitrificans* numbering) was mutated to a Cys. The Ser¹⁵⁷ is close to the two Cys residues coordinating the cluster, and it has already been shown in the yeast complex (86) that the mutation leads to the expression of the ISP protein without the cluster. The reason for the loss of the Rieske cluster is probably the formation of an internal disulphide bridge with one of the Cys involved in cluster coordination. Using the purified mutant, with only the apoprotein present in the complex for the experiments, monophasic kinetics were observed. The bimolecular rate constant was calculated to be about $2 \text{ M}^{-1}\text{s}^{-1}$, in line with the results of Julia Janzon (116). This represents the rate for the electron transfer between the cytochrome c_1 and ascorbate and indicates also that the slow phase observed with the wild type complex is, most likely, a process influenced by more factors than first thought.

To analyze the aforementioned electron transfer processes, a model has been developed at the university of Rome "La Sapienza" with Prof. Francesco Malatesta, which takes into account also the relative position of the ISP to cytochrome c_1 . The model is called "cube model" and is shown in Fig. 72.

Discussion

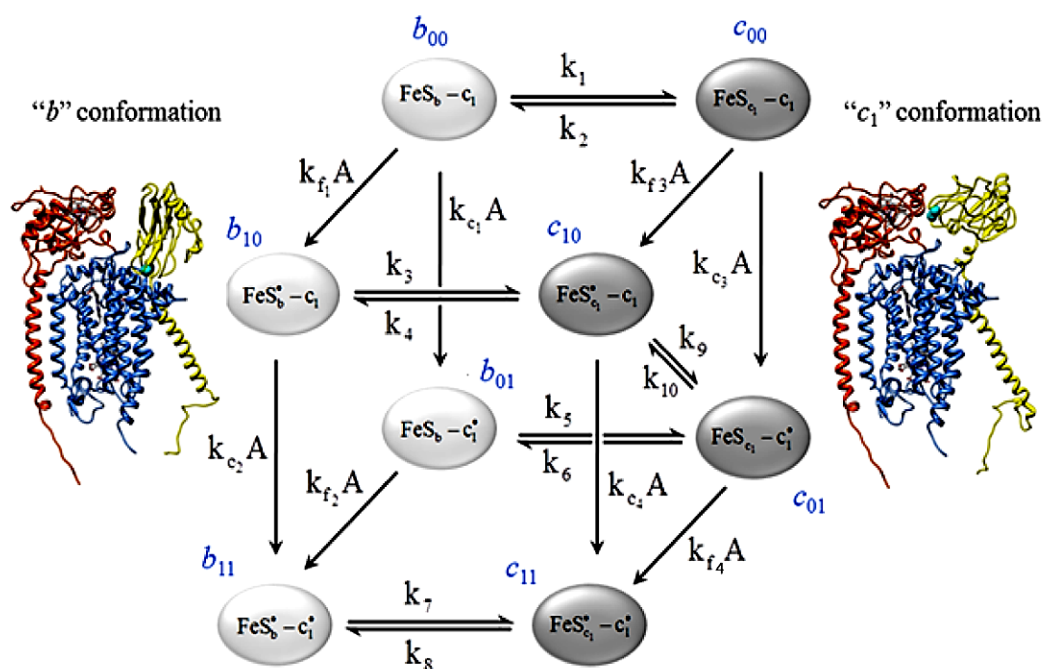


Fig. 72: Cube model for the reduction of cytochrome bc_1 by ascorbate under pseudo-first order conditions. Each species is labeled as follows: b_{00} and c_{00} = fully oxidized protein with the FeS protein in the “ b ” or “ c_1 ” position, respectively; b_{11} and c_{11} = corresponding to 2-electron reduced species (the electron being represented by a dot •); b_{10} and c_{10} are a 1-electron reduced species with the electron on the FeS protein; b_{01} and c_{01} are 1-electron reduced species with the electron on cytochrome c_1 . The species are connected by second-order processes (single headed arrows) with rate constants k_f 's and k_c 's multiplied by the ascorbate concentration (A). Horizontal double arrows represent the conformational transitions of the Rieske protein between “ b ” or “ c_1 ” states (light and dark grey ovals), and the diagonal double arrow direct ET between FeS and c_1 . Cytochrome b is colored in light blue, cytochrome c_1 in red and the Rieske protein in yellow with the 2 iron atoms of the FeS cluster shown as hard spheres in cyan. The structures were fitted by using the program Chimera of the USCF (208)

According to this model, ascorbate can reduce both cytochrome c_1 and the Rieske cluster. The latter can assume two different positions, the b position (light grey ovals) and the c_1 position (grey ovals). For simplicity, any intermediate configuration of the ISP head domain is not considered, and it is assumed that the reduction of the ISP and cytochrome c_1 does not change depending on the conformation of the first or the redox state of the redox cofactors. The fast phase is most likely described by the reduction of the FeS by ascorbate, the movement into direction of cytochrome c_1 and the reduction of it. The slow phase, on the other side, can be described as a complex function of the rate constants in the mechanism and is approximated by the pseudo-first order rate constant for reduction of cytochrome c_1

Discussion

by ascorbate. It is important to point out that the experiments are performed without addition of external substrate, and therefore the kinetic here described is only an approximation of the cytochrome c_1 reduction kinetics, which would resemble more the native situation in presence of substrate bound at the Q_o site. The saturation observed for the slow phase is probably due to competition between the reduction of cytochrome c_1 by ascorbate or the ISP. In the presence of stigmatellin, the fast phase becomes hyperbolically dependent on the ascorbate concentration, which could be explained by assuming that the inhibitor dissociates from the Q_o binding site and allows a portion of the ISP which is otherwise fixed in the b state to reach cytochrome c_1 and reduce it. In presence of the two Pm inhibitors, MOA-stilbene and myxothiazol, the k_{FAST} increases as a consequence of the displacement of the Rieske protein from the fixed position.

The analysis of the cube model has been performed by Prof. Francesco Malatesta. All the reactions involved in the mechanism are first order or pseudofirstorder reactions, which are dependent on the rate constant and the initial conditions of the reaction. The differential equations describing the time dependence of each species can be written as follows:

$$\frac{ds(t)}{dt} = K \cdot s(t) \quad \text{Equation 9}$$

K represents a matrix describing the kinetic constants for each reaction in the mechanism. From an Eigenvalues-Eigenvectors analysis of the matrix K , the following equation can be obtained:

$$s(t) = \sum_{i=1}^n c_i b_i e^{\lambda_i t} = \sum_{i=1}^n \alpha_i e^{\lambda_i t} \quad \text{Equation 10}$$

In this equation, c_i represents a vector related to initial conditions, b_i are column vectors of the eigenvector matrix and, λ_i are the Eigenvalues of K , i.e. the observed rate constants, which are determined experimentally and estimated by fitting the data to mono- or bi-exponential equations. The $\alpha_i = c_i b_i$ products represent the observed amplitudes, also determined experimentally.

Discussion

The mechanism has been simulated using the program MatLab and in Fig. 73 the time courses obtained from this simulation are shown.

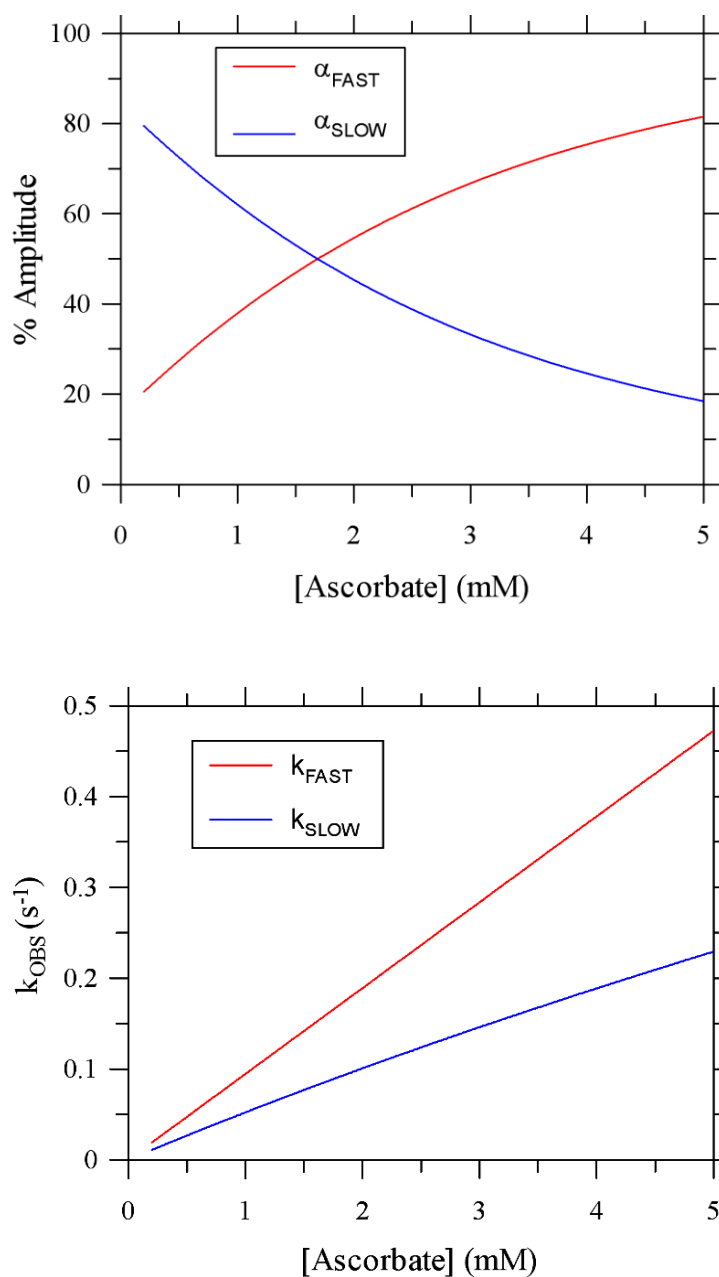


Fig. 73: Kinetic simulation of the amplitudes (upper panel) and for the rate constants (lower panel) for the fast and the slow phase obtained by using the cube model. In both cases a good simulation can be obtained for the experiments where no inhibitor have been added. Further simulations are currently going on.

Discussion

As visible from the Fig. 73, the cube model simulates quite well the experimental data obtained with the stopped-flow experiments for both amplitudes and rate constants. At the moment, further analysis is in progress for a more complete description of the model, in order to obtain a mathematical expression which can be used to completely fit the data and verify the simulations.

4.4 Deletion mutant of the cytochrome bc_1 complex from *P. denitrificans* and interaction with the substrate

The cytochrome bc_1 complex from *P. denitrificans* is unique, since its cytochrome c_1 protein has a 150 aminoacid long domain, which is rich in acidic residues (mostly Glu) and Pro, suggesting that the domain is not completely folded in a secondary structure, and, most likely, flexible. As already discussed in 1.2.3, in the eukaryotic complex a subunit is present, which is very rich in negatively charged residues as well. It is involved in long range interactions with the substrate. In *P. denitrificans*, without additional subunit is present, the acidic domain of the cytochrome c_1 leads to the question whether it may have a similar function.

In this work experiments have been performed with the deletion mutant of the complex, lacking the acidic domain. The complex has been purified by affinity chromatography, since the acidic domain was the feature which allowed the purification of the wild type complex on an ion exchange chromatography (DEAE). The tag of choice was a 10x His tag, introduced by SOEing PCR. Activity tests indicated that the affinity tag at the C-terminus of cytochrome b was not significantly affecting the turnover number of the complex or showing changes in redox spectra. The purification protocol using imidazole to elute the complex has been first established by Thomas Kleinschroth, who worked with the His tagged version of the wild type complex. The deletion mutant can only be purified efficiently by using an affinity chromatography. The first elution trial with the complex was performed with imidazole. The complex appeared fully normal in SDS PAGE, but the turnover number was very low (only 20 % residual activity) and the reducibility of the protein by ascorbate was strongly impaired. Dithionite fully reduced the complex, but ascorbate could only reduce a small amount of cytochrome b and only when present in strong excess. This is an unexpected result, since ascorbate can selectively reduce cytochrome c_1 and the Rieske cluster, because of its redox potential. In the literature, the same effect is described for the *Rhodobacter sphaeroides* cytochrome

Discussion

bc_1 complex (209), but the problem was solved by using histidine in the elution buffer instead of imidazole. The same strategy has been applied to the *P. denitrificans* complex, restoring the turnover number to values comparable to the wild type complex and the reducibility of cytochrome c_1 in presence of ascorbate. Imidazole is thought to change the network of hydrogen bonds in the heme cleft and therefore displacing the Met liganding the c_1 heme. This effect was observed only in the oxidized complex in *Rhodobacter sphaeroides*, since the reduced complex incubated with imidazole does not show any change in comparison with the wild type (178, 179).

The deletion mutant complex has been analyzed by LILBID (152, 177), revealing a dimeric structure. Even if the dimeric structure is expected for the cytochrome bc_1 complex, the wild type complex, analyzed with the same technique, appeared as a dimer of dimers (152). The deletion of the acidic domain seems to cause a change in the oligomerization state of the complex, determining the separation of the two dimers, otherwise purified together. How the acidic domain in the cytochrome c_1 affects the formation of dimers of dimers is not clear: one speculation is that the domain, probably not having a defined secondary structure, causes the aggregation of two dimers. If this is the case, this must happen on a site far away enough from the heme cleft so that the activity is not affected by the association of the two dimers. Interestingly, two dimers are present in the supercomplex purified from the digitonin solubilised membraned of *P. denitrificans* (151), so this unusual “tetrameric structure” could also be the natural association of two dimers in the supercomplex arrangement. Neither the wild type complex, nor the supercomplex have been crystallized so far, so no structural data are available. On the other hand, the crystal structure of the deletion mutant was obtained from it in collaboration with the group of Prof. Carola Hunte at the University of Freiburg (Kleinschroth *et al.* manuscript submitted) shows that the deletion has no effects on cytochrome c_1 folding. In section 3.4.2 it was shown that in the mutant complex cytochrome b can be reduced in presence of ascorbate, which was unexpected. The redox potentials have been checked to exclude any change which could justify the reduction of the low potential chain in presence of ascorbate, but no difference has been observed with the wild type. Probably, the dimer of dimers is not just the aggregation of two dimers in an unorganized manner, but a defined process which stabilizes the protein. The

Discussion

globular domain of the cytochrome c_1 seems to be more open and more accessible to small molecules (such as ascorbate).

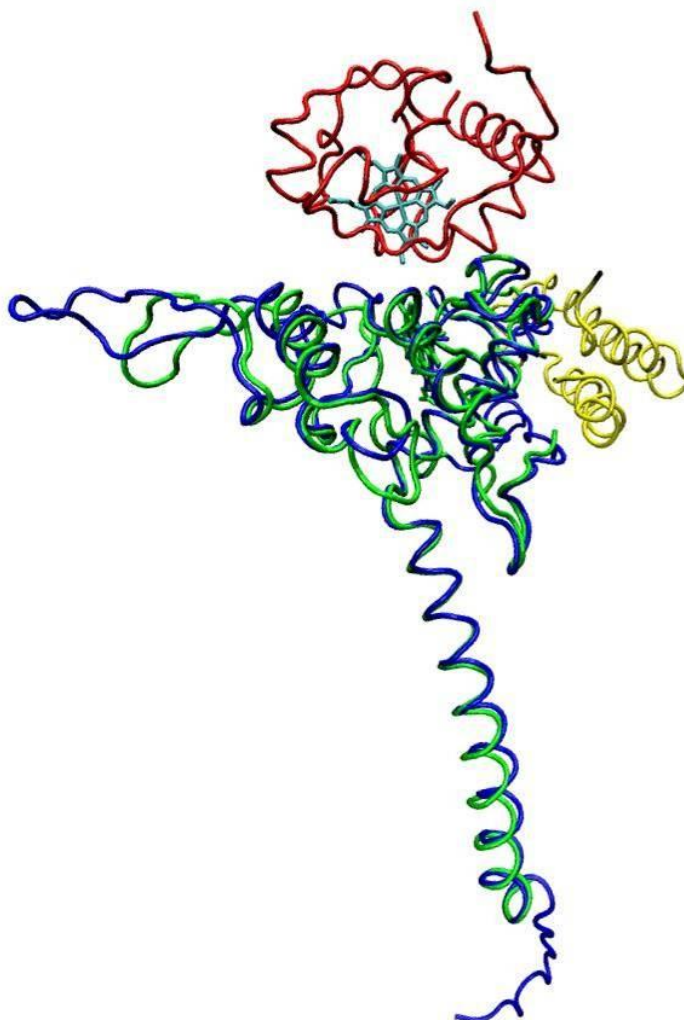


Fig. 74: Superimposition of the cytochrome c_1 structure of the acidic domain deletion complex and the yeast structure (pdb:1kyo). Red: cytochrome c from yeast. Yellow: Qcr6p. Blue: QcrC. Green: cytochrome $c_1^{\Delta ac}$. The structure of the deletion variant of the cytochrome c_1 from *P. denitrificans* clearly shows that the deletion does not cause any change in protein folding.

To test whether the acidic domain is involved in any interaction with the substrate, similar to the role played by the small acidic subunit in the eukaryotic complex (96-98, 102, 104, 106-108, 112, 210, 211), flash photolysis experiments have been performed using two different cytochromes c coupled to Ru as electron acceptors (119, 181). The proteins of choice are the isoform 1 of the yeast cytochrome c , known to have a strong association with the yeast cytochrome bc_1 complex (93, 113, 114, 119), and the correspondent cytochrome c in the aerobic respiratory chain of *P.*

Discussion

denitrificans, the cytochrome c_{552} . The latter being a membrane bound protein (149), a soluble fragment of it has been used and coupled to Ru, in order to avoid the additional purification of a membrane protein. A new crystal structure obtained from a different soluble fragment of cytochrome c_{552} (150) confirmed the previous, known structure of the heme binding domain, therefore indicating that the production of a soluble fragment does not change the heme binding or positioning and that soluble fragments represent a feasible to work with. The measurements presented in this work have already been performed previously using soluble fragments of the cytochrome c_1 and the same electron acceptors (116, 118), but studying the whole complex allows brings the situation closer to the scenario in membranes. Soluble fragments are free to diffuse in the buffer but whole membrane complex are embedded in a detergent micelles and much bigger than the soluble counterparts. This limits to free diffusion, and allows also the observation of eventual effects that the other redox cofactor in the protein have on the analyzed electron transfer. Moreover, the experiments discussed in this section represent a possibility to verify the results previously obtained with the soluble fragments.

From the results presented in section 3.3.5, it can be concluded that the deletion of the acidic domain does not affect the interaction with the substrate: The acidic domain interacts neither directly with the substrate, nor steers long range interactions with it (as observed for the small acidic subunit in the eukaryotic complex), otherwise altered ionic strength dependence should be observed in the Brønsted plot in the case of the deletion mutant. This is not the case, even if the electron acceptor is the yeast isoform 1 cytochrome c , meaning that the acidic domain on the cytochrome c_1 plays no role at all in the interaction with cytochrome c . Kinetic observation with the complexes from other organisms indicate that the interaction between the cytochrome bc_1 complex and the cytochrome c appears to share similar properties, where ionic long range interaction orientate the reaction partners and hydrophobic interactions define the binding of them (111, 114). Most likely, the acidic domain is involved in the interaction with one of the other c -type cytochromes taking part in the other metabolic pathways of *P. denitrificans*; as this bacterium possesses a quite versatile and flexible metabolism, allowing growth on different substrates and a fast adaptation to variations in the environment. The acidic domain could also define the interaction with other respiratory complexes

Discussion

under specific conditions, representing the possibility to connect otherwise separated metabolic pathways.

5 Summary

The ubiquinol:cytochrome *c* oxidoreductase is a key component of several aerobic respiratory chains in different organisms. It is an integral membrane protein complex, made up of three catalytic subunits (cytochrome *b*, cytochrome *c*₁ and Rieske iron sulphur protein) and up to eight additional subunits in mitochondria. The complex oxidizes one quinol molecules and reduces two cytochrome *c* during the Q cycle, originally described by Peter Mitchell. Electrons are split between the low and the high potential chain and protons are released on the positive side of the membrane, increasing the protonmotive force needed by the ATP-synthase for energy transduction. The cytochrome *bc*₁ complex from *P. denitrificans* is a perfect model for structural and functional studies. Bacteria are easy to grow and the genetic material is readily accessible for genetic manipulation. Moreover, the *P. denitrificans* aerobic respiratory chain is very close to the mitochondrial one: the complexes involved in electron transfer resemble the ones found in mitochondria, but lack most of the additional subunits. As a unique feature, *P. denitrificans* has a strongly acidic domain at the N-terminal region of the cytochrome *c*₁, a sequence of 150 aminoacids which does not correlate with any known protein. An analogous composition can be found in the eukaryotic cytochrome *bc*₁ complex as a part of an accessory subunit, proposed to be involved in facilitating electron transfer between the complex and the electron acceptor cytochrome *c*. In order to study the function of this domain in the *P. denitrificans* cytochrome *bc*₁ complex, a deletion mutant has been previously cloned and modified with an affinity tag as a C-terminal extension of cytochrome *b*.

The complex is purified by affinity chromatography and characterized by steady-state kinetics using not only horse heart cytochrome *c* but also the endogenous electron acceptor, the membrane bound cytochrome *c*₅₅₂, employed here as a soluble fragment. Steady-state kinetics indicate that the deletion of the long acidic domain had effects neither on the turnover rate nor on the apparent affinity for the substrate. To understand wether the deletion affects the reaction between the cytochrome *bc*₁ complex and the substrate, laser flash photolysis experiments are performed, showing that the interaction observed was not changed in the complex missing the acidic domain. The results presented in this work confirm the ones

Summary

previously obtained by Julia Janzon using soluble fragments of the same interaction partners.

The deletion, however, affected the oligomerization state of the complex, as shown by LILBID (Laser Induced Liquid Bead Ion Desorption) analysis. The wild type complex has a tetrameric structure, better described as a “dimer of dimers”. The deletion of the acidic domain on the cytochrome c_1 results in the separation of the two dimers, yielding the canonical dimer. Therefore, the complex deleted in the acidic domain is used for cloning and expression of a heterodimeric complex, containing an inactivating mutation in the quinol oxidation site in only one monomer, thus allowing a selective switch-off for half the complex. Such a complex is needed for the verification of an internal regulation mechanism, the half-of-the-sites reactivity. According to it, the dimeric structure of the cytochrome bc_1 complex has functional implications, since the two monomers can communicate and work in a coordinated manner. This approach confirms that substrate oxidation does effectively take place only in one of the two monomers constituting the dimer, and that the binding of substrate at the Q_o and Q_i site regulates the switch between active and inactive monomer. Moreover, this mechanism works also as an effective protection against the reaction of quinone intermediates with oxygen and the formation of reactive oxygen species (ROS), responsible for cellular aging.

The motion of the ISP head domain is also addressed in this work; in particular the mechanism which regulates the movements towards the cytochrome c_1 and the electron bifurcation at the quinol oxidation site. Laser flash kinetics in presence of several inhibitors and the substrate allow studying the response of the ISP to the binding of different species at the quinol oxidation site. The binding of ligand at the Q_o site in the complex triggers the conformational switch in the ISP head domain, supporting the mechanism proposed in the literature according to which the Q_o site is able to “sense” the presence of substrate and transfer the information to the ISP, regulating its mobility.

The internal electron pathway between the ISP and the cytochrome c_1 has been analyzed also by stopped-flow kinetics, in presence and absence of inhibitors. The results indicate that two kinetic phases describe the reduction of cytochrome c_1 by the ISP, and a model for the simulation of the data is proposed.

6 Zusammenfassung

Der Cytochrom bc_1 Komplex ist der zentrale Membranproteinkomplex der aeroben Atmungsketten vieler Organismen. Er besteht aus den drei redox-aktiven Untereinheiten Cytochrom b , Cytochrom c_1 und dem Rieske Eisen-Schwefel-Protein (ISP), sowie spezieabhängig aus bis zu acht weiteren akzessorischen Untereinheiten. Der Komplex oxidiert in einem kompletten katalytischen Zyklus zwei Chinol-Moleküle und reduziert hierbei zwei Cytochrom c und ein Chinon zu Chinol. Dieser als Q-Zyklus bekannte Mechanismus wurde ursprünglich von Peter Mitchell bereits in den 1960er Jahren vorgeschlagen. Dabei werden die Elektronen zwischen der *high potential* und der *low potential* Kette von Redoxkofaktoren aufgeteilt. Während dieses Prozesses werden Protonen auf der positiven Seite der Membran abgegeben, die zum Aufbau des chemiosmotischen Gradienten beitragen, der von der ATP-Synthase in zellulär verfügbare, chemisch gebundene Energie umgewandelt wird.

Der in dieser Arbeit untersuchte Cytochrom bc_1 Komplex des Bodenbakteriums *Paracoccus denitrificans* stellt aus mehreren Gründen ein geeignetes Studienobjekt dar: einerseits ist die aerobe Atmungskette dieses Bakteriums der der eukaryontischen Mitochondrien sehr ähnlich, jedoch vielfach als Minimal-Komplex aufgebaut aus den essentiellen Untereinheiten. In der Literatur wird davon ausgegangen, dass die heutigen Mitochondrien und *P. denitrificans* einen gemeinsamen Vorfahren hatten, der gemäß der Endosymbionten-Theorie von einer phagozytotisch lebenden Zelle aufgenommen und sich im Laufe der Evolution in die Organelle umgewandelt hat. Das Bakterium ist überdies im Labor gut zu kultivieren, die genetische Information durch etablierte Verfahren zugänglich, und gentechnische Veränderungen lassen sich im Vergleich zu Eukaryonten einfacher einfügen.

Der Cytochrom bc_1 Komplex von *P. denitrificans* weist im Cytochrome c_1 jedoch einen einzigartigen Unterschied zu anderen Komplexen auf. Er enthält am N-Terminus einen Einschub von 150 Aminosäuren, die zu 40 % saure Seitengruppen tragen. Für diese Domäne können aufgrund ihres ungewöhnlichen Aminosäure-Gehalts keine Sekundärstrukturen vorhergesagt werden. Eine ähnliche Zusammensetzung, mit hohem Anteil an sauren resten, findet sich in einer der akzessorischen Untereinheiten der eukaryontischen Komplexe, für die vorgeschlagen wurde, dass sie im Elektronentransfer die wichtige Ausrichtung des

Summary

Cytochrom *c* fördert. In dieser Arbeit wird deshalb eine Variante des *P. denitrificans* Komplexes ohne die saure Domäne ("Δac"), jedoch mit einem C-terminalen His-tag am Cytochrom *b*, untersucht.

Die Δac Variante des Komplexes wurde aufgereinigt und die Enzymaktivität mit ihren Michaelis-Menten-Parametern bestimmt. Die Deletion dieser großen Domäne hat keinen Einfluss auf die Enzymaktivität, unabhängig davon, ob mit dem nativen oder dem in den Standardaktivitätstest häufig verwendeten Cytochrom *c* aus Pferdeherz gemessen wurde. Zur Untersuchung der Elektronentransferprozesse und der für die Substratbindung beteiligten Ladungen wurden schnelle Kinetiken mit Hilfe der Methode der Laserblitz-Photolyse aufgenommen. In diesen Untersuchungen wurden vergleichbare Ergebnisse erzielt, so konnte zwischen Wildtyp und Variante kein Unterschied in den Brønstedt-Graphiken festgestellt werden, die die Zahl der an Interaktion beteiligten Ladungen definieren. Ein ähnlicher Trend wurde vorher bereits von Julia Janzon in einer vorangegangenen Arbeit mit löslichen Fragmenten des Cytochrom *c*₁ und Cytochrom *c* gezeigt. In einer weiteren Studie mit Hilfe der LILBID (*Laser Induced Liquid Bead Ion Desorption*)-Massenspektroskopie stellte sich heraus, dass der Unterschied zwischen Wildtyp und Variante in einem unterschiedlichen Oligomerisierungszustand liegt. Der Wildtyp liegt als Tetramer (Dimer aus zwei funktionellen Dimeren) vor, die Δac Varianten als funktionelles, für Cytochrome *bc*₁ Komplexe typischerweise beschriebenes Dimer.

Dieser Befund machte es möglich, in einem weiteren Projekt einen heterodimeren Komplex zu konstruieren, der durch eine Tandemaufreinigung mittels zweier verschiedener Affinitäts-*tags* isoliert werden konnte. Dies war vorher aufgrund des tetrameren Assoziationszustandes nicht gelungen. Für dieses Projekt wurde ein heterodimerer Komplex benötigt, der in einem Monomer dem Wildtyp entspricht und mit dem Strep-*tag* versehen ist und im anderen Monomer eine inaktivierende Mutation im Cytochrom *b* einführt und diese mit dem His-*tag* markiert. Die zur Kennzeichnung eingefügten *tags* wurden C-terminal am Cytochrom *b* angebracht. Hierfür wurden zwei entsprechende *fbc*-Operons konstruiert und in einen Cytochrom *bc*₁ Komplex Deletionsstamm eingebracht. Dies geschah mit Hilfe zweier Vektoren, die sich sowohl im *oriV* als auch in den vermittelten Antibiotikaresistenzen unterschieden. So konnte ein Stamm erzeugt werden, in dem beide Plasmide stabil replizieren und exprimieren. Der aus diesem Stamm nach Solubilisierung und

Summary

Tandemaufreinigung erhaltene Komplex wurde mittels Redox-Vis-Spektren untersucht und zeigte alle typischen Signale der Redoxkofaktoren. In der SDS-Elektrophorese konnten die drei Untereinheiten des Komplexes nachgewiesen werden. Dieser heterodimere Komplex wurde für *pre-steady-state* Kinetiken und Aktivitätsuntersuchungen herangezogen und lieferte eindeutige Ergebnisse, welche die seit langem kontrovers diskutierte *half-of-the-sites*-Hypothese bestätigten; sie schlägt eine interne Kommunikation und damit Regulation des Komplexes vor, in dem ein Monomer das andere Monomer abschalten kann. Sie beschreibt, dass unter normalen Umständen nur ein Monomer im Komplex aktiv ist und damit für die gesamte Aktivität verantwortlich ist, was für den hier vorgestellten heterodimeren Komplex klar bewiesen wird. Die Michaelis-Menten-Parameter für diese Reaktion zeigen, dass der heterodimere Komplex und der Wildtyp sich in der Substratbindung nicht unterscheiden. Für die *pre-steady-state* Kinetiken ergibt sich im Vergleich mit der Δac Variante und einer Mutante, welche die Mutation in beiden Monomeren trägt, dass der heterodimere Komplex eine biphasische Kinetik beschreibt aus den Phasen der jeweiligen homodimeren Komponenten. Eine vergleichende Inhibitortitration mit der Δac Variante und dem beschriebenen heterodimeren Komplex zeigt ebenfalls, dass die für den Wildtyp charakteristische Aktivierung des zweiten Monomers im Falle des heterodimeren Komplexes nicht mehr möglich ist. Zusammen mit der Möglichkeit, Elektronen zwischen den Monomeren auf der Ebene der b_L -Häme auszutauschen, dient dies dazu, möglichst viele Elektronenakzeptoren in der Niedrigpotentialkette zur Verfügung zu stellen, um damit die Bildung von Sauerstoff-Radikalen (ROS) zu vermindern. Diese spielen gerade im Hinblick auf Alterung und Zellschäden, zum Beispiel in Hochenergiedurchsatz Geweben wie Nervenzellen, eine entscheidende Rolle.

Die Elektronenübertragung zwischen dem Rieske-Protein und dem Cytochrom c_1 ist an eine vorherige Bewegung des Rieske-Proteins gekoppelt; von seiner Position am Cytochrom b , wo es zunächst an der Oxidation des Chinols beteiligt ist und reduziert wird, bewegt es sich zum Cytochrom c_1 , und reduziert es. Die Elektronenbifurkation, der Auslöser für die Ablösung vom Cytochrom b und für die Bewegung mit nachfolgender Reduktion des Cytochrom c_1 ist in dieser Arbeit mit Laserblitz-Photolyse und *Stopped Flow*-Experimenten untersucht, um ein breites Zeitfenster abzudecken. Die intrinsische Regulation der Elektronenbifurkation zwischen der Hoch- und Niedrigpotentialkette und deren Mechanismus und zeitlicher Ablauf

Summary

werden ebenfalls seit geraumer Zeit in der Literatur diskutiert. In den *Stopped Flow*-Experimenten wurde der mit Substrat oder verschiedenen Inhibitoren vorinkubierte Komplex mit Ascorbatlösung verschiedener Konzentrationen gemischt. Ascorbat reduziert spezifisch nur die *c*-Häme und das Rieske-Protein. Erstaunlicherweise ist eine biphasische Kinetik zu beobachten, die eine schnelle und eine langsame Phase enthält. Aus den Experimenten lässt sich schließen, dass die schnelle Phase die Übertragung von Elektronen vom zuvor reduzierten Rieske-Protein beschreibt mit anschließender Reduktion des Cytochrome c_1 . Die langsame, direkt Ascorbat-abhängige hyperbolische Phase ist die unmittelbare Reduktion des Cytochrome c_1 durch Ascorbat. Zur Klärung, welche der beiden Phasen die direkte Reduktion des Cytochrome c_1 durch Ascorbat ist, wurde eine Mutante des Rieske-Proteins ohne Eisen-Schwefelcluster verwendet (S157C^{ISP}), die eine monophasische Kinetik ergibt. Durch den Einsatz von Inhibitoren können die Anteile der schnellen und langsameren Phase verschoben werden, so dass durch den Einsatz von Stigmatellin (Pf Inhibitor), welches die bewegliche Domäne des Rieske-Proteins am Cytochrom *b* fixieren sollte, die schnelle Phase einen geringeren Anteil hat und die Abhängigkeit hyperbolisch wird. Die Pm Inhibitoren MOA-Stilben oder Myxothiazol erhöhen die Geschwindigkeit und führen zu einem höheren Anteil der schnellen Phase. Dies bedeutet, dass das Stigmatellin zwar das Rieske-Protein am Cytochrom *b* stabilisiert, jedoch eine Bewegung über längeren Zeiten nicht verhindern kann, möglicherweise durch die Entlassung des Inhibitors aus der Bindungsstelle. Die proximalen Inhibitoren führen zur Freisetzung der beweglichen Domäne und damit liegt das Rieske-Protein bereits vor der Reduktion durch Ascorbat näher am Cytochrom c_1 vor. Somit kann die schnelle Phase des Prozesses der Reduktion durch das Rieske-Protein zugeordnet werden. Zur weitergehenden mathematischen Analyse wurde in Zusammenarbeit mit Prof. F. Malatesta das „cube“-Modell entwickelt, welches sowohl die Bewegung des Rieske-Proteins, als auch die Elektronentransferprozesse berücksichtigt.

In den Laserblitz-Photolyse-Experimenten wurde der Elektronenübertrag vom Rieske-Protein auf das Ascorbat-vorreduzierte Cytochrom c_1 auf einer schnelleren Zeitskala untersucht. Hier zeigte sich, dass bei vermutlich nicht voll besetzter Q_o Bindungstasche ebenfalls zwei Phasen auftreten, die zu 9 und 17 % zur Reduktion des Cytochroms c_1 beitragen. Die schnelle Phase entspricht hierbei dem Elektronentransfer zwischen der bereits näher am Cytochrom c_1 liegende Rieske-

Summary

Domäne, und die langsamere Phase der noch in der *b*-Position vorliegenden Rieske Kopfdomäne. Durch Zugabe von Pm Inhibitoren ist mehr reduziertes Rieske-Protein an der Reaktion beteiligt, die schnelle Phase bleibt unverändert, die langsame Phase wird jedoch beschleunigt. Auch hier führen die Pm Inhibitoren zu einer höheren Aufenthaltswahrscheinlichkeit des löslichen Teils des Rieske-Proteins in der c_1 Position. Auf der kurzen Zeitskala dieser Experimente verhindert Stigmatellin durch Fixierung die Reduktion des Cytochrome c_1 vollständig. Ein weiterer Pf Inhibitor, JG-144, der keine Wasserstoffbrücke zum Rieske-Protein ausbildet, verlangsamt beide Phasen jedoch extrem. JG-144 ist demnach nicht in der Lage, das Rieske-Protein zu fixieren, jedoch wird seine Entlassung stark verlangsamt. Hieraus kann wiederum auf eine Beeinflussung des intrinsischen, regulatorischen Mechanismus durch die Bindung eines Moleküls an das Q_o -Zentrum geschlossen werden. Diese Daten untermauern den von Di Xia vorgeschlagenen Mechanismus der Regulation durch Verschiebung der *ef*-Schleife und bilden diesen Prozess erstmals auf kinetischer Ebene ab.

In dieser Arbeit wurde die Rolle untersucht, welche die saure Domäne im Cytochrom bc_1 Komplex von *P. denitrificans* spielt. Es konnte gezeigt werden, dass die Sequenz nicht am Elektronentransfer zwischen dem Cytochrom bc_1 Komplex und dem Cytochrom *c* beteiligt ist, möglicherweise aber für die Interaktion in anderen Stoffwechselwegen in *P. denitrificans* wichtig ist. Die Deletion führt zu einer Veränderung des Oligomerisierungszustandes des Komplexes und erlaubt die Verwendung der Δac Variante für die Validierung des *half-of-the-sites* Mechanismus. Durch die Bindung von Chinol am Q_i Zentrum wird die Aktivierung der Chinol-Oxidation auf einem oder auf beiden Monomeren des Cytochrom bc_1 Komplexes ausgeübt. Die kinetische Untersuchungen zeigen auch, dass die Bindung von Substrat im Q_o Zentrum nicht nur die Voraussetzung für die Katalyse ist; sie kontrolliert auch einen Mechanismus, der die Beweglichkeit des Rieske Proteins reguliert.

7 References

1. Margulis, L. (1970) Recombination of non-chromosomal genes in Chlamydomonas: assortment of mitochondria and chloroplasts?, *J Theor Biol* 26, 337-342.
2. Kurland, C. G., and Andersson, S. G. (2000) Origin and evolution of the mitochondrial proteome, *Microbiol Mol Biol Rev* 64, 786-820.
3. Mitchell, P. (1961) Coupling of phosphorylation to electron and hydrogen transfer by a chemi-osmotic type of mechanism, *Nature* 191, 144-148.
4. Morgan, D. J., and Sazanov, L. A. (2008) Three-dimensional structure of respiratory complex I from Escherichia coli in ice in the presence of nucleotides, *Biochim Biophys Acta*.
5. Efremov, R. G., Baradaran, R., and Sazanov, L. A. The architecture of respiratory complex I, *Nature* 465, 441-445.
6. Zickermann, V., Zwicker, K., Tocilescu, M. A., Kerscher, S., and Brandt, U. (2007) Characterization of a subcomplex of mitochondrial NADH:ubiquinone oxidoreductase (complex I) lacking the flavoprotein part of the N-module, *Biochim Biophys Acta* 1767, 393-400.
7. Vinogradov, A. D. (2001) Respiratory complex I: structure, redox components, and possible mechanisms of energy transduction, *Biochemistry (Mosc)* 66, 1086-1097.
8. Vinogradov, A. D., and Grivennikova, V. G. (2001) The mitochondrial complex I: progress in understanding of catalytic properties, *IUBMB Life* 52, 129-134.
9. Hinchliffe, P., and Sazanov, L. A. (2005) Organization of iron-sulfur clusters in respiratory complex I, *Science* 309, 771-774.
10. Hunte, C., Zickermann, V., and Brandt, U. Functional modules and structural basis of conformational coupling in mitochondrial complex I, *Science* 329, 448-451.
11. Sherwood, S., and Hirst, J. (2006) Investigation of the mechanism of proton translocation by NADH:ubiquinone oxidoreductase (complex I) from bovine heart mitochondria: does the enzyme operate by a Q-cycle mechanism?, *Biochem J* 400, 541-550.
12. Ackrell, B. A. (2000) Progress in understanding structure-function relationships in respiratory chain complex II, *FEBS Lett* 466, 1-5.
13. Huang, L. S., Borders, T. M., Shen, J. T., Wang, C. J., and Berry, E. A. (2005) Crystallization of mitochondrial respiratory complex II from chicken heart: a membrane-protein complex diffracting to 2.0 Å, *Acta Crystallogr D Biol Crystallogr* 61, 380-387.
14. Mitchell, P. (1975) The protonmotive Q cycle: a general formulation, *FEBS Lett* 59, 137-139.
15. Ostermeier, C., Harrenga, A., Ermler, U., and Michel, H. (1997) Structure at 2.7 Å resolution of the Paracoccus denitrificans two-subunit cytochrome c

References

- oxidase complexed with an antibody FV fragment, *Proc Natl Acad Sci U S A* 94, 10547-10553.
16. Iwata, S., Ostermeier, C., Ludwig, B., and Michel, H. (1995) Structure at 2.8 Å resolution of cytochrome c oxidase from *Paracoccus denitrificans*, *Nature* 376, 660-669.
 17. Ludwig, B., and Schatz, G. (1980) A two-subunit cytochrome c oxidase (cytochrome aa₃) from *Paracoccus denitrificans*, *Proc Natl Acad Sci U S A* 77, 196-200.
 18. Koepke, J., Olkhova, E., Angerer, H., Müller, H., Peng, G., and Michel, H. (2009) High resolution crystal structure of *Paracoccus denitrificans* cytochrome c oxidase: new insights into the active site and the proton transfer pathways, *Biochim Biophys Acta* 1787, 635-645.
 19. Belevich, I., Verkhovskiy, M. I., and Wikström, M. (2006) Proton-coupled electron transfer drives the proton pump of cytochrome c oxidase, *Nature* 440, 829-832.
 20. Fritz, M., Klyszejko, A. L., Morgner, N., Vonck, J., Brutschy, B., Müller, D. J., Meier, T., and Müller, V. (2008) An intermediate step in the evolution of ATPases: a hybrid F(0)-V(0) rotor in a bacterial Na(+) F(1)F(0) ATP synthase, *FEBS J* 275, 1999-2007.
 21. Meier, T., Morgner, N., Matthies, D., Pogoryelov, D., Keis, S., Cook, G. M., Dimroth, P., and Brutschy, B. (2007) A tridecameric c ring of the adenosine triphosphate (ATP) synthase from the thermoalkaliphilic *Bacillus* sp. strain TA2.A1 facilitates ATP synthesis at low electrochemical proton potential, *Mol Microbiol* 65, 1181-1192.
 22. Schagger, H., and Pfeiffer, K. (2000) Supercomplexes in the respiratory chains of yeast and mammalian mitochondria, *EMBO J* 19, 1777-1783.
 23. Couoh-Cardel, S. J., Uribe-Carvajal, S., Wilkens, S., and Garcia-Trejo, J. J. Structure of dimeric F₁F₀-ATP synthase, *J Biol Chem* 285, 36447-36455.
 24. Kagawa, Y. ATP synthase: from single molecule to human bioenergetics, *Proc Jpn Acad Ser B Phys Biol Sci* 86, 667-693.
 25. Beijerinck, M. (1910) Bildung und Verbrauch von Stickoxydul durch Bakterien, *Zentbl Bakteriol Parasitenkd Infektionskr Hyg Abt II* 25, 30-63.
 26. Harms, N., and van Spanning, R. J. (1991) C₁ metabolism in *Paracoccus denitrificans*: genetics of *Paracoccus denitrificans*, *J Bioenerg Biomembr* 23, 187-210.
 27. John, P., and Whatley, F. R. (1975) *Paracoccus denitrificans* and the evolutionary origin of the mitochondrion, *Nature* 254, 495-498.
 28. Kelly, D. P., Euzéby, J. P., Goodhew, C. F., and Wood, A. P. (2006) Redefining *Paracoccus denitrificans* and *Paracoccus pantotrophus* and the case for a reassessment of the strains held by international culture collections, *Int J Syst Evol Microbiol* 56, 2495-2500.
 29. Katayama, Y., Hiraishi, A., and Kuraishi, H. (1995) *Paracoccus thiocyanatus* sp. nov., a new species of thiocyanate-utilizing facultative chemolithotroph, and transfer of *Thiobacillus versutus* to the genus *Paracoccus* as

References

- Paracoccus versutus* comb. nov. with emendation of the genus, *Microbiology* 141 (Pt 6), 1469-1477.
30. Copeland, A., Lucas, S., Lapidus, A., Barry, K., Detter, J.C., Glavina del Rio, T., Hammon, N., Israni, S., Dalin, E., Tice, H., Pitluck, S., Munk, A.C., Brettin, T., Bruce, D., Han, C., Tapia, R., Gilna, P., Schmutz, J., Larimer, F., Land, M., Hauser, L., Kyrpides, N., Lykidis, A., Spiro, S., Richardson, D.J., Moir, J.W.B., Ferguson, S.J., van Spanning, R.J.M. and Richardson, P. (2006) Complete Sequence of the *Paracoccus denitrificans* Genome National Center for Biotechnology Information, NIH, Bethesda, MD 20894, USA.
 31. Baker, S. C., Ferguson, S. J., Ludwig, B., Page, M. D., Richter, O. M., and van Spanning, R. J. (1998) Molecular genetics of the genus *Paracoccus*: metabolically versatile bacteria with bioenergetic flexibility, *Microbiol Mol Biol Rev* 62, 1046-1078.
 32. Yip, C. Y., Harbour, M. E., Jayawardena, K., Fearnley, I. M., and Sazanov, L. A. Evolution of respiratory complex I: "supernumerary" subunits are present in the alpha-proteobacterial enzyme, *J Biol Chem* 286, 5023-5033.
 33. Yang, X. H., and Trumpower, B. L. (1986) Isolation of a three-subunit cytochrome bc1 complex from *Paracoccus denitrificans*, *Methods Enzymol* 126, 316-325.
 34. de Gier, J. W., Lubben, M., Reijnders, W. N., Tipker, C. A., Slotboom, D. J., van Spanning, R. J., Stouthamer, A. H., and van der Oost, J. (1994) The terminal oxidases of *Paracoccus denitrificans*, *Mol Microbiol* 13, 183-196.
 35. Schutz, M., Brugna, M., Lebrun, E., Baymann, F., Huber, R., Stetter, K. O., Hauska, G., Toci, R., Lemesle-Meunier, D., Tron, P., Schmidt, C., and Nitschke, W. (2000) Early evolution of cytochrome bc complexes, *J Mol Biol* 300, 663-675.
 36. Kurisu, G., Zhang, H., Smith, J. L., and Cramer, W. A. (2003) Structure of the cytochrome b6f complex of oxygenic photosynthesis: tuning the cavity, *Science* 302, 1009-1014.
 37. Smith, J. L., Zhang, H., Yan, J., Kurisu, G., and Cramer, W. A. (2004) Cytochrome bc complexes: a common core of structure and function surrounded by diversity in the outlying provinces, *Curr Opin Struct Biol* 14, 432-439.
 38. Stroebel, D., Choquet, Y., Popot, J. L., and Picot, D. (2003) An atypical haem in the cytochrome b(6)f complex, *Nature* 426, 413-418.
 39. Berry, E. A., Guergova-Kuras, M., Huang, L. S., and Crofts, A. R. (2000) Structure and function of cytochrome bc complexes, *Annu Rev Biochem* 69, 1005-1075.
 40. Berry, E. A., Huang, L. S., and DeRose, V. J. (1991) Ubiquinol-cytochrome c oxidoreductase of higher plants. Isolation and characterization of the bc1 complex from potato tuber mitochondria, *J Biol Chem* 266, 9064-9077.
 41. Berry, E. A., and Trumpower, B. L. (1985) Isolation of ubiquinol oxidase from *Paracoccus denitrificans* and resolution into cytochrome bc1 and cytochrome c-aa3 complexes, *J Biol Chem* 260, 2458-2467.

References

42. Carrell, C. J., Zhang, H., Cramer, W. A., and Smith, J. L. (1997) Biological identity and diversity in photosynthesis and respiration: structure of the lumen-side domain of the chloroplast Rieske protein, *Structure* 5, 1613-1625.
43. Schagger, H., Link, T. A., Engel, W. D., and von Jagow, G. (1986) Isolation of the eleven protein subunits of the bc1 complex from beef heart, *Methods Enzymol* 126, 224-237.
44. Hauska, G., Gabellini, N., Hurt, E., Krinner, M., and Lockau, W. (1982) Cytochrome b/c complexes with polyprenyl quinol:cytochrome c oxidoreductase activity from *Anabaena variabilis* and *Rhodospseudomonas sphaeroides* GA: comparison of preparations from chloroplasts and mitochondria, *Biochem Soc Trans* 10, 340-341.
45. Knaff, D. B. (1990) The cytochrome bc1 complex of photosynthetic bacteria, *Trends Biochem Sci* 15, 289-291.
46. Montoya, G., te Kaat, K., Rodgers, S., Nitschke, W., and Sinning, I. (1999) The cytochrome bc1 complex from *Rhodovulum sulfidophilum* is a dimer with six quinones per monomer and an additional 6-kDa component, *Eur J Biochem* 259, 709-718.
47. Palsdottir, H., Lojero, C. G., Trumpower, B. L., and Hunte, C. (2003) Structure of the yeast cytochrome bc1 complex with a hydroxyquinone anion Qo site inhibitor bound, *J Biol Chem* 278, 31303-31311.
48. Esser, L., Quinn, B., Li, Y. F., Zhang, M., Elberry, M., Yu, L., Yu, C. A., and Xia, D. (2004) Crystallographic studies of quinol oxidation site inhibitors: a modified classification of inhibitors for the cytochrome bc(1) complex, *J Mol Biol* 341, 281-302.
49. Iwata, S., Lee, J. W., Okada, K., Lee, J. K., Iwata, M., Rasmussen, B., Link, T. A., Ramaswamy, S., and Jap, B. K. (1998) Complete structure of the 11-subunit bovine mitochondrial cytochrome bc1 complex, *Science* 281, 64-71.
50. Crofts, A. R. (2004) The cytochrome bc1 complex: function in the context of structure, *Annu Rev Physiol* 66, 689-733.
51. Crofts, A. R., and Berry, E. A. (1998) Structure and function of the cytochrome bc1 complex of mitochondria and photosynthetic bacteria, *Curr Opin Struct Biol* 8, 501-509.
52. Xia, D., Yu, C. A., Kim, H., Xia, J. Z., Kachurin, A. M., Zhang, L., Yu, L., and Deisenhofer, J. (1997) Crystal structure of the cytochrome bc1 complex from bovine heart mitochondria, *Science* 277, 60-66.
53. Yu, C. A., Xia, D., Kim, H., Deisenhofer, J., Kachurin, A. M., Zhang, L., Deng, K. P., and Yu, L. (1998) Three-dimensional structure and functions of bovine heart mitochondrial cytochrome bc1 complex, *Biofactors* 8, 187-189.
54. Berry, E. A., Huang, L. S., Saechao, L. K., Pon, N. G., Valkova-Valchanova, M., and Daldal, F. (2004) X-Ray Structure of *Rhodobacter Capsulatus* Cytochrome bc (1): Comparison with its Mitochondrial and Chloroplast Counterparts, *Photosynth Res* 81, 251-275.
55. Berry, E. A., Huang, L. S., Zhang, Z., and Kim, S. H. (1999) Structure of the avian mitochondrial cytochrome bc1 complex, *J Bioenerg Biomembr* 31, 177-190.

References

56. Link, T. A. (1997) The role of the 'Rieske' iron sulfur protein in the hydroquinone oxidation (Q(P)) site of the cytochrome bc₁ complex. The 'proton-gated affinity change' mechanism, *FEBS Lett* 412, 257-264.
57. Dutton, P. L. (1978) Redox potentiometry: determination of midpoint potentials of oxidation-reduction components of biological electron-transfer systems, *Methods Enzymol* 54, 411-435.
58. Gennis, R. B., Barquera, B., Hacker, B., Van Doren, S. R., Arnaud, S., Crofts, A. R., Davidson, E., Gray, K. A., and Daldal, F. (1993) The bc₁ complexes of *Rhodobacter sphaeroides* and *Rhodobacter capsulatus*, *J Bioenerg Biomembr* 25, 195-209.
59. Hunte, C., Palsdottir, H., and Trumpower, B. L. (2003) Protonmotive pathways and mechanisms in the cytochrome bc₁ complex, *FEBS Lett* 545, 39-46.
60. Covian, R., Zwicker, K., Rotsaert, F. A., and Trumpower, B. L. (2007) Asymmetric and redox-specific binding of quinone and quinol at center N of the dimeric yeast cytochrome bc₁ complex. Consequences for semiquinone stabilization, *J Biol Chem* 282, 24198-24208.
61. Covian, R., and Trumpower, B. L. (2008) The dimeric structure of the cytochrome bc₁ complex prevents center P inhibition by reverse reactions at center N, *Biochim Biophys Acta* 1777, 1044-1052.
62. Covian, R., and Trumpower, B. L. (2008) Regulatory interactions in the dimeric cytochrome bc₁ complex: the advantages of being a twin, *Biochim Biophys Acta* 1777, 1079-1091.
63. Castellani, M., Covian, R., Kleinschroth, T., Anderka, O., Ludwig, B., Trumpower, B., L. (2010) Direct Demonstration of Half-of-the-sites Reactivity in the Dimeric Cytochrome bc₁ Complex. Enzyme with one inactive monomer is fully active but unable to activate the second ubiquinol oxidation site in response to ligand binding at the ubiquinone reduction site., *J Biol Chem* 285, 502-510.
64. Huang, L. S., Cobessi, D., Tung, E. Y., and Berry, E. A. (2005) Binding of the respiratory chain inhibitor antimycin to the mitochondrial bc₁ complex: a new crystal structure reveals an altered intramolecular hydrogen-bonding pattern, *J Mol Biol* 351, 573-597.
65. Esser, L., Elberry, M., Zhou, F., Yu, C. A., Yu, L., and Xia, D. (2008) Inhibitor-complexed structures of the cytochrome bc₁ from the photosynthetic bacterium *Rhodobacter sphaeroides*, *J Biol Chem* 283, 2846-2857.
66. Osyczka, A., Zhang, H., Mathe, C., Rich, P. R., Moser, C. C., and Dutton, P. L. (2006) Role of the PEWY glutamate in hydroquinone-quinone oxidation-reduction catalysis in the Q_o Site of cytochrome bc₁, *Biochemistry* 45, 10492-10503.
67. Gurung, B., Yu, L., and Yu, C. A. (2008) Stigmatellin induces reduction of iron-sulfur protein in the oxidized cytochrome bc₁ complex, *J Biol Chem* 283, 28087-28094.
68. Samoilova, R. I., Kolling, D., Uzawa, T., Iwasaki, T., Crofts, A. R., and Dikanov, S. A. (2002) The interaction of the Rieske iron-sulfur protein with

References

- occupants of the Qo-site of the bc1 complex, probed by electron spin echo envelope modulation, *J Biol Chem* 277, 4605-4608.
69. von Jagow, G., and Ohnishi, T. (1985) The chromone inhibitor stigmatellin--binding to the ubiquinol oxidation center at the C-side of the mitochondrial membrane, *FEBS Lett* 185, 311-315.
 70. Esser, L., Gong, X., Yang, S., Yu, L., Yu, C. A., and Xia, D. (2006) Surface-modulated motion switch: capture and release of iron-sulfur protein in the cytochrome bc1 complex, *Proc Natl Acad Sci U S A* 103, 13045-13050.
 71. Gao, X., Wen, X., Esser, L., Quinn, B., Yu, L., Yu, C. A., and Xia, D. (2003) Structural basis for the quinone reduction in the bc1 complex: a comparative analysis of crystal structures of mitochondrial cytochrome bc1 with bound substrate and inhibitors at the Qi site, *Biochemistry* 42, 9067-9080.
 72. Brandt, U., and Djafarzadeh-Andabali, R. (1997) Binding of MOA-stilbene to the mitochondrial cytochrome bc1 complex is affected by the protonation state of a redox-Bohr group of the 'Rieske' iron-sulfur protein, *Biochim Biophys Acta* 1321, 238-242.
 73. Crofts, A. R., Barquera, B., Gennis, R. B., Kuras, R., Guergova-Kuras, M., and Berry, E. A. (1999) Mechanism of ubiquinol oxidation by the bc(1) complex: different domains of the quinol binding pocket and their role in the mechanism and binding of inhibitors, *Biochemistry* 38, 15807-15826.
 74. Kim, H., Xia, D., Yu, C. A., Xia, J. Z., Kachurin, A. M., Zhang, L., Yu, L., and Deisenhofer, J. (1998) Inhibitor binding changes domain mobility in the iron-sulfur protein of the mitochondrial bc1 complex from bovine heart, *Proc Natl Acad Sci U S A* 95, 8026-8033.
 75. Bachmann, J., Bauer, B., Zwicker, K., Ludwig, B., and Anderka, O. (2006) The Rieske protein from *Paracoccus denitrificans* is inserted into the cytoplasmic membrane by the twin-arginine translocase, *FEBS J* 273, 4817-4830.
 76. Iwata, S., Saynovits, M., Link, T. A., and Michel, H. (1996) Structure of a water soluble fragment of the 'Rieske' iron-sulfur protein of the bovine heart mitochondrial cytochrome bc1 complex determined by MAD phasing at 1.5 Å resolution, *Structure* 4, 567-579.
 77. Link, T. A., Hagen, W. R., Pierik, A. J., Assmann, C., and von Jagow, G. (1992) Determination of the redox properties of the Rieske [2Fe-2S] cluster of bovine heart bc1 complex by direct electrochemistry of a water-soluble fragment, *Eur J Biochem* 208, 685-691.
 78. Graham, L. A., Brandt, U., Sargent, J. S., and Trumpower, B. L. (1993) Mutational analysis of assembly and function of the iron-sulfur protein of the cytochrome bc1 complex in *Saccharomyces cerevisiae*, *J Bioenerg Biomembr* 25, 245-257.
 79. Rieske, J. S., MacLennan, D. H., and Coleman, R. (1964) Isolation and properties of an iron-protein from the (reduced coenzyme Q)-cytochrome C reductase complex of the respiratory chain, *Biochemical and Biophysical Research Communications* 15, 338-344.
 80. Link, T. A. (1999) The structure of Rieske and Rieske-type proteins., *Advances in inorganic*

References

chemistry 47, 83-157.

81. Molik, S., Karnauchov, I., Weidlich, C., Herrmann, R. G., and Klosgen, R. B. (2001) The Rieske Fe/S protein of the cytochrome b6/f complex in chloroplasts: missing link in the evolution of protein transport pathways in chloroplasts?, *J Biol Chem* 276, 42761-42766.
82. Denke, E., Merbitz-Zahradnik, T., Hatzfeld, O. M., Snyder, C. H., Link, T. A., and Trumpower, B. L. (1998) Alteration of the midpoint potential and catalytic activity of the rieske iron-sulfur protein by changes of amino acids forming hydrogen bonds to the iron-sulfur cluster, *J Biol Chem* 273, 9085-9093.
83. Ding, H., Robertson, D. E., Daldal, F., and Dutton, P. L. (1992) Cytochrome bc1 complex [2Fe-2S] cluster and its interaction with ubiquinone and ubihydroquinone at the Qo site: a double-occupancy Qo site model, *Biochemistry* 31, 3144-3158.
84. Snyder, C. H., Merbitz-Zahradnik, T., Link, T. A., and Trumpower, B. L. (1999) Role of the Rieske iron-sulfur protein midpoint potential in the protonmotive Q-cycle mechanism of the cytochrome bc1 complex, *J Bioenerg Biomembr* 31, 235-242.
85. Schroter, T., Hatzfeld, O. M., Gemeinhardt, S., Korn, M., Friedrich, T., Ludwig, B., and Link, T. A. (1998) Mutational analysis of residues forming hydrogen bonds in the Rieske [2Fe-2S] cluster of the cytochrome bc1 complex in *Paracoccus denitrificans*, *Eur J Biochem* 255, 100-106.
86. Gutierrez-Cirlos, E. B., Merbitz-Zahradnik, T., Trumpower B. L.. . (2002) Failure to Insert the Iron-Sulfur Cluster into the Rieske Iron-Sulfur Protein Impairs Both Center N and Center P of the Cytochrome bc1 Complex. , *J Biol Chem* 277, 50703-50709.
87. Darrouzet, E., Valkova-Valchanova, M., Ohnishi, T., and Daldal, F. (1999) Structure and function of the bacterial bc1 complex: domain movement, subunit interactions, and emerging rationale engineering attempts, *J Bioenerg Biomembr* 31, 275-288.
88. Zhang, Z., Huang, L., Shulmeister, V. M., Chi, Y. I., Kim, K. K., Hung, L. W., Crofts, A. R., Berry, E. A., and Kim, S. H. (1998) Electron transfer by domain movement in cytochrome bc1, *Nature* 392, 677-684.
89. Tian, H., White, S., Yu, L., and Yu, C. A. (1999) Evidence for the head domain movement of the rieske iron-sulfur protein in electron transfer reaction of the cytochrome bc1 complex, *J Biol Chem* 274, 7146-7152.
90. Tian, H., Yu, L., Mather, M. W., and Yu, C. A. (1998) Flexibility of the neck region of the rieske iron-sulfur protein is functionally important in the cytochrome bc1 complex, *J Biol Chem* 273, 27953-27959.
91. Darrouzet, E., Valkova-Valchanova, M., and Daldal, F. (2000) Probing the role of the Fe-S subunit hinge region during Q(o) site catalysis in *Rhodobacter capsulatus* bc(1) complex, *Biochemistry* 39, 15475-15483.
92. Obungu, V. H., Wang, Y., Amyot, S. M., Gocke, C. B., and Beattie, D. S. (2000) Mutations in the tether region of the iron-sulfur protein affect the activity and assembly of the cytochrome bc(1) complex of yeast mitochondria, *Biochim Biophys Acta* 1457, 36-44.

References

93. Hunte, C., Koepke, J., Lange, C., Rossmann, T., and Michel, H. (2000) Structure at 2.3 Å resolution of the cytochrome bc₁ complex from the yeast *Saccharomyces cerevisiae* co-crystallized with an antibody Fv fragment, *Structure* 8, 669-684.
94. Lange, C., and Hunte, C. (2002) Crystal structure of the yeast cytochrome bc₁ complex with its bound substrate cytochrome c, *Proc Natl Acad Sci U S A* 99, 2800-2805.
95. Gencic, S., Schagger, H., and von Jagow, G. (1991) Core I protein of bovine ubiquinol-cytochrome-c reductase; an additional member of the mitochondrial-protein-processing family. Cloning of bovine core I and core II cDNAs and primary structure of the proteins, *Eur J Biochem* 199, 123-131.
96. Kim, C. H., Balny, C., and King, T. E. (1987) Role of the hinge protein in the electron transfer between cardiac cytochrome c₁ and c. Equilibrium constants and kinetic probes, *J Biol Chem* 262, 8103-8108.
97. Kim, C. H., and Zitomer, R. S. (1990) Disruption of the gene encoding subunit VI of yeast cytochrome bc₁ complex causes respiratory deficiency of cells with reduced cytochrome c levels, *FEBS Lett* 266, 78-82.
98. Ohta, S., Goto, K., Arai, H., and Kagawa, Y. (1987) An extremely acidic amino-terminal presequence of the precursor for the human mitochondrial hinge protein, *FEBS Lett* 226, 171-175.
99. Trumpower, B. L. (1990) Cytochrome bc₁ complexes of microorganisms, *Microbiol Rev* 54, 101-129.
100. Trumpower, B. L. (1990) The protonmotive Q cycle. Energy transduction by coupling of proton translocation to electron transfer by the cytochrome bc₁ complex, *J Biol Chem* 265, 11409-11412.
101. Yang, X. H., and Trumpower, B. L. (1986) Purification of a three-subunit ubiquinol-cytochrome c oxidoreductase complex from *Paracoccus denitrificans*, *J Biol Chem* 261, 12282-12289.
102. Kurowski, B., and Ludwig, B. (1987) The genes of the *Paracoccus denitrificans* bc₁ complex. Nucleotide sequence and homologies between bacterial and mitochondrial subunits, *J Biol Chem* 262, 13805-13811.
103. John, P., and Whatley, F. R. (1975) *Paracoccus denitrificans*: a present-day bacterium resembling the hypothetical free-living ancestor of the mitochondrion, *Symp Soc Exp Biol*, 39-40.
104. Ludwig, B., Suda, K., and Cerletti, N. (1983) Cytochrome c₁ from *Paracoccus denitrificans*, *Eur J Biochem* 137, 597-602.
105. Rath, A., Glibowicka, M., Nadeau, V. G., Chen, G., and Deber, C. M. (2009) Detergent binding explains anomalous SDS-PAGE migration of membrane proteins, *Proc Natl Acad Sci U S A* 106, 1760-1765.
106. Kim, C. H., and King, T. E. (1983) A mitochondrial protein essential for the formation of the cytochrome c₁-c complex. Isolation, purification, and properties, *J Biol Chem* 258, 13543-13551.
107. Nakai, M., Endo, T., Hase, T., Tanaka, Y., Trumpower, B. L., Ishiwatari, H., Asada, A., Bogaki, M., and Matsubara, H. (1993) Acidic regions of

References

- cytochrome c1 are essential for ubiquinol-cytochrome c reductase activity in yeast cells lacking the acidic QCR6 protein, *J Biochem* 114, 919-925.
108. Schmitt, M. E., and Trumpower, B. L. (1990) Subunit 6 regulates half-of-the-sites reactivity of the dimeric cytochrome bc₁ complex in *Saccharomyces cerevisiae*, *J Biol Chem* 265, 17005-17011.
 109. Gerhus, E. (1992) PhD thesis Molekularbiologische und funktionelle Untersuchungen zum Cytochrome bc₁ Komplex aus *Paracoccus denitrificans*, Medical University Lübeck, Germany.
 110. Castellani, M. (2006) Functional studies on the interaction between *Paracoccus denitrificans* complex III and its substrates, in *Facolta 'di Scienze MM.FF.NN*, p 83, Universita' degli studi di L'Aquila, L'Aquila.
 111. Solmaz, S., and Hunte, C. (2008) Structure of complex III with bound cytochrome c in reduced state and definition of a minimal core interface for electron transfer, *J Biol Chem* 283, 17542-17549.
 112. Kim, C. H., and King, T. E. (1987) Preparation and properties of cardiac cytochrome c1, *Biochemistry* 26, 1955-1961.
 113. Hunte, C., Solmaz, S., and Lange, C. (2002) Electron transfer between yeast cytochrome bc(1) complex and cytochrome c: a structural analysis, *Biochim Biophys Acta* 1555, 21-28.
 114. Nyola, A., and Hunte, C. (2008) A structural analysis of the transient interaction between the cytochrome bc₁ complex and its substrate cytochrome c, *Biochem Soc Trans* 36, 981-985.
 115. Ubbink, M., Ejdeback, M., Karlsson, B. G., and Bendall, D. S. (1998) The structure of the complex of plastocyanin and cytochrome f, determined by paramagnetic NMR and restrained rigid-body molecular dynamics, *Structure* 6, 323-335.
 116. Janzon, J. (2007) Elektronentransfer zwischen Komplex III und Komplex IV der Atmungskette von *Paracoccus denitrificans* und *Thermus thermophilus*, in *Molekulare Genetik*, Goethe Universität, Frankfurt am Main.
 117. Janzon, J., Eichhorn, A. C., Ludwig, B., and Malatesta, F. (2008) Electron transfer kinetics between soluble modules of *Paracoccus denitrificans* cytochrome c1 and its physiological redox partners, *Biochim Biophys Acta* 1777, 250-259.
 118. Janzon, J., Yuan, Q., Malatesta, F., Hellwig, P., Ludwig, B., Durham, B., and Millett, F. (2008) Probing the *Paracoccus denitrificans* cytochrome c(1)-cytochrome c(552) interaction by mutagenesis and fast kinetics, *Biochemistry* 47, 12974-12984.
 119. Tian, H., Sadoski, R., Zhang, L., Yu, C. A., Yu, L., Durham, B., and Millett, F. (2000) Definition of the interaction domain for cytochrome c on the cytochrome bc(1) complex. Steady-state and rapid kinetic analysis of electron transfer between cytochrome c and *Rhodobacter sphaeroides* cytochrome bc(1) surface mutants, *J Biol Chem* 275, 9587-9595.
 120. Wikstrom, M. K., and Berden, J. A. (1972) Oxidoreduction of cytochrome b in the presence of antimycin, *Biochim Biophys Acta* 283, 403-420.

References

121. Crofts, A. R., Guergova-Kuras, M., Huang, L., Kuras, R., Zhang, Z., and Berry, E. A. (1999) Mechanism of ubiquinol oxidation by the bc(1) complex: role of the iron sulfur protein and its mobility, *Biochemistry* 38, 15791-15806.
122. Brandt, U. (1998) The chemistry and mechanics of ubihydroquinone oxidation at center P (Qo) of the cytochrome bc1 complex, *Biochim Biophys Acta* 1365, 261-268.
123. Berry, E. A., and Huang, L. S. (2003) Observations concerning the quinol oxidation site of the cytochrome bc1 complex, *FEBS Lett* 555, 13-20.
124. Ding, H., Moser, C. C., Robertson, D. E., Tokito, M. K., Daldal, F., and Dutton, P. L. (1995) Ubiquinone pair in the Qo site central to the primary energy conversion reactions of cytochrome bc1 complex, *Biochemistry* 34, 15979-15996.
125. Brandt, U. (1999) Control of ubiquinol oxidation at center P (Qo) of the cytochrome bc1 complex, *J Bioenerg Biomembr* 31, 243-250.
126. Bartoschek, S., Johansson, M., Geierstanger, B. H., Okun, J. G., Lancaster, C. R., Humpfer, E., Yu, L., Yu, C. A., Griesinger, C., and Brandt, U. (2001) Three molecules of ubiquinone bind specifically to mitochondrial cytochrome bc1 complex, *J Biol Chem* 276, 35231-35234.
127. Xia, D., Esser, L., Yu, L., and Yu, C. A. (2007) Structural basis for the mechanism of electron bifurcation at the quinol oxidation site of the cytochrome bc1 complex, *Photosynth Res* 92, 17-34.
128. Zhu, J., Egawa, T., Yeh, S. R., Yu, L., and Yu, C. A. (2007) Simultaneous reduction of iron-sulfur protein and cytochrome b(L) during ubiquinol oxidation in cytochrome bc(1) complex, *Proc Natl Acad Sci U S A* 104, 4864-4869.
129. Yu, C. A., Cen, X., Ma, H. W., Yin, Y., Yu, L., Esser, L., and Xia, D. (2008) Domain conformational switch of the iron-sulfur protein in cytochrome bc1 complex is induced by the electron transfer from cytochrome bL to bH, *Biochim Biophys Acta* 1777, 1038-1043.
130. Cen, X., Yu, L., and Yu, C. A. (2008) Domain movement of iron sulfur protein in cytochrome bc1 complex is facilitated by the electron transfer from cytochrome b(L) to b(H), *FEBS Lett* 582, 523-526.
131. Cape, J. L., Bowman, M. K., and Kramer, D. M. (2007) A semiquinone intermediate generated at the Qo site of the cytochrome bc1 complex: importance for the Q-cycle and superoxide production, *Proc Natl Acad Sci U S A* 104, 7887-7892.
132. de Vries, S., Albracht, S. P., Berden, J. A., and Slater, E. C. (1981) A new species of bound ubisemiquinone anion in QH2: cytochrome c oxidoreductase, *J Biol Chem* 256, 11996-11998.
133. Rotsaert, F. A., Ding, M. G., and Trumpower, B. L. (2008) Differential efficacy of inhibition of mitochondrial and bacterial cytochrome bc1 complexes by center N inhibitors antimycin, ilicicolin H and funiculosin, *Biochim Biophys Acta* 1777, 211-219.

References

134. Forquer, I., Covian, R., Bowman, M. K., Trumpower, B. L., and Kramer, D. M. (2006) Similar transition states mediate the Q-cycle and superoxide production by the cytochrome bc₁ complex, *J Biol Chem* 281, 38459-38465.
135. Yang, S., Ma, H. W., Yu, L., and Yu, C. A. (2008) On the mechanism of quinol oxidation at the QP site in the cytochrome bc₁ complex: studied using mutants lacking cytochrome bL or bH, *J Biol Chem* 283, 28767-28776.
136. Osyczka, A., Moser, C. C., and Dutton, P. L. (2005) Fixing the Q cycle, *Trends Biochem Sci* 30, 176-182.
137. Rich, P. R. (2004) The quinone chemistry of bc complexes, *Biochim Biophys Acta* 1658, 165-171.
138. Mulkidjanian, A. Y. (2007) Proton translocation by the cytochrome bc₁ complexes of phototrophic bacteria: introducing the activated Q-cycle, *Photochem Photobiol Sci* 6, 19-34.
139. Hunte, C. (2005) Specific protein-lipid interactions in membrane proteins, *Biochem Soc Trans* 33, 938-942.
140. Lange, C., Nett, J. H., Trumpower, B. L., and Hunte, C. (2001) Specific roles of protein-phospholipid interactions in the yeast cytochrome bc₁ complex structure, *EMBO J* 20, 6591-6600.
141. Covian, R., and Trumpower, B. L. (2009) Illicilin Inhibition and Binding at Center N of the Dimeric Cytochrome bc₁ Complex Reveal Electron Transfer and Regulatory Interactions between Monomers, *J Biol Chem* 284, 8614-8620.
142. Trumpower, B. L. (2002) A concerted, alternating sites mechanism of ubiquinol oxidation by the dimeric cytochrome bc₁ complex, *Biochim Biophys Acta* 1555, 166-173.
143. Covian, R., Kleinschroth, T., Ludwig, B., and Trumpower, B. L. (2007) Asymmetric binding of stigmatellin to the dimeric *Paracoccus denitrificans* bc₁ complex: evidence for anti-cooperative ubiquinol oxidation and communication between center P ubiquinol oxidation sites, *J Biol Chem* 282, 22289-22297.
144. Covian, R., and Trumpower, B. L. (2005) Rapid electron transfer between monomers when the cytochrome bc₁ complex dimer is reduced through center N, *J Biol Chem* 280, 22732-22740.
145. Covian, R., and Trumpower, B. L. (2006) Regulatory interactions between ubiquinol oxidation and ubiquinone reduction sites in the dimeric cytochrome bc₁ complex, *J Biol Chem* 281, 30925-30932.
146. De Vries, S., Albracht, S. P., Berden, J. A., and Slater, E. C. (1982) The pathway of electrons through OH₂:cytochrome c oxidoreductase studied by pre-steady-state kinetics, *Biochim Biophys Acta* 681, 41-53.
147. Snyder, C. H., and Trumpower, B. L. (1999) Ubiquinone at center N is responsible for triphasic reduction of cytochrome b in the cytochrome bc₁ complex, *J Biol Chem* 274, 31209-31216.
148. Covian, R., Gutierrez-Cirlos, E. B., and Trumpower, B. L. (2004) Anti-cooperative oxidation of ubiquinol by the yeast cytochrome bc₁ complex, *J Biol Chem* 279, 15040-15049.

References

149. Harrenga, A., Reincke, B., Ruterjans, H., Ludwig, B., and Michel, H. (2000) Structure of the soluble domain of cytochrome c(552) from *Paracoccus denitrificans* in the oxidized and reduced states, *J Mol Biol* 295, 667-678.
150. Rajendran, C., Ermler, U., Ludwig, B., and Michel, H. Structure at 1.5 Å resolution of cytochrome c(552) with its flexible linker segment, a membrane-anchored protein from *Paracoccus denitrificans*, *Acta Crystallogr D Biol Crystallogr* 66, 850-854.
151. Stroh, A., Anderka, O., Pfeiffer, K., Yagi, T., Finel, M., Ludwig, B., and Schagger, H. (2004) Assembly of respiratory complexes I, III, and IV into NADH oxidase supercomplex stabilizes complex I in *Paracoccus denitrificans*, *J Biol Chem* 279, 5000-5007.
152. Kleinschroth, T. (2008) PhD thesis Untersuchung zur Struktur-Funktionsbeziehung des Cytochrom bc_1 Komplexes aus *Paracoccus denitrificans*, Goethe Universität Frankfurt am Main, Germany.
153. Saribas, A. S., Ding, H., Dutton, P. L., and Daldal, F. (1995) Tyrosine 147 of cytochrome b is required for efficient electron transfer at the ubihydroquinone oxidase site (Qo) of the cytochrome bc_1 complex, *Biochemistry* 34, 16004-16012.
154. Ding, H., Daldal, F., and Dutton, P. L. (1995) Ion pair formation between basic residues at 144 of the Cyt b polypeptide and the ubiquinones at the Qo site of the Cyt bc_1 complex, *Biochemistry* 34, 15997-16003.
155. Humphrey, W., Dalke, A., and Schulten, K. (1996) VMD: visual molecular dynamics, *J Mol Graph* 14, 33-38, 27-38.
156. Pfitzner, U., Odenwald, A., Ostermann, T., Weingard, L., Ludwig, B., and Richter, O. M. (1998) Cytochrome c oxidase (heme aa₃) from *Paracoccus denitrificans*: analysis of mutations in putative proton channels of subunit I, *J Bioenerg Biomembr* 30, 89-97.
157. Yanisch-Perron, C., Vieira, J., and Messing, J. (1985) Improved M13 phage cloning vectors and host strains: nucleotide sequences of the M13mp18 and pUC19 vectors, *Gene* 33, 103-119.
158. Antoine, R., and Locht, C. (1992) Isolation and molecular characterization of a novel broad-host-range plasmid from *Bordetella bronchiseptica* with sequence similarities to plasmids from gram-positive organisms, *Mol Microbiol* 6, 1785-1799.
159. Arslan, E., Schulz, H., Zufferey, R., Kunzler, P., and Thony-Meyer, L. (1998) Overproduction of the *Bradyrhizobium japonicum* c-type cytochrome subunits of the *cbb3* oxidase in *Escherichia coli*, *Biochem Biophys Res Commun* 251, 744-747.
160. Reincke, B., Thony-Meyer, L., Dannehl, C., Odenwald, A., Aidim, M., Witt, H., Ruterjans, H., and Ludwig, B. (1999) Heterologous expression of soluble fragments of cytochrome c552 acting as electron donor to the *Paracoccus denitrificans* cytochrome c oxidase, *Biochim Biophys Acta* 1411, 114-120.
161. Hanahan, D. (1983) Studies on transformation of *Escherichia coli* with plasmids, *J Mol Biol* 166, 557-580.
162. Hanahan, D. (1985) *DNA Cloning*, Vol. 1, IRL Press.

References

163. Hanahan, D., and Meselson, M. (1983) Plasmid screening at high colony density, *Methods Enzymol* 100, 333-342.
164. Devries, G. E., Harms, N., Hoogendijk, J., and Stouthamer, A. H. (1989) Isolation and Characterization of *Paracoccus denitrificans* Mutants with Increased Conjugation Frequencies and Pleiotropic Loss of a (Ngatcn) DNA-Modifying Property, *Archives of Microbiology* 152, 52-57.
165. Sanger, F., Nicklen, S., and Coulson, A. R. (1977) DNA sequencing with chain-terminating inhibitors. 1977, *Biotechnology* 24, 104-108.
166. Lowry, O. H., Rosebrough, N. J., Farr, A. L., and Randall, R. J. (1951) Protein measurement with the Folin phenol reagent, *J Biol Chem* 193, 265-275.
167. Von Jagow, G., and Schagger, H., (1994) *A practical guide to membrane protein purification, in Separation, Detection and Characterization of Biological Macromolecules*, A. R., Ed., Academic Press, Inc., San Diego, California, USA.
168. Crane, F. L., Barr, R., Donald, B. M., and Lemuel, D. W. (1971) [220] Determination of ubiquinones, in *Methods in Enzymology*, pp 137-165, Academic Press.
169. Kroger, A., Sidney, F., and Lester, P. (1978) [56] Determination of contents and redox states of ubiquinone and menaquinone, in *Methods in Enzymology*, pp 579-591, Academic Press.
170. Anderka, O. (2005) PhD thesis Strukturelle und funktionelle Untersuchungen am Cytochrom *bc₁*-Komplex aus *Paracoccus denitrificans*, p 229, Johann Wolfgang Goethe Universität Frankfurt am Main, Germany.
171. Zaugg, W. S., and Rieske, J. S. (1962) The quantitative estimation of cytochrome b in sub-mitochondrial particles from beef heart, *Biochem Biophys Res Commun* 9, 213-217.
172. Chance, B. (1957) Techniques for the assay of the respiratory enzymes, *Methods Enzymol* 4, 273-329.
173. Berden, J. A., and Slater, E. C. (1970) The reaction of antimycin with a cytochrome b preparation active in reconstitution of the respiratory chain, *Biochim Biophys Acta* 216, 237-249.
174. Malatesta, F. (2005) The study of bimolecular reactions under non-pseudo-first order conditions, *Biophys Chem* 116, 251-256.
175. Heacock, D. H., 2nd, Liu, R. Q., Yu, C. A., Yu, L., Durham, B., and Millett, F. (1993) Intracomplex electron transfer between ruthenium-cytochrome c derivatives and cytochrome c₁, *J Biol Chem* 268, 27171-27175.
176. Janzon, J. e. a. (2008) Electron transfer kinetics between soluble modules of *Paracoccus denitrificans* cytochrome c₁ and its physiological redox partners, *Biochimica et Biophysica Acta* 1777, 250-259.
177. Morgner, N., Kleinschroth, T., Barth, H. D., Ludwig, B., and Brutschy, B. (2007) A novel approach to analyze membrane proteins by laser mass spectrometry: from protein subunits to the integral complex, *J Am Soc Mass Spectrom* 18, 1429-1438.

References

178. Kokhan, O., Shinkarev, V. P., and Wraight, C. A. Binding of imidazole to the heme of cytochrome c1 and inhibition of the bc1 complex from *Rhodobacter sphaeroides*: I. Equilibrium and modeling studies, *J Biol Chem* 285, 22513-22521.
179. Kokhan, O., Shinkarev, V. P., and Wraight, C. A. Binding of imidazole to the heme of cytochrome c1 and inhibition of the bc1 complex from *Rhodobacter sphaeroides*: II. Kinetics and mechanism of binding, *J Biol Chem* 285, 22522-22531.
180. Novick, R. P. (1987) Plasmid incompatibility, *Microbiol Rev* 51, 381-395.
181. Sadoski, R. C., Engstrom, G., Tian, H., Zhang, L., Yu, C. A., Yu, L., Durham, B., and Millett, F. (2000) Use of a photoactivated ruthenium dimer complex to measure electron transfer between the Rieske iron-sulfur protein and cytochrome c(1) in the cytochrome bc(1) complex, *Biochemistry* 39, 4231-4236.
182. Engstrom, G., Xiao, K., Yu, C. A., Yu, L., Durham, B., and Millett, F. (2002) Photoinduced electron transfer between the Rieske iron-sulfur protein and cytochrome c(1) in the *Rhodobacter sphaeroides* cytochrome bc(1) complex. Effects of pH, temperature, and driving force, *J Biol Chem* 277, 31072-31078.
183. Bechmann, G., Weiss, H., and Rich, P. R. (1992) Non-linear inhibition curves for tight-binding inhibitors of dimeric ubiquinol-cytochrome c oxidoreductases. Evidence for rapid inhibitor mobility, *Eur J Biochem* 208, 315-325.
184. Crofts, A. R., Holland, J. T., Victoria, D., Kolling, D. R., Dikanov, S. A., Gilbreth, R., Lhee, S., Kuras, R., and Kuras, M. G. (2008) The Q-cycle reviewed: How well does a monomeric mechanism of the bc(1) complex account for the function of a dimeric complex?, *Biochim Biophys Acta* 1777, 1001-1019.
185. Crofts, A. R., Shinkarev, V. P., Kolling, D. R., and Hong, S. (2003) The modified Q-cycle explains the apparent mismatch between the kinetics of reduction of cytochromes c1 and bH in the bc1 complex, *J Biol Chem* 278, 36191-36201.
186. Gisi, U., Sierotzki, H., Cook, A., and McCaffery, A. (2002) Mechanisms influencing the evolution of resistance to Qo inhibitor fungicides, *Pest Manag Sci* 58, 859-867.
187. Mather, M. W., Darrouzet, E., Valkova-Valchanova, M., Cooley, J. W., McIntosh, M. T., Daldal, F., and Vaidya, A. B. (2005) Uncovering the molecular mode of action of the antimalarial drug atovaquone using a bacterial system, *J Biol Chem* 280, 27458-27465.
188. Vaidya, A. B., and Mather, M. W. (2005) A post-genomic view of the mitochondrion in malaria parasites, *Curr Top Microbiol Immunol* 295, 233-250.
189. Kessl, J. J., Lange, B. B., Merbitz-Zahradnik, T., Zwicker, K., Hill, P., Meunier, B., Palsdottir, H., Hunte, C., Meshnick, S., and Trumppower, B. L. (2003) Molecular basis for atovaquone binding to the cytochrome bc1 complex, *J Biol Chem* 278, 31312-31318.
190. di Rago, J. P., and Colson, A. M. (1988) Molecular basis for resistance to antimycin and diuron, Q-cycle inhibitors acting at the Qi site in the

References

- mitochondrial ubiquinol-cytochrome c reductase in *Saccharomyces cerevisiae*, *J Biol Chem* 263, 12564-12570.
191. Gao, X., Wen, X., Yu, C., Esser, L., Tsao, S., Quinn, B., Zhang, L., Yu, L., and Xia, D. (2002) The crystal structure of mitochondrial cytochrome bc1 in complex with famoxadone: the role of aromatic-aromatic interaction in inhibition, *Biochemistry* 41, 11692-11702.
 192. Borek, A., Sarewicz, M., and Osyczka, A. (2008) Movement of the iron-sulfur head domain of cytochrome bc(1) transiently opens the catalytic Q(o) site for reaction with oxygen, *Biochemistry* 47, 12365-12370.
 193. Droese, S., and Brandt, U. (2008) The mechanism of mitochondrial superoxide production by the cytochrome bc1 complex, *J Biol Chem*.
 194. Ransac, S., and Mazat, J. P. How does antimycin inhibit the bc1 complex? A part-time twin, *Biochim Biophys Acta* 1797, 1849-1857.
 195. Ransac, S., Parisey, N., and Mazat, J. P. (2008) The loneliness of the electrons in the bc1 complex, *Biochim Biophys Acta* 1777, 1053-1059.
 196. Swierczek, M., Cieluch, E., Sarewicz, M., Borek, A., Moser, C. C., Dutton, P. L., and Osyczka, A. An electronic bus bar lies in the core of cytochrome bc1, *Science* 329, 451-454.
 197. Guergova-Kuras, M., Kuras, R., Ugulava, N., Hadad, I., and Crofts, A. R. (2000) Specific mutagenesis of the rieske iron-sulfur protein in *Rhodobacter sphaeroides* shows that both the thermodynamic gradient and the pK of the oxidized form determine the rate of quinol oxidation by the bc(1) complex, *Biochemistry* 39, 7436-7444.
 198. Mulkidjanian, A. Y. (2005) Ubiquinol oxidation in the cytochrome bc1 complex: reaction mechanism and prevention of short-circuiting, *Biochim Biophys Acta* 1709, 5-34.
 199. Ritter, M., Anderka, O., Ludwig, B., Mantele, W., and Hellwig, P. (2003) Electrochemical and FTIR spectroscopic characterization of the cytochrome bc1 complex from *Paracoccus denitrificans*: evidence for protonation reactions coupled to quinone binding, *Biochemistry* 42, 12391-12399.
 200. Wenz, T., Covian, R., Hellwig, P., Macmillan, F., Meunier, B., Trumpower, B. L., and Hunte, C. (2007) Mutational analysis of cytochrome b at the ubiquinol oxidation site of yeast complex III, *J Biol Chem* 282, 3977-3988.
 201. Sharp, R. E., Moser, C. C., Gibney, B. R., and Dutton, P. L. (1999) Primary steps in the energy conversion reaction of the cytochrome bc1 complex Qo site, *J Bioenerg Biomembr* 31, 225-233.
 202. Crofts, A. R., Lhee, S., Crofts, S. B., Cheng, J., and Rose, S. (2006) Proton pumping in the bc1 complex: a new gating mechanism that prevents short circuits, *Biochim Biophys Acta* 1757, 1019-1034.
 203. Hong, S., Ugulava, N., Guergova-Kuras, M., and Crofts, A. R. (1999) The energy landscape for ubihydroquinone oxidation at the Q(o) site of the bc(1) complex in *Rhodobacter sphaeroides*, *J Biol Chem* 274, 33931-33944.
 204. Cooley, J. W. A structural model for across membrane coupling between the Qo and Qi active sites of cytochrome bc1, *Biochim Biophys Acta* 1797, 1842-1848.

References

205. Cooley, J. W., Ohnishi, T., and Daldal, F. (2005) Binding dynamics at the quinone reduction (Qi) site influence the equilibrium interactions of the iron sulfur protein and hydroquinone oxidation (Qo) site of the cytochrome bc1 complex, *Biochemistry* **44**, 10520-10532.
206. Cooley, J. W., Lee, D. W., and Daldal, F. (2009) Across membrane communication between the Q(o) and Q(i) active sites of cytochrome bc(1), *Biochemistry* **48**, 1888-1899.
207. Klishin, S. S., Junge, W., and Mulkidjanian, A. Y. (2002) Flash-induced turnover of the cytochrome bc1 complex in chromatophores of *Rhodobacter capsulatus*: binding of Zn²⁺ decelerates likewise the oxidation of cytochrome b, the reduction of cytochrome c1 and the voltage generation, *Biochim Biophys Acta* **1553**, 177-182.
208. Pettersen, E. F., Goddard, T. D., Huang, C. C., Couch, G. S., Greenblatt, D. M., Meng, E. C., and Ferrin, T. E. (2004) UCSF Chimera--a visualization system for exploratory research and analysis, *J Comput Chem* **25**, 1605-1612.
209. Guergova-Kuras, M., Salcedo-Hernandez, R., Bechmann, G., Kuras, R., Gennis, R. B., and Crofts, A. R. (1999) Expression and one-step purification of a fully active polyhistidine-tagged cytochrome bc1 complex from *Rhodobacter sphaeroides*, *Protein Expr Purif* **15**, 370-380.
210. Kim, C. H., and King, T. E. (1981) The indispensibility of a mitochondrial 15K protein for the formation of the cytochrome C1-cytochrome c complex, *Biochem Biophys Res Commun* **101**, 607-614.
211. Schoppink, P. J., Hemrika, W., Reynen, J. M., Grivell, L. A., and Berden, J. A. (1988) Yeast ubiquinol: cytochrome c oxidoreductase is still active after inactivation of the gene encoding the 17-kDa subunit VI, *Eur J Biochem* **173**, 115-122.

8 Publications

Castellani, M., Covian, R., Kleinschroth, T., Anderka, O., Ludwig, B., Trumpower, B.,L.. (2010) Direct Demonstration of Half-of-the-sites Reactivity in the Dimeric Cytochrome bc_1 Complex. Enzyme with one inactive monomer is fully active but unable to activate the second ubiquinol oxidation site in response to ligand binding at the ubiquinone reduction site., *J Biol Chem* 285, 502-510.

Castellani, M., Havens, J., Kleinschroth, T., Millett, F., Durham, B., Malatesta, F., Ludwig, B., (2011) The acidic domain of cytochrome c_1 in *Paracoccus denitrificans*, homologous to the acidic subunit in eukaryotic bc_1 complexes, is not involved in the electron transfer reaction to the cytochrome c_{552} . Submitted.

Kleinschroth, T., Castellani, M., Trinh, C., Morgner, N., Brutschy, B., Ludwig, B., Hunte, C., (2011) Structure of the cytochrome bc_1 complex of *Paracoccus denitrificans* at 2.7 Å. Submitted.

Havens, J.*, Castellani, M.*, Kleinschroth, T., Ludwig, B., Durham, B., Millett, F., (2011) Photo-Initiated Electron Transfer Within the *P.denitrificans* Cytochrome bc_1 Complex: The mobility of the Iron Sulfur Protein is modulated by the occupant of the Q_o site. Submitted. *: first authors

Abbreviations

9 Abbreviations

abs.	Absorbance
Amp	Ampicillin
APS	Ammoniumpersulfate
ATP	Adenosine triphosphate
Heme b_H	high potential heme b
Heme b_L	low potential heme b
bp	Base pairs
BSA	Bovine serum albumine
BCIP	5-Bromo-4-chloro-3-indolylphosphate
CD	Circular dichroism spectroscopy
CIAP	Calf Intestinal Alkaline Phosphatase
Cyt b	Cytochrome b
Cyt c	Cytochrome c
Cyt c_1	Cytochrome c_1
CV	Column volume
Δ ac	Acidic domain deletion mutant complex
dNTP	Desoxy-NTP
DDM	β -D-Dodecylmaltoside
DMSO	Dimethylsulfoxide
DNA	Desoxyribonucleic acid
DSC	Double sector cuvette
EDTA	Ethylen diamine tetra-acetic acid
EPR	Electron paramagnetic resonance
FAD	Flavin adenine dinucleotide
Gm	Gentamycin
His	Histidine
[I]	Ionic strength
ISC	Iron sulphur cluster
ISP	Iron sulphur protein
kbp, kb	Kilo base pairs
kD	Kilodalton
Km	Kanamycin
KP _i	Potassium phosphate

Abbreviations

k_{CAT}	Catalytic constant, turnover number
K_{M}	Michaelis constant
k_{OBS}	Observed rate constant
k_{FAST}	Fast phase rate constant
k_{SLOW}	Slow phase rate constant
LB	Luria-Bertani
LILBID	Laser-induced liquid bead ion desorption
μs	Microseconds
mA	Milliampere
MES	2-(N-morpholino)-ethansulfonsäure
MMP	<i>Mitochondrial matrix processing peptidase</i>
MOAS	Methoxyacrylate-stilbene
MOPS	3-(N-morpholino)propanesulfonic acid
MS	Mass spektrometry
mV	Millivolt
NADH	Nicotin adenine dinucleotide
NaP_i	Sodium phosphate
NBT	Nitro blue tetrazolium
NCS	<i>New Born Calf Serum</i>
NQNO	2-n-nonyl-4-hydroxyquinoline N oxide
NMR	Nuclear magnetic resonance
OD	Optical density
<i>p.a</i>	<i>Pro analysi</i>
PAGE	Polyacrylamide gel electrophoresis
PCR	<i>Polymerase chain reaction</i>
PDB	<i>Protein Data Base</i>
PFO	Pseudo first order
PNK	Polynucleotide kinase
Q_o	Quinol oxidation site
Q_i	Quinone reduction site
Q- pool	Quinone pool
Rif	Rifampicin
Ru_z	(2,2'-bipyridine) ₂ (bromomethyl-4'-methyl-2,2'-bipyridine)
Ru2D	[Ru(bpy)2]2(qpy)(PF6)4; qpy, 2,2':4',4'':2'',2'''-quaterpyridine

Abbreviations

UV	Ultra violet light
rpm	Rounds per minute
ROS	Reactive oxygen species
SDS	Sodium dodecylsulfate
Sm	Streptomycin sulfate
SOEing PCR	<i>Splicing by overlap extension</i> PCR
SQR	Succinate dehydrogenase, complex II
TBE	Trisboric acid EDTA
TBS	Tris buffered saline
TBS-TT	TBS Triton Tween
TEMED	N, N, N', N'-Tetramethylethylenediamin
TMBZ	3,3',5,5'-Tetramethylbenzidin
TNM	Tris-sodium chloride magnesium chloride
Tris	Tris-(hydroxymethyl)-aminomethane
UHDBT	5-n-undecyl-6-hydroxy-4,7-dioxobenzothiazole
UQ6	Ubiquinone 6
V	Volt
w/w	Weight/weight
w/v	Weight/volume

Eidstattliche Erklärung

Eidesstattliche Erklärung

Hiermit erkläre ich, Michela Castellani, dass ich die vorliegende Arbeit selbständig und nur mit den angegebenen Quellen und Hilfsmitteln angefertigt habe.

Frankfurt am Main

Michela Castellani

Curriculum Vitae

WORK EXPERIENCE

- 02/2007 - to date Research assistant / doctoral student in biochemistry
Goethe University, Frankfurt am Main, Germany
- 2004/2005 Working student Assistant in the Library of the University of
L'Aquila, Italy
- 07/2002 -
09/2002 Sales assistant (part time) in the book shop "Il Cercalibro"
L'Aquila, Italy
- 07/2001 -
09/2001

EDUCATION

- 08/2009 Working experience in the USA, in the labs of Prof. Dr. Bernard
09/2009 Trumpower, Dartmouth (NH), Prof. Dr. Francis Millett,
Fayetteville (AR) and Prof. Dr. Anthony Crofts, Urbana (IL)
- 04/2008 to Four visits in the laboratory of Prof. Francesco Malatesta
01/2011 (University of Rome) for kinetic analysis of the cytochrome *bc₁*
complex from *P. denitrificans*
- 12/2006 Master degree in Applied Biology and Biological Quality,
University of L'Aquila (Italy) Grade 110/110 magna cum laude
Title: "Functional studies on the interaction between *Paracoccus*
denitrificans complex III and its substrates"
- 08/2005 - Erasmus exchange program, Molecular Genetics group
03/2006 Prof. Dr. Bernd Ludwig Goethe University, Frankfurt am Main
- 10/2004 Bachelor degree in Molecular Biology University of L'Aquila
(Italy) Grade 110/110 magna cum laude
Title: "Sequencing of the *nqr* operon from *Marinobacter*
hydrocarbonoclasticus ATCC 50418
- 09/1996 - Secondary school "Liceo Classico D. Cotugno"
06/2001 Grade 97/100

Acknowledgments

Acknowledgments

I would like to thank Prof. Dr. Bernd Ludwig for the opportunity he offered me, to work on the cytochrome bc_1 complex. He assigned me a very exciting topic, and gave me the chance to travel for conferences and for cooperations in many different places.

I also want to thank Prof. Dr. Klaas Martinus Pos for kindly accepting to be my second referent for the PhD thesis.

A huge thanks goes to Prof. Dr. Francesco Malatesta, who followed me from the Bachelor to the PhD thesis, worked with me and transferred me the passion for kinetics. I thank him for always being there, on Skype, live in Frankfurt, in Rome, and for all the exciting and loooooong days in front of the stopped flow. Grazie di tutto Prof!

I want to thank also Prof. Dr. Bernard Trumpower, Dr. Raul Covian, Prof. Dr. Francis Millett and his (now) postdoctoral student Jeffrey Havens, for the very nice time in America, for the exciting experiments and for the wonderful work we achieved together. My American expedition has been very successful and very nice thanks to you!

Prof. Dr. Petra Hellwig and Youssef provided quickly and very nicely some last-minute data, and for this I am thankful to them.

I have to thank Werner Müller (Topolino) and Andrea Herrmann (Frau Herrmann) for the excellent technical support, and for always being available for a coffee, a cigarette, or just to help me cool down after a tough day in the lab. And also for slapping me whenever I've been BOSE.

Edith, our secretary, Achim, Alena, Caro, Jule, Peter, Anna, Vicky, Axel, Daniela, Oli and Ole for the nice time in the lab, the funny grill-evenings and for the friendship we developed, which is one of the nicest memories of the time I spent here.

All the persons I met on the way, or whom I worked with, who helped me in any way and all the names are too many to be written here: thanks for being there when I needed you and for making my day sometimes!!

Un grazie speciale va alla mia famiglia, al di fuori del mondo scientifico e forse proprio per questo in grado di minimizzare tante piccole tragedie della vita di ogni giorno nel laboratorio. Mi avete aiutato a guardare in modo diverso molte cose ma soprattutto siete sempre stati lì dove siete anche ora. Siete stati uno dei pochi punti fermi negli sconvolgimenti degli ultimi anni, un porto dove tornare sempre, anche dopo il terremoto, e quando sei sola via da casa, questa é la certezza piú grande e uno stimolo a fare sempre di piú. A voi il merito se ho tenuto i piedi per terra nei momenti belli e brutti, perché mi avete sempre ricordato che al di fuori di queste

Acknowledgments

mura c'è il mondo reale! Grazie per il passato, per il presente, e per il futuro dove so che sarete sempre al mio fianco.

Thanks to my German family, who were also there whenever I needed them, for the nice time together and for being just a phone call away, all the time.

And to Thomas, mein schatz, for you wouldn't be another 200 pages enough to tell you how grateful I am, and I'm missing any word which could help express what I feel. That's why I will just say "Thank you". For everything. Yesterday, today and tomorrow.

Und damit, kann ich endlich mal stolz sagen: ICH HABE FERTIG!